DOCTORAL THESIS

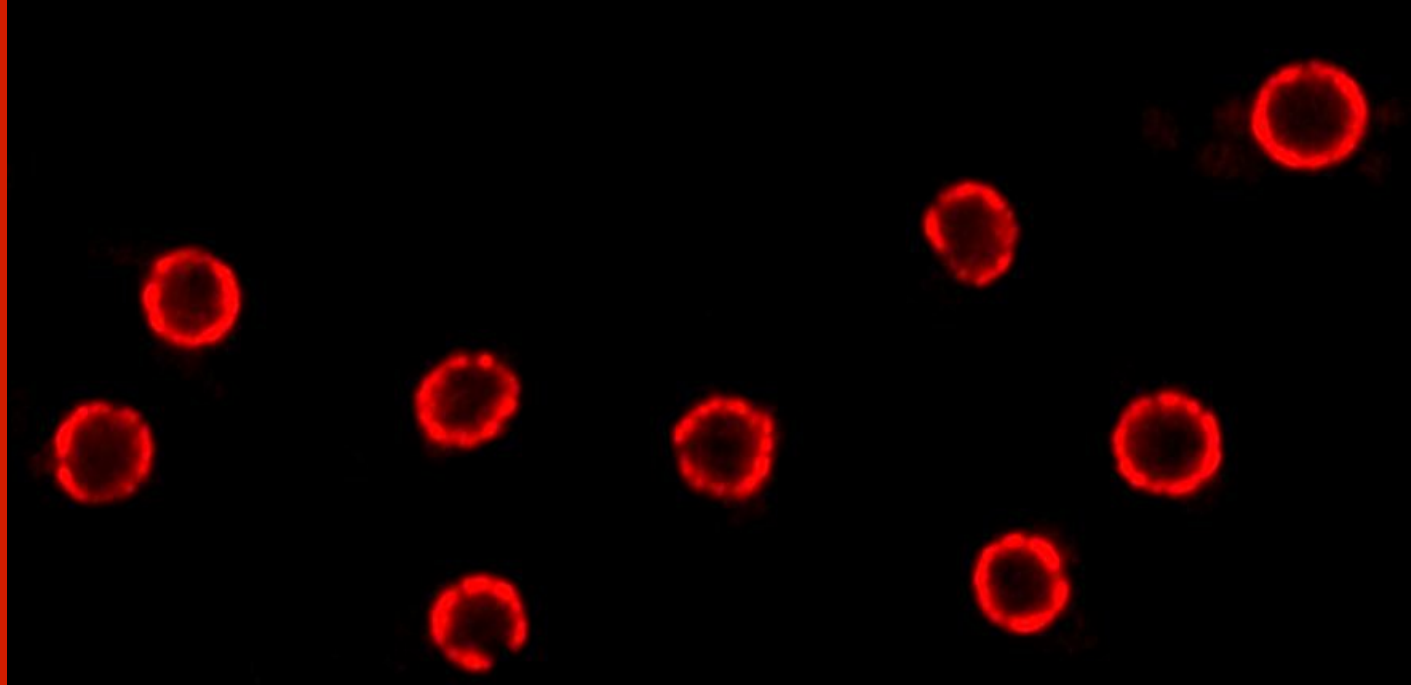

Functional Characterization of the Nuclear Basket TPR Nucleoporins in the Fission Yeast

Paola Gallardo Palomo

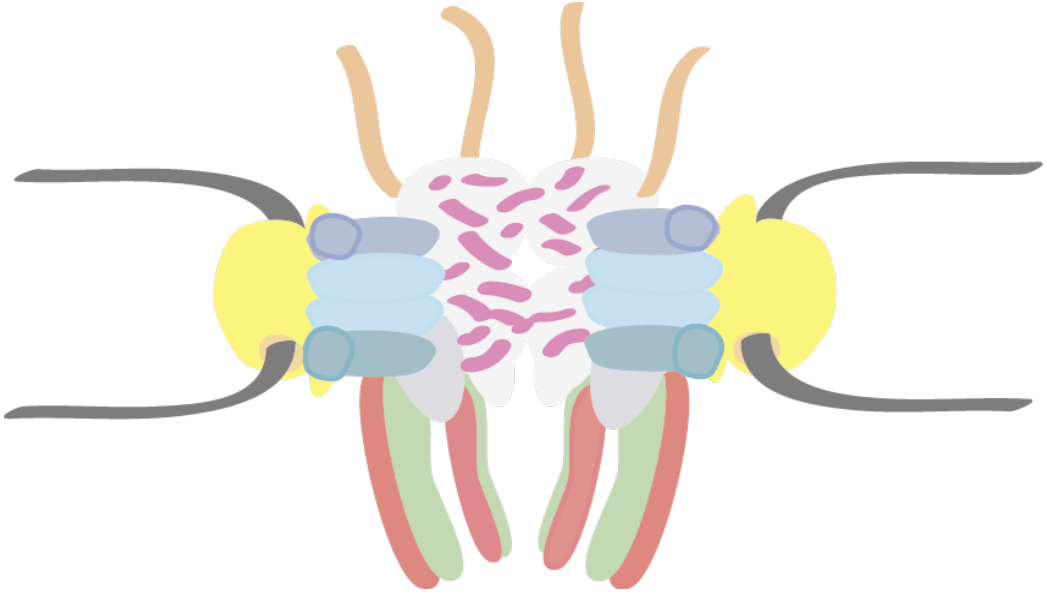

Universidad Pablo de Olavide

Sevilla, 2020

Departamento de Biología Molecular e Ingeniería Bioquímica

UNIVERSIDAD PABLO DE OLAVIDE

Doctoral Thesis

Functional Characterization of the Nuclear Basket TPR Nucleoporins in the Fission Yeast

Paola Gallardo Palomo

PhD Advisors

Dr. Rafael Rodríguez Daga

Dra. Silvia Salas Pino

Sevilla, 2020

El **Dr. Rafael Rodríguez Daga**, profesor titular del Área de Genética de la Universidad Pablo de Olavide, y la **Dra. Silvia Salas Pino**, profesora contratada doctora del Área de Genética de la Universidad Pablo de Olavide, en calidad de Directores, certifican que:

El trabajo titulado ***Functional characterization of the Nuclear Basket TPR nucleoporins in the fission yeast*** ha sido realizado por **Paola Gallardo Palomo** bajo su dirección y supervisión, y que a su juicio reúne las condiciones de originalidad y calidad necesarias para constituir una Tesis doctoral y optar al grado de Doctor por la Universidad Pablo de Olavide.

Y para que conste, expedimos el presente certificado en Sevilla, a 1 de mayo de 2020.

Fdo.: Dr. Rafael Rodríguez Daga

RODRIGUEZ DAGA RAFAEL - 52575222M

Firmado digitalmente por RODRIGUEZ DAGA RAFAEL - 52575222M
Nombre de reconocimiento (DN): c=ES, serialNumber=IDCES-52575222M, givenName=RAFAEL, sn=RODRIGUEZ DAGA, cn=RODRIGUEZ DAGA RAFAEL - 52575222M
Fecha: 2020.05.05 00:23:40 +02'00'

Fdo.: Dra. Silvia Salas Pino

SALAS PINO SILVIA - 25592856C

Firmado digitalmente por SALAS PINO SILVIA - 25592856C
Nombre de reconocimiento (DN): c=ES, serialNumber=25592856C, sn=SALAS PINO, givenName=SILVIA, cn=SALAS PINO SILVIA - 25592856C
Fecha: 2020.05.05 00:24:09 +02'00'

This Doctoral Thesis has been performed under the Doctorate Program in Biotechnology, Engineering and Chemical Technology, in the research group Nuclear Architecture and Dynamics of the Andalusian Centre for Developmental Biology, and has been conducted under the supervision of Dr. Rafael Rodriguez Daga and Dra. Silvia Salas Pino, belonging to the Genetics Area, Department of Molecular Biology and Biochemical Engineering of the Pablo de Olavide University.

The work of this Doctoral Thesis has been funded by the Spanish Miinistry of Economy and Competitiveness (BFU2015-70604-P and PGC2018-099849-B-I00 to R.R. Daga), and a predoctoral grant by the Pablo de Olavide University (PPI-1402 to P. Gallardo).

LIST OF PAPERS

This thesis is based on the following papers:

Salas-Pino P* , **Gallardo P*** , Barrales RR, Braun S, Daga RR. (2017) The fission yeast nucleoporin Alm1 is required for proteasomal degradation of kinetochore components. *J Cell Biol*. 6 Nov; 216(11):3591-3608. * Co-first authors.

Gallardo P, Real-Calderon P, Santana C, Devos D, Salas-Pino S, Daga RR. (2020) Nuclear basket interaction with mRNA-binding proteins facilitates mRNP docking and export in fission yeast. *Manuscript in preparation.*

Gallardo P, Real-Calderon P, Flor-Parra I, Salas-Pino S, Daga RR. (2020) Reversible aggregation of NPC components and mRNA machinery into nucleolar rings during acute heat stress. *Under review in Cell Reports. CELL-REPORTS-D-20-01067*

Papers by the author not included in this thesis:

Expósito-Serrano M*, Sánchez-Molina A*, **Gallardo P**, Salas-Pino S, Daga RR. (2020) Selective nuclear pore complex removal drives nuclear envelope division in the fission yeast. *Under review in Current Biology*. CURRENT-BIOLOGY-D-20-00391 * Co-first authors.

Gallardo P, Barrales RR, Daga RR, Salas-Pino S. (2019) Nuclear mechanics in the fission yeast. *Cells*. 20 Oct 8 (10). pii: E1285.

Gallardo P, Salas-Pino S, Daga RR. (2017) A new role for the nuclear basket network. *Microbial Cell*. 27 Nov; Vol.4, No.12, 423-425.

Flor-Parra I, Zhurinsky J, Bernal M, **Gallardo P**, Daga RR. (2014) A Lallzyme MMX-based rapid method for fission yeast protoplast preparation. *Yeast*. 31(2):61-6.

"Success is not final, failure is not fatal:
it is the courage to continue that counts."

Winston S. Churchill

ABSTRACT

Research performed over the last years has changed the view of NPCs as simple nucleo-cytoplasmic trafficking channels into a more comprehensive understanding of the multiples roles of the NPCs, which range from chromatin regulation to the maintenance of genome integrity. The most nucleoplasm-facing structure of the NPC is the nuclear basket. While in higher eukaryotes the main structural component of the nuclear basket is the translocated promoter region (TPR) nucleoporin, most yeasts possess two orthologs: Mlp1/Mlp2 in *Saccharomyces cerevisiae* and Nup211/Alm1 in *Schizosaccharomyces pombe*. Although it is known that most nuclear basket functions have been conserved along evolution, it remains unclear how TPR nucleoporins are assembled into the NPCs and the roles that they perform in the fission yeast.

Previous data from our laboratory described that the absence of Alm1 leads to chromosome missegregation and altered kinetochore behaviour. In order to avoid erroneous microtubule-kinetochore attachments and chromosome segregation defects, it is required a proper centromere and kinetochore structural organization, which is regulated by proteasomal degradation. Proteasome is enriched in the nucleus, specially at the nuclear periphery, although how this localization is regulated and its biological implications are unclear. In the first part of this thesis, we have characterized the role of the nuclear basket component Alm1 in the spatial regulation of the proteasome, which is key for chromosome segregation through the regulation of the kinetochore homeostasis.

The different steps of mRNA biogenesis, including transcription, processing, quality control and export are closely coordinated, and the nuclear basket has been proposed to act as a physical platform that couples such processes. *nup211*$^{+}$ was previously described as required for mRNA export. However, it remains unknown its specific role in mRNA docking and export. In the second part of this thesis, we have characterized how the two TPR nucleoporins in the fission yeast, Nup211 and Alm1, are assembled into the nuclear basket and how they anchor to the NPC. Additionally, we have performed a genetic and functional analysis to dissect the functions of Nup211 and Alm1 in mRNA docking, quality control and export.

Heat shock deeply compromise cell viability due to protein denaturation and aggregation. In order to ensure survival cells activate the evolutionary conserved *heat shock response* (HSR), which results in profound changes in mRNA metabolism and nuclear organization. How this switch is achieved is not fully understood. In the third part of this study, we have characterized how heat stress leads to the inhibition of bulk mRNA export and the arrest of cell growth, concomitant with the aggregation of NPC components, the mRNA processing and export machinery, cell cycle regulators, and protective chaperones and disaggregases into ring-like structures proximal to the nucleolus. We propose that these structures, named “nucleolar rings” (NuRs), are formed by the reversible aggregation of nuclear components, and constitute storage sites for those activities that are inhibited during HS and have to be protected in order to re-start cellular metabolism when normal conditions are restored.

RESUMEN

Las investigaciones realizada en los últimos años han permitido ampliar la visión de los NPCs (Complejos del poro nuclear) como simples canales que median el tránsito nucleo-citoplásmico hacia una comprensión más integral de las múltiples funciones que realizan los NPCs, que van desde la regulación de la cromatina al mantenimiento de la integridad genómica. La parte nucleoplásmica de los NPC se denomina cesta del poro. Mientras que en eucariotas superiores la cesta del poro está constituida principalmente por las nucleoporinas TPR (*translocated promoter region*), la mayor parte de levaduras poseen dos ortólogos: Mlp1/Mlp2 en *Saccharomyces cerevisiae* y Nup211/Alm1 en *Schizosaccharomyces pombe.* Aunque se sabe que la mayoría de las funciones de la cesta del poro se han conservado a lo largo de la evolución, se desconoce cómo las nucleoporinas TPR se ensamblan en los NPCs y qué funciones realizan en la levadura de fisión.

Datos previos de nuestro laboratorio describieron que en ausencia de Alm1 se producen defectos en la segregación cromosómica y en la dinámica del cinetocoro. Para evitar interacciones erróneas entre los microtúbulos-cinetocoros y, en consecuencia, defectos en la segregación cromosómica, es necesaria una correcta organización estructural de los centrómeros y cinetocoros, lo cual está regulado por el proteosoma. Aunque se ha descrito que el proteosoma localiza principalmente en el núcleo y la envuelta nuclear, se desconoce cómo se regula esta localización y cuáles son sus implicaciones biológicas. En la primera parte de esta tesis hemos caracterizado la función de la nucleoporina Alm1 en la regulación espacial del proteasoma, la cual es necesaria para que se mantenga la homeostasis del cinetocoro y que se produzca una correcta segregación cromosómica.

Los diferentes pasos que dan lugar a la generación de los RNA mensajeros, incluídos su transcripción, procesamiento, control de calidad y exporte, están estrechamente coordinados y, de hecho, se ha propuesto que la cesta del poro actúa como una plataforma física que conecta dichos procesos. Se ha descrito que Nup211 participa en el exporte de ARNm. Sin embargo, se desconoce el papel específico de ésta en el anclaje y exporte de ARNm. En la segunda parte de esa tesis hemos caracterizado cómo las dos nucleoporinas TPR en *S. pombe*, Nup211 y Alm1, se ensamblan en la cesta nuclear y se anclan al NPC. Además, hemos realizado un análisis genético y funcional para diseccionar las funciones de Nup211 y Alm1 en el anclaje, control de calidad y exporte del ARNm.

El estrés térmico compromete la viabilidad celular debido a la desnaturalización y agregación de proteínas. Para garantizar su supervivencia, las células activan la respuesta a estrés térmico (HSR, *heat shock response*), la cual desencadena cambios considerables en el metabolismo del ARNm y en la organización nuclear. Actualmente, no se conoce completamente cómo se producen estos cambios. En la tercera parte de este estudio, hemos caracterizado cómo el estrés térmico conduce a la inhibición del exporte general de ARNm y al bloqueo del crecimiento celular, al mismo tiempo que en la periferia del nucleolo se produce la agregación de diversos componentes celulares, incluyendo componentes del poro, la maquinaria de procesamiento y exporte de ARNm, reguladores del ciclo

celular, así como las chaperonas y desagregasas. Proponemos que estas estructuras, denominadas NuRs (*nucleolar rings*), se forman por la agregación reversible de componentes nucleares y constituyen estructuras para el almacenamiento de aquellas actividades que se inhiben durante la estrés térmico y deben ser protegidas para reiniciar el metabolismo celular cuando se reestablezcan las condiciones normales de crecimiento.

CONTENTS

ABBREVIATIONS

A	Adenosine
Ab	Antibody
APC/C	Anaphase-promoting complex/cyclosome
ATP	Adenosine triphosphate
AU	Arbitrary units
BCA	Bicinchoninic acid
bp	Base pair
BSA	Bovine serum albumin
cAMP/PKA	Cyclic AMP/protein kinase A
CBC	Cap binding complex
CCAN	Constitutive-centromere-associate network
Cdk	Cyclin-dependent kinase
cDNA	Complementary DNA
ChIP	Chromatin immunoprecipitation
CHX	Cycloheximide
CLRC	Clr4-containing complex
cnt	Centromere core domain
COC	Chromosome-organizing clamp
CP	Core particle
CPF	Cleavage and polyadenylation factor
CTD	Carboxy-terminal domain
kDa	KiloDalton
DAPI	4′,6-diamidino-2-phenylindole
DMSO	Dimethyl sulfoxide
DNA	Deoxyribonucleic acid
dNTP	Deoxynucleotide triphosphate
DTT	Dithiothreitol
EDTA	Ethylenediaminetetraacetic acid
EJC	Exon-junction complex
EMM	Edinburgh minimal media
EtBr	Ethidium bromide
FG	Phenylalanine/glycine
FISH	Fluorescence *in situ* hybridization
FOA	5-fluoroorotic acid
GDP	Guanosine diphosphate
GFP	Green fluorescence protein
GH	Guanidinium hydrochloride
GO	Gene ontology
GRS	Gene recruitment sequence
GTP	Guanosine-5'-triphosphate
HDAC	Histone deacetylase
hnRNP	Heterogeneous nuclear RNP
HRP	Horseradish peroxidase
HS	Heat shock
HSE	Heat shock element
HSP	Heat shock protein
HSR	Heat shock response
Hyg	Hygromycin B
IF	Immunofluorescence
IgG	Immunoglobulin G
imr	Innermost repeats
INM	Inner nuclear membrane
IP	Immunoprecipitation
IP6	Inositol hexakisphosphate
IR	Inverted repeat
Kap	Karyopherin
Kb	Kilobase
KMN	KNL-1/Mis12 complex/Ndc80 complex network
KT	Kinetochore
LB	Luria-Bertani medium
LiAc	Litium acetate
LINC	Linker of nucleoskeleton and cytoskeleton
lncRNA	long non-coding RNA
MAPK	Mitogen-activated protein kinase
mAb	Monoclonal antobody
Mb	Megabase
MCC	Mitotic checkpoint complex
miRNA	MicroRNA
ml	Milliliter
Mlp	Myosin-like protein
MM	Minimal medium
mRNA	Messenger RNA
mRNP	Messenger ribonucleoprotein
MT	Microtubule
MTOC	Microtubule-organizing centres
MTREC	Mtl1-Red1 core complex
NA	Numerical aperture
NE	Nuclear envelope
NEM	N-Ethylmaleimide

NES	Nuclear export signal
NLS	Nuclear localization signal
NPC	Nuclear pore complex
ns	Non-significant
Nup	Nucleoporin
NURS	Nuclear RNA silencing complex
OD	Optical density
otr	Outermost repeats
PABP	Poly(A)-binding protein
PBS	Phosphate Buffered Saline
PCR	Polymerase chain reaction
PEG	Polyethylene glycol
pFA	Paraformaldehyde
PMSF	Phenylmethylsulfonyl fluoride
pAb	Polyclonal antobody
QC	Quality control
qPCR	Quantitative polymerase chain reaction
Ran-GAP	Ran GTPase activating protein
Ran-GEF	Ran guanine nucleotide exchange factor
RBP	RNA-binding protein
rDNA	Ribosomal DNA
RFP	Red fluorescence protein
RITS	RNA-induced transcriptional silencing
RNA	Ribonucleic acid
RNAi	RNA interference
RNAP	RNA Polymerase
RNase	Ribonuclease
RP	Regulatory particle
rpm	Revolutions per minute
RT-qPCR	Reverse transcription quantitative PCR
SAC	Spindle assembly checkpoint
SAGA	Spt-Ada-Gcn5 acetyltransferase
SD	Standard deviation
SDS	Sodium dodecyl sulfate
SG	Stress granule
SGA	Synthetic genetic array
SHREC	Snf2/Hdac Repressive Complex
sHSP	Small HSPs
siRNA	Small interfering RNA
snRNA	Small nuclear RNA
SOC	Super Optimal broth with Catabolite repression
SPA	Sporulation Agar
SPB	Spindle pole body
SR	Serine-arginine
STRE	Stress responsive elements
TBE	Tris/Borate/EDTA
TBZ	Thiabendazole
TCA	Trichloroacetic acid
TE	Tri-EDTA
TERRA	Telomeric repeat-containing RNA
TOR	Target of rapamycin
TPR	Translocated promoter region
TRAMP	Trf4/Air2/Mtr4p polyadenylation
TREX	Transcription-export
tRNA	transfer RNA
ts	Thermosensitive
Ub	Ubiquitin
UPS	Ubiquitin-proteasome system
UTR	Untranslated region
UV	Ultraviolet
v/v	Volume/volume
VRC	Ribonucleoside vanadyl complexes
w/v	Weight/Volume
WB	Western blot
YES	Yeast Extract with Supplements
YFP	Yellow fluorescent protein
µl	Microliter
µm	Micrometer
µM	Micromolar

INTRODUCTION

THE NUCLEAR PORE COMPLEX

Overview of the NPC

One of the distinctive features of eukaryotic cells is the presence of membrane-encircled organelles that perform specific functions, of which the nucleus is the largest one. The nuclear envelope (NE) is a lipid bilayered-membrane that physically separates the DNA-containing nucleoplasm and the cytoplasm. Even though nuclear compartmentalization has enabled a tighter regulation of nuclear processes, it also represents a considerable logistic challenge. This has been solved along evolution with the development of channels that control the trafficking between the nucleus and the cytoplasm: the nuclear pore complexes (NPCs). Embedded at the NE, NPCs are the only gates connecting the cytoplasm and the nucleus and, therefore, are responsible for the selective and bidirectional exchange of proteins between both compartments and the export of RNAs to the cytoplasm, while allow the free difusion of small metabolites, such as water, ions or sugars (Davis, 1995; Knockenhauer and Schwartz, 2016; Suntharalingam and Wente, 2003; Terry and Wente, 2009; Wente and Rout, 2010).

Firstly described in 1949 using electron microscopy in amphibian oocytes (Callan et al., 1949), several studies have described that while yeast nucleus contains ~100-200 NPCs, human cells possess on average 3000 NPCs (Bui et al., 2013; Maul et al., 1972; Winey et al., 1997). NPCs are enormous macromolecular structures with an estimated single molecular mass of ~50 MDa in yeasts (45.8–47.8 MDa in the fission yeast) and 100–130 MDa in *Homo sapiens* (Alber et al., 2007; Asakawa et al., 2014; Reichelt et al., 1990). Despite this large size, they are composed by a reduced number of different proteins (~30), called nucleoporins (hereinafter referred to as Nups, listed in Table I1), which are repetitively arranged into the different subcomplexes that comprise the NPC (Asakawa et al., 2014; Beck and Hurt, 2017; Cronshaw et al., 2002; Pante and Aebi, 1996; Rout et al., 2000; Schwartz, 2016). In the past four decades, the combined efforts of several groups have provided a complete depiction of the composition and architecture of the NPC for different eukaryotes, demonstrating that although Nups have diverged at the sequence level, most nucleoporins as well as their structural arrangement show a remarkable conservation between species (Table I1) (DeGrasse et al., 2009; Field et al., 2014; Holzer and Antonin, 2018; Kim et al., 2018; Mosalaganti et al., 2018; Neumann et al., 2010; Rajoo et al., 2018; Yang et al., 1998).

The Nuclear Pore Complex structure

The most complete 3D map of the NPC structure comes from *Saccharomyces cerevisiae* (Kim et al., 2018; Rout et al., 2000). Broadly, Nups are assembled into subcomplexes that constitute the building blocks of the NPC, which in turn interact with each other to create the higher-order structure of the NPC. The central body of the NPC is a symmetrical cylinder formed by the inner and outer rings (Fig. I1 A). This core scaffold represents the anchorage for the other modules of the NPC; it is connected outwards to the nuclear envelope through the membrane ring, and inwards to channel Nups (Alber et al., 2007; Grossman et al., 2012; Kim et al., 2018; Rout et al., 2000; Schwartz, 2016).

Table A1. List of nucleoporins in *S. pombe* and their orthologs in *S. cerevisiae* and *H. sapiens*.

Subcomplex	*S. pombe*	*S. cerevisiae*	*H. sapiens*
Inner Rings	Nup97	*Sc*Nic96	*Hs*Nup93
	Npp106		
	Nup186	*Sc*Nup192	*Hs*Nup205
	Nup184	*Sc*Nup188	*Hs*Nup188
	Nup40	*Sc*Nup53 *Sc*Nup59	*Hs*Nup35
	Nup155	*Sc*Nup157 *Sc*Nup170	*Hs*Nup155
Outer Rings	Nup37	—	*Hs*Nup37
	Nup96 (spNup189c)	*Sc*Nup145C	*Hs*Nup96
	Nup85	*Sc*Nup85	*Hs*Nup85
	Ely5	—	*Hs*ELYS
	Nup120	*Sc*Nup120	*Hs*Nup160
	Seh1	*Sc*Seh1	*Hs*Seh1
	Nup131	*Sc*Nup133	*Hs*Nup133
	Nup132		
	Nup107	*Sc*Nup84	*Hs*Nup107
	—	*Sc*Sec13	*Hs*Sec13
	—	—	*Hs*Nup43
Membrane Ring	Pom34	*Sc*Pom34	—
	Cut11	*Sc*Ndc1	*Hs*Ndc1
	Pom152	*Sc*Pom152	—
	Tts1	*Sc*Pom33 *Sc*Per33	*Hs*Pom121
	—	—	*Hs*Gp210 (Nup210) *Hs*Pom121
Central channel	Nsp1	*Sc*Nsp1	*Hs*Nup62
	Nup44	*Sc*Nup57	*Hs*Nup54
	Nup45	*Sc*Nup49	*Hs*Nup58
	Nup98	*Sc*Nup145n *Sc*Nup100 *Sc*Nup116	*Hs*Nup98
Cytoplasmic filaments	Nup82	*Sc*Nup82	*Hs*Nup88
	Nup146	*Sc*Nup159	*Hs*Nup214
	Amo1	*Sc*Nup42 (Rip1)	*Hs*Nlp1
	—	—	*Hs*ALADIN *Hs*Nup358
Nuclear Basket	Nup124	*Sc*Nup1	*Hs*Nup153
	Nup60	*Sc*Nup60	—
	Nup61	*Sc*Nup2	*Hs*Nup50
	Nup211	*Sc*Mlp1	*Hs*TPR
	Alm1	*Sc*Mlp2	

Adapted from (Asakawa et al., 2019; Asakawa et al., 2014).

Cytoplasmic and nucleoplasmic filaments extent out from the core scaffold, conferring asymmetry to the NPC. At the nuclear side, the filaments converge to form the nuclear basket (Fig. I1 A) (Cordes et al., 1997; Kiseleva et al., 2004; Kosova et al., 2000; Krull et al., 2004; Strambio-de-Castillia et al., 1999).

- **NPC core scaffold**

The core scaffold constitutes the channel through which macromolecular exchange occurs. The most basic modules of the core scaffold are termed “spokes”. Eight spokes are interconnected with each other, shaping a cylinder with octagonal symmetry around the central axis. This assembly is composed of two adjacent inner rings sandwiched by two distal outer rings in yeasts (four outer rings in metazoans) (Holzer and Antonin, 2018; Lin et al., 2016; Rout et al., 2000; Szymborska et al., 2013). The inner rings comprise the Nup170 subcomplex in budding yeast (Nup155 subcomplex in metazoans and Nup93 subcomplex in fission yeast; Fig. I1 B) (Asakawa et al., 2014; Boehmer et al., 2003; Kim et al., 2018; Kosinski et al., 2016; Rout et al., 2000). The outher rings are constituted by the Y-shaped subcomplexes, which correspond to the Nup84 complex in budding yeast (Nup107 in metazoans and Nup107-Nup160 in *S. pombe*; Fig. I1 B and C) (Asakawa et al., 2014; Belgareh et al., 2001; Bui et al., 2013; Siniossoglou et al., 2000; Siniossoglou et al., 1996; von Appen et al., 2015; Wente and Rout, 2010). The rigid, and still flexible, ring structure of the core scaffold is supported by linker Nups. Among them, *Sc*Nic96 (*Sp*Npp106 and *Sp*Nup97/*Hs*Nup93) bridges the inner and outer rings and serves as attachment site for other Nups, while *Sc*Nup192 (*Sp*Nup186/ HsNup205) connects adjacent spokes (Fischer et al., 2015; Grandi et al., 1997; Kim et al., 2018; Schwartz, 2016; Vollmer and Antonin, 2014).

While composition and structure of the inner rings show a high degree of conservation, the outer rings have apparently diverged along evolution, but still the Y-subcomplex is required for NPC organization and assembly (Boehmer et al., 2003; Harel et al., 2003; Walther et al., 2003). Yeast possesses two outer rings (each one containing eight Y-subcomplexes, located at the cytoplasmic and at the nucleoplasmic faces), whereas human NPCs have two concentric rings at each side of the core scaffold (Fig. I1 C). Consistently, human outer rings contain twice the number of Y-subcomplex Nups than yeast (16 copies in yeasts and 32 in humans) (Bui et al., 2013; Holzer and Antonin, 2018, 2019; Ma et al., 2017; Obado et al., 2016; Rajoo et al., 2018; von Appen et al., 2015). Moreover, even though the Y-subcomplex has conserved its distinctive conformation in most organisms, the number of constituent nucleoporins differs: seven in *S. cerevisiae,* nine in *S. pombe* and ten humans (Asakawa et al., 2019; Bai et al., 2004; Bui et al., 2013; Chopra et al., 2019; DeGrasse et al., 2009; Kim et al., 2018; von Appen et al., 2015). Its name, Y-subcomplex, arises from the structural arrangement that its components adopt (Fig. I1 C). In *H. sapiens*, Nup85, Nup43, and Seh1 form the short arm, Nup160, Nup37, and ELYS constitute the long arm, and through Nup96 and Sec13 they interact with Nup107 and Nup133, which shape the long stem (Bui et al., 2013; Kim et al., 2018; Knockenhauer and Schwartz, 2016; Lutzmann et al., 2002; Stuwe et al., 2015b; von Appen et al., 2015). Importantly, a

recent study has described that fission yeast Y-subcomplex has lost its symmetrical composition and localization; *Sp*Nup132 and *Sp*Nup107 are located exclusively at the nucleoplasmic side of the NPC, while *Sp*Nup131, *Sp*Nup120, *Sp*Nup85, *Sp*Nup96, *Sp*Nup37, *Sp*Ely5 and *Sp*Seh1 are only present at the cytoplasmic side (Fig. I1 B and C) (Asakawa et al., 2019).

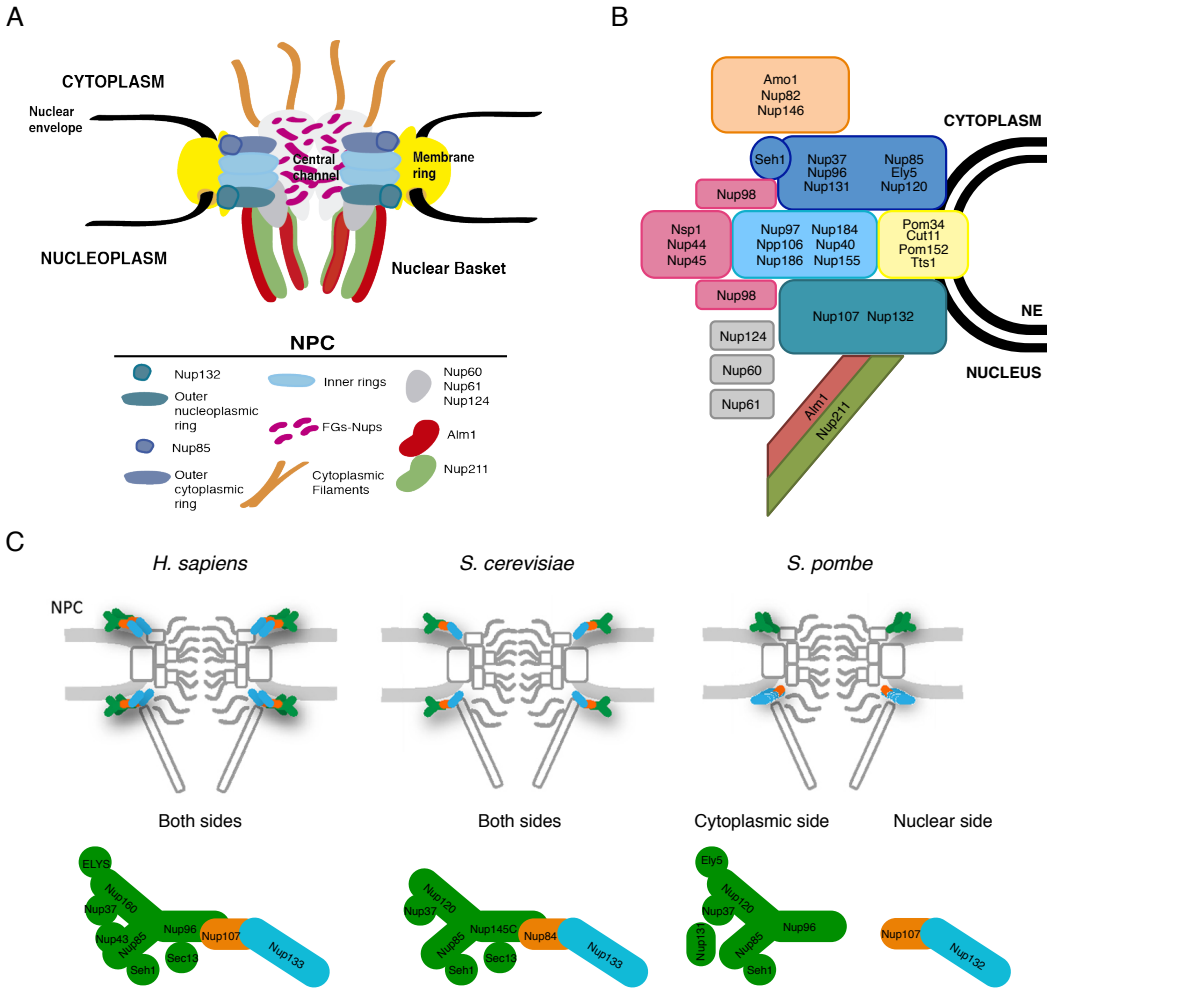

Figure I1. Schematic illustration of the Nuclear Pore Complex structure and composition. (A) Structure of the NPC. The NPC is composed by a cylindrical central scaffold, formed by the inner and outer rings (shown in blue), displaying an eightfold rotational symmetry. The membrane ring (yellow) anchors the core scaffold to the NE (black) through transmembrane nucleoporins. The central channel is lined by FG-nucleoporins (pink), which regulate NPC transport and create the permeability barrier. Cytoplasmic filaments projecting towards the cytoplasm constitute the platform for mRNA export remodeling (orange). The nuclear filaments converge to form the nuclear basket (green and red). Although the molecular mass of the NPC increases from yeast (50 kDa) to mammals (120kDa), its modular structure as well as most of nucleporins are evolutionarily conserved. (B) Composition of the NPC in the fission yeast. The picture shows the different nucleoporins that are contained in each subcomplex, including the core scaffold (formed by the cytoplasmic and nucleoplasmic outer rings, and the inner rings, blue), the membrane ring (yellow), the FG-nucleoporins of the central channel (pink), the cytoplasmic filaments (orange), and the nuclear basket (FG-Nups in grey and TPR Nups in red and green). Fission yeast Y-subcomplex has lost its symmetrical composition: *Sp*Nup132 and *Sp*Nup107 are located exclusively at the nucleoplasmic side of the NPC, while *Sp*Nup131, *Sp*Nup120, *Sp*Nup85, *Sp*Nup96, *Sp*Nup37, *Sp*Ely5 and *Sp*Seh1 are only present at the cytoplasmic side of the NPC. For further information about the nucleoporins of each subcomplex and its orthologs in *S. cerevisiae* and *H. sapiens*, see Table I1. (Adapted from Terry and Wente, 2007; Alber et al., 2007; Wente and Rout, 2010; Strambio-De-Castilla et al., 2010; Stuwe et al., 2015b; Asakawa et al., 2019) (C) Schematic picture of the NPC, highlighting the localization (upper panel) and the structural composition (lower panel) of the Y-subcomplexes in *H. sapiens* (left), *S. cerevisiae* (middle) and *S. pombe* (right). See NPC core scaffold for further information. (Asakawa et al., 2019)

- **Membrane Ring**

The NPC core scaffold is anchored to the NE directly interacting with the pore membrane, the region of the NE where the NPC is embedded, or through the membrane ring, which is essential for the assembly of the NPC and the maintenance of its structural integrity. The inner rings are anchored to the membrane ring and to the pore membrane through the membrane-binding domains of Nup157, Nup170, Nup53 and Nup59 in *S. cerevisiae*. The outer rings are anchored to the pore membrane through *Sc*Nup120 and *Sc*Nup133 (Eisenhardt et al., 2014; Kim et al., 2018; Kim et al., 2014; Onischenko et al., 2009; Vollmer et al., 2012). In the fission yeast membrane ring comprises the nucleoporins Cut11, Pom34, Pom152 and Tts1 (Fig. I1 B) (Ndc1, Pom34, Pom152, Pom33 and Per33 in budding yeast), characterized by the presence of transmembrane α-helices domains (Alber et al., 2007; Asakawa et al., 2014; Chadrin et al., 2010; Mitchell et al., 2010; Onischenko et al., 2009; Upla et al., 2017; Zhang and Oliferenko, 2014). Beyond their roles in the attachment of the NPC to the NE, these membrane Nups have been related to additional functions. For example, Cut11 is involved in anchoring the spindle pole body (SPB, centrosome homolog) to the NE and in spindle assembly, being required for correct chromosome segregation during mitosis (West et al., 1998); while Tts1 facilitates SPB insertion, together with Cut11, and participates in NE remodeling and NPC distribution during mitosis (Zhang and Oliferenko, 2014).

- **Channel Nups**

Lining the innermost part of the nuclear pore, channel nucleoporins are the flexible gates that control the passive and active transport across NPCs (Knockenhauer and Schwartz, 2016; Solmaz et al., 2011; Tetenbaum-Novatt and Rout, 2010). Channel Nups belong to a unique family of NPC proteins termed phenylalanine-glycine Nucleoporins (FG-Nups). FG-Nups are characterized by the presence of natively unfolded domains that lack secondary structure, separated by spacer sequences, what makes them highly dynamic (Lim et al., 2006; Patel et al., 2007; Rout and Wente, 1994; Stuwe et al., 2015a). FG-Nups also possess a small structured domain to anchor to the core scaffold, preferentially to linker Nups and to the inner rings, contributing to the stabilization of the NPC structure (Denning et al., 2003; Kim et al., 2018; Li et al., 2016; Onischenko et al., 2017; Strawn et al., 2004; Terry and Wente, 2009; Tetenbaum-Novatt and Rout, 2010). There exist three types of FG-Nups, according to their repeated sequence, FG (Phe-Gly) FXFG (Phe-X-Phe-Gly) and GLFG (Gly-Leu-Phe-Gly) (Allen et al., 2001; Frey and Gorlich, 2009; Onischenko et al., 2017).

Stoichiometric analyses of NPC composition have determined that FG repeats are found in about one third of all Nups, which can be symmetrically or asymmetrically located. Symmetric FG-Nups (Nsp1, Nup49, Nup57 in *S. cerevisiae* and Nsp1, Nup44 and Nup45, Nup98 in *S. pombe*, Fig. I1 B) fill the central channel and are found at both sides of the NPC, while asymmetric FG-Nups occupy peripheral positions facing the cytoplasm or the nucleoplasm (see below) (Denning et al., 2003; Kim et al., 2018; Onischenko et al., 2017; Rout et al., 2000; Suntharalingam and Wente, 2003; Terry and Wente, 2009). FG-Nups create a highly effective permeability barrier: while ions, small metabolites

and molecules up to 10 nm or 40 kDa freely diffuse across the NPCs, larger macromolecules require carriers that facilitate their nucleo-cytoplasmic translocation by interacting with FG-Nups. Given their relevant function, their structure and organization are conserved among eukaryotes (Li et al., 2016; Shulga et al., 2000; Terry and Wente, 2009; Tetenbaum-Novatt and Rout, 2010).

- **Peripheral filaments**

Peripheral filaments extend from the core scaffold outer rings into the cytoplasm or the nucleoplasm, providing asymmetry to the NPC. Most of their components are FG-Nups (Kim et al., 2018; Kiseleva et al., 2004; Terry and Wente, 2009). Interestingly, while the nucleoporins of the core scaffold seem to be very stable and posses longer lifetimes, peripheral components show fast turnover rates (D'Angelo et al., 2009; Denning et al., 2001; Rabut et al., 2004).

- **Cytoplasmic filaments**

Budding yeast Nup82 subcomplex includes *Sc*Nup82 and two FG-Nups (*Sc*Nup159 and *Sc*Nup42), which are anchored by cytoplasmic connectors (GLFG-containing *Sc*Nup100, *Sc*Nup116) (Alber et al., 2007; Bailer et al., 1998; Gaik et al., 2015; Kim et al., 2018; Terry and Wente, 2007, 2009). In *S. pombe* Nup82, Nup146 and Amo1 have been described as components of the cytoplasmic filaments (Fig. I1 C) (Asakawa et al., 2014). Cytoplasmic filaments function as docking sites for karyopherin transport factors during protein import and for nucleoporin-associated mRNA export factors; therefore, they are also called the export platform (Alcazar-Roman et al., 2006; Fernandez-Martinez et al., 2016; Kraemer et al., 1995; Schmitt et al., 1999; Strawn et al., 2001; Weirich et al., 2004).

- **The Nuclear Basket**

At the nuclear side, eight filaments converge distally into a ring, forming a basket-like assembly, named nuclear basket. The morphological structure of the nuclear basket has been conserved in a wide range of eukaryotes, including fungi, trypanosomes, amoebae, metazoan and plants. Despite its morphological conservation, the composition of the nuclear basket seems to be quite divergent between species. In budding yeast, it is composed of a nucleoplasmic connector *Sc*Nup145n (GLFG-Nup), *Sc*Nup1 and *Sc*Nup2 (FXFG Nups), *Sc*Nup60 (FXF-containing), and the non-FG Nups Mlp1 and Mlp2 (Denning et al., 2001; Kim et al., 2018; Rout et al., 2000; Terry and Wente, 2009). Nup1 and Nup60 interact with both the nuclear membrane and the NPC core scaffold, regulating the membrane curvature (Meszaros et al., 2015). In *S. pombe* the nuclear basket comprises five nucleoporins: Nup60, Nup61, Nup124, Nup211 and Alm1 (Fig. I1 B) (Asakawa et al., 2019; Salas-Pino et al., 2017). The main scaffolding elements of the nuclear basket are the large (~200 kDa) coiled-coil TPR (translocated promoter region) proteins: *S. cerevisiae* Mlp1 and Mlp2, *S. pombe* Nup211 and Alm1, and vertebrate TPR. Long repeated coiled-coil domains of TPR proteins could be key for their tertiary structure, their anchoring to the NPC, and their interaction with numerous proteins, partly due to their ability to nucleate and anchor molecular complexes (Asakawa et al., 2019; Cordes et al., 1997; Field et al., 2014; Frosst et al., 2002; Galy et al., 2004; Gu et al., 2012; Hase et al., 2001; Knockenhauer and Schwartz, 2016; Salas-Pino et al., 2017; Strambio-de-Castillia et al., 1999).

FUNCTIONS OF THE NUCLEAR BASKET

The view of the NPCs as simple channel for the nucleocytoplasmic transport has been expanded over the last years, highlighting the integral roles that they perform in several key cellular processes. At the nucleoplasmic side, the TPR nucleoporins form the nuclear basket and constitute an extensive network underlying the NE, connecting neighbouring NPCs. Therefore, it has been proposed that the absence of nuclear lamina in yeasts is partially fulfilled by the these TPR-like proteins (Niepel et al., 2013; Niepel et al., 2005). The nuclear basket is involved in the regulation of several nuclear functions, most of which have been conserved during evolution, such as functional organization of nuclear compartments (Casolari et al., 2005; Feuerbach et al., 2002; Hediger et al., 2002a; Krull et al., 2010), chromatin organization (Brickner et al., 2019; Fiserova et al., 2017; Iglesias et al., 2020; Kuhn and Capelson, 2019), spatio-temporal regulation of SAC components (Ding et al., 2012; Lee et al., 2008a; Lince-Faria et al., 2009; Rodriguez-Bravo et al., 2014; Salas-Pino et al., 2017; Schweizer et al., 2013), transcriptional regulation (Brickner et al., 2007; Cabal et al., 2006; Feuerbach et al., 2002; Light and Brickner, 2013; Mendjan et al., 2006; Vaquerizas et al., 2010), and recruitment of RNA processing and export factors (Bonnet and Palancade, 2014; Coyle et al., 2011; Galy et al., 2004; Green et al., 2003; Rajanala and Nandicoori, 2012; Terry and Wente, 2007). The following sections will provide a general overview of these processes and the contribution of the nuclear basket to their regulation.

Nucleo-cytoplasmic transport

Nucleocytoplasmic transport is one of the best-characterized functions of the nuclear pores. In simple terms, during nucleo-cytoplasmic trafficking, transport receptors bind to their cargo and dock to the asymmetric FG-Nups that work as a platform for transporters, located exclusively at the cytoplasmic or nucleoplasmic sides of the NPC (Kim et al., 2018; Li et al., 2016; Terry and Wente, 2009; Tran and Wente, 2006); then, transporters escort the cargo through the NPC by interacting with the FG-Nups that line the central channel, and finally release the cargo into the appropriate compartment. In general, protein transport is bidirectional and depends on the Ran-GTPase system, while export of messenger ribonucleoproteins (mRNPs) is independent on the Ran-GTPase system (see mRNP export below for further information) (Pemberton and Paschal, 2005; Tetenbaum-Novatt and Rout, 2010; Wente and Rout, 2010). Interestingly, it has been suggested the existence of different transport routes, keeping protein transport and mRNP export apart, as a consequence of the preferential interaction of transporters with FG-Nups (Ma and Yang, 2010; Strasser et al., 2000; Strawn et al., 2004; Terry and Wente, 2007, 2009; Tran and Wente, 2006; Yamada et al., 2010).

The most common transport receptors are the karyopherins (Kaps), of the importin β superfamily, which can be importins or exportins. Kap cargoes include proteins and different types of RNAs (tRNA, rRNA, miRNA and snRNA), which are recognized directly or using adaptors (Sloan et al., 2016). Transport directionality depends on two factors: the RanGTP gradient (higher RanGTP levels in the

nucleoplasm and RanGDP in the cytoplasm) and the presence of asymmetrical FG-Nups exposed towards the cytoplasmic or nucleoplasmic compartments (Cook et al., 2007; Macara, 2001; Mosammaparast and Pemberton, 2004; Walde and Kehlenbach, 2010).

During nuclear import (Fig. I2 A), importin β Kaps recognize nuclear localization signal (NLS) in their specific cargoes, directly or using importin α as adaptor (Dingwall and Laskey, 1991), and this complex translocates, interacting with FG-Nups, to the nucleoplasmic side of the NPC. Here, RanGTP induces a conformational change in the transport receptors, which dissociate from the cargoes. Then, Kap-RanGTP travels back to the cytoplasm, where Ran-GTPase activating protein (Ran-GAP, *Sc*Rna1) catalyzes the conversion of RanGTP into RanGDP (Rexach and Blobel, 1995). During nuclear export (Fig. I2 B), nuclear Ran-GTP allows Kaps (*Crm1p* in *S. pombe*) (Kudo et al., 1999) recognition of nuclear export signal (NES) in their cargoes (la Cour et al., 2004). Once this trimeric complex has crossed the NPC and reached the cytoplasmic side, Ran-GAP hydrolyzes RanGTP to RanGDP, which produces a conformational change in the Kap that releases the cargo. Then, RanGDP makes the return trip to the nucleus by nuclear transport factor-2 (NTF2, *Cse1p* in *S. pombe*) (Chen et al., 2004; Ribbeck et al., 1998), where it is recycled back to RanGTP by the Ran guanine nucleotide exchange factor (Ran-GEF, *Hs*RCC1/*Sc*Prp12/*Sp*Pim1) (Cook et al., 2007; Sorokin et al., 2007; Stewart, 2019; Tetenbaum-Novatt and Rout, 2010; Yoshida and Sazer, 2004).

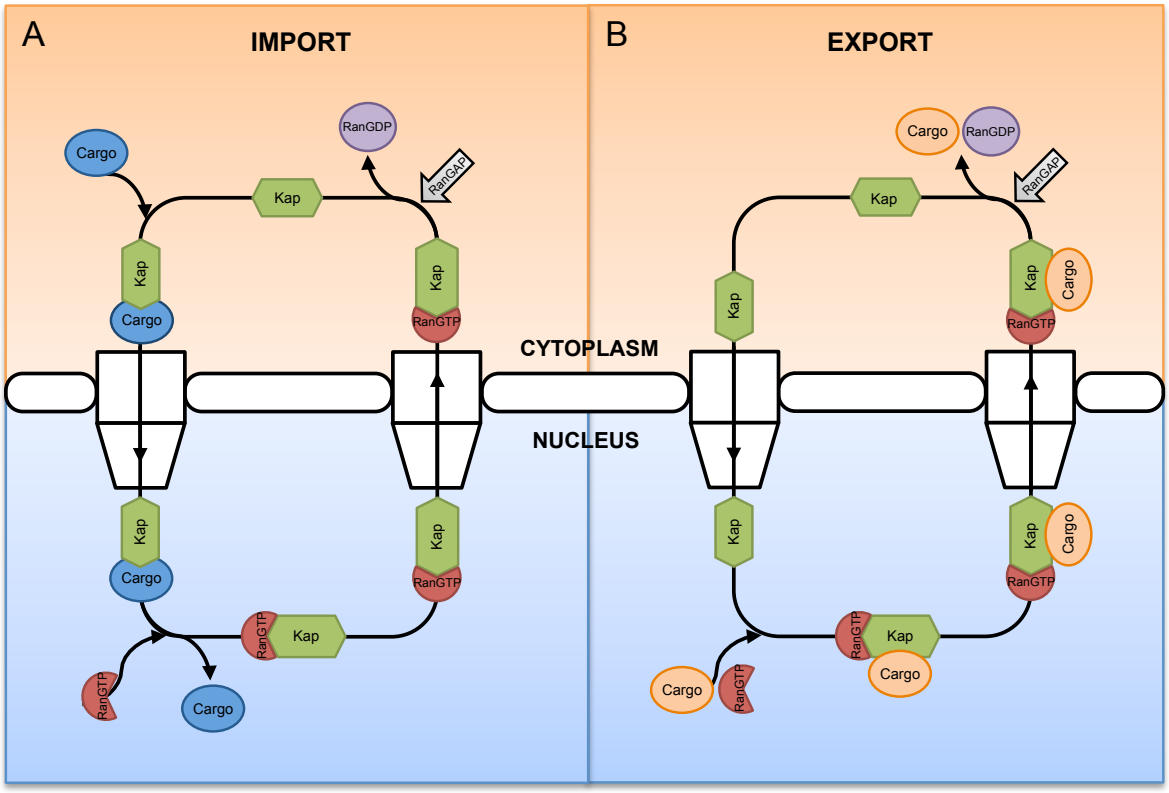

Figure I2. Schematic of the Ran-dependent nucleo-cytoplasmic transport of proteins. (A) Nuclear import. Protein cargoes (blue) containing a NLS are imported by karyopherins (importins, green) into the nucleus, where RanGTP (red) binds to karyopherins and promotes cargo release. Then, RanGTP-bound karyopherins return into the cytoplasm being recycled by Ran-GAP (grey), which transform RanGTP into RanGDP (purple). (B) Nuclear export. NES-containing proteins (orange) associate in the nucleus to RanGTP-bound karyopherins (exportins), which mediate their export to the cytoplasm. There, Ran-GAP releases RanGTP and cargoes from karyopherins, which return into the nucleoplasm. See text for further information. (Adapted from Sloan et al., 2016; Stewart, 2019)

Different nucleoporins display especific functions during nucleo-cytoplasmic transport of proteins (reviewed in Walde and Kehlenbach, 2010). Regarding the roles of the nuclear basket in nucleo-cytoplasmic trafficking, both vertebrate Nup50/Npap60 and its *S. cerevisiae* homolog Nup2 are mobile nucleoporins that shuttle between the cytoplasmic and the nucleoplasmic sides of the NPC to escort the cargoes (Denning et al., 2001; Dilworth et al., 2005; Lindsay et al., 2002; Makise et al., 2012). In vertebrates, Nup50 simultaneously interacts with both importin β and its adaptor importin α to increase their affinity, enhancing the nuclear import of NLS-containing cargoes. A similar function has been described for budding yeast Nup2, which associated with importin β and α (Kap95 and Kap60, respectively). This interaction would increase the targeting of cargoes to the NPC and their translocation through the central channel. Nup2 also form a multiprotein complex with Nup60, Kap60, Kap95, Ran-GEF, and RanGTP, which stimulates the release of Kap60 protein cargoes (Denning et al., 2001; Gilchrist et al., 2002). Besides, budding yeast Nup1 regulates the accumulation of certain Kaps and RanGTP at the nucleoplasmic side of the NPCs and stimulates importin β-dependent translocation (Liu and Stewart, 2005; Pyhtila and Rexach, 2003). On the other hand, the nuclear basket TPR participates in nucleo-cytoplasmic transport as well, acting as a binding site for both karyopherin CRM1, during the export of CRM1-containing complexes, and importin-β, during the import of cargoes and the recycling of cargo-free importin β (Ben-Efraim et al., 2009; Frosst et al., 2002).

Chromatin-dependent nuclear organization

Chromosome painting and high resolution Hi-C studies have demonstrated that, from yeast to humans, chromosomes are not randomly distributed at the nuclear interior, but genomes are organized in distinct genomic foci or chromosome territories (Mizuguchi et al., 2015; Scherthan et al., 1994; Zimmer and Fabre, 2011). The nuclear periphery, through inner nuclear membrane (INM) proteins and the NPCs, plays a pivotal role in the chromatin-dependent nuclear organization. Chromosome organization is key for the regulation of nuclear processes, such as gene expression, DNA replication or genome stability; and, in turn, chromatin state influences the spatial arrangement of the genome (Lemaitre and Bickmore, 2015; Ptak and Wozniak, 2016; Sun et al., 2019; Zuleger et al., 2011)

• Chromatin domains

Eukaryotic genomes are organized into a complex structure known as chromatin. The basic unit of chromatin is the nucleosome, which is made up of a histone octamer (formed by two copies each of the histone proteins H2A, H2B, H3 and H4) and 146 base pairs (bps) of genomic DNA coiled around it (Luger et al., 1997). Histones are subjected to a wide range of post-translational modifications, which regulates DNA packaging and accessibility of transcription factors to chromatin. Covalent modifications of histones are read and interpreted by the cellular machinery to establish functional

chromatin domains, namely euchromatin and heterochromatin (Cam and Grewal, 2004; Woolcock and Buhler, 2013). Euchromatin domains are low condensed, gene-rich and usually transcriptionally active. Heterochromatin domains are highly condensed, gene-poor and transcriptionally repressed (Allshire and Ekwall, 2015; Cam and Whitehall, 2016; Huisinga et al., 2006). Heterochromatin and euchromatin domains are isolated by boundary elements, or insulators, which define the limits between them and shield functional chromatin domains from the surrounding environment (Barkess and West, 2012). The recruitment of factors to these chromatin boundaries precludes the inappropriate spreading of heterochromatin, while promotes the interaction between different regions of the genome, establishing chromosome spatial domains (Cam and Grewal, 2004; Iwasaki and Noma, 2012; Mizuguchi et al., 2015; Tanizawa et al., 2010).

Fission yeast genome is formed by three chromosomes, each one containing two major heterochromatin regions: centromeres and telomeres (Fig. I3 A). Besides, heterochromatin can be found in other genomic loci, such as the mating-type locus located at Chromosome II; the ribosomal DNA (rDNA), a ~500–1000 kb tandem array located at both ends of chromosome III containing the ribosomal genes; and chromosome-organizing clamps (COCs), sites scatered across the genome that are binding sites of the transcription factor TFIIIC (Allshire and Ekwall, 2015; Cam and Whitehall, 2016; Noma et al., 2006). All heterochromatin domains at centromere, telomere and mating-type locus share an essential internal structure, containing a high density of repetitive sequences (full or parts of *dg* and *dh* repeats in fission yeast), recognition targets of the RNAi (RNA interference) heterochromatin machinery, responsible for their transcriptionally silenced state (Cam et al., 2005; Grewal and Moazed, 2003; Volpe and Martienssen, 2011).

Centromeric structure of *S. pombe* resembles those of higher eukaryotic organisms. They range from 35 to 110 kb in length and are formed by a centromere core domain (*cnt*) surrounded by pericentromeric heterochromatin. Each central core is ~11-15 kb long and is defined by the histone variant CENP-A/Cnp1. They are flanked by ~12-20 kb domains of pericentromeric heterochromatin, which comprises the innermost repeats (*imr*), specific of each chromosome, and the outermost repeats (*otr*), composed of *dg* and *dh* repetitive elements, whose arrangement differs between chromosomes (Fig. I3 A). Centromeric insulators are tRNAs (transference RNAs) and IRs (inverted repeats) (Appelgren et al., 2003; Cam et al., 2005; Kniola et al., 2001; Partridge et al., 2000; Pidoux and Allshire, 2004; Volpe and Martienssen, 2011). Fission yeast telomeres contain three subdomains: a 3'-single stranded GT-rich overhang (G-tail), a specific GT-rich repetitive DNA duplex and the subtelomeric region (Mandell et al., 2005; Paeschke et al., 2010). Maintenance of telomere integrity and homeostasis are intrinsically linked to the binding of chromatin remodellers at insulators located at subtelomeric borders (Stralfors et al., 2011), to its heterochromatin features (Moser and Nakamura, 2009), and to the protection by different telomere-associated proteins, such as Rif1 (Dan et al., 2014; Kanoh and Ishikawa, 2001), or shelterins Ccp1 and Taz1 (Buhler and Gasser, 2009; Kanoh et al., 2005; Moser and Nakamura, 2009; van Emden et al., 2019).

- **Heterochromatin regulation**

In fission yeast the RNAi machinery is the main responsible for the initiation and maintenance of centromeric heterochromatin. The process of heterochromatin assembly can be divided in three steps: establishment, spreading and maintenance (Fig. I3 B) (Martienssen and Moazed, 2015; Moazed et al., 2006; Verdel and Moazed, 2005; Zofall and Grewal, 2006). In general terms, establishment of heterochromatin regions depends on the DNA repetitive sequences and the epigenetic marks on histones, usually characterized by hypoacetylation and hypermethylation (Cam et al., 2005; Chen et al., 2008; Nakayama et al., 2001; Yamada et al., 2005). This imprinting determines the DNA nucleation sites by recruiting the RNAi machinery, consisting of three main players: the RNA-dependent RNA polymerase Rdp1, the RNase III enzyme Dicer (Dcr1) and the small RNA-binding protein Argonaute (Ago1) (Cam and Grewal, 2004; Noma et al., 2004). Pericentromeric repeated sequences are transcribed bidirectionally by the RNA polymerase II (RNAPol II) into long non-coding RNAs, which are loaded into RITS (RNA-induced initiation of transcriptional silencing) complex through Ago1. RITS recruits the RNA polymerase Rdp1, responsible for RNA amplification and double stranded RNA (dsRNA) formation. dsRNA are cleaved by Dcr1 into small interfering RNAs (siRNAs). These siRNAs are incorporated into RITS, which recruits the the Clr4-containing complex (CLRC), responsible for H3K9 methylation, to complementary DNA regions, initiating a positive feedback loop (Moazed et al., 2006; Motamedi et al., 2004; Noma et al., 2004; Sugiyama et al., 2005; Verdel and Moazed, 2005; Zhang et al., 2008; Zofall and Grewal, 2006). H3K9-methylation epigenetic mark constitutes a binding site for chromodomain-containing proteins, such as HP1 homologs Swi6 and Chp2, and Chp1, which mediate the spreading from initial nucleation sites to nearby sequences (Fischer et al., 2009; Maksimov et al., 2018; Nakayama et al., 2001; Thon and Verhein-Hansen, 2000). Then, heterochromatin spreads in cis until the RNAi machinery finds a boundary element that hinders its extension. One of the best-known boundary factors is Epe1, which restricts heterochromatin spreading beyond boundaries by interacting with Swi6 (Isaac et al., 2007; Zofall and Grewal, 2006). Silencing of heterochromatin RNAs requires RNAi-dependent and RNAi-independent mechanisms (Buhler et al., 2007; Reyes-Turcu and Grewal, 2012). Chp1 anchoring to H3K9-me2 recruits RITS complex to chromatin to mediate the degradation of heterochromatic transcripts by a mechanism termed cotranscriptional gene silencing (CTGS) (Moazed et al., 2006; Verdel et al., 2004). On the other hand, Swi6 and Chp2 create a platform for recruiting the TRAMP (Trf4/Air2/Mtr4p Polyadenylation) complex, which targets RNAs for exosome-dependent degradation, and the SHREC complex (Snf2/Hdac Repressive Complex), an effector complex for heterochromatic transcriptional silencing that contains the histone deacetylase (HDAC) Clr3. This way, Swi6 and Chp2 constribute to restricting RNA Pol II occupancy and shutting off transcription, by a mechanism termed transcriptional gene silencing (TGS) (Fischer et al., 2009; Keller et al., 2012; Maksimov et al., 2018; Noma et al., 2004; Sugiyama et al., 2007; Thon and Verhein-Hansen, 2000; Volpe et al., 2002; Yamada et al., 2005).

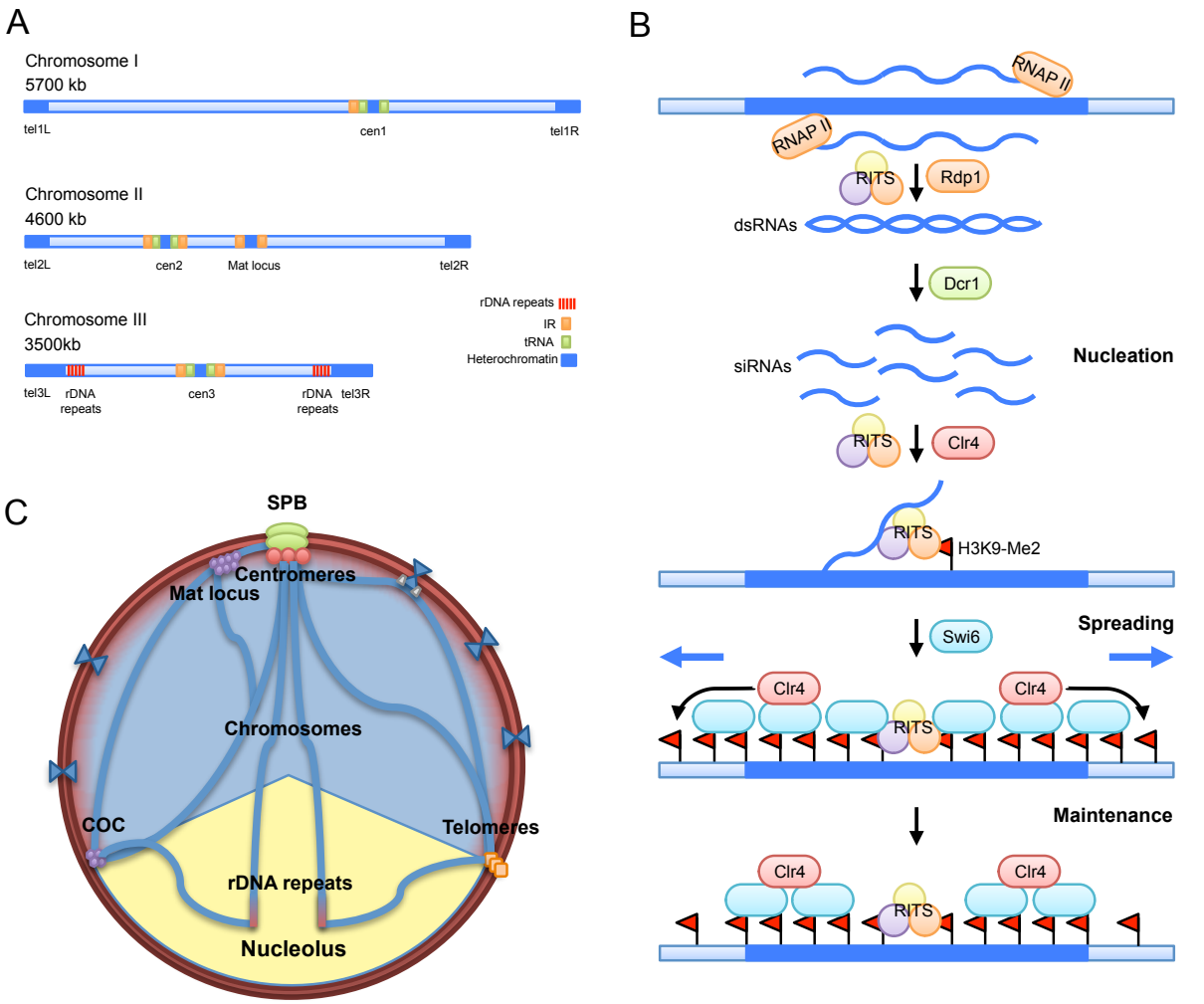

Figure I3. Chromosome domains and nuclear organization of fission yeast genome. (A) Representation of the three *S. pombe* chromosomes, Chromosome I (5,7 Mb), Chromosome II (4,6 Mb), and Chromosome III (3,5 Mb). Each chromosome contains heterochromatin regions (dark blue) at centromeres and telomeres, besides the mating-type locus located in Chromosome II. Centromeres range in size from 35 to 100 kb and are organized in a central core domain (cnt), site of kinetochore assembly, surrounded by the pericentromeric domains, innermost repeats (imr) and outermost repeats (otr), which are isolated by tRNAs (orange) and inverted repeats (IRs, green), boundary elements that prevents heterochromatin spreading. rDNA is located at both arms of Chromosome III. (B) Model of RNAi-dependent heterochromatin formation in fission yeast. RNA polymerase II (RNAP II) transcribes heterochromatin repetitive sequences in long non-coding RNAs (blue line), which are loaded into RITS through Ago1, transformed into dsRNAs (double stranded RNAs) by Rdp1, and cleaved into siRNAs (small interfering RNAs) by Dcr1. siRNAs are incorporated into RITS, which is targeted to nascent RNAs for amplification or to complementary DNA sequence regions for the recruitment of heterochromatin assembly factors, such as the methyltransferase Clr4. Clr4 methylates H3K9, acting as a signal for Swi6 binding. Swi6 spreads to adjacent sequences until it finds a boundary element and silences heterochromatin formation by recruiting boundary factors, such as Epe1, and by promoting the activity TRAMP (Trf4/Air2/Mtr4p Polyadenylation) and SHREC (Snf2/Hdac Repressive Complex) complexes (See text for further details). (Adapted from Cam and Grewal, 2004). (C) Cartoon of nuclear organization in fission yeast during interphase. Heterochromatin domains are anchored to the NE (red). Centromeres (red circles) are clustered and attached to the SPB (green circles); while telomeres occupy an opposite localization at the nuclear periphery, closer to the nucleolus, anchored to the NE forming a bouquet through interaction between telomere binding proteins and INM proteins (orange). The mating type locus (purple) localizes at the vicinity of the SPB. rDNA, at the ends of Chromosome III, is confined at the nucleolus (yellow), opposite to the SPB, which represents roughly one third of the nuclear volume. Other DNA elements scattered along chromosomes, such as chromosome organizing clamps (COCs), retrotransposons, or tRNAs, tether to the nuclear periphery and contribute to chromosome organization. Actively transcribed genes can be found in the proximity of the NPCs, which favors mRNA export, although the interaction of the NPC with transcriptionally silenced domains further contributes to chromatin regulation (see text for details). (Zimmer and Fabre, 2011; Mizuguchi et al., 2015; Matsuda et al., 2017).

Although less is known about heterochromatin regulation in telomeres, the presence of heterochromatin factors into these regions suggests that they share common and additional heterochromatin assembly mechanisms (Nakayama et al., 2001; Shankaranarayana et al., 2003; Thon and Verhein-Hansen, 2000; Verdel and Moazed, 2005). For example, apart from the RNAi machinery, SHREC, Ccq1 and Taz1 also contribute to heterochromatin formation in telomeres (Kanoh et al., 2005; Sugiyama et al., 2007; van Emden et al., 2019). Similarly, heterochromatin assembly in the mating-type locus depends on two pathways, the RNAi machinery (Hall et al., 2002) and DNA-binding of specific proteins, such as histone deacetylases or stress-activated ATF/CREB family proteins (Atf1 and Pcr1) (Jia et al., 2004; Yamada et al., 2005).

- **The nuclear periphery in nuclear organization**

It has long been described that heterochromatin domains associate to the nuclear periphery, while euchromatin or transcribed genes occupy more interior position inside the nucleus. However, recent works have illustrated that this picture is not so simple. The nuclear periphery plays a critical role in anchoring both active and repressed domains, being differentially regulated depending on the environment where they are located (Fig. I3 C) (Akhtar and Gasser, 2007; Mekhail and Moazed, 2010; Tanizawa et al., 2010). Anchoring of heterochromatin domains to the free-pore regions of the NE by INM proteins contributes to higher-order nuclear organization. Of note, certain domains that share similar functional features are clustered, and can be visualized in nuclear foci (Alfredsson-Timmins et al., 2007; Iwasaki and Noma, 2012; Noma, 2017; Woolcock and Buhler, 2013). For example, during interphase centromeres are clustered at the SPBs, the mating-type region is close to centromeres, and telomeres are attached to the opposite site of the nucleus, near the nucleolus, through the interaction between telomere-binding proteins and INM proteins, forming a bouquet (Fig. I3 C). This chromosomal arrangement is named Rabl conformation (Chikashige et al., 1997; Funabiki et al., 1993; Matsuda et al., 2017; Mizuguchi et al., 2015).

Several studies point to a conserved funtion of nucleoporins in chromatin regulation and nuclear organization (Kuhn and Capelson, 2019; Ptak and Wozniak, 2016; Sun et al., 2019). The nuclear basket contributes to chromatin organization by delimiting heterochromatin free zones under the NPC to ensure the accessibility for nucleo-cytoplasmic trafficking (Iglesias et al., 2020; Krull et al., 2010; Kylberg et al., 2010; Niepel et al., 2013), or by interacting with chromatin insulators (Kalverda and Fornerod, 2010; Woolcock et al., 2012). For example, *Sc*Nup2 prevents heterochromatin spreading into euchromatin regions by association with boundary elements (Dilworth et al., 2005; Ishii et al., 2002). A recent study in fission yeast has stablished that the inner nucleoporin Npp106 (*Sc*Nic96 and *Hs*Nup93) and the nuclear basket TPR Nup211, among other nucleoporins, are associated to heterochromatin domains, but not to euchromatin regions. Consistently, Npp106 is involved in heterochromatin silencing, peripheral clustering and epigenetic inheritance (Iglesias et al., 2020). Interestingly, the RNAi machinery component Dcr1, the RNase III enzyme involved in the processing of double-stranded RNAs into small interfering RNAs, is enriched at the nuclear periphery in a NPC-

dependent manner and its delocalization leads to defects in heterochromatin assembly (Emmerth et al., 2010). Budding yeast nucleoporin Nup107 is also involved in chromatin silencing and telomere anchoring to the nuclear periphery (Lapetina et al., 2017; Van de Vosse et al., 2013). Besides, inducible genes associate to the nuclear basket to positively and negatively regulate transcription (see Transcriptional regulation; Brickner et al., 2019; Burns and Wente, 2014; Randise-Hinchliff and Brickner, 2016; Sood and Brickner, 2014). The environment created by heterochromatin inhibits gene expression, but also takes part in other key cellular processes, like DNA repair and recombination, chromosome stability and segregation, or maintenance of kinetochore structure (Allshire et al., 1995; Cam et al., 2005; Hall et al., 2003; Pidoux and Allshire, 2004; Ptak and Wozniak, 2016).

SAC regulation and chromosome segregation

Fission yeast undergoes a closed mitosis in which the NE does not break down, and just concomitant with mitotic entry, duplicated SPBs are inserted into the nuclear envelope surface. Then, kinetochores, multiprotein structures assembled on centromeres that constitute the linkage between the chromosomes and the spindle microtubules, are released from the SPBs (Musacchio and Hardwick, 2002; Musacchio and Salmon, 2007). At this point, kinetochores can be observed as multiple and independent foci, while nuclear microtubules nucleated by SPBs immediately after their NE insertion start to establish contacts with kinetochores. The close proximity between clustered kinetochores and SPBs during interphase facilitates their rapid capture by mitotic spindle microtubules at the beginning of mitosis to drive chromosome segregation to daughter cells (Funabiki et al., 1993; Gachet et al., 2008; Hou et al., 2012; Mekhail and Moazed, 2010). Faithful chromosome segregation is of extreme importance for the transmission of the genetic information and, thus, cells possess control mechanisms (Cheeseman, 2014; Santaguida and Musacchio, 2009).

• Spatio-temporal regulation of SAC

The Spindle Assembly Checkpoint (SAC), composed of Mad1, Mad2, Mad3 (BubR1), Bub1, Bub3 and Mph1 (Mps1) in *S. pombe,* is the surveillance mechanism that detects erroneous kinetochore-microtubule attachments and halts mitotic progression until all kinetochores are properly attached by microtubules of the mitotic spindle, preventing thus chromosome missegregation. During interphase, SAC components Mad1 and Mad2 localize to the nuclear periphery, docked to the nuclear basket, whereas in mitosis both Mad1 and Mad2 relocate to kinetochores, where they are essential for SAC activation (Fig. I4). The recruitment of the SAC machinery to kinetochores at the mitotic onset initiates a response that inhibit the anaphase-promoting complex APC/cyclosome (APC/C) by sequestering its co-factor Cdc20 (*Sp*Slp1) in the Mitotic Checkpoint Complex (MCC), formed by Mad2, BubR1, Bub3, and Cdc20. At the metaphase-anaphase transition, once kinetochores have been properly captured, MCC inhibition ceases and Cdc20 is released, promoting the APC/C-mediated polyubiquitynation of mitotic proteins, which are degraded by the 26S proteasome (see The ubiquitin-proteasome system

for further information). The targets of the ubiquitin ligase APC/C include two key anaphase substrates, cyclin B and securin (an inhibitor of the protease separase). Their degradation results in lowering CDK1 activity, leading to mitotic exit, and the activation of separase, which in turn cleaves cohesins, leading to sister chromatids separation (Fig. I4) (Corbett, 2017; Kops and Shah, 2012; Lara-Gonzalez et al., 2012; Musacchio and Desai, 2017; Musacchio and Salmon, 2007; Silva et al., 2011).

One of the conserved functions of TPR nucleoporins is the spatio-temporal regulation of the SAC components Mad1 and Mad2 (Fig. I4). During interphase Mad1 and Mad2 are docked to the nuclear basket TPRs (De Souza et al., 2009; Ding et al., 2012; Lee et al., 2008b; Rajanala et al., 2014; Salas-Pino et al., 2017; Schweizer et al., 2013; Scott et al., 2005). Upon entry into mitosis, phosphorylation of TPR triggers the release of Mad1/Mad2, which travel from the nuclear periphery to kinetochores (Cunha-Silva et al., 2020; Rajanala et al., 2014). Nuclear basket anchoring of these SAC components during interphase is important for the formation and signaling of the MCC, to ensure the inhibition of the APC/C prior to mitosis and the delay of the anaphase onset (Lee et al., 2008b; Rodriguez-Bravo et al., 2014). Moreover, it has been described that TPR-dependent localization of Mad1/Mad2 regulates SAC proteostasis (Schweizer et al., 2013). Accordingly, lack of TPR results in detachment of SAC components from the NPC, which leads to defective SAC regulation and, consequently, to genome instability.

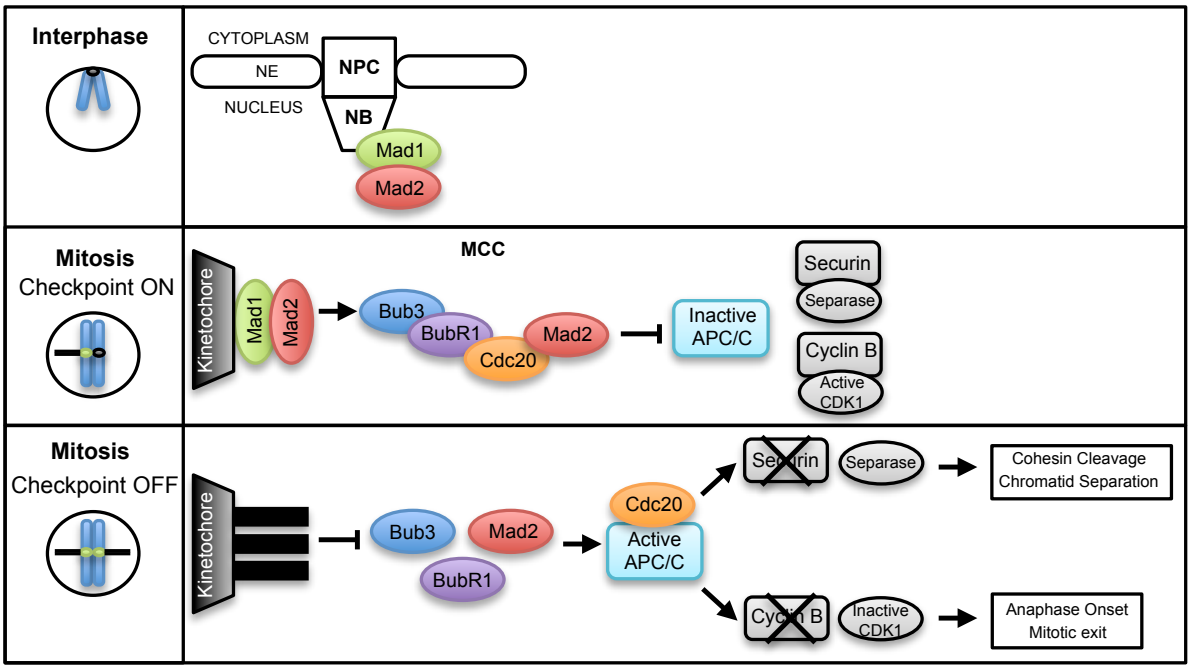

Figure I4. Simplified scheme of SAC regulation. The Spindle Assembly Checkpoint ensures chromosome segregation by monitoring proper kinetochore-microtubule attachment during mitosis. During interphase Mad1/Mad2 are anchored to the Nuclear Basket (NB) of Nuclear Pore Complex (NPC). At mitosic onset Mad1/Mad2 are released and bind to kinetochores. At this stage, in the presence of unattached kinetochores, the SAC is turned on and the MCC (Mad2, Bub1, BubR1/Mad3 and Cdc20) sequesters Cdc20 and inhibits the APC/C to halt mitotic progression. When all chromosomes have been properly captured by the spindle microtubules, the SAC is turned off, Cdc20 is released and the APC/C is activated. This triggers the APC/C-dependent ubiquitination and proteasome-dependent degradation of securin, which leads to separase activation (resulting in chromatid separation), and cyclin B, which leads to CDK1 inactivation (resulting in anaphase onset and mitotic exit). (Adapted from Silva et al., 2011)

• Kinetochores

Kinetochores are multiprotein structures assembled on the central core domain of centromeres required for the interaction between chromosomes and spindle microtubules during mitosis (Fig. I5) (reviewed in Cheeseman and Desai, 2008; Musacchio and Desai, 2017; Santaguida and Musacchio, 2009). Composition, structural modularity and functions of the kinetochores show a high degree of conservation among species (Roy et al., 2013; Santaguida and Musacchio, 2009; Westermann and Schleiffer, 2013; Yamagishi et al., 2014). Several studies have contributed to define the principles that govern kinetochore assembly (Hinshaw and Harrison, 2018; Perpelescu and Fukagawa, 2011). Kinetochores are composed of an inner layer that directly binds to the centromeric chromatin, known as CCAN (constitutive centromere-associated network; Hara and Fukagawa, 2017; McAinsh and Meraldi, 2011), and an outer layer that constitutes the attachment site for microtubules, also known as KMN (KNL-1/Mis12 complex/Ndc80 complex network; Santaguida and Musacchio, 2009; Varma and Salmon, 2012). The following section will provide a brief description of kinetochore structure and composition.

- **Kinetochore structure**

Inner kinetochore

- CENP-A/*Sp*Cnp1/*Sc*Cse4. At the central core domain of centromeres the histone H3 is replaced by the histone variant CENP-A, Cnp1 in fission yeast (Catania et al., 2015; Earnshaw et al., 2013; Stoler et al., 1995; Sullivan et al., 1994). CENP-A/Cnp1 is considered the epigenetic mark that defines centromere identity, since the kinetochore is assembled over this Cnp1-defined region (Catania and Allshire, 2014; Logsdon et al., 2015; Meluh et al., 1998; Palmer et al., 1987). Its deposition occurs through multiple pathways, which involve heterochromatin factors (Folco et al., 2008; Roy and Sanyal, 2011), the chaperone Scm3 (Pidoux et al., 2009; Williams et al., 2009) and other inner kinetochore components, such as Cnp3, Cnp20 and Mis6 complex (Hayashi et al., 2004; Hori et al., 2013; Okada et al., 2006; Suma et al., 2018; Takahashi et al., 2000). In *S. pombe*, Cnp1 is incorporated in a cell cycle-dependent manner (by the GATA factor Ams2 and the histone cell cycle regulator HIRA homolog Hip1, during S and G2 phases, respectively) (Takahashi et al., 2005; Takayama et al., 2008). In addition, its loading and distribution is tightly regulated by ubiquitin-mediated proteolysis in several eukaryotes (Collins et al., 2004; Kitagawa et al., 2014; Moreno-Moreno et al., 2006; Ranjitkar et al., 2010).

- CENP-S-T-W-X complex. CENP-S-T-W-X (Mhf1, Cnp20, New1/Wis1, and Mhf2 in fission yeast; Fig. I5) is a non-canonical nucleosome-like complex formed by two heterodimers, CENP-TW and CENP-SX (Takeuchi et al., 2014). This complex directly interacts with centromeric DNA and contributes to the stablishment of centromeric chromatin structure. Moreover, CENP-T acts as a linker between CENP-A and the outer kinetochore. The absence of any of the elements of this complex results in defective kinetochore structure and leads to chromosome

missegregation (Amano et al., 2009; Folco et al., 2015; Gascoigne et al., 2011; Hori et al., 2008; Huis In 't Veld et al., 2016; Nishino et al., 2013; Rago et al., 2015; Schleiffer et al., 2012; Takeuchi et al., 2014).

- **CENP-C/*Sc*Mif2/*Sp*Cnp3.** This protein directly associates to CENP-A/Cnp1-containing chromatin through its C-terminal domain (Carroll et al., 2010; Kato et al., 2013; Sugimoto et al., 1997; Trazzi et al., 2009). CENP-C also contributes to the docking of outer kinetochore components of the KMN network through its N-terminal domain (Gascoigne et al., 2011; Klare et al., 2015; Milks et al., 2009; Przewloka et al., 2011; Rago et al., 2015; Screpanti et al., 2011). Moreover, several inner kinetochore components, including CENP-L/Fta1, CENP-K/Sim4, or the monopolin complex (Pcs1-Mde4), are loaded in a CENP-C-dependent manner (Fig. I5) (Carroll et al., 2010; Corbett et al., 2010; Liu et al., 2005; Tanaka et al., 2009). Therefore, CENP-C/Cnp3 has been defined as the structural platform for kinetochore assembly (Klare et al., 2015; Przewloka et al., 2011; Tanaka et al., 2009).

- **CENP-HIK/ Mis6-Sim4-Mal2 complex**. Composed of 12 different subunits, including Sim4, Mal2 and several Fta and Mis proteins, this complex participates in the maintenance of chromatin and kinetochore structure (Kerres et al., 2006; Liu et al., 2005; Okada et al., 2006; Pidoux et al., 2003; Shiroiwa et al., 2011). Its incorporation depends on several kinetochore components, including Cnp1, Cnp20 and Cnp3 (Basilico et al., 2014; Carroll et al., 2010; Milks et al., 2009; Tanaka et al., 2009), and the Mis16-18-19 complex (Hirai et al., 2014). This complex also interacts with the outer kinetochore components Knl1 and DASH complex (Cheeseman and Desai, 2008; Kerres et al., 2006; Liu et al., 2005).

- ***Sp*Mis16-Mis18-Mis19-Mis20 complex**. This complex is part of the CENP-A recruitment pathway and interacts with outer kinetochore factors. Contrary to the vast majority of kinetochore components, Mis16 complex only localizes at kinetochore during interphase, but not in mitosis (Hayashi et al., 2014; Hayashi et al., 2004; Hirai et al., 2014; Kornter-Vetter et al., 2019; Liu et al., 2005; Subramanian et al., 2014).

Outer kinetochore

- **NMS complex**: It is composed of Ndc80 complex, MIND/Mis12 complex and Spc7/Spc105 complex (so it has been termed NMS complex, Fig. I5), with a 1:1:1 stoichiometry. NMS complex establishes multiple internal and external contacts, highlighting a hierarchical and co-dependent assembly, essential for proper kinetochore structure and functions. In general terms, Mis12 and Ndc80 complexes mediate KMN assembly and interaction with the inner kinetochore, Knl1 subunit represents the docking site for the SAC machinery, and Ndc80 complex is the microtubule receptor (Cheeseman et al., 2006; Cheeseman and Desai, 2008; Liu et al., 2005; McCleland et al., 2003; Roy et al., 2013; Takeuchi and Fukagawa, 2012).

- **DASH/Dam1 complex**: This complex represent the most external part of the kinetochore,

which forms a ring structure that accommodates around the microtubule during mitosis (Buttrick and Millar, 2011). It is one of the most dissimilar complexes of the kinetochore. Dam1 complex assembly depends on Cse4 and NMS complex in budding yeast (Cheeseman et al., 2001; Collins et al., 2005; Enquist-Newman et al., 2001; Hofmann et al., 1998) and on its own components and Mis6 complex in fission yeast (Liu et al., 2005; Sanchez-Perez et al., 2005). While the DAM complex is essential for cell viability in the budding yeast, it is not in *S. pombe*. Importantly, in yeasts only localizes at kinetochores during mitosis (Enquist-Newman et al., 2001; Hofmann et al., 1998; Li et al., 2002; Liu et al., 2005; Sanchez-Perez et al., 2005).

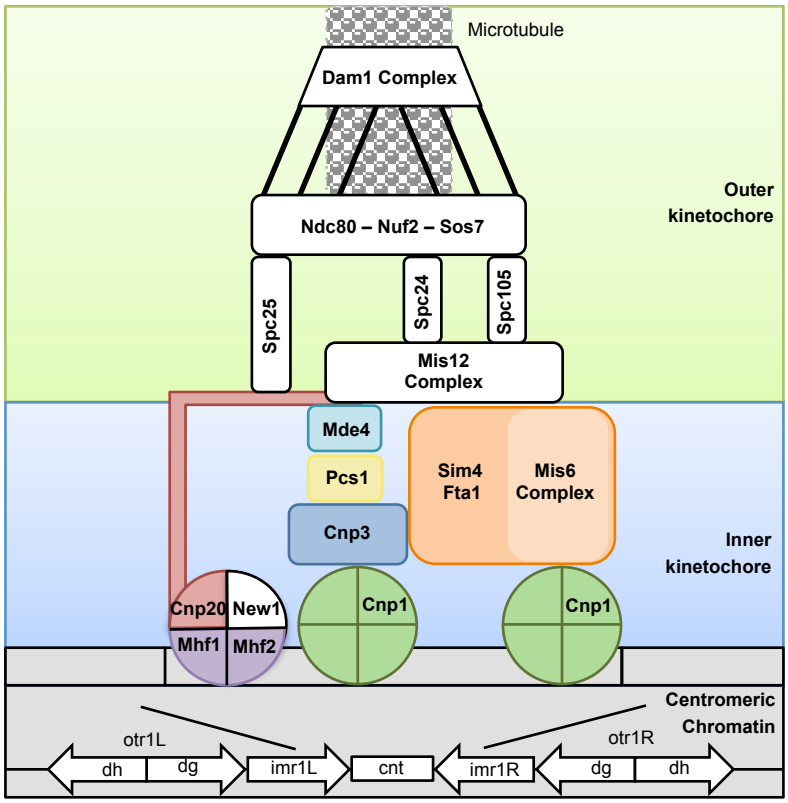

Figure I5. Simplified scheme of kinetochore structure and composition in *S. pombe*. Kinetochores are assembled at central core region (*cnt*) of centromeres (grey). Kinetochore structure can be divided in two subdomains. The inner kinetochore (squared in blue) is associated to the centromeric chromatin, and comprises the histone Cnp1 (CENPA, green), the non-canonical nucleosome components (Mhf1, Mhf2, Cnp20 and New1), Cnp3, the Mis6-Sim4-Mal2 complex, and the monopolin complex (Pcs1 and Mde4). The outer kinetochore (squared in green) comprises the Ndc80, Mis12 and Spc105-Spc7 (NMS) complexes, which links to the inner kinetochore and interacts with microtubules, and the Dam1/DASH complex, which constitutes the microtubule-binding ring during mitosis. (Adapted from Roy et al., 2013; Yamagishi et al., 2014)

- **Kinetochore functions during the cell cycle**

Albeit the high conservation between yeast and metazoan kinetochores, comparisons between organisms has highlighted that their assembly, composition and dynamics are influenced by their cell-cycle specific characteristics (Chan et al., 2005; Nagpal and Fukagawa, 2016). In *S. cerevisiae* SPBs are embedded in the NE throughout the cell cycle, and kinetochore are continuously assembled and tethered to SPBs by microtubules (except for a brief period of time during S phase for DNA replication) (Kitamura et al., 2007). In metazoans, inner kinetochore components (CCAN) are assembled

constitutively, whereas outer kinetochore components (KMN) dynamically change in a cell-cycle dependent manner (Cheeseman and Desai, 2008; Hori et al., 2008; Musacchio and Desai, 2017). In interphase metazoan cells, microtubule-organizing centres (MTOCs) are located outside the NE and centromeres are dispersed within the nucleus. During mitosis, the NE breaks down, allowing kinetochore-microtubule interactions (Guttinger et al., 2009; Maiato et al., 2004).

In *S. pombe* an intermediate situation has been observed: most inner kinetochore components are constitutive, and DASH complex and motor proteins are recruited transiently at mitosis onset (Liu et al., 2005; Sanchez-Perez et al., 2005). Noteworthy, in fission yeast SUN-KASH (also called LINC complex for linker of nucleoskeleton and cytoskeleton) links interphase kinetochores to the SPBs, which are attached to the cytoplasmic side of NE (De Souza and Osmani, 2007; Hou et al., 2012; Jaspersen and Ghosh, 2012; Kim et al., 2015; Tapley and Starr, 2013). The linkage between the kinetochores and SPBs is mediated by the interaction of Csi1 and the SUN protein Sad1 with centromere-assembled kinetochores (Ding et al., 1997; Hou et al., 2012; King et al., 2008). Therefore, proper kinetochore structure is required for clustering and tethering of centromeres to the SPB during interphase (Funabiki et al., 1993; Hou et al., 2012) and influences heterochromatin formation (Allshire and Ekwall, 2015).

Apart from microtubule interaction, kinetochores perform additional key functions during both mitotic and meiotic cell cycles (reviewed Cleveland et al., 2003; McCleland et al., 2003; Santaguida and Musacchio, 2009). During mitosis, the KMN complex is key for monitoring proper kinetochore-microtubules attachment by the recruitment of the SAC machinery (Varma and Salmon, 2012). *S. pombe* NMS complex, which is constitutively assembled at the outer kinetochore during the mitotic cell cycle, dissociates during meiotic prophase I and is reassembled before metaphase I. This leads to the detachment of centromeres from the SPB and the attachment of telomeres to the SPB (Chikashige et al., 1997; Hayashi et al., 2006). Intriguingly, the Y-subcomplex component Nup132 is required for avoiding the precocious assembly of the KMN complex during prophase I, which would lead to chromosome segregation defects during meiosis (Yang et al., 2015).

The ubiquitin-proteasome system

The ubiquitin-proteasome system (UPS) is the main degradation pathway responsible for protein homeostasis by removal of most short-lived and misfolded proteins in eukaryotes. In growing cells, the proteasome is involved in approximately the 80-90% of protein degradation (Enenkel, 2014; Finley et al., 2012; Ravid and Hochstrasser, 2008). It is also required for quality control of damaged and unnecessary proteins (reviewed in Boban and Foisner, 2016; Nielsen et al., 2014). Proteasome degradation targets include proteins associated to a broad range of cellular processes, including DNA damage (Gumeni et al., 2017), cell-cycle regulation (Foster and Morgan, 2012; Varetti et al., 2011), gene expression (Kwak et al., 2011; Muratani and Tansey, 2003), or stress response (Aiken et al., 2011; Miller et al., 2015). Therefore UPS is key for the regulation of a wide range of cellular processes

(Fig. I6 A). Accordingly, most genes that encode for proteasome subunits are essential for cell viability (Laporte et al., 2008).

Proteins targeted for proteasomal degradation are previously marked by the addition of ubiquitins (Ubs), which requires the concerted action of three enzymes: the ATP-dependent ubiquitin activating enzyme (E1), the ubiquitin conjugating enzymes (E2) and the family of ubiquitin ligases (E3). This process starts with the ATP-dependent covalent binding of ubiquitin to E1, which is subsequently bound to the E2 active site. Then, the ubiquitin is transferred to the target protein substrate through the action of E3, which also primes the addition of more ubiquitins, forming a poly-ubiquitin chain (polyUb). Finally, the proteasome complex recognizes the poly-ubiquitinated target (at least four Ub are required for proteasome recognition), cleaves the polyUb to be recycled, unfolds the protein and degrades it (Fig. I6 B) (Finley et al., 2012; Nandi et al., 2006).

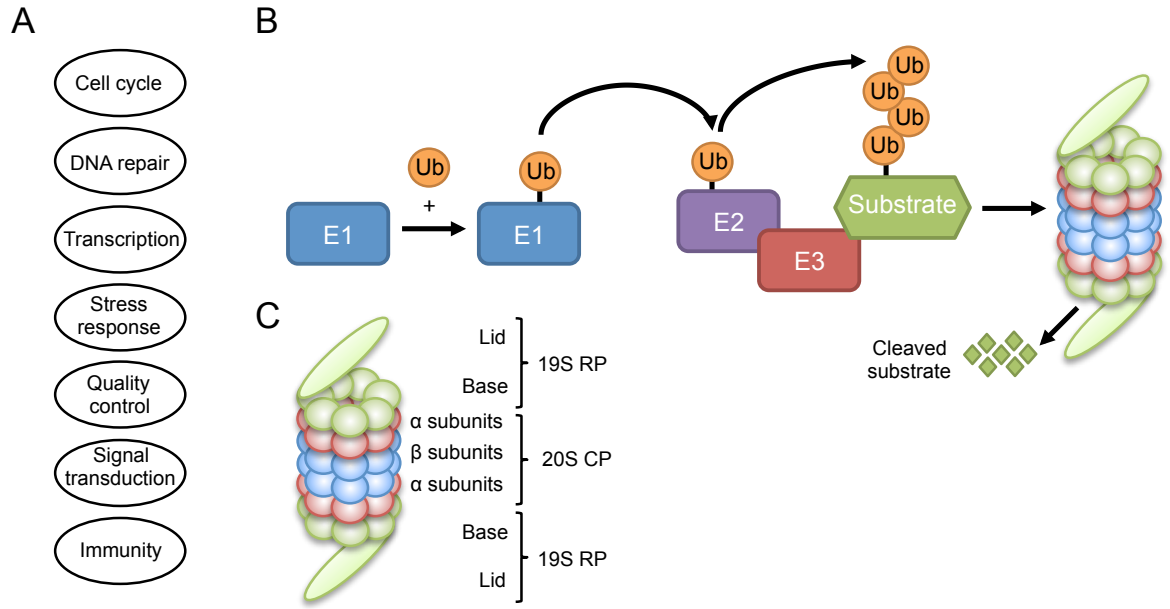

Figure I6. Schematic of ubiquitin-proteasome system. (A) UPS is key for a great number of cellular processes, including cell cycle, DNA repair, transcription, stress response, quality control, signal transduction and immunity. (B) The UPS pathway requires the ATP-dependent ubiquitin activating enzyme (E1, blue), the ubiquitin conjugating enzymes (E2, purple) and the family of ubiquitin ligases (E3, red). A small protein ubiquitin (Ub) is covalently bound to E1, which is subsequently transferred to E2. Then, E3 transfers the ubiquitin to the target substrate (green), which become poly-ubiquitinated. Finally, the poly-ubiquitinated substrate is recognized and cleaved by the proteasome complex. (C) Structure of the proteasome. The proteasome consists of the 20S catalytic particle (CP) and one or two 19S regulatory particles (RP). The CP comprises two inner β-rings (blue) and two outer α-rings (red). The RP (green) is formed by a base and a lid. The lid cleaves the polyUb from poly-ubiquitinated proteins to be recycled, while the base mediates the substrate recognition, unfolding and translocation into the catalytic chamber inside the CP, where the substrate is degraded into oligopeptides. (Adapted from Saeki and Tanaka, 2012; Tomko and Hochstrasser, 2013)

- **Proteasome structure**

Both the composition and the structure of the proteasome are highly conserved among eukaryotes (Dahlmann et al., 1989). The proteasome is a macromolecular complex composed of two modules, the 20S core particle (CP) and the 19S regulatory particle (RP), which confer the catalytic activity and the recognition specificity, respectively (Fig. I6 C). Proteasome exists as a holo-enzyme that is usually constituted by one CP and one or two RPs, forming the 26S proteasome or the 30S proteasome (Coux

et al., 1996; Eytan et al., 1989; Finley, 2009). Even though some recent advances have been made in other organisms, the vast majority of the information regarding the composition of the proteasome and how it is assembled comes from studies in *S. cerevisiae* (reviewed in Saeki and Tanaka, 2012; Sahara et al., 2014; Wehmer and Sakata, 2016).

The 20S core particle contains seven different α subunits and seven distinct β subunits. At the structural level, α and β subunits form four independent heptameric rings, which stack together and conform a cylinder comprising two inner β-rings and two outer α-rings (Fig. I6 C). While the α-rings constitute the gates that allow substrate entry, the β-rings bear the proteolytic activity (Groll et al., 2000; Unno et al., 2002). The RP is the gate of the proteasome and confers the specificity for substrate recognition. The RP is formed by two submodules, the base and the lid. The RP base is constituted by five non-ATPase subunits and six ATPase subunits, which mediate the recognition of the polyUb-bound proteins and the unfolding and translocation of the substrates into the CP, respectively. The RP lid comprises at least nine different non-ATPase subunits that cleave the poly-ubiquitin chains from the substrates, which will be re-used thereafter (Budenholzer et al., 2017; Glickman et al., 1998; Saeki and Tanaka, 2012; Sauer and Baker, 2011; Tomko et al., 2010).

- **Proteasome localization**

Ubiquitin-dependent degradation of proteins has been described to be mainly nuclear, as suggests the localization of many specific substrates, such as cell-cycle regulators or transcription factors (Fig. I6 A) (Bader et al., 2007; Chowdhury and Enenkel, 2015; Enenkel et al., 1998; Salomons et al., 2010). Indeed, several works have described that misfolded proteins can be imported into the nucleus for degradation, even though some proteins also travel to the cytoplasm to be degraded (Chen and Madura, 2014; Park et al., 2013; Prasad et al., 2010; Smoyer and Jaspersen, 2019). Therefore, in dividing yeast and mammalian proliferating cells the proteasome is enriched in the nucleus (Amsterdam et al., 1993; Chowdhury and Enenkel, 2015; Enenkel, 2014; Enenkel et al., 1998; Hugle et al., 1983; Laporte et al., 2008; McDonald and Byers, 1997; Russell et al., 1999; Scharf et al., 2007). In higher eukaryotes the proteasome show different cellular distributions, depending on the cell type and the developmental stage (Amsterdam et al., 1993; Brooks et al., 2000; Lafarga et al., 2002; Palmer et al., 1994; Wojcik et al., 2000). In *S. pombe*, the proteasome localizes both at the cytoplasm and inside the nucleus, although it is enriched predominantly at the nuclear periphery (Voges et al., 1999; Wilkinson et al., 1998). The nuclear envelope protein Cut8, homolog of budding yeast Sts1, interacts with the proteasome and acts as a sensor that regulates its enrichment at the nuclear periphery, as in its absence the proteasome becomes mainly cytoplasmic (Takeda and Yanagida, 2005; Tatebe and Yanagida, 2000), similar to *sts1* mutant phenotypes (Chen et al., 2011b). Analogously to the proteasome itself, Cut8 participates in the regulation of the histone variant CENP-A/Cnp1 levels and distribution at the centromeric chromatin (Collins et al., 2004; Hewawasam et al., 2010; Kitagawa et al., 2014; Moreno-Moreno et al., 2006; Ranjitkar et al., 2010). Cut8 has also been involved in anaphase progression and DNA repair (Kearsey et al., 2007; Tatebe and Yanagida, 2000).

It has been reported that in *S. cerevisiae* the proteasome interacts with the nuclear basket through Esc1 (Niepel et al., 2013), while in *Chlamydomonas reinhardtii* the 26S proteasome tethers to two specific NPC locations, the nuclear basket and the inner nuclear membrane surrounding the NPC (Albert et al., 2017), where it acts as a protein quality control system that degrades membrane and soluble proteins crossing the NPC, respectively (Boban and Foisner, 2016; Nielsen et al., 2014). Moreover, in *S. pombe* the multifunctional protein Dss1 (*Sc*Sem1) acts as a 26S ubiquitin receptor that localizes at the NPC and functions in several nuclear processes, including protein degradation, DNA repair, transcription and mRNA export, among others (Josse et al., 2006; Mannen et al., 2008; Paraskevopoulos et al., 2014; Schenstrom et al., 2018; Selvanathan et al., 2010). However, it remains unclear the precise biological meaning of the proteasome enrichment at the nuclear periphery, its degree of conservation among species, and the involvement of the NPC in proteasome anchoring. In the first part of this thesis, we have characterized the role of the nuclear basket TPR nucleoporin Alm1 in the spatial regulation of the proteasome at the nuclear periphery, which in turn is key for the maintenance of kinetochore homeostasis and chromosome segregation.

From transcription to mRNA export

In addition to the transport of proteins, the NPCs is also invoved in the export of mRNAs out of the nucleus. But before being allowed to exit the nucleus, nascent transcripts undergo a complex maturation process that results in the formation of export-competent messenger RNA ribonucleoprotein (mRNPs) complexes. To obtain competency, pre-mRNA transcripts are subjected to a number of modifications, including capping of the 5' end, splicing, and poly-adenylation of the 3' end (Bjork and Wieslander, 2017; Dimaano and Ullman, 2004; Jensen et al., 2003). Along these processes transcripts are coated with a broad range of mRNA binding proteins that not only protect the mRNAs, but also are directly involved in their processing and export (Baejen et al., 2014; Kelly and Corbett, 2009; Rougemaille et al., 2008; Singh et al., 2015). When the mRNP has reached full competency, the export factors to which is bound mediate its translocation through the NPC. Once at the cytoplasmic side of the NPC, the export factors release their mRNP cargo and shuttle back into the nucleoplasm, while the mRNA is translated into proteins (Fig. I7) (Carmody and Wente, 2009; Delaleau and Borden, 2015; Iglesias and Stutz, 2008; Stewart, 2010; Stutz and Izaurralde, 2003).

The different steps of mRNA biogenesis, including transcription, processing, quality control, and export, are closely coordinated, and the nuclear basket has been proposed to act as a physical platform that couples such processes. In this regard, the nuclear basket physically and genetically interacts with the multiple players involved in RNA biogenesis, in order to provide a more accurate coordination (Akhtar and Gasser, 2007; Ptak et al., 2014; Raices and D'Angelo, 2017; Schmid and Jensen, 2008; Sommer and Nehrbass, 2005; Stewart, 2019; Strambio-De-Castillia et al., 2010; Vinciguerra and Stutz, 2004). But how does the nuclear basket influence mRNA biogenesis and export?

- **Transcriptional regulation**

Back in 1985, Blobel proposed the visionary gene-gating hypothesis, according to which anchoring of transcribing genes to NPCs would favor mRNA export (Blobel, 1985). Studies in the budding yeast have revealed that upon activation, certain inducible genes, such as *INO1, GAL, HSP104* or *HXK1*, among others, are translocated from the nucleoplasm to the nuclear periphery (Brickner and Walter, 2004; Cabal et al., 2006; Casolari et al., 2004; Dieppois et al., 2006; Luthra et al., 2007; Schmid et al., 2006; Taddei et al., 2006). This nuclear positioning of specific gene loci in the vicinity of the NPC is not exclusive of inducible gene, as highly expressed and constitutively active genes have also been demonstrated to anchor to the NPCs (Casolari et al., 2005; Light and Brickner, 2013; Schmid et al., 2006; Vaquerizas et al., 2010). NPC tethering of inducible genes is based on the recognition of DNA elements, called gene recruitment sequences (GRSs), located in the promoters of the regulated genes, which are binding sites for transcription factors (Ahmed and Brickner, 2010). Indeed, different genes that share the same GRS cluster together (Brickner et al., 2012; Randise-Hinchliff et al., 2016). Nuclear basket components, such as Mlp1 and Nup1, interact with these GRSs through the transcription co-activator SAGA (Spt-Ada-Gcn5 acetyltransferase) complex and TREX2 (transcription and export complex 2, composed of Sac3, Thp1, Sem1, Sus1, and Cdc31 in budding yeast), respectively. NPC-gene anchoring is promoted by Sus1, a common component of SAGA and TREX2 complexes. This assists the coupling of transcription and export by association with the nuclear basket (Cabal et al., 2006; Fischer et al., 2002; Garcia-Oliver et al., 2012; Jani et al., 2014; Luthra et al., 2007; Pascual-Garcia et al., 2008; Rodriguez-Navarro et al., 2004; Schubert and Kohler, 2016).

Several studies point to similar evolutionarily conserved mechanism in higher eukaryotes (Brown et al., 2008; Capelson et al., 2010b; Kurshakova et al., 2007; Mendjan et al., 2006; Rohner et al., 2013; Sood and Brickner, 2014), even though association between the nuclear basket nucleoporins and activated genes usually takes places in the nucleoplasm (Capelson et al., 2010b; Kalverda et al., 2010). For instance, TPR regulates gene expression and export through interaction with TREX2 (GANP, THP1, DSS1 and ENY2 in metazoans), which in turn recruits the mRNA export factor NXF1, involved in mRNP transport across the NPCs (Jani et al., 2012; Umlauf et al., 2013). Moreover, TPR also interacts with the promoter of certain stress-responsive genes through the transcription factor HSF1 (Skaggs et al., 2007). In *Drosophila melanogaster* one quarter of the genome, including active transcription sites, is bound to the nuclear basket components Nup153 and Megator (Mtor, *Dm*TPR; Vaquerizas et al., 2010) and some inducible genes are associated to the NPC via Nup98 (Pascual-Garcia et al., 2017). In humans Nup93 regulates super-enhancers association to the nuclear periphery, influencing the expression of cell identity genes (Ibarra et al., 2016).

Despite the fact that this process has not been studied in depth in *S. pombe,* collected data suggest a similar regulatory mechanism. *S. cerevisiae* GRS sequences promote targeting of a reporter locus to the nuclear periphery in the fission yeast, although it is unknown if this also have an impact on gene expression (Ahmed and Brickner, 2010); highly expressed, co-regulated or functionally related genes also colocalize, which relies on the presence of putative transcription factor binding domains

located in their promoters (Tanizawa et al., 2010); and most of the factors implicated in transcriptional regulation and gene anchoring, such as SAGA, TREX2 and the nuclear basket, are present in the fission yeast as well (Asakawa et al., 2014; Helmlinger et al., 2008; Schenstrom et al., 2018; Watanabe et al., 2012).

Although nuclear basket-dependent positioning of genes usually correlates positively with transcriptional activity and mRNA production, it has also been suggested that the nuclear basket participates in transcriptional repression of *GAL* and ribosomal genes, and their release from the NPC correlates with their expression (Green et al., 2012; Labade et al., 2016; Van de Vosse et al., 2013; Yoshida et al., 2010). However, the existence of a repressive environment around the NPCs that promotes gene silencing is still under debate (Hediger et al., 2002a; Hediger et al., 2002b; Ptak et al., 2014; Sood and Brickner, 2014). In the fission yeast it has been demonstrated that the interaction of NPC components with the RNAi machinery, canonically involved in the establishment of centromeric chromatin, prevents the expression of stress response genes under normal conditions through cotranscriptional gene silencing (CTGS). Mechanistically, the RNAi machinery, including Dcr1, degrades stress-inducible transcripts under normal conditions, while promotes transcriptional activation of Atf1-bound genes under stress. The interaction between the RNAi machinery and these Atf1-bound genes occurs ar the nuclear pores (Woolcock et al., 2012). This highlights a new transcriptional regulation pathway in the nuclear pore, which depends on the RNAi machinery. Importantly, several examples show that this processes might be conserved in higher eukaryotes. In human cells the association of the nuclear basket component Nup153 with DICER is important for transcriptional regulation during heat shock stress response (Ando et al., 2011; Cernilogar et al., 2011), while n mouse embrionic stem cells Nup153 promotes gene repression of developmental genes (Jacinto et al., 2015), Besides, human Nup93 is responsible for *HOXA* gene cluster silencing (Labade et al., 2016) and *Drosophila* Nup93 has been reported to participate in silencing and clustering of Polycomb genes (Gozalo et al., 2020).

Additionally, it has been described a third class of NPC-gene anchoring in yeasts, which has been associated with transcriptional memory, a process in which once repressed inducible genes (*GAL1*, *INO1* and *HXK1*) remain associated to the nuclear pore for several generations for a faster transcriptional reactivation (Brickner, 2009; D'Urso and Brickner, 2014, 2017; Laine et al., 2009; Tan-Wong et al., 2009). A similar phenomenon of epigenetic transcriptional memory has been described for other eukaryotes, regulating the expression of interferon-γ genes in metazoans and stress responsive genes in plants (Gialitakis et al., 2010; Kundu and Peterson, 2009; Lamke et al., 2016; Light and Brickner, 2013; Light et al., 2013; Pascual-Garcia et al., 2017).

Nevertheless, which are the biological implications of NPC-gene anchoring? It has been suggested that gene association with the nuclear basket provides an additional level of transcriptional regulation, which increases gene expression rates and favors mRNA export (Akhtar and Gasser, 2007; Brickner and Walter, 2004; Taddei et al., 2006; Van de Vosse et al., 2011). Additionally, clustering of co-regulated genes could be considered as a mechanism to recruit transcription factors more efficiently,

both in yeasts and in higher eukaryotes (Brickner and Brickner, 2012; Brown et al., 2008; Randise-Hinchliff et al., 2016; Schmid et al., 2006; Schoenfelder et al., 2010; Xu and Cook, 2008). Along these lines, several studies in higher eukaryotes have illustrated that NPC anchoring of chromatin is involved in the fine-tune regulation of gene expression (Ruault et al., 2008), in tissue-specific differenciation, or in cellular response to environmental cues inducing transcriptional programs (D'Angelo et al., 2012; Ibarra et al., 2016; Liang et al., 2013; Liu et al., 2019; Raices et al., 2017; Su et al., 2018; Toda et al., 2017).

- **mRNP processing and assembly**

Early during transcription initiation several factors are recruited to the nascent transcript through the RNA Polymerase II elongating complex. The carboxy-terminal domain (CTD) of RNAPII is phosphorilated at the Ser5, which results in the co-transcriptional recruitment of the capping enzymes and the attachment of the cap binding complex (CBC) to the 5' end of the pre-mRNA that is being synthesized (Fig. I7 A) (Andersen et al., 2013a; Hsin et al., 2014; Komarnitsky et al., 2000). Latter on, the spliceosome is recruited co-transcriptionally, via serine-arginine (SR) splicing factors, such as Npl3 (Das et al., 2007; Hurt et al., 2004; Kress et al., 2008; Muller-McNicoll et al., 2016). The spliceosome removes the introns from the pre-mRNA, depositing an exon junction complex (EJC) near to the two joined exons (Fica and Nagai, 2017; Woodward et al., 2017).

The next pre-mRNA processing step consists on the poly-adenilation of the 3'-end. The length of the poly(A) tail (about 60 nucleotides in *S. cerevisiae* and 250 in higher eukaryotes) is important for the stability, nuclear export and translation of the mRNA. Therefore, this process is highly regulated by the multiprotein CPF (Cleavage and polyadenylation factor) (Eckmann et al., 2011; Kelly et al., 2014; Tudek et al., 2018a). Firstly, the CPF nuclease module cleaves the 3'-UTR of the pre-mRNA; then, the CPF polymerase module containing the poly(A)-polymerase Pap1 catalyzes the addition of adenosines to form the poly(A) tail. During the poly(A) tail synthesis, poly(A)-binding proteins (PABPs), such as Nab2 (*Hs*ZC3H14) and Pab2 (*Hs*PABPN1) (Kelly et al., 2014; Kuhn et al., 2017; Leung et al., 2009; Muniz et al., 2015; Soucek et al., 2016) are recruited (Fig. I7 A). Afterward, the CPF phosphatase module triggers the termination of poly-adenilation, which is signalled by Pcf11 through conformational changes in the mRNP (Chan et al., 2011; Di Giammartino and Manley, 2014; Johnson et al., 2009; Katahira, 2012). The PABPs play a key role in this process, as binding of enough Nab2 to the poly(A)-tail induces Nab2 dimerization, which results in the inhibition and detachment of Pap1 (Casanal et al., 2017; Soucek et al., 2012; Wahle, 1995). Dimerization of Nab2 also contributes to mRNP compaction by interacting with different regions of the transcript (Aibara et al., 2017; Fasken et al., 2019; Hector et al., 2002; Viphakone et al., 2008).

Together, transcription elongation, capping, splicing and poly-adenilation are signaled by the recruitment of the TREX (transcription and export) complex to the mRNP (Fig. I7 A) (Abruzzi et al., 2004; Cheng et al., 2006; Chi et al., 2013; Luo et al., 2001; Masuda et al., 2005; Meinel et al., 2013; Viphakone et al., 2019). TREX complex comprises the transcription elongation subcomplex THO

(composed of Hpr1, Tho2, Thp2, Tex1, and Mft1 in budding yeast), the RNA-binding protein Yra1 (*Hs*ALY/REF) and the ATP-dependent RNA helicase Sub2 (*Hs*UAP56). TREX couples transcription and mRNP export and is required for the remodeling of the mRNP, contributing to the loading of RNA adaptors, such as Yra1, Nab2 and Npl3, among others (Chi et al., 2013; Jimeno et al., 2002; Katahira, 2012; Strasser et al., 2002; Zenklusen et al., 2002). In turn, these adaptors promote the recruitment of mRNA export factors, such as Mex67-Mtr2 heterodimer (TAP/NXF1-p15/NXT1 in metazoans; Hautbergue et al., 2008; Hurt et al., 2004; Rougemaille et al., 2008; Strasser and Hurt, 2000; Strasser et al., 2002; Viphakone et al., 2012; Zenklusen et al., 2001), although it has also been proposed that Mex67 is recruited to pre-mRNPs earlier during transcription through the TREX complex component Hpr1 (Gwizdek et al., 2005; Gwizdek et al., 2006). According to the “hand-over” model, prior to export the mRNP undergoes further rearrangements, which involve Yra1/ALY/REF removal from the mRNP as a result of Sub2/UAP56-dependent remodeling of the mRNPs (Strasser and Hurt, 2001), arginine methylation (Hung et al., 2010), and Tom1 E3 ligase-dependent ubiquitination (Iglesias et al., 2010). This remodeling promotes the further loading of Mex67 by increasing its RNA-binding affinity, which ultimately generates export competent mRNPs (Hautbergue et al., 2008). These steps of mRNP maturation occur in the proximity of the NPCs and might be facilitated by the interaction of mRNP with the nuclear basket (Abruzzi et al., 2006; Bjork and Wieslander, 2017; Gilbert and Guthrie, 2004; Hautbergue et al., 2008; Oeffinger and Zenklusen, 2012; Stewart, 2019; Tutucci and Stutz, 2011).

- **mRNP docking**

Prior to export, mRNPs are docked to the nucleoplasmic side of the NPC. This step is favored by TREX and TREX2 complexes, which integrate gene expression and processing with mRNA export by bridging the transcription machinery to the entrance of the NPC. Co-transcriptional recruitment of mRNA export factors, such as Mex67/NXF1, facilitates the transfer of the mRNP from the transcription site to the NPC (Chekanova et al., 2008; Dieppois et al., 2006; Fischer et al., 2002; Garcia-Oliver et al., 2012; Raices and D'Angelo, 2017; Rodriguez-Navarro et al., 2004). Mammalian TREX-2 is also a key player in coupling transcription and export machineries through association with the nuclear basket TPR (Dimitrova et al., 2015; Jani et al., 2012; Umlauf et al., 2013). Moreover, the physical interaction of mRNPs adaptor and export factors with the nuclear basket further contributes to mRNP docking (Bailer et al., 1998; Green et al., 2003; Strawn et al., 2001; Vinciguerra et al., 2005). Mlp1 interaction with Nab2 helps in the recognition and concentration of correctly processed mRNPs at the nuclear pore, contributing to efficient export, while Mlp2 has also been associated with Yra1, especially in conditions of mRNP processing impairment (Fasken and Corbett, 2009; Galy et al., 2004; Vinciguerra et al., 2005). Specifically, it has been described that the C-terminal domain of *Sc*Mlp1 (and probably hTPR) binds to the N-terminal domain of Nab2, which facilitates mRNP interaction with the nuclear basket (Fasken et al., 2008; Grant et al., 2008; Green et al., 2003).

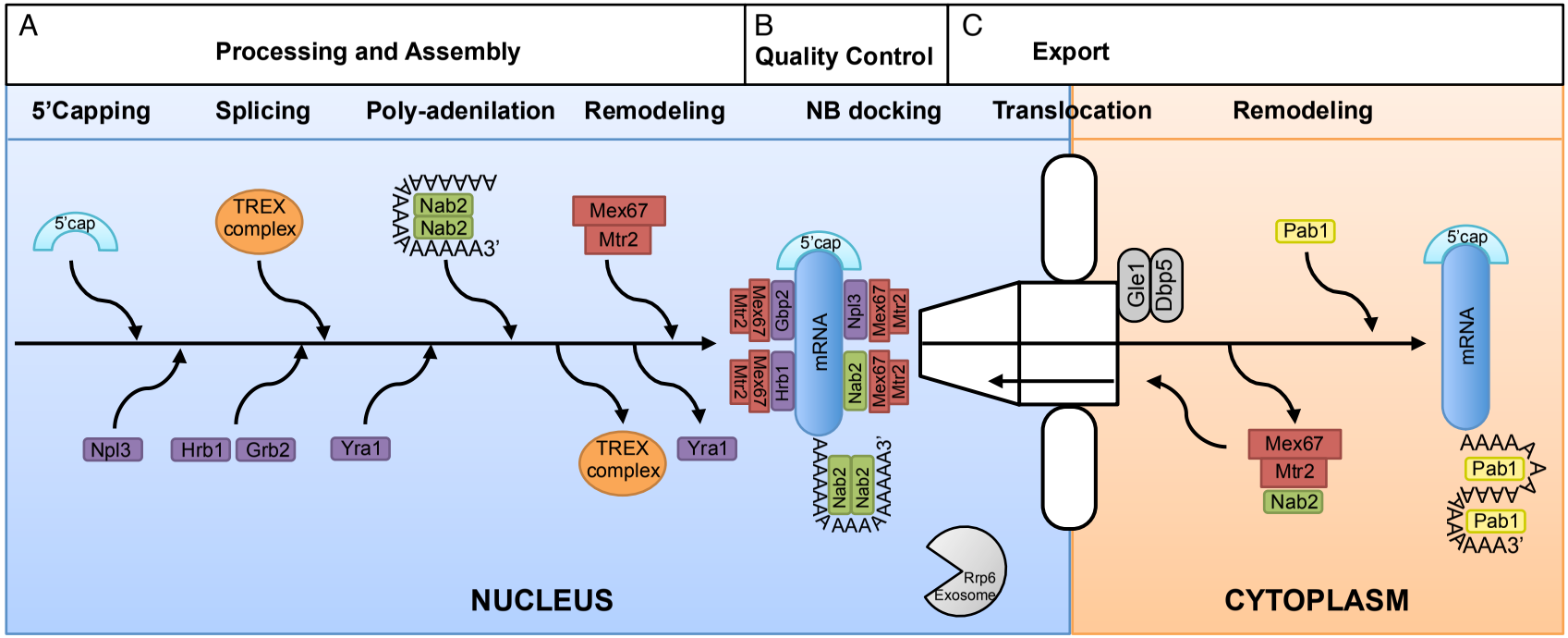

Figure I7. Schematic of RNA life cycle, from transcription to export in *S. cerevisiae*. (A) During transcription, immature transcripts are processed, which includes capping of the 5' end, removal of introns by the spliceosome, and poly-adenilation of the 3' end. During these processing steps, the pre-RNA molecule is coated with different proteins, forming the mRNP. These includes the TREX complex, and export adaptors (Npl3, Hrb1, Grb2, Yra1, Nab2). If every maturation step has been successfully accomplished, the mRNP is remodeled and the heterodimeric mRNA export factor Mex67:Mtr2 gains access to the mRNP via interaction with adaptors proteins. (B) If a problem has occurred, nuclear surveillance mechanisms retain the mRNP, which its is degraded via the Rrp6-containing exosome. The mRNP is docked to the nuclear basket of the NPC, where the last quality control is performed. (C) Then, the export factors facilitate mRNP translocation through the NPC. At the cytoplasmic side of the NPC, adaptor and export factors, such as Mex67 and Nab2, dissociate from the mRNP via Gle1 and Dbp5-dependent remodeling, and travel back to the nucleoplasm. Finally, the mRNA is loaded with the PABP Pab1 and is directed to translation. See text for further details. (Adapted from Zander et al., 2016; Stewart, 2019)

- **mRNP surveillance and quality control**

In order to prevent the export of improperly processed or immature mRNPs, which would interfere with mRNA biogenesis or protein homeostasis, cells possess nuclear surveillance quality control mechanisms that monitor the quality of the mRNPs during all the steps of the RNA biogenesis (Fig. I7 B). Nuclear RNA quality control pathways depends on the recognition of defective transcripts by the TRAMP (Trf4/Trf5, Air1/Air2, Mtr4 polyadenylation) complex and their degradation by the exosome (Doma and Parker, 2007; Porrua and Libri, 2013; Schmid and Jensen, 2008; Soheilypour and Mofrad, 2018). The exosome is an evolutionarily conserved 3'–5' ribonuclease complex that contains two exoribonucleases, Dis3 and Rrp6, involved in RNA quality control and degradation of most unprocessed RNAs. All exosome components localize in the cytoplasm and in the nucleoplasm, except for Rrp6 that is a central player in the nuclear mRNA decay (Doma and Parker, 2007; Fasken and Corbett, 2005; Fox and Mosley, 2016; Houseley et al., 2006; Schmid and Jensen, 2008).

mRNP quality control checkpoint relies on the co-transcriptional loading of adaptor and export factors into pre-mRNAs at the different processing steps; for instance, Npl3 associates near the 5' cap and 3' end, Hrb1 and Gbp2 are loaded during splicing, and Nab2 is recruited to the poly(A) tail (Fig. I7 A and B) (Baejen et al., 2014; Hackmann et al., 2014; Jensen et al., 2003; Peck et al., 2019; Tutucci and Stutz, 2011). Accordingly, defects in mRNA capping, splicing, polyadenilation or assembly lead to the retention of faulty mRNPs near the transcription sites for further processing or degradation (Hilleren and Parker, 2001; Jensen et al., 2001; Paul and Montpetit, 2016; Thomsen et al., 2003; Zenklusen et al., 2002). In fact, Rrp6 interacts with newly synthesized transcripts through these RNA binding proteins and has been proposed to escort them to the nuclear pore (Hessle et al., 2012). Export impairment also leads to the accumulation of poly(A)-RNAs in nuclear foci close to nuclear pores, which become hyperadenylated and degraded by the Rrp6-exosome (Paul and Montpetit, 2016; Tudek et al., 2018b).

Mlps/TPR are part of a final quality control at the NPC that either allows mRNA export or retain unspliced or defective mRNAs for degradation by interacting with RNP adaptor proteins (Fig. I7 B). Consistently, the Mlp1 recognizes poly-adenilated/unspliced RNAs, which are marked by TRAMP for degradation by the exosome, while quality-controlled mRNAs are allowed to further associate with Mex67 and are licensed to export (Fasken and Corbett, 2009; Hackmann et al., 2014; Iglesias et al., 2010; Soheilypour and Mofrad, 2018; Tudek et al., 2018a). Accordingly, the absence of Mlp1 results in the leakage of unspliced and defective mRNPs into the cytoplasm (Galy et al., 2004). In *S. cerevisiae* several nuclear pore associated proteins have been functionally linked to this QC mechanism, including the the RNA adaptor Nab2, the endoribonuclease Swt1, the desumoylating enzyme Ulp1, NE-associated Esc1, and Pml39 (Bonnet et al., 2015; Galy et al., 2004; Hackmann et al., 2014; Lewis et al., 2007; Palancade et al., 2005; Skruzny et al., 2009). Indeed, the endoribonuclease Swt1 has been proposed to play a role in the degradation of aberrant mRNAs (Skruzny et al., 2009) and Pml39 is described as an upstream effector of Mlp1 required for the retention of faulty mRNPs (Palancade et al., 2005). Although less studied, in the fission yeast two Poly(A) RNA binding proteins, Nab2 and

Pab2, have been implicated in Rrp6-dependent quality control, in a similar mechanism than that operating in *S. cerevisiae* (Schmid et al., 2012). Nab2 associates preferentially to unspliced mRNAs, protecting them from exosome degradation, while Pab2 (an ortholog of human PABPN1 that is not present in *S. cerevisiae* genome) binds to mRNAs and promotes Rrp6-dependent degradation (Grenier St-Sauveur et al., 2013; Lemieux et al., 2011; St-Andre et al., 2010).

- **mRNP export**

Contrary to protein transport, the translocation of mRNPs is independent of the Ran-GTPase system. However, the transport directionality is provided as well by the asymmetric presence of nucleoporins at the nucleoplasmic and cytoplasmic sides of the NPC (Grunwald et al., 2011; Kohler and Hurt, 2007; Terry and Wente, 2009; Tran and Wente, 2006). Despite some differences, most of the players of the mRNA export pathways and their functions have been conserved along evolution. Mex67 (TAP/NXF1 in metazoans) is the main mRNP export factor, which forms a heterodimeric complex with Mtr2 (p15/NXT1) (Gruter et al., 1998; Hurt et al., 2000; Katahira et al., 1999; Santos-Rosa et al., 1998; Segref et al., 1997; Tan et al., 2000; Yoon et al., 2000). As described above, Mex67-Mtr2 binding to RNAs is non-specific, and different adaptor proteins participate in its recruitment to mRNPs (Rodriguez-Navarro and Hurt, 2011; Stewart, 2010). Prior to NPC translocation, remodeling of mRNPs acts as a signal of mRNP competency, which allows Mex67-bound mRNPs to interact with nucleoporins (Dieppois et al., 2006; Hautbergue et al., 2008; Iglesias and Stutz, 2008; Iglesias et al., 2010; Viphakone et al., 2012). Then, Mex67-Mtr2, together with its adaptors (Nab2, Nlp3, among others), escort mRNPs from the nucleoplasm to the cytoplasm through interaction with FG nucleoporins of the central channel (Fig. I7 C) (Santos-Rosa et al., 1998; Strasser et al., 2000; Strawn et al., 2001). *Sc*Gle2 (RAE1 in metazoans and Rae1 *S. pombe*), a well-conserved nuclear pore-associated mRNA export factor, helps Mex67-Mtr2 during translocation (Bharathi et al., 1997; Blevins et al., 2003; Brown et al., 1995; Murphy et al., 1996; Pritchard et al., 1999).

Once at the cytoplasmic side of the NPC, mRNP is remodeled again to release the mRNA (Fig. I7 C). This step requires the Nup42 and Nup159 nucleoporins, which dock mRNP transport receptors, and the DEAD-box RNA-helicase Dbp5 (*Hs*DDX19), which becomes activated by the cytoplasmic filament component Gle1 (*Hs*GLE1) bound to inositol hexakisphosphate (IP6). As a result, Mex67 and its adaptors are removed from the mRNP and are recycled back into the nucleus (Alcazar-Roman et al., 2006; Ben-Yishay et al., 2019; Hodge et al., 2011; Montpetit et al., 2011; Strahm et al., 1999; Tieg and Krebber, 2013; Tran et al., 2007; Weirich et al., 2004). Then, the mRNP, bound to the shuttling poly(A)-binding protein Pab1, gets its way to the ribosome for translation (Brune et al., 2005; Dunn et al., 2005). Interestingly, while transport through the central channel of the NPC occurs in miliseconds, interaction with nucleoplasm-facing nups is a rate-limiting step, caused by mRNP remodeling and nuclear surveillance mechanisms (Grunwald and Singer, 2010; Grunwald et al., 2011; Kelich and Yang, 2014; Ma and Yang, 2010; Siebrasse et al., 2012).

Genetic screenings performed in fission yeast have led to the identification of several nucleoporins and NPC-associated proteins involved in mRNA docking and export. These include nucleoporins of the central channel, FG nucleoporins, such as Nup214, Nup98 or Nup85, and the nuclear basket (Bae et al., 2009; Bai et al., 2004; Bailer et al., 1998; Brown et al., 1995; Thakurta et al., 2004; Yoon et al., 2000). Fission yeast Rae1 (*Sc*Gle2) is a constitutive element of the NPC that interacts with the multifunctional factor Dss1 (*Sc*Sem1) and with the TREX complex RNA helicase Uap56 (*Sc*Sub2). In turn, these factors are associated to Mlo3 (*Sc*Yra1), assisting the loading of Mex67 into the mRNP. Similar to *S. cerevisiae*, it has been proposed that Uap56 and Mex67 bind to Mlo3 in a mutually exclusive manner, and loading of Mex67 could displace Uap56 prior to export. Rae1, Dss1, Mlo3 and Mex67 have been shown to interact with FG-Nups, Nup146 (*Sc*Nup159) and Nup189 (*Sc*Nup98), contributing to mRNP targeting to the NPC (Thakurta et al., 2005; Thakurta et al., 2004; Thakurta et al., 2007; Yoon et al., 2000).

Previous works have shown that deregulation of Mlp1 causes altered poly(A)-RNA trafficking, which has been associated to its QC function (Galy et al., 2004; Green et al., 2003; Lewis et al., 2007; Palancade et al., 2005; Vinciguerra et al., 2005), while human TPR participates in nuclear export of intron containing mRNAs (Bangs et al., 1998; Rajanala and Nandicoori, 2012; Shibata et al., 2002; Umlauf et al., 2013). Overexpression and downregulation of *nup211*$^{+}$ lead to the accumulation of mRNA inside the nucleus (Bae et al., 2009). Nevertheless, it remains unknown which is the functional involvement of the nuclear basket in mRNA docking, quality control and export. In the second part of this work, we have characterized how the two nuclear basket TPR nucleoporins in the fission yeast, Nup211 and Alm1, are assembled and anchored to the NPC, and we have examined the functional connection between the nuclear basket and the mRNA processing and export machinery.

The Heat Shock Response

Both unicellular and pluricellular organisms are constantly challenged by changing environmental conditions. Under such circumstances, they have two options, adapt or perish. In order to become resistant to the stress and ensure cell survival, organisms have to respond to a wide spectrum of external insults in an immediate and proportional manner (Hohmann, 2003). In other case, cell viability could be deeply compromised. This ability to tolerate environmental fluctuations provide a competitive advantage and, consequently, evolution has provided unicellular and pluricellular organisms an amazing toolbox to overcome external insults. Some of these insults include nutrient starvation, abrupt temperature fluctuations, changes in osmotic conditions, or the exposition to toxic compounds. Cells react according to the type of stress, triggering general and specific pathways in a very rapid manner (Bahn et al., 2007; Hohmann, 2003). Although stress response regulatory networks may have diverged along evolution, the final phenotypic outputs compensate the stress conditions (Lelandais and Devaux, 2010; Tirosh et al., 2011).

- **Regulation of the Heat Shock Response**

How cells respond to heat shock stress has been object of study over the last decades (reviewed in Morano et al., 2012; Trott A., 2003; Verghese et al., 2012). To withstand severe thermal stress, cells take action at multiple levels, starting with the activation the heat shock response (HSR), an universal process that results in cell cycle arrest, metabolic reprogramming, and cell wall and membrane changes (reviewed in Imazu and Sakurai, 2005; Kuhl and Rensing, 2000; Levin, 2005; Rowley et al., 1993; Sorger, 1991; Strassburg et al., 2010; Trott A., 2003; Verghese et al., 2012; Walther et al., 2010). HSR induces a drastic and transient reprogramming of the gene expression profile, which includes the shut-down of housekeeping gene transcription and the up-regulation of stress-responsive genes, mostly heat shock proteins (HSPs) and molecular chaperones that prevent damaged and denatured proteins to interfere with cellular processes (reviwed in Trott A., 2003). The global switch in the transcriptional program critically accelerates the HSR and facilitates the rapid adaptation to temperature fluctuations (Bond, 2006; Sadis et al., 1988; Yost and Lindquist, 1991). HSR-dependent transcriptional reprogramming is mainly mediated by Hsf1 and Msn2/4 transcription factors (reviewed in Amoros and Estruch, 2001; Becerra et al., 2003; Boy-Marcotte et al., 2006; Brunquell et al., 2016; Causton et al., 2001; Chen et al., 2003; Craig, 1985; Gasch et al., 2000; Hahn et al., 2004; Richter et al., 2010; Trinklein et al., 2004; Verghese et al., 2012; Yamamoto et al., 2005).

Hsf1 is considered the master regulator of the HSR, as this transcription factor controls the expression of molecular chaperones under thermal stress (Amoros and Estruch, 2001; Boy-Marcotte et al., 2006; Brunquell et al., 2016; Cotto and Morimoto, 1999; Gasch et al., 2000; Hahn et al., 2004; Solis et al., 2016; Trinklein et al., 2004; Yamamoto et al., 2008). Hsf1 shows a high degree of conservation among organisms, although its family members vary among species; most yeasts and *Caenorhabditis elegans* only possess one copy, humans have at least five HSF genes, and *Arabidopsis thaliana* contains 21 (Akerfelt et al., 2010; Liu et al., 1997; Morano et al., 2012). In *S. cerevisiae* Hsf1 is constitutively active and inside the nucleus, regulating the expression of genes in unperturbed conditions (Hahn et al., 2004; Jakobsen and Pelham, 1988; Sorger et al., 1987). In higher eukaryotes, however, Hsf1 is kept inactive in the cytoplasm as a monomer, bound to the chaperones Hsp90 and Hsp70-Hsp40 (Brunquell et al., 2016; Krakowiak et al., 2018; Shi et al., 1998; Sorger et al., 1987; Voellmy, 2004; Voellmy and Boellmann, 2007; Zheng et al., 2016). In *S. pombe*, regulation of Hsf1 activity is similar to metazoan, although it is essential for cell viability even under normal growth conditions (Gallo et al., 1993; Gallo et al., 1991).

According to the “chaperone titration model” the accumulation of unfolded proteins during thermal stress results in the release of Hsf1 from its sequestering chaperones Hsp90 and Hsp70-Hsp40, as these now bind preferently to unfolded proteins than to Hsf1. After displacement from this allosteric inhibition, Hsf1 monomers form trimers and translocate from the cytoplasm into the nucleoplasm (Fig. I8 A). This homotrimeric form of Hsf1 is subjected to a number of posttranslational modifications, and becomes hyperactivated and competent to bind with high affinity to specific heat shock elements (HSEs), located in the promoter region of its target genes. This leads to the RNA polymerase II-

dependent expression of stress-responsive genes, mainly chaperones that buffer protein aggregation and denaturation (Baler et al., 1993; Hashikawa et al., 2007; Masser et al., 2019; Peffer et al., 2019; Sakurai and Takemori, 2007; Sarge et al., 1993; Shi et al., 1998). Importantly, since RNA polymerase II activity is also partially block during a severe heat shock, most Hsf1 target genes become highly expressed during the recovery period after thermal stress, which has been termed delayed upregulation (Yamamoto et al., 2008). Once physiological conditions are restored, the increased accumulation of those chaperones induced by Hsf1 during the period of recovery causes the restraint of Hsf1. This negative feedback loop is key to reprogram gene expression and to resume normal cell growth (Krakowiak et al., 2018; Sakurai and Ota, 2011; Shi et al., 1998; Vjestica et al., 2013; Zheng et al., 2016; Zou et al., 1998). In addition to the negative regulation by chaperone sequestration, Hsf1 activity is fine-tuned by posttranscriptional modifications, such as phosphorylation, acetylation and sumoylation (Akerfelt et al., 2010; Baler et al., 1993; Guettouche et al., 2005; Hashikawa et al., 2006; Hong et al., 2001; Kim et al., 2005; Sorger and Pelham, 1988; Westerheide et al., 2009; Zheng et al., 2016). The subcellular localization of Hsf1 represents another regulatory mechanism, as Hsf1 exits from the nucleus following a heat shock (Herbomel et al., 2013; Jolly et al., 1999; Kim et al., 2005; Sarge et al., 1993; Vujanac et al., 2005).

In a parallel pathway, the general stress response transcription factors Msn2 and Msn4 activate the gene expression of common and additional stress responsive genes, binding to specific promoter sequences termed stress response elements (STREs) (Amoros and Estruch, 2001; Martinez-Pastor et al., 1996; Schmitt and McEntee, 1996). Msn2/4 target genes, some of which are shared with Hsf1, include HSPs and proteins involved in carbohydrate metabolism and protection against oxidative stress (Boy-Marcotte et al., 2006; Gasch et al., 2000; Martinez-Pastor et al., 1996; Treger et al., 1998). Msn2/4 localization and activity are regulated by phosphorylation, via cAMP/PKA (cyclic AMP protein kinase A) and TOR (target of rapamycin) pathways (Fig. I8 B) (Ferguson et al., 2005; Lee et al., 2008a; Santhanam et al., 2004), nucleocytoplasmic shuttling (Jacquet et al., 2003) and the Rpd3L deacetylase complex (Ruiz-Roig et al., 2010). The mitogen-activated protein kinase (MAPK) pathway is another key cascade for the general stress regulation (Lee et al., 2008a; Levin, 2005; Truman et al., 2007). Accordingly, MAPK Sty1/Spc1 (Hog1 in *S. cerevisiae*, and p38 and JNK in mammals) becomes activated under different type of stresses, including osmotic stress, UV, peroxide or heat shock (Degols et al., 1996; Regot et al., 2013; Tibbles and Woodgett, 1999). It has been described that the inhibition of the tyrosine phosphatase Pyp1 under heat stress results in Sty1 activation (Nguyen and Shiozaki, 1999; Shiozaki et al., 1998); Sty1 relocalizes to the nucleus and phosphorylates transcription factors, such as Atf1 (Gaits et al., 1997; Salat-Canela et al., 2017; Sanchez-Mir et al., 2018; Wilkinson et al., 1996). However, in *S. pombe* the expression of heat responsive genes is only partially dependent on Sty1 (Chen et al., 2003; Paredes et al., 2004).

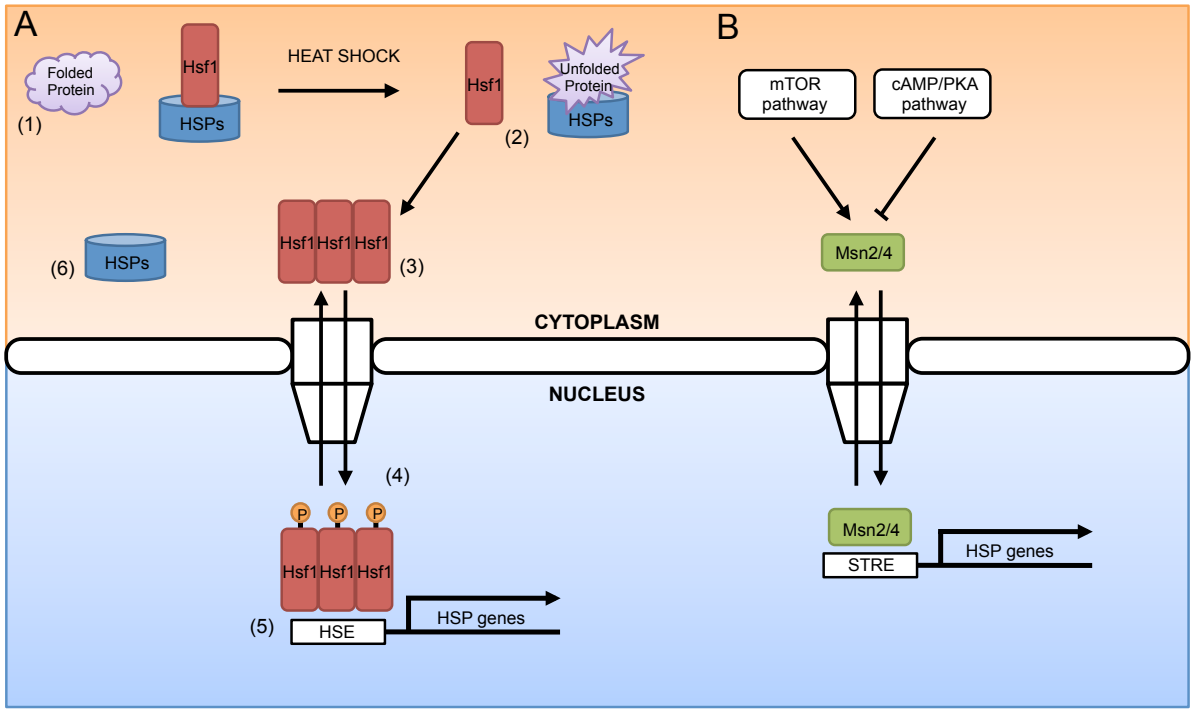

Figure I8. Schematic of Heat Shock Response pathways. (A) Hsf1 regulation. In unperturbed conditions, inactive Hsf1 is bound to HSPs, such as Hsp70 and Hsp90 (1). Under heat stress, the increase in unfolded proteins draws Hsp70 and Hsp90 away from Hsf1 (2). This leads to Hsf1 activation, caused by Hsf1 homotrimerization (3), translocation into the nucleus and phosphorylation (4). As a result, activated Hsf1 binds to HSE located in the promoter of HSP genes, and promotes their transcription (5). The increase in the concentration of chaperones helps protein refolding and avoids misfolded protein aggregation. Then, Hsp70-90-dependent feedback loop contributes to repress Hsf1 activity by direct association (6). (B) Msn2/4 regulation. Msn2/4 transcription factors localize at the cytoplasm in unperturbed condition. Under stress conditions, mTOR and cAMP/PKA pathways contribute to Msn2/4 activation positively and negatively, respectively. Activated Msn2/4 enter into the nucleus to promote the expression of stress response genes, binding to STRE located in the promoters of their target genes. P, phosphorylation; HSE, heat shock element; STRE, stress response element. (Adapted from Vabulas et al., 2010; Morano et al., 2012; Verghese et al., 2012)

- **Transcriptional reprogramming during heat shock**

As a result of the stress-dependent transcriptional reprograming, transcription, export and translation of housekeeping transcripts responsible for normal cell growth, such as ribosomal components or RNA-processing factors, are blocked until physiological conditions are restored (Bond, 1988, 2006; Sadis et al., 1988; Yost and Lindquist, 1991). This is concomitant with the expression of stress-responsive genes, most of which encode for molecular chaperones and other heat shock response proteins (Craig, 1985; Gasch et al., 2000; Lindquist and Craig, 1988; Richter et al., 2010; Trott A., 2003; Verghese et al., 2012). Other activated genes are related to protein ubiquitination and degradation, vesicular transport, cell wall integrity and metabolism (Chen et al., 2003; Hahn et al., 2004; Hahn et al., 2006; Imazu and Sakurai, 2005; Solis et al., 2016; Strassburg et al., 2010; Walther et al., 2010). Heat shock also induces the accumulation of trehalose, a disaccharide of glucose responsible for the prevention of protein aggregation and the stabilization of structures and proteins during thermal stress, including Hsf1. Thus, trehalose is considered one of the most important thermoprotectant (Conlin and Nelson, 2007; De Virgilio et al., 1991; De Virgilio et al., 1990; Hottiger et

al., 1994; Piper, 1998; Ribeiro et al., 1997). Interestingly, studies in several organisms have revealed that many of the up-regulated genes under heat shock are also transcribed under other type of stresses. As a result, cells under a type of stress acquire tolerance to subsequent different stresses, which has been termed “cross-protection” (Piper, 1995; Verghese et al., 2012). For instance, in *S. pombe* about 300 genes are induced under heat stress; while one third are common to the general stress response, about 40 of them are HSR exclusive (Chen et al., 2003).

Among stress-responsive factors, HSPs limit stress-induced damage by preventing protein denaturation and aggregation, and help in the folding and degradation of injured proteins, which in other case would lead to cell death. Some HSPs are required under normal conditions and become overexpressed during HS, while others are exclusively produced under heat stress (Bond, 2006; Lindquist and Craig, 1988; Parsell and Lindquist, 1993; Parsell et al., 1993; Pincus, 2017; Riezman, 2004; Trinklein et al., 2004; Verghese et al., 2012; Vogel et al., 1995). The most important HSPs are described below:

- Hsp70. Chaperones of the Hsp70 family are highly conserved along evolution. *S. cerevisiae* possesses several Hsp70 members, which differ in localization and expression. One of the most studied subfamilies is Ssa (Ssa1-4 in *S. pombe*), whose members display redundant and specific functions. In general, Ssa chaperones are present in unperturbed conditions, although they are heat-inducible (Hasin et al., 2014; Lindquist and Craig, 1988; Lotz et al., 2019; Morano et al., 2012; Werner-Washburne et al., 1987). Hsp70 localizes predominantly in the cytoplasm in unperturbed conditions, and accumulates in the nucleus under HS, both in yeasts and in mammalian cells (Oda et al., 2014; Pelham et al., 1984; Velazquez and Lindquist, 1984; Welch and Feramisco, 1984). Hsp70 functions in the folding of new proteins and in the refolding of misfolded and aggregated proteins (Glover and Lindquist, 1998; Horton et al., 2001; Lindquist and Craig, 1988; Parsell and Lindquist, 1993). In *D. melanogaster* Hsp70 is the main chaperone conferring thermotolerance under severe temperatures (Solomon et al., 1991), while in *C. elegans* it has been involved in the clearance of protein aggregates (Kirstein et al., 2017).

- Hsp104. Hsp104 is a disaggregase that recognizes misfolded proteins within an aggregate and participates in their solubilization together with the Hsp70/40 complex (Ssa2-Mas5 in fission yeast) (Bosl et al., 2006; Glover and Lindquist, 1998; Glover and Lum, 2009; Kaimal et al., 2017; Parsell et al., 1994; Vogel et al., 1995). In budding yeast Hsp104 is essential for thermotolerance and its expression is highly induced when cells are recovering from a heat stress (Lindquist and Kim, 1996; Mosser et al., 2004; Sanchez and Lindquist, 1990; Senechal et al., 2009).

- Hsp90. During thermal stress this chaperone acts selectively in the last steps of protein maturation and in the assembly of macromolecular complexes (Nathan et al., 1997; Pearl and Prodromou, 2006; Zhao and Houry, 2005).

- Small HSPs (sHSPs). This group includes several ubiquitous molecular chaperones, such as Hsp26 and Hsp42, which form co-aggregates with damaged proteins, preventing their aggregation

and assisting their later solubilization by other chaperones (Haslbeck et al., 2004; Haslbeck et al., 2005; Haslbeck et al., 1999).

It has been demonstrated that pretreatment with a mild heat shock prior to a severe heat shock increase considerably cell survival, a phenomenon that has been termed acquired thermotolerance. This effect has been attributed to the expression of some chaperones (*e.g.* Hsp104) during the mild heat shock, which confer protection for a subsequent and more severe stress (Bond, 2006; Bracken and Bond, 1999; De Virgilio et al., 1991; Gross and Watson, 1998; Parsell and Lindquist, 1993; Sanchez and Lindquist, 1990; Yost and Lindquist, 1991).

- **mRNP biogenesis during heat shock**

In order to respond to external insults as fast and efficiently as possible, transcriptional reprogramming under elevated temperatures is accompanied by the inhibition of the RNA Polymerase II-dependent transcription, which reduces the synthesis of normal mRNAs. This is coordinated with the inactivation of splicing and RNA processing, and the block of bulk mRNA export, presumably to favor the selective export and translation of heat shock mRNAs (Bond, 1988, 2006; Bracken and Bond, 1999; Castells-Roca et al., 2011; Kay et al., 1987; Krebber et al., 1999; Saavedra et al., 1996; Sadis et al., 1988; Shalgi et al., 2014; Shin et al., 2004; Tani et al., 1996; Yost and Lindquist, 1986, 1991). This raised the question of how cells are able to discern between housekeeping and HS transcripts to prioritize the export and translation of stress-responsive genes.

Under normal conditions, mRNA molecules exist as mRNPs, coated with several RNA-binding proteins that not only protect the transcripts but are also involved in the different processing and assembly steps of the RNA lifecycle (Fig. I9 A) (as described in section From transcription to mRNA export). Several works have shown that under heat stress the dissociation of mRNA adaptor and export elements from the mRNP particles could contribute to the inhibition of normal mRNA export in *S. cerevisiae*. A number of RNA-binding proteins (RBPs) involved in the different stages of RNA processing, such as Npl3, Gbp2, Hrb1 and Nab2, uncouple from regular mRNAs to prevent their export, whereas direct binding of Mex67 to stress transcripts without the need of any adaptor promotes their export (Fig. I9 B). Mex67 recruitment to HS mRNAs directly depends on Hsf1 (Krebber et al., 1999; Rollenhagen et al., 2007; Zander et al., 2016). Similarly, in higher eukaryotes it has been reported the disruption of mRNP complexes and the inhibition of splicing and nucleocytoplasmic transport during an acute heat shock (Bond, 1988; Bracken and Bond, 1999; Hochberg-Laufer et al., 2019; Kay et al., 1987; Lutz et al., 1988; Mahl et al., 1989; Mayrand and Pederson, 1983; Sadis et al., 1988).

Apart from the remodeling of mRNPs, a sub-set of RBPs relocalizes in stress-induced bodies both in the nucleoplasm and in the cytoplasm. These include paraspeckles, cytoplasmic stress granules (SG), processing bodies (P-bodies), and nucleolar caps (Anderson and Kedersha, 2006; Kedersha et al., 2005; Ninomiya et al., 2020; Parker and Sheth, 2007; Protter and Parker, 2016; Shav-Tal et al.,

2005; Sheinberger and Shav-Tal, 2017). Additionally, heterogeneous nuclear RNPs (hnRNPs) constituents are packaged in RNA-containing nuclear stress bodies, called perichromatin granules, formed by the association of Hsf1 with specific DNA loci, which drives the RNAP II- dependent transcription (Chiodi et al., 2000; Denegri et al., 2001; Mahl et al., 1989; Weighardt et al., 1999). It has been proposed that some of these ribonucleoprotein assemblies constitute mRNA reservoirs that

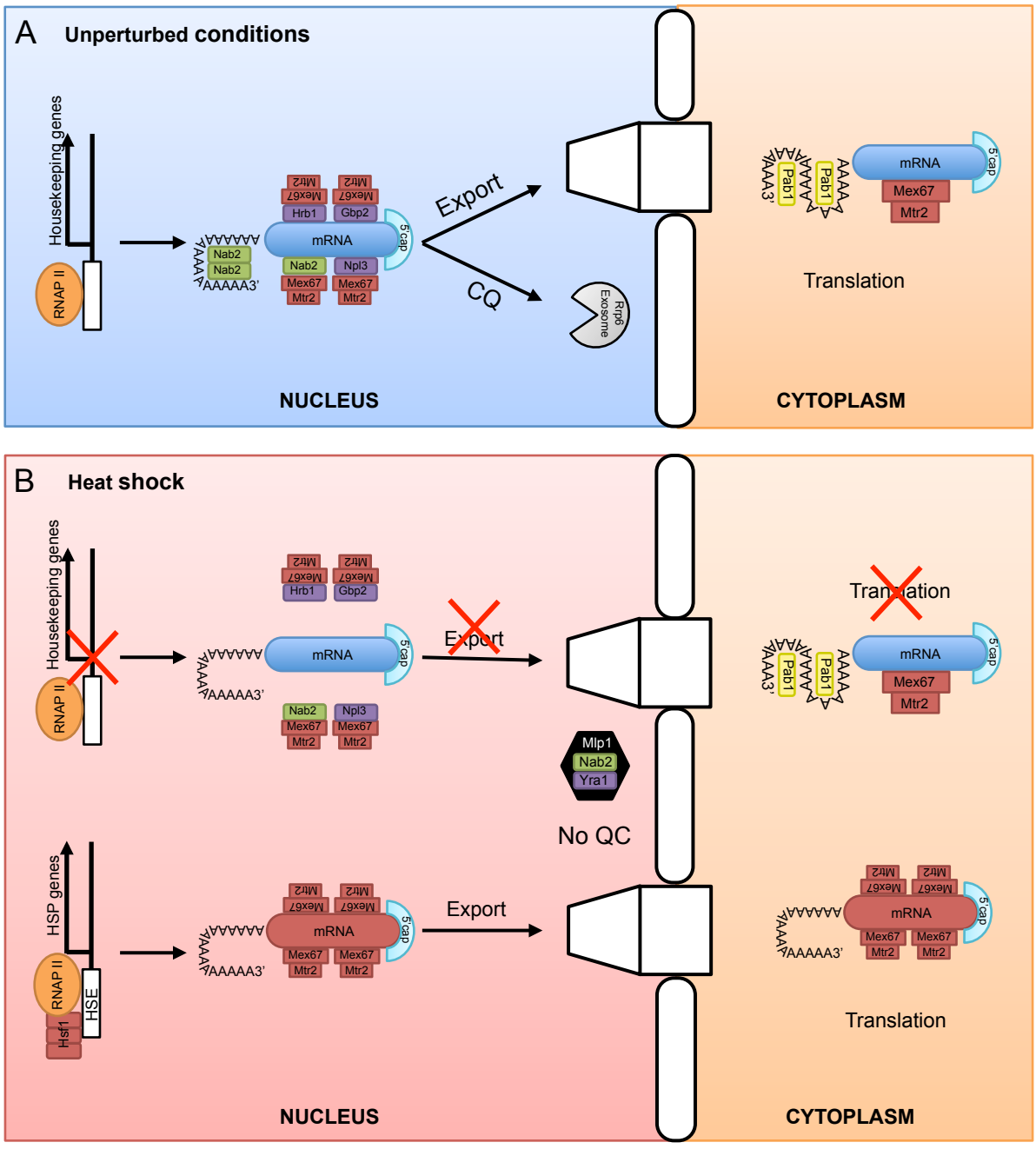

Figure I9. Schematic of mRNA biogenesis in unperturbed conditions and under heat shock in *S. cerevisiae*. (A) In unperturbed conditions adaptors proteins are loaded into housekeeping mRNAs during the maturation steps, and recruit the export factor Mex67. Once mRNPs have passed quality control and are docked to the NPC, they are exported to the cytoplasm. (B) During heat shock stress, the expression of housekeeping genes is inhibited and the export of normal transcripts is blocked, due to the dissociation of adaptors and export factors. Nab2 and Yra1 form nuclear aggregates in a Mlp1-dependent manner. Conversely, heat shock genes are highly transcribed, promoted by the binding of Hsf1 to HSE elements located in the promoters of HS genes. Hsf1-dependent recruitment of Mex67 to HS mRNAs favors the rapid export of stress responsive transcripts, which are not subjected to quality control. (Adapted from Zander et al., 2016; Zander and Krebber, 2017)

would either contribute to the degradation or protection of mRNAs. For example, cytoplasmic SGs, the best characterized structures formed under thermal stress, contain mRNAs and translation initiation factors, which has been considered a mechanism to restrict the translation of transcripts during stress conditions, while these RNAs could be ready for translation upon the recovery of physiological conditions (Buchan and Parker, 2009; Chiodi et al., 2000; Parker and Sheth, 2007).

Regarding the NPC, first studies in budding yeast proposed the existence of a specialized export pathway for HS mRNAs (Saavedra et al., 1997; Stutz et al., 1997). Later works have shown that most of the structural nuclear pore components required for normal mRNA export also participate in the HS export pathway (Hurt et al., 2000; Kendirgi et al., 2005; Rollenhagen et al., 2004; Vainberg et al., 2000). Interestingly, one of the NPC subcomplexes essential for mRNA export during heat stress in *S. cerevisiae* is the cytoplasmic Nup82 subcomplex, composed of Nup82, Rat7p, Nsp1p, Gle1p and Rip1p. In particular, Rip1 is key to stabilize the Nup82 subcomplex under heat stress conditions, since in its absence Gle1p and Rat8p delocalize from the NPC and HS mRNA export efficiency is reduced. The essentiality of Rip1 during heat shock could be due to a direct role as binding site during mRNA export or to an indirect role in the maintenance of NPC integrity (Hodge et al., 2011; Rollenhagen et al., 2004; Saavedra et al., 1997; Strahm et al., 1999). Moreover, *Sc*Gle2, homolog of Rae1, has been shown to dissociated from the NPC under heat shock, while its interacting partners Rip1p and Nup116p remain associated, which has been attributed to changes in the membrane fluidity (Izawa et al., 2004; Vigh et al., 2007). On the other hand, at the nucleoplasmic side of the NPC, it has been observed that heat shock results in the dissociation of the nuclear basket TPRs, Mlp1/2, and their accumulation in nuclear foci together with the RNA-binding proteins Yra1 and Nab2, in a sort of mechanism to inhibit the quality control and export of normal mRNAs, while promoting the export of HS mRNAs (Carmody et al., 2010; Zander et al., 2016; Zander and Krebber, 2017).

- **Nuclear reorganization during heat shock**

Earlier studies described that heat shock cause drastic changes in the structural organization of the nucleus, observed as chromatin rearrangement and nucleolar disruption (Jolly et al., 1999; Welch and Suhan, 1985). It was hypothesize that the disassembly of macromolecular complexes and the inhibition of splicing and mRNA export could be associated to this nuclear reorganization. More recent research has highlighted that nuclear structure is dynamically and reversibly remodeled upon a thermal stress in most of the studied eukaryotes (Bond, 2006; Boulon et al., 2010; Chowdhary et al., 2017). For instance, Hsf1 can dynamically rearrange the 3D organization of yeast genome by driving the coalescence of its target genes (Chowdhary et al., 2019; Ray et al., 2019).

Nucleolus is the ribosome factory of cells, a membrane-less subnuclear organelle where rRNAs synthesis and processing, and ribonucleoprotein pre-assembly take place (Hernandez-Verdun et al., 2010; Raska et al., 2006; Shaw and Jordan, 1995). The nucleolus represents approximately 80% of the total transcription activity, both in yeast and in proliferating mammalian cells (Bersaglieri and

Santoro, 2019; Jacob, 1995; Warner, 1999). Besides this, several works have position the nucleolus as an emerging hub that senses and coordinates different cellular stresses, contributing to safeguard cell viability (reviewed in Boisvert et al., 2007; Boulon et al., 2010; Hayashi and Matsunaga, 2019; Mayer and Grummt, 2005; Olson, 2004; Olson et al., 2002; Yang et al., 2018). Heat shock causes structural changes in the nucleolar morphology, concomitant with the inhibition of rRNA transcription and the redistribution of many nuclear and nucleolar proteins (Andersen et al., 2005; Hayashi and Matsunaga, 2019; Jacob et al., 2013; Mayer and Grummt, 2005; Nazer et al., 2011, 2012; Nemeth and Grummt, 2018; Olson, 2004; Shav-Tal et al., 2005). Indeed, the inhibition of rRNA synthesis was suggested to be responsible for the mayor changes in the nucleolus, due to the relocation of nucleolar proteins, such as the fibrillarin ortholog Nop1 (Liu et al., 1996). However, the molecular mechanisms underlying the spatio-temporal coordination between nuclear reorganization and mRNA export inhibition are starting to be elucidated.

In the third part of this thesis work, we describe and characterize unprecedented NPC structural changes induced by HS that are concomitant with the inhibition of bulk mRNA export and the remodeling of mRNPs. Additionally, we have further studied the mechanisms and biological consequences of the heat shock-induced nuclear protein unfolding and aggregation for cell survival.

SCHIZOSACCHAROMYCES POMBE AS MODEL ORGANISM

This work has been performed using *Schizosaccharomyces pombe* as model organism. *S. pombe* is a rod-shaped unicellular eukaryote, also known as fission yeast due to its characteristic pattern of cell division by medial fission. Firstly isolated in 1893 by Paul Lindner and developed as model organism since 1946 by Urs Leupold, over the last decades *S. pombe* has become a remarkable experimental model in molecular and cellular biology (Egel, 2004; Fantes and Hoffman, 2016; Hoffman et al., 2015; Mitchison, 1990). Fission yeast offers a number of advantages as model organism. It is easily grown in the laboratory, is non-pathogenic, possesses a short generation time (2-4 hours), and it is naturally maintained as haploid cells, which facilitates the genetic analysis, although cells can also turn into diploids in certain experimental conditions (Egel, 1989, 2004). In fact, *S. pombe* cells are naturally homothallic (referred to as h^{90}), but heterothallic strains of mating types h^+ and h^- have been experimentally designed to facilitate the genetic manipulation of this organism in the laboratory. During the exponential vegetative (asexual) growth *S. pombe* cells posses a cylindrical shape of 7-14 µm in length and 3-4 µm in diameter. *S. pombe* grows by polarized growth at the cell tips, and divide symmetrically at the cell middle once cells have reached a minimal size threshold to enter into mitosis (Fig. I10 A). As in metazoans, cell division requires the assembly and contraction of an actomyosin ring, which generates two daughter cells of nearly equal size (Marks et al., 1986). In conditions of nitrogen starvation fission yeast cells are blocked in stationary phase (sometimes referred to as G0) and initiate a sexual cell cycle that starts with the conjugation of two haploid cells of opposite mating type to form a diploid zygote (Fig. I10 B). This zygote can be maintained as a diploid or undergo meiosis. During meiosis, one round of DNA replication is followed by two consecutives nuclear divisions to produce four spores, or gametes. These spores will germinate and start a vegetative cell cycle when environmental conditions are restored (Egel, 1989, 2004).

Fission yeast research started with the study the mating-type system and the sexual cell cycle (Mitchison, 1971; Mitchison, 1990), and lately centered in cell growth, mitosis and meiosis (Bresch et al., 1968; Egel, 1973). Nowadays, *S. pombe* is used for studying a wide range of cellular processes, most of which are conserved in metazoans, including cell cycle regulation, cellular morphogenesis, DNA replication, DNA damage repair, chromatin regulation and epigenetics, or chromosome dynamics, among others (Hoffman et al., 2015). Importantly, *S. pombe* is suitable for microscopic observation due to the size of cellular organelles and structures. *S. pombe* is genetically tractable, allows a highly efficient homologous recombination and its genome has been fully sequenced (Wood et al., 2002). Fission yeast genome size is 13.8 Mb and contains about 5000 open reading frames, distributed in three chromosomes: I (5,7 Mb), II (4,6 Mb) and III (3,5 Mb) (Wood et al., 2002; Wood et al., 2012). Its genome organization shares many features with higher eukaryotes: each chromosome contains a large centromere and two telomeres (Mizuguchi et al., 2015; Olsson and Bjerling, 2011); *S. pombe* possesses a highly conserved RNAi-dependent heterochromatin formation (Allshire and Ekwall, 2015; Volpe et al., 2002), has large replication origins (Mojardin et al., 2013; Xu et al., 2012),

and around one third of intron-containing genes (Wilhelm et al., 2008). Moreover, more than two third of protein coding genes possess human orthologs (Hoffman et al., 2015; Lock et al., 2018; McDowall et al., 2015; Wood et al., 2002; Wood et al., 2012). In recent years, the development of new tools, including a wide range of mutants, tagged strains and protocols (Bahler et al., 1998; Fennessy et al., 2014; Hayles et al., 2013; Kim et al., 2010; Moris et al., 2016; Sato et al., 2005; Sun et al., 2013; Tasto et al., 2001), along with high-throughput screenings and quantitative transcriptomic datasets (Carpy et al., 2014; Chen and Runge, 2009; Chen et al., 2003; Hayles et al., 2013; Marguerat et al., 2012; Matsuyama et al., 2006; Rallis and Bahler, 2016; Rhind et al., 2011; Swaffer et al., 2018) have contributed to the establishment and development of *S. pombe* as model organism. All these reasons, along with its greater similarities with human cells, have lead to the use of *S. pombe* to understand the basic principles that govern the eukaryotic cell.

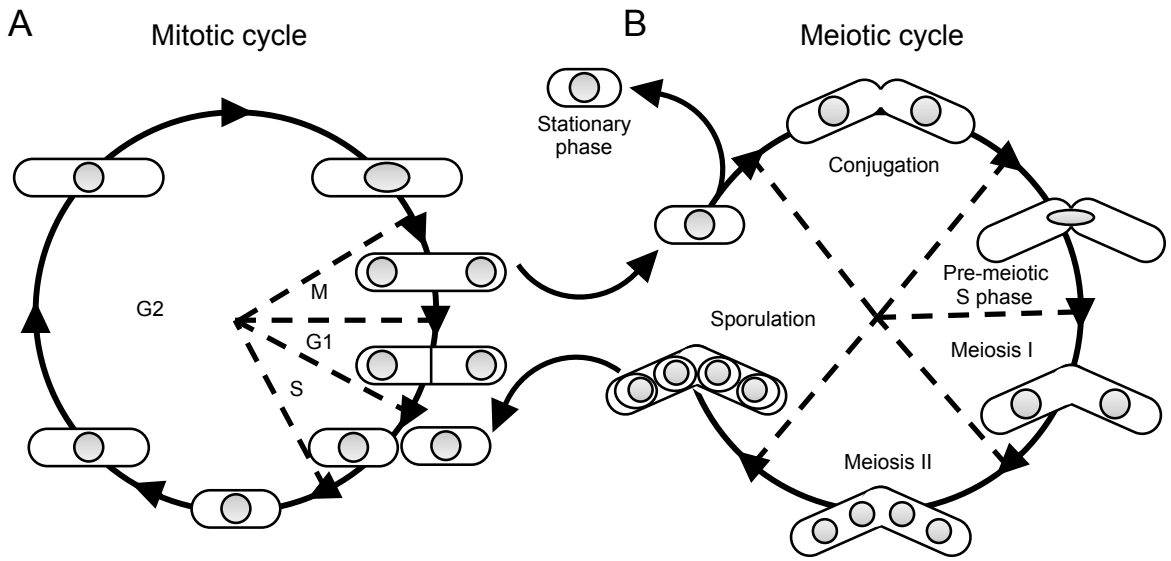

Figure I10. Cell cycle of *S. pombe* model organism. (A) During a vegetative (mitotic) cell cycle, cells proceed through four phases: G1, S (DNA replication), G2, and M (mitosis). While G2 is a long phase (about 70% of the division time), the other phases are shorter (about 10% each one). (B) In response to nutrient limitation, haploid cells are arrested into a stationary phase. However, if cells find an appropriate mating partner, they enter into a meiotic cell cycle. In the sexual or meiotic cell cycle, cells conjugate in response to mating pheromones and fuse their nuclei, to form a diploid zygote. This is followed by a pre-meiotic S phase and two meiotic divisions (I and II), in which four haploid spores are formed, packaged into a tetrad ascus. If propitious environmental conditions are restored, cells return to a vegetative cell cycle. (Adapted from dornsife.usc.edu/pombenet/fission-yeast-cell-cycle/)

ANTECEDENTS

Previous results from our lab showed that cells lacking Alm1 (*alm1Δ*) presented defective mitosis. During this work it was determined that this TPR nucleoporin is key to maintain genome stability. Analysis of chromosome segregation during mitosis in *alm1Δ* cells showed a striking phenotype of asymmetric nuclear divisions, increased loss of non-essential minichromosomes and altered ploidy. A deeper characterization of *alm1Δ* missegregation phenotypes showed uncoordinated segregation of sister chromatids, the presence of lagging chromosomes in around one third of cells, and an altered kinetochore dynamics during anaphase (Fig. I11 A-C) (Salas-Pino et al., 2017).

Since the capture of kinetochores by the spindle MTs is an error-prone process, SAC constitutes the safeguard mechanism that prevents erroneous attachments, which would lead to aneuploidy. Previous work from the lab revealed that the recruitment of the SAC components Mad1 and Mad2 to the NE during interphase is Alm1-dependent (Salas-Pino et al., 2017). This anchoring function of the SAC machinery to the nuclear basket is highly conserved among eukaryotes (Cunha-Silva et al., 2020; De Souza et al., 2009; Ding et al., 2012; Lee et al., 2008b; Lince-Faria et al., 2009; Rajanala et al., 2014; Rodriguez-Bravo et al., 2014; Schweizer et al., 2013; Scott et al., 2005). However, their localization at kinetochores during mitosis is not affected in *alm1Δ* cells. Indeed, SAC is not only functional in the absence of Alm1, but required for cell viability, as demonstrates the sustained localization of Mad2 and Bub1 at kinetochore during mitosis in *alm1Δ* mutant (Fig. I11 D-E). Together, these data suggested that the genomic instability and chromosome segregation defects of *alm1Δ* cells could be a consequence erroneous KT-MTs attachments.

We also found that the absence of Alm1 also resulted in the partial detachment of the other nuclear basket TPR protein, Nup211, from the NPC (Fig. I11 F), suggesting that Nup211 association to NPCs is partially dependent on Alm1. These two TPR protein in the fission yeast, as happens in the budding yeast, emerged from an early event of gene duplication that, furthermore, was independent in both yeasts; therefore, they are not orthologs to each other (Field et al., 2014). This offers a unique situation to study new functions that might have arisen after the duplication of the single TPR in both organisms. Consistent with this idea neither *S. cerevisiae* Mlps nor *S. pombe* Alm1 are required for cell viability (Niepel et al., 2005; Palancade et al., 2005; Salas-Pino et al., 2017), while *nup211* is an essential gene, and has been previously reported to be critical for mRNA export (Bae et al., 2009). These data suggested that both TPR proteins might have specialized and distinctive functions.

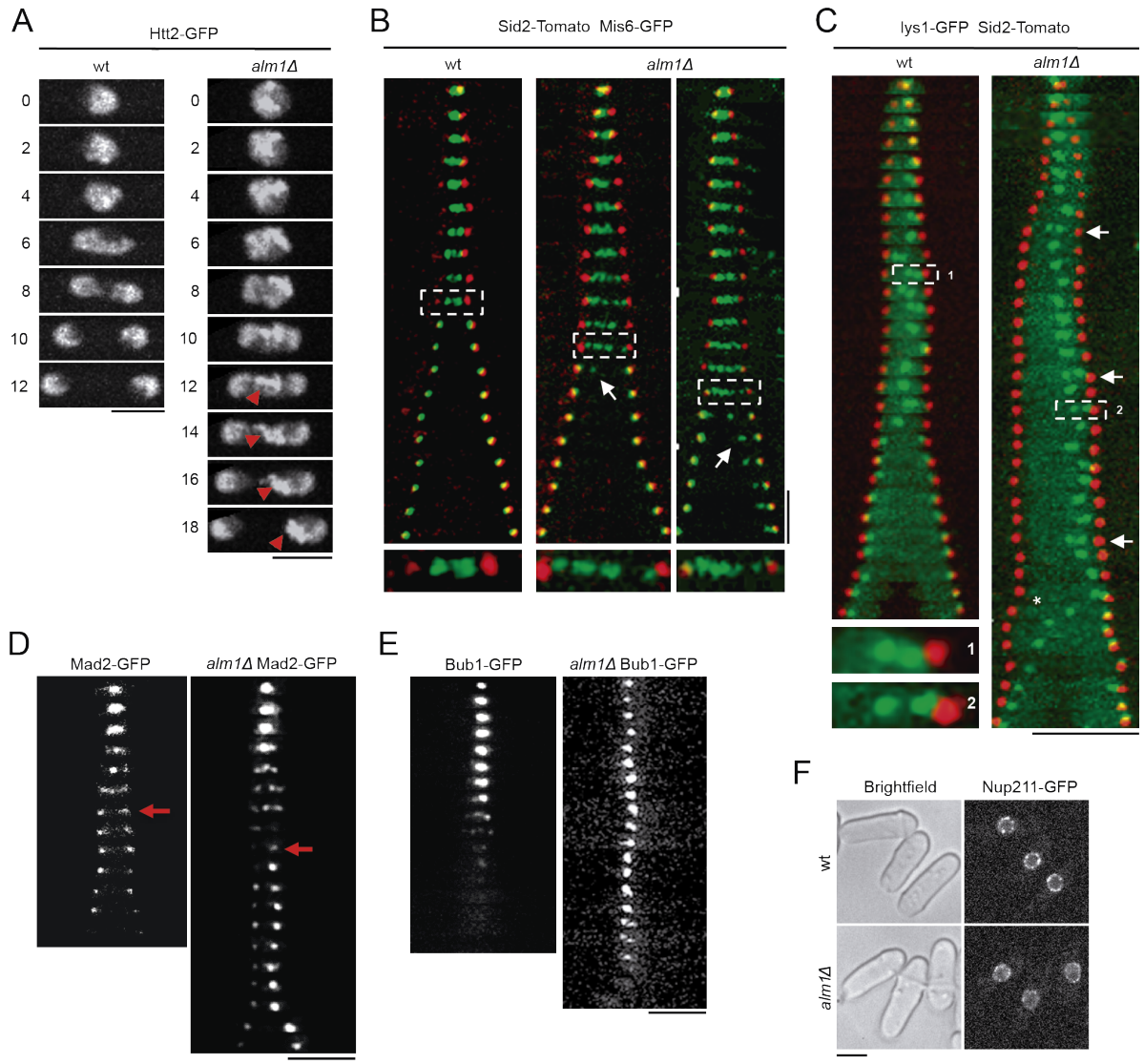

Figure I11. Lack of Alm1 results in chromosome missegregation and SAC activation. (A) Representative fluorescence microscopy images of *wt* and *alm1Δ* cells during mitosis expressing the histone H3 variant Hht2-GFP. Arrowheads indicate lagging masses of DNA. Time is indicated in minutes. Scale bar: 5 µm. (B) Representative fluorescence microscopy images of *wt* and *alm1Δ* cells during mitosis expressing sid2-Tomato (SPB marker) and mis6-GFP (kinetochore marker). Time between frames is 1 min. Arrows indicate lagging kinetochores. Magnifications of the regions indicated by dashed boxes are shown below. Scale bar: 5 µm. (C) Representative fluorescence microscopy images of *wt* and *alm1Δ* cells during mitosis expressing sid2-tomato and lacI-GFP bound to a tandem array repeats of lacO at the *lys1* locus (Chromosome I). Asterisk marks a lagging chromatid. Arrows indicate increased interkinetochore distance. Time between frames is 1 minute. Magnifications of the regions indicated by dashed boxes are shown below. Scale bar: 5 µm. (D, E) Representative fluorescence microscopy images of *wt* and *alm1Δ* cells during mitosis expressing Mad2-GFP (D) and Bub1-GFP (E). Time between frames is 1 minute. Scale bar: 5 µm. Arrows indicate the accumulation of Mad2-GFP at spindle poles. (F) Brightfield and fluorescence images of *wt* and *alm1Δ* cells expressing Nup211-GFP, grown at 25ºC. Scale bar: 5 µm. (Salas-Pino et al., 2017)

SCOPE OF THIS STUDY

The main structural elements of the nuclear basket in the fission yeast are Nup211 and Alm1 (Asakawa et al., 2019; Field et al., 2014; Salas-Pino et al., 2017), functional homologs of *S. cerevisiae* Mlp1 and Mlp2, and vertebrates TPR (Bangs et al., 1998; Cordes et al., 1997; Frosst et al., 2002; Hase et al., 2001; Kosova et al., 2000; Krull et al., 2004; Shibata et al., 2002). These nuclear basket TPR nucleoporins form a dynamic network, connecting NPCs and acting as a platform for the anchoring of a wide range of nuclear components (Niepel et al., 2013; Strambio-de-Castillia et al., 1999; Zimowska et al., 1997). Although most nuclear basket functions have seemingly been conserved along evolution, it is still unclear how the TPR nucleoporins are assembled in the fission yeast NPC and which functions do they perform. Therefore, the general objective of this thesis was to characterize the assembly and the functions of the nuclear basket TPR nucleoporins Nup211 and Alm1.

Specific objectives

1. To characterize the role of the nuclear basket nucleoporin Alm1 in chromosome segregation.
2. To study the assembly of the fission yeast nuclear basket and dissect the functions of Alm1 and Nup211 in mRNA docking and export.
3. To investigate the remodeling of the NPC-Nuclear Basket during mRNA export inhibition induced by heat shock.

RESULTS AND DISCUSSION

Chapter 1

The fission yeast nucleoporin Alm1 is required for proteasomal degradation of kinetochore components

1.1 SGA assay based on TBZ sensitivity identifies genetic factors that contribute to maintain KT structure and functionality.

It has been described that mutants affecting centromere and kinetochore function show lagging chromosomes and uneven DNA segregations, similar to the phenotypes observed in the *alm1*-deleted mutant (Fig. I11 A-C), as well as sensitivity to microtubule-disturbing drugs (Ekwall et al., 1999; Pidoux et al., 2003; Takahashi et al., 1994). To further characterize the role of *alm1* in chromosome segregation, we assessed whether the presence of the microtubule-destabilising drug TBZ affected cell viability of the *alm1Δ* mutant. For that, we initially performed a drop assay in plates containing a concentration of 15 µg/ml of thiabendazole (TBZ) (Fig. 1.1 A), which is tolerated by the wildtype strain. As positive control we used *clr4Δ* mutant. Clr4 is a histone H3 lysine methyltransferase required for centromere silencing and kinetochore function, and its deletion is known to be hypersensitive to TBZ (Zhang et al., 2008). We found that *alm1Δ* cells are sensitive to microtubule perturbation, since this mutant exhibits a growth inhibition in the presence of TBZ, compared to the wildtype strain, although not as pronounced as *clr4* deletion (Fig. 1.1 A).

In order to gain further insights into the functional role of Alm1, we took advantage of the TBZ sensitivity of *alm1Δ* cells to screen for genome wide genetic interactions related to kinetochore function. We followed a high-throughput genetic approach by performing a Synthetic Genetic Array (SGA) assay (Tong et al., 2001) in the presence of TBZ. First, *alm1Δ* mutant was automatically crossed to a collection of 3,400 viable haploid single deletion mutants (Bioneer library v.3), and plated onto media with and without TBZ. Then, to obtain quantitative data of possible genetic interactions, measurements of single and double mutant colony-size were used as readout of cellular fitness (Fig. 1.1 B, see Methods: SGA assay for further information). Finally, we performed a clustering analysis according to the growth of single and double mutants in media with and without TBZ, selecting those gene clusters in which the degree TBZ sentisitivity of double mutants with *alm1Δ* is greater than in the single mutants (Fig. 1.1 C). Gene Ontology (GO) enrichment analysis for biological processes of those genes that show synthetic interaction with the *alm1Δ* mutant (Fig. 1.1 D) revealed an enrichment of genes encoding for SAC components (*e.g. bub1*, *mad1* and *mad2,* p-value 9.08E-03), elements associated to kinetochore-microtubule attachment (*e.g. spc19*, *dis2* or *ask1, p-value* 3.54E-02), proteins involved in ubiquitin-dependent proteolysis (*e.g. ubp2,* p-value 2.23E-02), chromatin regulators (*e.g. spt6, pdp3, fft3*, and Swr1 complex subunits, p-value 4.27E-02), regulation of mRNA processing (GO:0050684, *dsk1, tls1,* p-value 1.93E-02), ribonucleoprotein complex biogenesis (GO:0022613, *mex67, nxt1, sen1,* p-value 4.27E-02), positive regulation of stress-activated protein kinase signaling cascade (GO:0070304, *mpr1, mcs4*, p-value 2.91E-02), response to stress (GO:0006950, p-value 4.42E-02) and *de novo* protein folding (GO:0006458, *sks2, btf3*, p-value 2.91E-02), among others.

The enrichment in SAC and kinetochore components in this analysis suggests a possible functional relationship between Alm1 and kinetochores that might explain the genetic instability and TBZ sensibility of *alm1Δ* cells. Notice that this enrichment in kinetochore mutants could be understimated

as most of the centromere and kinetochore components are essential for cell survival, and the SGA was performed with a deletion library containing non-essential genes. Therefore, we next examined possible genetic interactions between *alm1Δ* and additional mutants of kinetochore components using

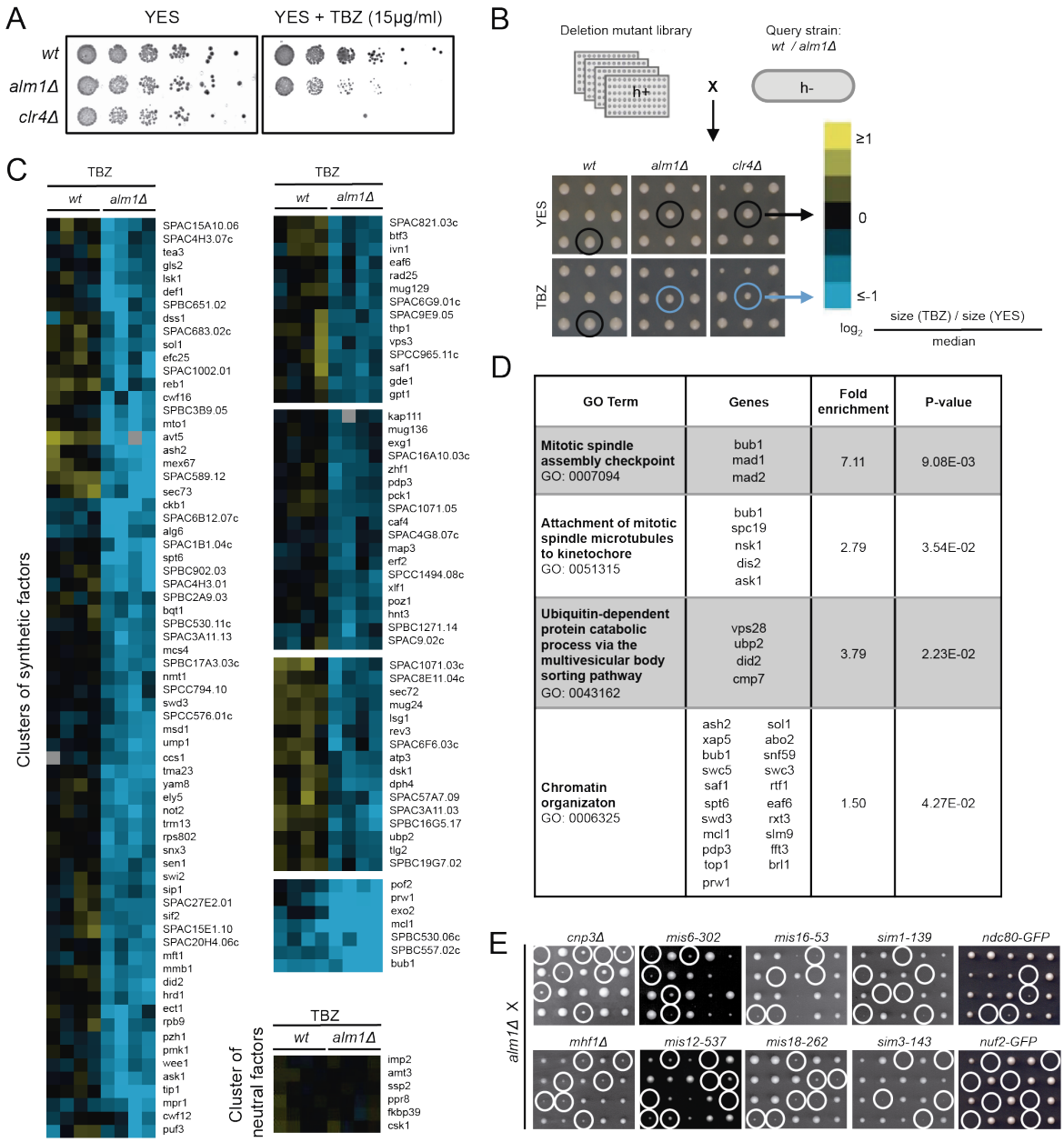

GO Term	Genes	Fold enrichment	P-value
Mitotic spindle assembly checkpoint GO: 0007094	bub1 mad1 mad2	7.11	9.08E-03
Attachment of mitotic spindle microtubules to kinetochore GO: 0051315	bub1 spc19 nsk1 dis2 ask1	2.79	3.54E-02
Ubiquitin-dependent protein catabolic process via the multivesicular body sorting pathway GO: 0043162	vps28 ubp2 did2 cmp7	3.79	2.23E-02
Chromatin organizaton GO: 0006325	ash2 xap5 bub1 swc5 saf1 spt6 swd3 mcl1 pdp3 top1 prw1 sol1 abo2 snf59 swc3 rtf1 eaf6 rxt3 slm9 fft3 brl1	1.50	4.27E-02

Figure 1.1. SGA assay based on TBZ sensitivity identifies genetic factors that contribute to maintain KT structure and functionality. (A) Drop assay showing sensitivity to TBZ of *wt*, *alm1Δ* and *clr4Δ* cells. Cells spotted correspond to 5-fold dilutions with an initial O.D. of 0.3. (B) Flow-through of the SGA screenning to search for genetic interactors of *alm1Δ* mutant in TBZ. *wt* and *alm1Δ* query strains were crossed with the *Bioneer* haploid deletion mutant library (*v.3*), and single and double mutants were spotted on YES and TBZ-containing plates. The colony size of single and double mutants was measured in both media, and we compared the ratio with the median ratio. Blue indicates small colony size and yellow indicates large colony size. See Materials and Methods: SGA assay for further information. (C) Gene clusters showing those mutants with a negative genetic interaction with *alm1Δ* in TBZ sensitivity. Clustering analysis showing one group of neutral genes with no sensitivity to TBZ, neither in the single deleted mutant nor the double mutant with *alm1Δ* (bottom). Blue indicates synthetic interaction, yellow indicates suppressive interaction, black indicates no interaction, and grey indicates the absence of data. Data correspond to four independent replica. (D) GO enrichment analysis for biological processes of those genes obtained in the TBZ-based SGA screenning that show a synthetic interaction with *alm1Δ* mutant. The table contains the corresponding fold change and p-value of the indicated GO groups. (E) Tetrad dissection analysis of crosses between *alm1Δ* and strains with the indicated genotypes. Double mutants between *alm1Δ and* the indicated mutant backgrounds are encircled.

available thermosensitive alleles (Fig. 1.1 E). Tetrad dissection showed that *alm1Δ* is synthetically lethal with all centromere and kinetochore mutants used in this assay (*i.e. cnp3*, *mhf1*, *mis6* or *mis12)*. Furthermore, *alm1* deletion resulted to be lethal in combination with alleles of kinetochore components that are simply tagged with GFP (Ndc80-GFP and Nuf2-GFP). This data pointed to a functional relationship between Alm1 and components of the kinetochore and centromeric chromatin.

1.2 Centromeric chromatin is altered in the absence of Alm1.

Kinetochore assembly and chromatin state are intrinsically linked; while loading of kinetochore proteins into the central core domain affects chromatin silencing, heterochromatin contribute to kinetochore assembly by creating an appropriate chromatin environment (Pidoux and Allshire, 2004). Consistently, mutants affecting chromatin silencing at centromeres usually show defects in kinetochore assembly that leads to high levels of lagging chromosomes and are also sensitive to MT-disrupting drugs (Ekwall et al., 1999; Gregan et al., 2007). The negative genetic interaction between *alm1Δ* and deletion mutants involved in chromatin organization found in the SGA (Fig. 1.1 D), prompted us to test whether the chromatin silencing state at centromeres where altered in *alm1* deletion.

Fission yeast centromeres are composed of two domains: the heterochromatin outer repeats (containing the *otr* and the *imr* repeats) and the central core (*cnt*), both of which are transcriptionally silenced (Pidoux and Allshire, 2005). To examine the transcriptional state of the centromeric region we used a fission yeast strain in which the reported gene *ura4*$^{+}$ is inserted at distinct locations within the centromere, such as the *imr* repeats of chromosome I (*imr1L*) (Fig. 1.2 A) and the central core of chromosome II, *cnt2* (Fig. 1.2 B). This allows studying in a simple manner the centromeric silencing by monitoring cell growth in nonselective (EMM), selective (EMM-URA), and counter selective 5-fluoro-orotic acid (FOA) plates (Allshire et al., 1994). The FOA is a toxic compound that blocks the growth of *ura4*$^{+}$ cells (Boeke et al., 1984; Boeke et al., 1987). As described, wildtype cells in which the *ura4*$^{+}$ gene was inserted at *imr1* (*imr1L:ura4*$^{+}$*)* showed a reduced growth on plates without uracil (EMM-Ura), and normal growth on plates containing FOA, indicative of low *ura4+* expression. However, compared to control wiltype cells, the *alm1Δ* mutant showed a reduced growth on EMM-Ura plates, and a increased growth on EMM+FOA plates. The decreased *ura4*$^{+}$ expression suggests that this pericentromeric domain could be more silenced in *alm1Δ* mutant (Fig. 1.2 C). On the other hand, when assessing the silencing behavior of the central core region (*cnt2:ura4*$^{+}$), wildtype and *alm1Δ* mutant cells displayed apparently the same behavior (Fig. 1.2 D). This could be due to the extremely reduced levels of *ura4*$^{+}$ expression when inserted at the central core. Then, we assessed the centromeric silencing state by measuring the levels of transcription from the heterochromatin repeats (*imr, dg* and *dh*) and the central core (*cnt*) by reverse transcriptase quantitative PCR (RT-qPCR). We observed a statistically significant reduction in the abundance of *dg* and *imr* transcripts in the *alm1Δ* genetic background in comparison to the wildtype (Fig. 1.2 E). This is consistent with the results obtained in the cell growth-based silencing assay, and is indicative of a more repressed

heterochromatin at these centromeric regions. Additionally, we detected a 3-fold increase in transcripts originated from the centromeric central core in the *alm1Δ* background (Fig. 1.2 E), which is indicative of derepressed chromatin at this region.

Given that centromere and telomere silencing is regulated by the same heterochromatin formation pathways (Nakayama et al., 2001; Shankaranarayana et al., 2003; Thon and Verhein-Hansen, 2000; Verdel and Moazed, 2005), we examined the effect of deleting *alm1* on heterochromatic telomere silencing, specifically in *tlh1/2*, two coding sequences located at the end of chromosomes I and II, and in *TERRA* (telomeric repeat-containing RNA), a long non-coding RNA (lncRNA) part of the telomeric heterochromatin (Luke and Lingner, 2009). RT-qPCR revealed that *alm1Δ* cells display an increased transcription derived from telomere heterochromatin repeats, both in *tlh1/2* and *TERRA*, similar to the results obtained from centromeric central core (Fig. 1.2 F).

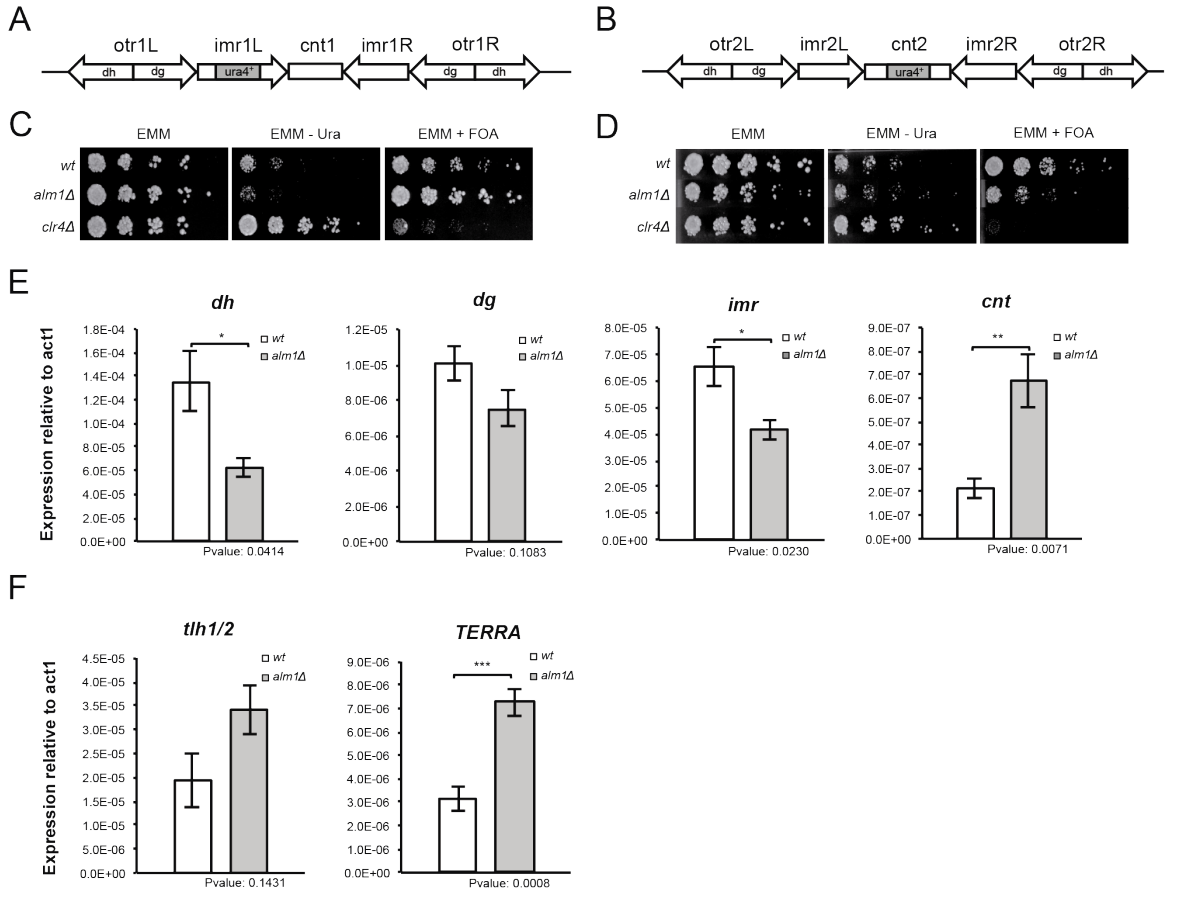

Figure 1.2. Centromeric chromatin is altered in the absence of Alm1. (A) Schematic representation of centromere I with the ura4+ reporter gene inserted in the left innermost repeat (*imr1L*) region. (B) Schematic representation of centromere II with the ura4+ reporter gene inserted in the central core (*cnt2*) region. (C) Silencing assay of *wt*, *alm1Δ* and *clr4Δ* strains harboring the ura4$^+$ reporter gene inserted in the *imrL1* region of centromere I as depicted in A. Cells were plated on nonselective EMM, EMM-Ura and EMM+FOA media, and grown at 25ºC. Spotted cells correspond to 5-fold dilutions with an initial O.D. of 0.2. (D) Silencing assay of *wt*, *alm1Δ* and *clr4Δ* strain backgrounds harboring the ura4$^+$ reporter gene inserted in the cnt2, as represented in B. Cells were plated on nonselective EMM, EMM-Ura and EMM+FOA media, and grown at 25ºC. Spotted cells correspond to 5-fold dilutions with an initial O.D. of 0.2. (E) RT-qPCR analysis of centromere I (*dh, dg, imr and cnt*) transcript levels (normalized to *act1*$^+$ transcript levels) of *wt* and *alm1Δ* mutant. Error bars represent SEM. n =5. (F) RT-qPCR analysis of telomere (*tlh1/2* and *TERRA*) transcript levels (normalized to act1$^+$ transcript levels) of *wt* and *alm1Δ* mutant. Error bars represent SEM. n =5. *, $P < 0.05$; **, $P < 0.001$; ***, $P < 0.001$.

Together, these results demonstrate that centromeric chromatin silencing is altered in the absence of *alm1*, being more repressed in the pericentromeric regions, and derepressed at the central core region, where kinetochores are assembled. Furthermore, this chromatin deregulation is not exclusive of centromeres, as telomeric chomatin silencing is also altered in *alm1*-deleted cells. Thus, these observations reveal an unexpected functional connection between Alm1 and the state of chromatin silencing. As the silencing state of centromeric chromatin is critical for the assembly of fully functional kinetochores, we wondered whether this could have an impact in the kinetochore structure of *alm1* mutant.

1.3 *alm1Δ* mutant shows abnormal accumulation of centromere–kinetochore proteins.

Kinetochores are assembled over the central core domain of centromeres, which contains the histone H3 variant CENP-A/Cnp1 (Cse4 in *S. cerevisiae*). CENP-A/Cnp1, together with the noncanonical nucleosome complex CENP-S-T-W-X (Mhf1, Cnp20, New1 and Mhf2), define the landmark of central core chromatin (Fig. I5) (Hori et al., 2013; Meluh et al., 1998; Nishino et al., 2013), and thus are essential for kinetochore establishment and function (Amano et al., 2009; Folco et al., 2015; Hori et al., 2013; Takeuchi et al., 2014). The synthetic lethality between *alm1Δ* mutant and deletions of non-essential centromeric and kinetochore components found in the SGA, prompted us to test whether Alm1 could have a role in the loading of Cnp1 and Mhf1/Cnp20/New1/Mhf2 complex into this region. To do that, we analyzed by fluorescence microscopy the localization and accumulation of these centromere components, expressed from their native locus, in *wt* and *alm1Δ* cells. While the levels of Cnp1 were apparently unaffected in *alm1Δ* cells (Fig. 1.3 A and B), several of these centromeric proteins were deregulated, although the most remarkable difference found was in Cnp20, with a 1.3-fold increase in signal intensity in *alm1Δ* compared to the wildtype.

Previous works have defined Cnp1 as a scaffold that determines the site of kinetochore assembly by interacting with inner kinetochrore proteins, such as CENP-C/Cnp3 (Klare et al., 2015; Przewloka et al., 2011; Tanaka et al., 2009). In turn, Cnp3 is known to be a structural hub for kinetochrore assembly as it participates in the recruitment of several kinetochore components, such as Mis6 complex-containing CENP-L/Fta1 and CENP-L/Sim4, and Pcs1-Mde4 monopolin complex (Carroll et al., 2010; Corbett et al., 2010; Tanaka et al., 2009). Analysis of these centromere-kinetochore proteins in *wt* and *alm1Δ* cells revealed significant increased levels of Cnp3, with a 1.8-fold increase in *alm1Δ* compared to the wildtype (Fig. 1.3 A and C). Other kinetochore components, such as Mde4, and Fta1 were also upregulated (Fig. 1.3 C). Western blot analysis showed that the over-accumulation of Cnp3 at kinetochores in the *alm1Δ* mutant correlates with an increase in total Cnp3 protein, but not Cnp20 protein (Fig. 1.3 D). To discard the possibility that Alm1 could have an indirect effect in the accumulation of these kinetochore proteins by regulating their transcription, we performed RT-PCR of *cnp1*, *cnp20* and *cnp3*. The analysis of steady-state levels of both *cnp20* and *cnp3* mRNAs did not show significant differences compared to those of wildtype cells (Fig. 1.3 E). This suggests that the

increased levels of Cnp3 observed in *alm1Δ* cells are not due to their transcriptional upregulation, but instead, it might be the result of deregulated protein stability or turnover.

It has been shown that *cnp1* overexpression leads to its spreading from the centromeric central core to adjacent heterochromatin regions (Castillo et al., 2013; Choi et al., 2012; Gonzalez et al., 2014). This results in altered chromatin silencing at centromeres that leads to chromosome missegregation (Castillo et al., 2007), similar to *alm1*-deletion phenotypes. To test whether the excess of Cnp3 in *alm1Δ* spreads laterally from the central core towards adjacent *imr* regions, we performed chromatin immunoprecipitation experiments (ChIP) using endogenously expressed Cnp3-GFP. Cnp3 distribution pattern at centromeric region in *alm1Δ* was similar to the wildtype (Salas-Pino et al., 2017), indicating that the excess of Cnp3 protein in *alm1Δ* mutant cells does not spread into adjacent pericentromeric chromatin. Thus, taken together, the synthetic lethality with kinetochore mutants and

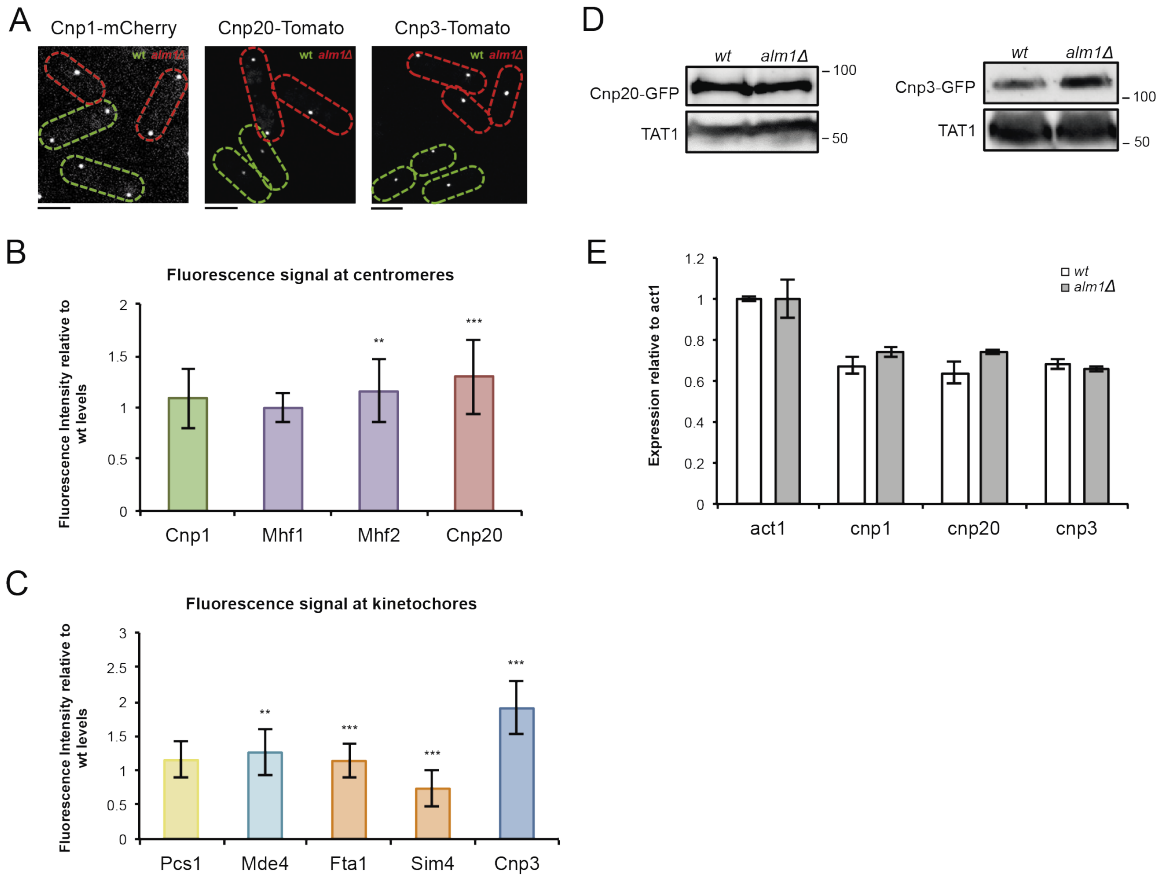

Figure 1.3. *alm1Δ* mutant shows abnormal accumulation of centromere–kinetochore proteins. (A) Representative fluorescence microscopy images of *wt* (delineated in green) and *alm1Δ* (delineated in red) cells expressing Cnp1-mCherry, Cnp20-Tomato and Cnp3-Tomato from their endogenous promoter. Maximal projections of 18 z-sections 0.3 µm step size. Scale bar: 5 µm. (B) Quantification of the indicated centromere components (Cnp1-mCherry, Mhf1-GFP, Mhf2-GFP, Cnp20-GFP) by fluorescence microscopy, colored as represented in Fig. I5. Graphs represent mean fluorescence intensity levels in *alm1Δ* cells relative to *wt* cells. Error bars represent SD. n=50. (C) Quantification of the indicated kinetochore components (Pcs1-GFP, Mde4-GFP, Fta1-GFP, Sim4-Tomato and Cnp3-Tomato) by fluorescence microscopy, colored as represented in Fig. I5. Graphs represent mean fluorescence intensity levels in *alm1Δ* cells relative to *wt* cells. Error bars represent SD. n=50. **, $P < 0.001$; ***, $P < 0.001$. (D) Western blot analysis of total Cnp20-GFP protein (left panel) and Cnp3-GFP protein (right panel) from the indicated strains using anti-GFP mAb to detect Cnp20-GFP and Cnp3-GFP (upper panel), and anti-tubulin (TAT1) mAb as a loading control (lower panel). Positions of molecular weight markers are indicated in kDa. (E) RT-PCR analysis of *act1* (control), *cnp1*, *cnp20*, and *cnp3* mRNA levels, of *wt* and *alm1Δ* cells. Graph represents the average transcript levels normalized to *act1*$^{+}$ mRNA levels of three independent biological repeats. Error bars represent SD.

the abnormal accumulation of centromere-kinetochore proteins show that centromere-kinetochrore structure is altered in *alm1Δ* cells. This would result in a not fully functional kinetochore assembly that might impair microtubule-kinetochore attachment, leading to chromosome missegregation and, consequently, to genome instability in the absence of Alm1.

1.4 Ectopic accumulation of Cnp3 at kinetochores impairs chromosome segregation.

We speculated that if the chromosome missegregations observed in *alm1Δ* cells are caused by the abnormal accumulation of Cnp3 at kinetochores, then, the overexpression of this protein in wildtype cells would lead to similar chromosome segregation defects. To test this hypothesis, we ectopically expressed an additional copy of *cnp3-GFP* under the control of the medium strenght *nmt41* promoter (*pINT-cnp3-GFP*) (Fennessy et al., 2014) in wildtype and *alm1Δ* backgrounds. Fluorescence microscopy analysis confirmed that, in conditions of moderate overexpression (*i.e.* in rich medium), Cnp3-GFP levels at the kinetochore are increased by 2.4-fold in a wildtype background and 1.4-fold in the *alm1Δ* background, compared to their corresponding non-overexpression control backgrounds (Fig. 1.4 A and B). Similar results were obtained when analyzing total Cnp3-GFP protein levels by western blot (Fig. 1.4 C). Once confirmed that moderated Cnp3 overexpression resulted in its accumulation at kinetochores, we further examined chromosome segregation by time-lapse fluorescence microscopy in these cells (Fig. 1.4 D and E). We found that, similar to *cnp1* overexpression, an excess of Cnp3 results in an increased of lagging chromosomes both in wildtype and in *alm1Δ* cells (Fig. 1.4 D and E). Thus, an excess of Cnp3 at kinetochores is enough to phenocopy chromosome segregation defects observed in the *alm1* deletion.

Having addressed the consequences of Cnp3 overexpression, we next tested whether the reduction of Cnp3 kinetochore levels in a *alm1Δ* background would rescue its chromosome missegregation phenotype. For that, we replaced *cnp3* endogenous promoter by the weak thiamine-repressible *nmt81* promoter in the *alm1Δ* background. When expression from the *nmt81* promoter is inhibited by thiamine, we still observed Cnp3 localization at the kinetochores, since expression is not completely abolished (Fig. 1.4 F). Under these conditions, Cnp3 accumulation at kinetochores was reduced to levels comparable to wildtype cells (Fig. 1.4 G), and total Cnp3 protein decreased accordingly (Fig. 1.4 H). Consistently, chromosome segregation defects were reduced compared to those of *alm1Δ* cells, although not to the levels observed in wildtype cells (Fig. 1.4 I).

Therefore, from this set of experiments we concluded that the excess of Cnp3 could be responsible for the defective chromosome segregations in the *alm1Δ* mutant. Nevertheless, we cannot rule out the possibility that the other kinetochore components that are deregulated in the absence of Alm1 may also contribute to chromosome missegregation.

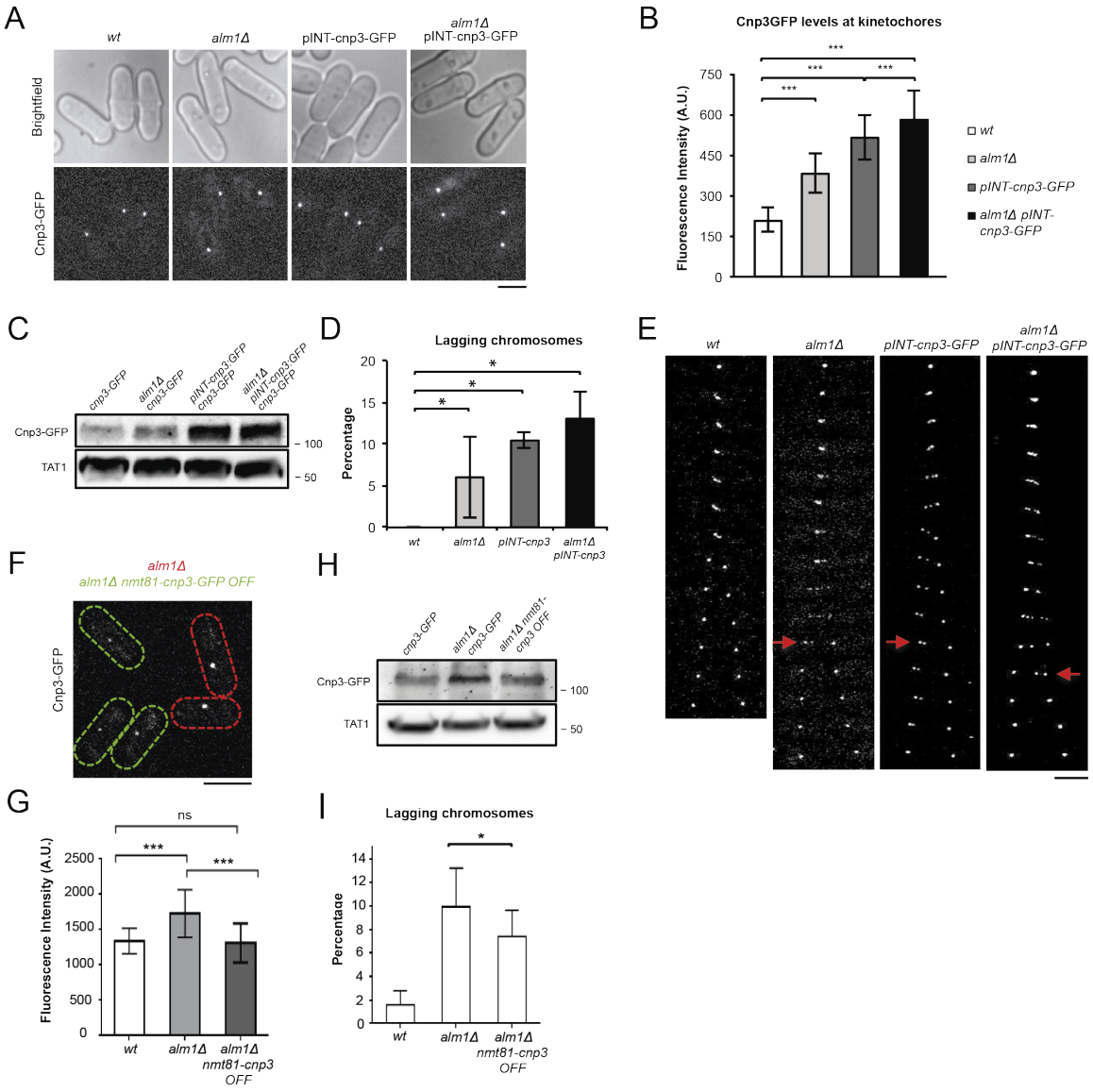

Figure 1.4. Ectopic accumulation of Cnp3 at kinetochores impairs chromosome segregation. (A) Representative fluorescence microscopy images of *wt* and *alm1Δ* cells expressing *cnp3-GFP* from their endogenous locus, and *wt* and *alm1Δ* cells expressing an additional copy of *cnp3-GFP* from the medium strength promoter *nmt41* (pINT-Cnp3-GFP) in repressed conditions (YES media). Maximal projections of 18 0.3 µm z sections. Scale bar: 5 µm. (B) Quantification of kinetochore Cnp3-GFP intensity levels of the indicated backgrounds. Graph represents mean fluorescence intensity levels and error bars represent SD. n= 50. (C) Western blot analysis of total Cnp3-GFP protein of cultures with the indicated genetic backgrounds using anti-GFP mAb (upper panel) to detect Cnp3-GFP and anti tubulin mAb (TAT1) as loading control (lower panel). Positions of molecular weight markers are indicated in kDa. (D) Quantification of mitotic defects (lagging kinetochores during anaphase B) of the indicated strains by *in vivo* fluorescence microscopy. Graphs represent mean and SD. n= 50. (E) Time-lapse fluorescence images of the indicated strains showing kinetochore segregation during mitosis using Cnp3-GFP as kinetochore marker. Arrows denote lagging kinetochores. Time between frames is 2 minutes. Maximal projections of 18 0.3 µm z sections. Scale bar: 5 µm. (F) Representative fluorescence microscopy images of *alm1Δ* cells expressing *cnp3-GFP* from the endogenous promoter (delineated in red) and *alm1Δ* cells expressing *cnp3-GFP* from the *nmt81* promoter (delineated in green) under repressed conditions (EMM+thiamine). Maximal projections of 18 0.3 µm z sections. Scale bar: 5 µm. (G) Quantification of kinetochore Cnp3-GFP intensity levels of the indicated backgrounds. Graph represents mean fluorescence intensity levels. Error bars represent SD. n= 50. (H) Western blot analysis of total Cnp3-GFP protein of cultures with the indicated genetic backgrounds grown in EMM+thiamine, using anti-GFP mAb (upper panel) to detect Cnp3-GFP and anti tubulin mAb (TAT1) as loading control (lower panel). Positions of molecular weight markers are indicated in kDa. (I) Quantification of mitotic defects (lagging kinetochores during anaphase B) of the indicated strains by *in vivo* fluorescence microscopy. Graphs represent mean and SD. n= 50. *, $P < 0.05$; **, $P < 0.001$; ***, $P < 0.001$.

1.5 Proteasome function and localization are required for stoichiometric accumulation of Cnp3 at kinetochores.

Previously, we have shown that the increased levels of Cnp3 in *alm1Δ* cells were not due to its transcriptional upregulation (Fig. 1.3 E), which suggest that Cnp3 stability or turnover could be deregulated in the absence of Alm1. It is known that centromeric levels and distribution of CENP-A/Cnp1 are regulated by ubiquitin-dependent proteasome degradation, a mechanism that has been conserved from yeast to humans (Collins et al., 2004; Kitagawa et al., 2014; Moreno-Moreno et al., 2006; Ranjitkar et al., 2010). To test whether Cnp3 is regulated by proteasomal degradation, we analyzed Cnp3 protein levels after compromising proteasome activity. For that, we used a thermosensitive allele of *mts4*, which encodes for a non-ATPase subunit of the 19S regulatory particle of the proteasome (Wilkinson et al., 1997). Quantification of Cnp3-GFP levels by fluorescence microscopy showed a significant increased of Cnp3 accumulation at kinetochores in the *mst4* mutant relative to the wildtype background, both at permissive (by 2-fold increase) and at restrictive temperature (by 3.6 fold) (Fig. 1.5 A). Of note, while the single mutants *mts4* and *alm1Δ* reached similar Cnp3 levels, the double mutant *alm1Δ mts4* showed a further increase in Cnp3 levels at kinetochores at the permissive temperature (Fig. 1.5 A). These results were further confirmed by western blot analysis of total Cnp3-GFP protein levels (Fig. 1.5 B), suggesting that Cnp3 turnover is regulated by ubiquitin-dependent proteolysis. We also determined that, even at permissive temperature, the *mts*4 proteasome mutant displayed a 2-fold increase of lagging chromosomes compared to wildtype cells (Fig. 1.5 C).

The 26S proteasome localizes to different cellular compartments, although it is accumulated in the nucleus both in yeast as in animal cells (Amsterdam et al., 1993; Chowdhury and Enenkel, 2015; Enenkel et al., 1998; Russell et al., 1999; Wilkinson et al., 1998). In fission yeast, the enrichment of the proteasome at the NE depends on Cut8. Consistently, this protein is essential for cell viability, specially at elevated temperatures (Takeda and Yanagida, 2005; Tatebe and Yanagida, 2000). First, we checked by live-cell microscopy that in the *cut8-563* thermosensitive mutant (Samejima and Yanagida, 1994) the proteasome localization at the NE is reduced (Fig. 1.5 D). Then, we analyzed whether the proper localization of the proteasome was required for regulating Cnp3 turnover, by quantifying Cnp3 kinetochore levels in *cut8-563* mutant cells. Results confirmed that compromising the proteasome localization at the nuclear envelope results in the aberrant accumulation of Cnp3 at kinetochores. This was observed even at permissive temperature, but especially at restrictive growing conditions, with a further 2-fold increase of Cnp3 (Fig. 1.5 E). This was further confirmed by western blot analysis (Fig. 1.5 F). Moreover, *alm1Δ* and *cut8-563* showed a synthetically lethal genetic interaction. Altogether, these results suggest that Cut8 and the proteasome itself are required for proper degradation of Cnp3.

Then, we followed a biochemical approach to further confirm that the proteasome indeed regulates kinetochore composition and stoichiometry. First, we analyzed by western blot Cnp3 protein stability in

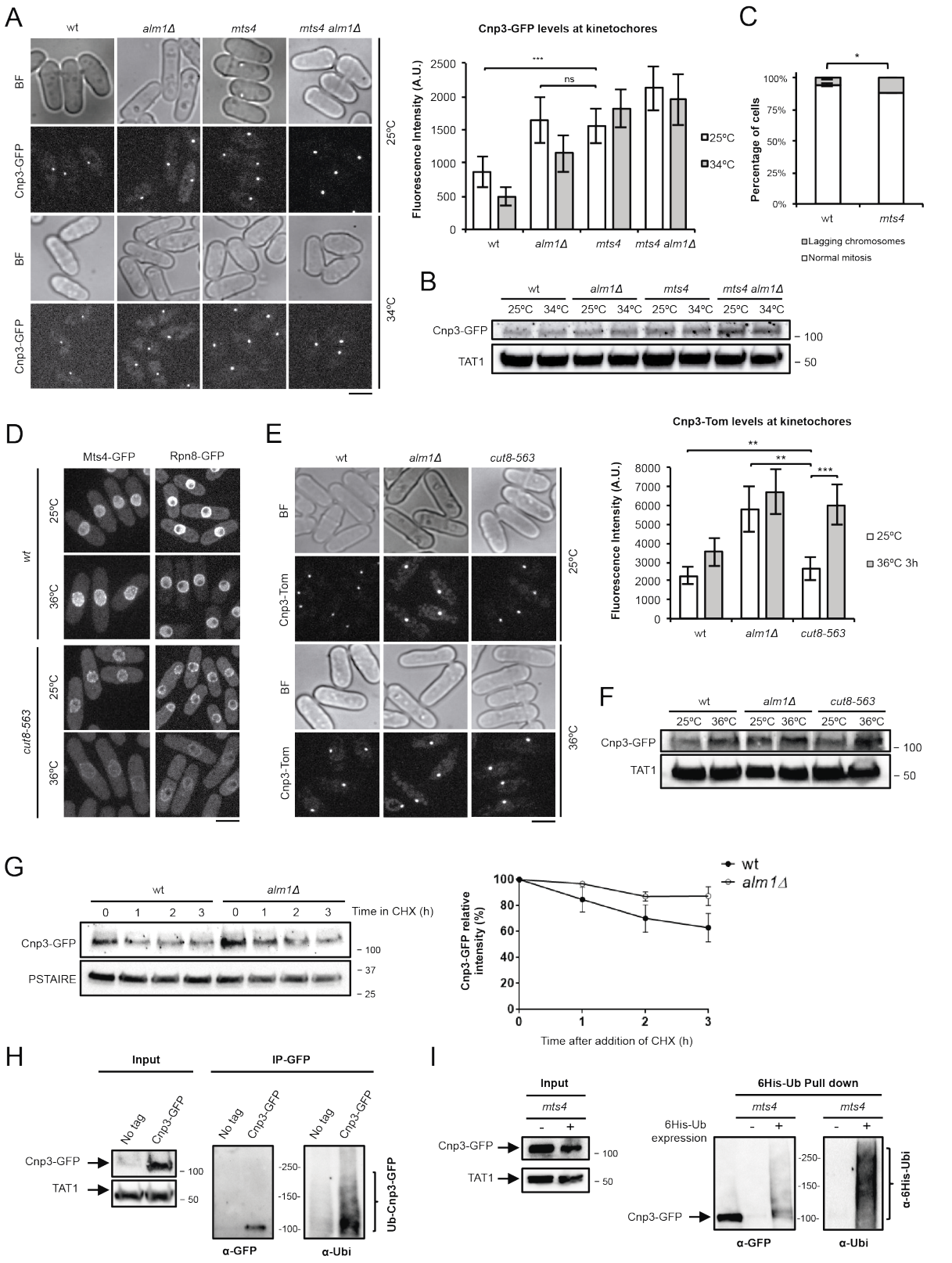

Figure 1.5. Proteasome function and localization are required for stoichiometric accumulation of Cnp3 at kinetochores. (A) Representative fluorescence microscopy images, and their corresponding brightfield images, of the indicated strains expressing Cnp3-GFP from their endogenous promoter, from cells cultured at 25ºC and shifted to 34ºC for 1 hour (left panel). Maximal projections of 18 0.3 µm z sections. Scale bar: 5 µm. Quantification of kinetochore Cnp3-GFP intensity levels of the indicated backgrounds and at the indicated Tªs (right panel). Graph represents mean fluorescence intensity levels. Error bars represent SD. n= 50. (B) Western blot analysis of total Cnp3-GFP protein, using anti-GFP mAb to detect Cnp3-GFP (upper panel) and anti-tubulin (TAT1) mAb as a loading control (lower panel). Positions of molecular weight markers are indicated in kDa. (C) Quantification of

mitotic defects (lagging KTs during anaphase B) of *wt* and *mts4* cells at 25ºC by *in vivo* fluorescence microscopy using Cnp3-GFP as kinetochore marker. n=140-200. (D) Representative fluorescence microscopy images of *wt* and thermosensitive *cut8-563* mutant cells expressing the proteasome components mts4-GFP and rpn8-GFP from their endogenous promoter. Cells were cultured at 25ºC and shifted to 36ºC for 3 hours. Maximal projections of three central 0.3 µm z sections. Scale bar: 5 µm. (E) Representative fluorescence microscopy images, and their corresponding brightfield images, of the indicated strains expressing Cnp3-Tomato from their endogenous promoter (left panel). Cells were cultured at 25ºC and shifted to 36ºC for 3 hours. Maximal projections of 18 0.3 µm z sections. Scale bar: 5 µm. Quantification of kinetochore Cnp3-Tomato intensity levels of the indicated backgrounds and at the indicated T^{a}s (right panel). Graph represents mean fluorescence intensity levels. Error bars represent SD. n= 50. ns, non-significant; **, $P < 0.001$; ***, $P < 0.001$. (F) Western blot analysis of total Cnp3-GFP protein, using anti-GFP mAb to detect Cnp3-GFP (upper panel) and anti-tubulin (TAT1) mAb as a loading control (lower panel). Positions of molecular weight markers are indicated in kDa. (G) Cnp3 protein stability in *wt* and *alm1Δ* cells in the presence of cycloheximide (CHX; left panel). Cnp3-GFP was detected by immunoblotting with anti-GFP mAb and anti-PSTAIR mAb was used as loading control. Quantification of Cnp3-GFP protein stability (right panel). Cnp3-GFP band intensities were normalized to PSTAIR signals. Relative intensity at time 0 was set up as 100% in each case. Graphs represent mean and error bars represent SD from three independent experiments. (H) Analysis of Cnp3 ubiquitination. *mts4* cells expressing Cnp3-GFP and untagged *mts4* cells were grown to mid-log phase at 25ºC and then shifted to 36ºC for 3 hours. Samples were collected and a fraction of the whole cell extract (Input) was immunoblotted with anti-GFP mAb to detect Cnp3-GFP and anti-tubulin mAb (TAT1) was used as loading control (left). Samples were subjected to anti-GFP immunoprecipitation (IP-GFP). Immunoprecipitated proteins were immunoblotted with anti-GFP mAb to detect Cnp3-GFP (α-GFP) and anti-ubiquitin pAb to detect ubiquitinated proteins (α-Ubi). (I) Analysis of Cnp3 ubiquitination. *mts4* cells overexpressing Cnp3-GFP (-) or Cnp3-GFP and His_6-Ubiquitin (+) were grown in EMM to mid-log phase at 25ºC and then shifted to 36ºC for 3 hours. Samples were collected and a fraction of the whole cell extract (Input) with equal amount of total protein was immunoblotted with anti-GFP mAb to detect Cnp3-GFP and anti-tubulin mAb (TAT1) as loading control (left). Polyubiquitinated proteins were purified with Ni^2–NTA beads in denaturing conditions. Ubiquitinated proteins were detected by immunoblotting with anti-Ubiquitin pAb (α-Ubi) and ubiquitinated forms of Cnp3 were detected by immunoblotting using anti-GFP mAb (α-GFP). Positions of molecular weight makers are indicated in kDa.

wildtype and *alm1Δ* cells in conditions of protein synthesis inhibition using cycloheximide (CHX). Quantification of Cnp3 protein levels revealed that only a pool Cnp3 is degraded in wildtype cells. However, the Cnp3 decay was delayed in *alm1Δ* cells compared to wildtype cells (Fig. 1.5 G). Based on the observed proteasome dependency for Cnp3 regulation, we next determined whether Cnp3 is ubiquitinated, which would be consistent with that hypothesis. Thus, we immunoprecipitated native Cnp3 from *mts4* mutant cells, a condition in which Cnp3 was drastically accumulated (Fig. 1.5 A), and probed the immunoblot with an antibody against ubiquitin (see Methods: Protein immunoprecipitation for further information). This experiment revealed the typical smear of poly-ubiquitinated proteins (Fig. 1.5 H). Using a complementary approach, we co-expressed Cnp3-GFP and 6His-tagged ubiquitin in *mts4* mutant cells and performed pull-down experiments for His-tagged ubiquitin under denaturing conditions (see Methods: Ubiquitin pull down assay for further information). In this case, we analyzed the fraction enriched in ubiquitinated-proteins by anti-GFP immunoblotting, where we detected a smear of slower migrating ubiquitinated forms of Cnp3-GFP (Fig. 1.5 I). Therefore, both experiments are consistent with Cnp3 being ubiquitinated *in vivo*. Altogether, these data indicate that Cnp3 is regulated by ubiquitin-dependent proteasomal degradation.

1.6 Alm1 is required for proper localization of the 26S proteasome to the NE.

Cut8, as the 26S proteasome itself, localizes to the nucleus and the nuclear periphery (Tatebe and Yanagida, 2000). Cut8 is directly associated to the nuclear membrane, although it has been proposed that both the import and targeting of the proteasome to the nuclear periphery partially depend on the NPC (Savulescu et al., 2011; Takeda et al., 2011; Takeda and Yanagida, 2005; Tatebe and Yanagida,

2000). Accordingly, both Cut8 and Alm1 localize to the nuclear periphery (Fig. 1.6 A). In order to determine whether the absence of Alm1 could affect the localization of Cut8, we analyzed by

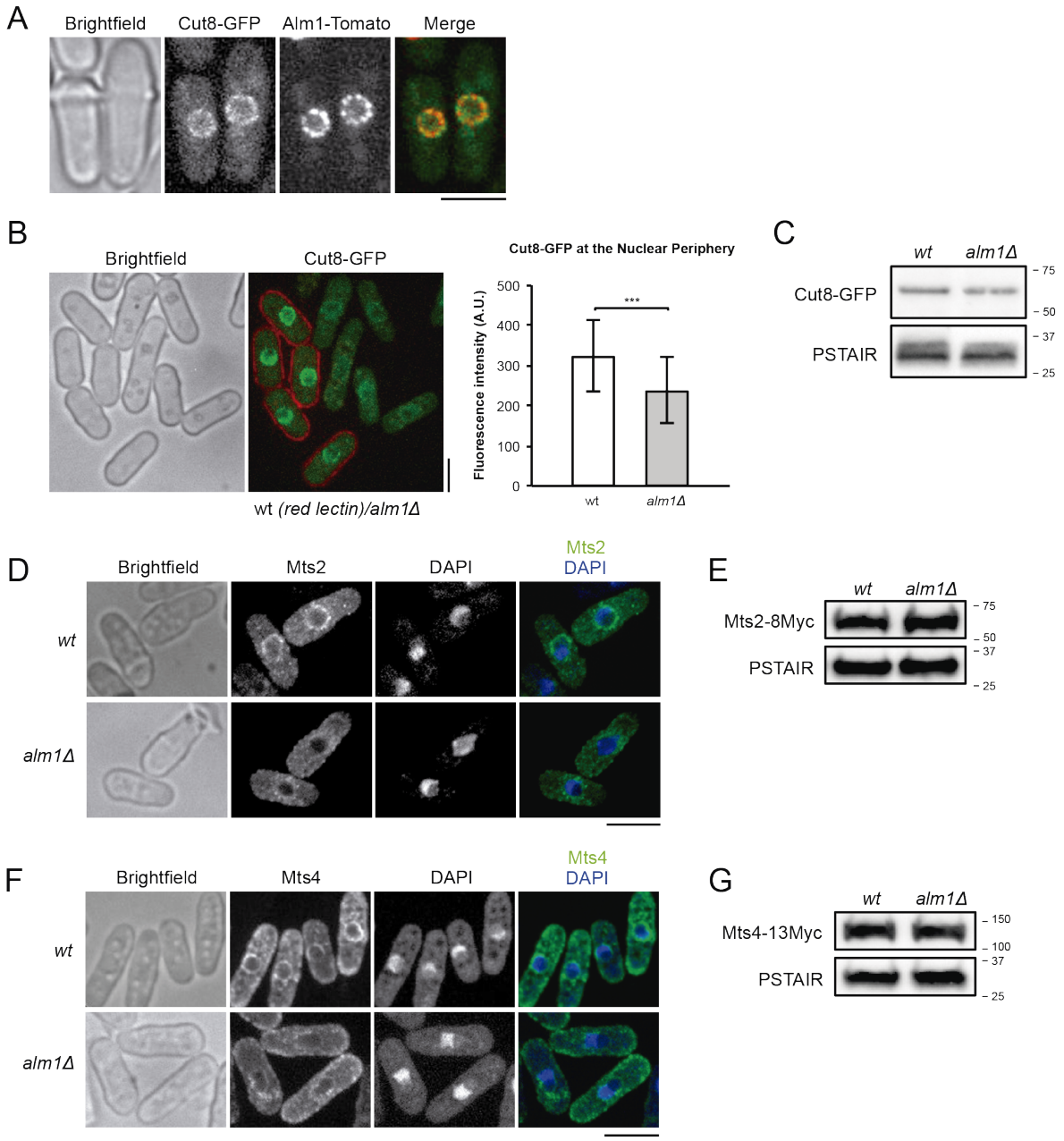

Figure 1.6. Alm1 is required for proper localization of the 26S proteasome to the NE. (A) Representative fluorescence microscopy images of *wt* cells expressing cut8-GFP and alm1-Tomato, and the corresponding brightfield images. Maximal projections of three central 0.3 µm z sections. Scale bar: 5 µm. (B) Representative fluorescence microscopy images of *wt* cells (red lectin stained) and *alm1Δ* cells expressing cut8-GFP, and the corresponding brightfield images (left panel). Maximal projections of three 0.3 µm z sections. Scale bar: 5 µm. Quantification of Cut8-GFP intensity levels at the NE in *wt* and *alm1Δ* cells (right panel). Graphs represent mean and SD, from three independent experiments. n= 69. ***, P < 0.001. (C) Western blot analysis of total Cut8-GFP protein of *wt* and *alm1Δ* cells using anti-GFP mAb to detect Cut8-GFP (upper panel) and anti-PSTAIR mAb as a loading control (lower panel). Positions of molecular weight makers are indicated in kDa. (D) Representative brightfield and immunofluorescence images of *wt* and *alm1Δ* cells expressing Mts2-8myc, using anti-myc antibody against Mts2-myc (green) and DAPI to stain DNA (blue). Scale bar: 5 µm. (E) Western blot analysis of total Mts2-8Myc protein in *wt* and *alm1Δ* cells using anti-myc antibody to detect Mts2-8Myc (upper panel) and anti-PSTAIR antibody as a loading control (lower panel). Positions of molecular weigh markers are indicated in kDa. (F) Representative brightfield and immunofluorescence images of *wt* and *alm1Δ* cells expressing Mts4-13myc, using anti-myc antibody against Mts4-13myc (green) and DAPI to stain DNA (blue). Scale bar: 5 µm. (G) Western blot analysis of total Mts4-13Myc protein in *wt* and *alm1Δ* cells using anti-myc antibody to detect Mts4-13Myc (upper panel) and anti-PSTAIR antibody as a loading control (lower panel). Positions of molecular weigh markers are indicated in kDa.

fluorescence microscopy the distribution of Cut8 in wildtype and *alm1Δ* cells. Strikingly, we observed that in the *alm1Δ* mutant Cut8-GFP localization at the NE was reduced, compared to the wildtype strain (Fig. 1.6 B). However, Cut8 protein levels were unaffected (Fig. 1.6 C).

Given that Cut8 is a nuclear envelope protein that physically interacts with the proteasome and mediates its tethering to the nuclear envelope (Takeda et al., 2011; Takeda and Yanagida, 2005), we wondered if the localization of the 26S proteasome was also altered in the absence of Alm1. To do this, we analyzed by immunostainning the localization of the proteasome subunits Mts2 (Rpt2) and Mts4 (Rpn1), two components of the proteasome 19S regulatory particle (Wilkinson et al., 1997). As expected, we discovered that both subunits failed to localize properly to the nuclear periphery in the absence of Alm1, while total protein levels were unaffected (Fig. 1.6 D-G). Altogether, these data suggest that Alm1 is involved in the proper localization of the proteasome anchor Cut8 and the proteasome itself to the NE. Therefore, the absence of Alm1 could negatively impact the proteasome-dependent degradation at the nuclear periphery of specific substrates, such as centromere and kinetochore proteins.

Discussion

1.1 *alm1Δ* mutant shows a genetic interaction with chromatin and kinetochore mutants.

Previous work from our laboratory described that the absence of Alm1 leads to chromosome segregation defects during mitosis (Fig. I11 A-C). Mutants affecting centromere or kinetochore functions usually display DNA segregation defects and are sensitive to microtubule perturbation (Ekwall et al., 1999; Pidoux et al., 2003; Takahashi et al., 1994). The reduced cell viability observed in the *alm1Δ* mutant in the presence of the MT-depolymerizing drug TBZ (Fig. 1.1 A) pointed to a defect in kinetochore function. In order to deepen the possible role of Alm1 in the regulation of kinetochore, we performed an SGA analysis of *alm1Δ* cells in the presence of TBZ (Fig. 1.1 B), which provided a valuable set of genes and genetic pathways that could be functionally linked to Alm1 function (Fig. 1.1 C and D).

From this analysis we obtained a gene cluster related to the SAC machinery (Fig. 1.1 D). This result is in agreement the phenotype of *alm1Δ* in chromosome missegregation and confirmed the dependency of SAC machinery for the viability of *alm1Δ* cells, especially in conditions of microtubule impairment, which validates our study. One of the conserved and best characterized functions of the TPR proteins is the spatio-temporal regulation of SAC components, Mad2 and Mad1 (De Souza et al., 2009; Ding et al., 2012; Lee et al., 2008b; Lince-Faria et al., 2009; Rodriguez-Bravo et al., 2014; Schweizer et al., 2013). As happens for the rest of the nuclear basket TPR proteins of the studied model organisms, Alm1 participates in the anchoring of both SAC components to the NPC during interphase, since Mad1-2 delocalize to the nucleoplasm in the *alm1Δ* mutant (Salas-Pino et al., 2017). However, during mitosis, SAC components relocalize to the kinetochores, where they are required for monitoring proper attachment of kinetochores by spindle microtubules prior to chromosome

segregation (Lara-Gonzalez et al., 2012; Silva et al., 2011). Even though Alm1 conserves this function, SAC components not only localize properly to kinetochores during mitosis, but also they are essential for cell survival in the absence of Alm1. In agreement with this, we observed a sustained localization of Mad2 at kinetochores during mitosis (Fig. I11 D) (Salas-Pino et al., 2017). Thus, the aberrant chromosome segregation observed in *alm1Δ* cells is not consequence of defective SAC, but instead to an faulty kinetochore. Consistently, genetic crosses with thermosensitive mutants in essential centromere-kinetochore components by manual tetrad dissection, revealed a synthetically lethal genetic interaction between *alm1Δ* and the entire set of kinetochore mutant tested (Fig. 1.1 E). We speculated that these phenotypes might arise as a result of defective attachment of kinetochores by the spindle microtubules.

Additionally, GO enrichment analysis also identified synthetic factors related to chromatin organization. This cluster includes deletion of *eaf6,* a subunit of the Mst2/NuA4 complex involved in histone incorporation and acetylation, which is key for several cellular processes, such as transcription, cellular response to DNA damage, and cell-cycle progression (Allard et al., 1999; Altaf et al., 2010; Doyon and Cote, 2004; Hodges et al., 2019). We also found *fft3*, an ATP-dependent DNA helicase required for the maintenance of proper chromatin structure at centromeres and subtelomeres by preventing euchromatin spreading into these regions and for the association of specific chromatin domains to the nuclear envelope (Steglich et al., 2015; Stralfors et al., 2011). Several mutants of the Swr1 complex were also present in the chromatin organization cluster; Swr1 is an ATP-dependent chromatin-remodeling complex that participates in the incorporation of the histone variant H2A.Z into chromatin (Altaf et al., 2010; Lu et al., 2009), preferentially in the promoter regions of certain genes (such as *INO1* and *GAL1*), which is necessary for their localization at the nuclear periphery and for their transcriptional reactivation (Brickner et al., 2007; Light et al., 2010). This data is of special interest, as analysis of chromatin state revealed that in the absence of Alm1 the centromeric chromatin region is deregulated (Fig. 1.2). While pericentromeric chromatin is excessively repressed, transcription from central core domain is increased (Fig. 1.2 E). Centromeric chromatin is transcriptionally silenced; however, while transcriptional silencing at *imr/otr* domains depends on the canonical heterochromatin marks (H3K9me2) and HP1/Swi6 binding, transcriptional silencing at the central core relies on the centromeric histone H3 variant, CENP-A/Cnp1 (Castillo et al., 2007; Pidoux and Allshire, 2005). Fluorescence microscopy quantification did not revealed any significant difference in the *alm1*-deleted mutant in the levels of centromeric Cnp1, but rather in Cnp20 levels (Fig. 1.3 A and B); however, given the technical limitations due to microscopy resolution, we cannot discard the possibility that Cnp1 levels/distribution could be altered as well. Therefore, the silencing defects of *alm1Δ* mutant could be the result of a deregulation of the chromatin formation/maintenance pathways *per se*. Alternatively, taking into account the functional interconnection between centromeric chromatin and kinetochores (Allshire and Ekwall, 2015), the unbalanced stoichiometric composition of kinetochores in *alm1Δ* (Fig. 1.3 A-C) could negatively impact the chromatin state of centromeric region.

1.2 Kinetochore stoichiometry is altered in the absence of Alm1.

A common feature of centromere and kinetochore mutants is that most of them display chromosome segregation defects, since proper centromere and kinetochore structural organization is key to avoid erroneous microtubule-kinetochore attachments (Bernard et al., 2001; Goshima et al., 1999; Gregan et al., 2007; Nonaka et al., 2002; Pidoux and Allshire, 2005; Pidoux et al., 2003). For example, both inactivation and overexpression of Cnp1/CENP-A, which affects the loading of other centromere and kinetochore components, results in chromosome missegregations (Castillo et al., 2007; Folco et al., 2015; Tanaka et al., 2009). We hypothesized that the unbalance of centromere-kinetochore factors observed in the absence of Alm1, especially in Cnp3 levels (Fig. 1.3 A and C), could be responsible for the kinetochore disfunction and, consequently, provoke chromosome segregation defects. In line with this assumption, overexpression of Cnp3 is sufficient to cause chromosome missegregation in wildtype cells (Fig. 1.4 A-E). However, reduction of Cnp3 protein levels in *alm1Δ* cells, by changing its native promoter by a repressible promoter, only partially rescues chromosome lagging (Fig. 1.4 F-I). This data suggests that, even though Cnp3 levels are important for kinetochore function, the unbalance of other centromere/kinetochore components in *alm1Δ* mutant could also contribute to kinetochore disfunction and, as a result, to chromosome missegregation.

Quantification of several inner kinetochore components revealed that the altered composition of kinetochores not only affects one but several components, which suggests an interdependent recruitment. This raised the issue of whether there is a primal element that establishes and determines the stoichiometry of the other kinetochore components. If this were the case, defects in the accumulation of such key kinetochore component would trigger a chain reaction that might lead to a general deregulation of the entire kinetochore stoichiometry. It has been described that Cnp1 defines the landmark for kinetochore assembly. While Cnp20 is directly recruited by the N-tail domain of Cnp1 (Folco et al., 2015), CENP-C/Cnp3 binds to CENP-A/Cnp1 nucleosomes via its C-tail (Carroll et al., 2010; Kato et al., 2013). Accordingly, inactivation of CENP-A/Cnp1 negatively affects the loading of other kinetochore proteins, such as CENP-T/Cnp20 or CENP-I/Mis6, and overexpression of Cnp1 results in increased levels of centromeric Cnp3, Mal2 and Sim4 (Castillo et al., 2007; Folco et al., 2015; Tanaka et al., 2009). Therefore, there exist two independent but parallel pathways for the recruitment of outer kinetochore components, which depends on CENP-T and CENP-C. CENP-T (Cnp20) directs the assembly of the outer kinetochore via interaction with Mis12 complex and Ndc80 complex, which acts as the primary microtubule-binding interface at kinetochores (Hori et al., 2008; Huis In 't Veld et al., 2016; Nishino et al., 2013; Rago et al., 2015). Concurrently, human CENP-C (Cnp3) also participates in the recruitment of both Mis12 and Ndc80 complexes (Hori et al., 2008; Huis In 't Veld et al., 2016; Petrovic et al., 2016; Rago et al., 2015; Screpanti et al., 2011). Importantly, KMN network recruitment throught CENP-T and CENP-C is competitive (Huis In 't Veld et al., 2016) and is promoted by two different cell cycle kinases, cyclin-dependent kinase and Aurora B kinase, respectively (Rago et al., 2015). Of note, Cnp20 and Cnp3 are the two proteins that show a higher accumulation at the kinetochore in the absence of Alm1 (Fig. 1.3 B and C).

The C-terminal region of CENP-C/Cnp3 protein possesses two Mif2p homology domains, which have been conserved along evolution. While Mif2p homology domain II mediates CENP-C binding to the centromeric chromatin, Mif2-homology domain III is responsible for the homodimerization of CENP-C and for the recruitment of other kinetochore components (Cohen et al., 2008; Sugimoto et al., 1997; Trazzi et al., 2002; Trazzi et al., 2009). On the one hand, it would be reasonable to hypothesize that the excess of Cnp3 that we observe in the absence of Alm1 might result in the ectopic accumulation of Cnp3 by self-association. However, the increased levels of Cnp3 protein does not result in its spreading into adjacent heterochromatin domains. On the other hand, given the key role of Cnp3 as hub for other kinetochore components, the overload of Cnp3 could also cause the abnormal accumulation of such components. Accordingly, levels of Fta1, which is part of the Sim4 complex (Tanaka et al., 2009), are also increased in *alm1Δ* cells (Fig. 1.3 C), suggesting that an excess of Cnp3 might drive the ectopic accumulation of other kinetochore components. However, this is not the only possibility (see below).

1.3 Alm1 regulates proteasome function or localization at the NE.

Previous works have described that centromere and kinetochore component homeostasis is regulated by proteasomal degradation. Cnp1 distribution is altered in *rpt3* and *cut8* mutants, which encode for a subunit of the 19S proteasome and the anchor of the proteasome to the NE, respectively, resulting in altered chromatin silencing and genome instability (Collins et al., 2004; Kitagawa et al., 2014; Moreno-Moreno et al., 2006; Ranjitkar et al., 2010). CENP-T and CENP-W protein stability are also regulated by the proteasome and by CSN5, a component of the COP9 signalosome, homolog to the lid subcomplex of the 26S proteasome, which possesses de-ubiquitinating activity and functions in the ubiquitin-proteasome pathway (Chun et al., 2016; Chun et al., 2013; Wei and Deng, 2003). Importantly, inner and outer kinetochore components maintain a similar stoichiometric composition (Cheeseman et al., 2006). Of note, deletion of Psh1, an ubiquitin ligase that controls the loading and distribution of inner kinetochore proteins, shows elevated levels of Cse4 and other inner kinetochores components, and results in chromosome segregation defects. However, the levels of outer kinetochore proteins do not increase, suggesting that the altered stoichiometry between inner and outer kinetochore is sufficient to impair chromosome segregation (Herrero and Thorpe, 2016). Besides, in fission yeast, the proteasome has been associated to a quality control pathway for several kinetochore components, including Spc7 or Mis6, which ensures kinetochore proteostasis and genome integrity (Kriegenburg et al., 2014). In the present study, we show that Cnp3 stability is regulated in a proteasome-dependent manner. When the function of the proteasome is impaired (in the *mts4* mutant) or when the proteasome does not localize properly to the NE (in the *cut8-563* mutant), Cnp3 levels are increased (Fig. 1.5). Moreover, ubiquitinated forms of Cnp3 can be detected when proteasomal degradation is compromised (Fig. 1.5 H-I). This led us to hypothesize the proteasome function and localization at the NE is required for Cnp3 proteostasis. However, it remains unknown if the proteasome control the levels of several inner kinetochore components or whether

Cnp3 is exclusively regulated in a proteasome-dependent manner, and an increase in its levels due to proteasome disfunctioning is sufficient to alter the kinetochore stoichiometry.

In fission yeast, the three centromeres cluster together and are anchored at the NE in interphase cells. During mitosis, they are released from the NE and captured by the mitotic spindle that leads them to the cell poles. Thus, except for a brief period during mitosis, centromeres-kinetochores stay in contact with the NE (De Souza and Osmani, 2007; Ding et al., 1997; Hou et al., 2012; Jaspersen and Ghosh, 2012; Mekhail and Moazed, 2010). It remains unknown whether there exist a connection between kinetochore attachment to the SPB during interphase and the role of the proteasome at the NE. However, it has been suggested that the localization of the proteasome correlates with the subnuclear distribution of its substrated (Scharf et al., 2007), and indeed proteasome-dependent degradation occurs in different subnuclear domains or nucleoplasmic foci (Rockel et al., 2005).

Noteworthy, we found that Alm1 is required to maintain the proteasome and its anchor Cut8 at the NE (Fig. 1.6). At the structural level, Cut8 contains an N-terminal lysine-rich domain, required for the interaction with the proteasome, a dimerization domain, and a six-helix bundle, similar to the 14-3-3 phosphoprotein-binding domain, involved in liposome and cholesterol binding, required for membrane binding (Takeda et al., 2011). Cut8 enrichment at the nuclear periphery is regulated by the ubiquitin-conjugating enzyme Rhp6 (Rad6), the ubiquitin-ligase Ubr1 and the proteasome itself (Takeda and Yanagida, 2005; Tatebe and Yanagida, 2000). However, although no clear higher eukaryote orthologs for Cut8 have been found, this mechanism could be a conserved (Takeda and Yanagida, 2005). Shortly after the finalization of this study, it was published that in *Chlamydomonas reinhardtii* the 26S proteasome tethers via Rpn9 to two specific NPC locations, the nuclear basket and the inner nuclear membrane surrounding the NPC (Albert et al., 2017). This study suggests that the anchoring of the

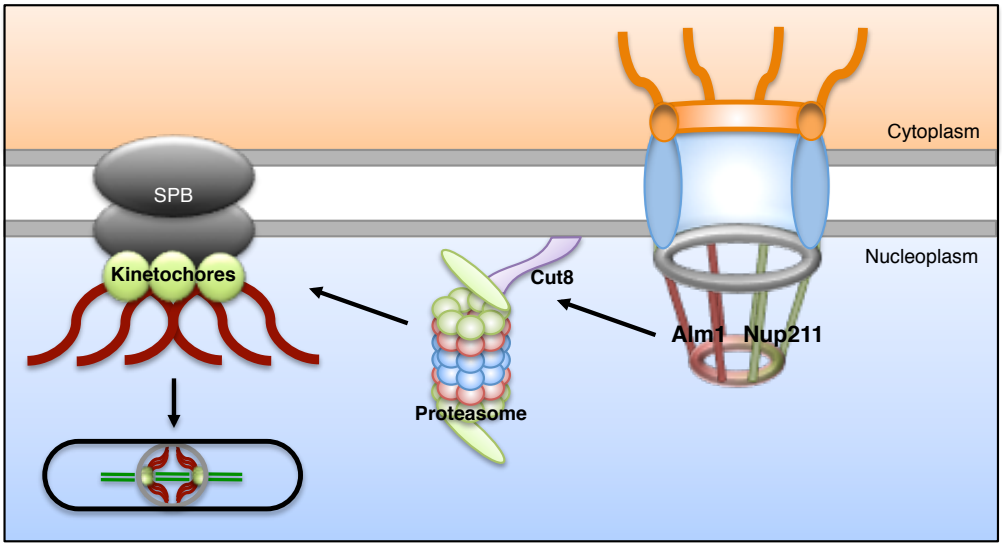

Figure 1.7. The fission yeast nuclear basket component Alm1 is required for proper localization of the proteasome and its anchor Cut8 to the NE. Alm1 might directly regulate or stabilize Cut8 localization at the NE, or alternatively, Alm1 might function as scaffold for proteasomal assembly or regulation, which would indirectly impact Cut8-NE localization. Deregulation/delocalization of the proteasome from the NE results in unbalanced kinetochore homeostasis, which leads to chromosome missegregation.

proteasome to the NE and the NPC is part of a protein quality control system that act as a degradation center for membrane proteins and soluble proteins crossing the NPC, respectively. Thus, Alm1 could be involved in the recruitment of Cut8 and the proteasome to the nuclear periphery or it may provide a platform for the assembly or targeting of functional proteasomal complexes to the NE.

In conclusion, this work reveals a novel role of the TPR nucleoporin Alm1 in the regulation of the function and the spatial distribution of the proteasome within the fission yeast nucleus (Fig. 1.7). This regulation is critical to maintain proper kinetochore proteostasis and, consequently, the stability of the genome.

Chapter 2

Nuclear basket interaction with mRNA-binding proteins facilitates mRNP docking and export in fission yeast

2.1 Nup211 and Alm1 interaction is required for their assembly at the nuclear basket.

The main structural components of the nuclear basket are the TPR nucleoporins. While higher eukaryotes and some fungi only have a single TPR (Bangs et al., 1998; Cordes et al., 1997; Coyle et al., 2011), *S. cerevisiae* and *S. pombe* have two copies, Mlp1-Mlp2 and Nup211-Alm1, respectively (Asakawa et al., 2019; Field et al., 2014; Kosova et al., 2000; Niepel et al., 2005; Salas-Pino et al., 2017; Strambio-de-Castillia et al., 1999). Although Nup211 and Alm1 proteins have been described as equivalent to *S. cerevisiae* Mlp1 and Mlp2, phylogenetic analyses have revealed that these proteins emerged from independent events of gene duplication and, therefore, they are not real orthologs to each other (Field et al., 2014). This offers a unique situation to study new functions that may have arisen after the duplication of the single TPR in both organisms.

In order to study how the nuclear basket operates in the fission yeast and to dissect the functions of Nup211 and Alm1, we generated thermosensitive (ts) alleles of both TPR genes. These thermosensitive alleles were obtained by random mutagenesis and integrated at the endogenous locus (see Methods: Random mutagenesis). *nup211*$^{+}$ is an essential gene (Bae et al., 2009) and, consequently, *nup211* thermosensitive mutant (*nup211ts*) is unable to grow at non-permissive temperature (36ºC), while cell viability is not affected at 25ºC (Fig. 2.1 A). Since *alm1* is not an essential gene, to obtain thermosensitive mutants we used the *nup132Δ* genetic background, in which *alm1*$^{+}$ becomes essential for cell viability (Salas-Pino et al., 2017). The selected mutant of *alm1*$^{+}$ gene (hereafter *alm1ts*) is not lethal at any temperature *per se*, as happens for *alm1Δ*, whereas the *nup132Δ alm1ts* double mutant is inviable at restrictive temperature (36ºC) (Fig. 2.1 B).

Then, we analyzed by fluorescence microscopy the localization of the *ts* mutants proteins, Nup211ts-GFP and Alm1ts-Tomato, at permissive temperature (25ºC) and after incubation at restrictive temperature (36ºC) for four hours. Both proteins localize properly at the nuclear periphery at 25ºC. However, after incubation at 36ºC, Nup211ts-GFP was mostly delocalized from NPCs, although it was also observed in few aberrant aggregation foci at the nuclear periphery (Fig. 2.1 C). Similarly, after four hours at 36ºC, Alm1ts-Tomato intensity levels at the nuclear periphery were reduced, compared to Alm1-Tomato, and instead accumulated in the nucleoplasm (Fig. 2.1 C), showing that inactivation of both *ts* alleles impairs their localization at NPCs.

Nup211-GFP and Alm1-Tomato show an identical localization pattern at the nuclear envelope (Fig. 2.1 D), which suggests a direct interaction between both proteins at NPCs. Since the localization of these nuclear basket *ts* mutant proteins is compromised at restrictive temperature, we tested whether inactivation of one of the TPR Nup would compromise the localization of the other. As expected, Alm1-Tomato accumulation at the nuclear periphery was reduced in the *nup211ts* mutant at restrictive temperature. Likewise, Nup211 partially delocalized from the nuclear periphery in the *alm1ts* background (Fig. 2.1 D), with only a few remaining foci associated to the NPCs. Of note, in all cases the colocalization of Alm1 and Nup211 was maintained in these perinuclear foci (Fig. 2.1 D, arrowheads). These data demonstrate that TPR nucleoporins Nup211 and Alm1 display an

interdependent localization at the NPC and suggest that the direct interaction between both nucleoporins is required for their anchoring to the NPC.

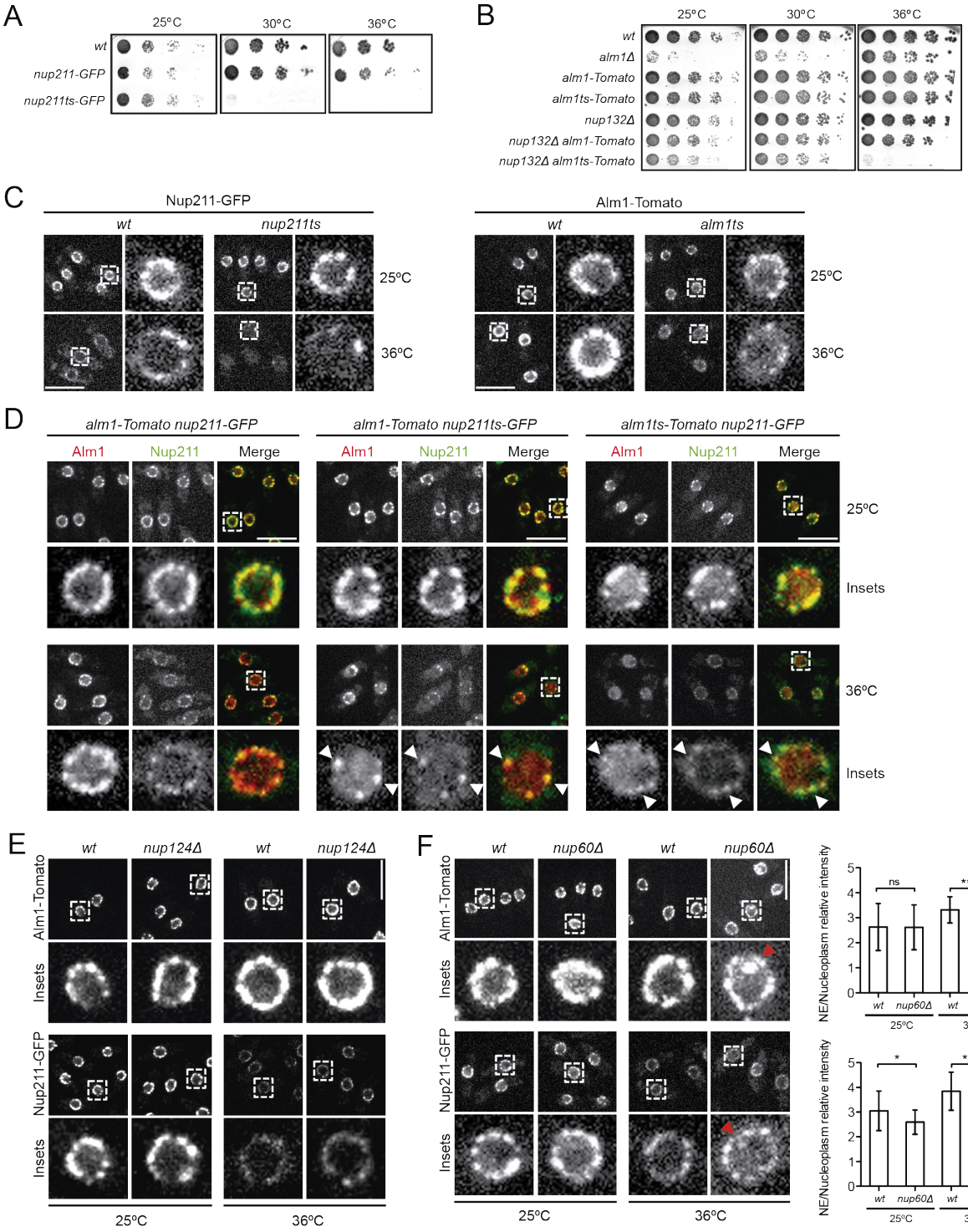

Figure 2.1. Nup211 and Alm1 interaction is required for their assembly at the nuclear basket. (A) Drop assay comparing the cell viability of the indicated strains in rich media (YES). Spotted cells correspond to 10-fold dilutions with an initial O.D. of 0.2. (B) Drop assay comparing the cell viability of the indicated strains in YES. Spotted cells correspond to 5-fold dilutions with an O.D of 0.3. Cells were grown at 25ºC, and plates were incubated at 25ºC, 30ºC and 36ºC. (C) Representative fluorescence microscopy images of *wt* Nup211-GFP and mutant Nup211ts-GFP (left) and *wt* Alm1-Tomato and mutant Alm1ts-Tomato (right) proteins at the indicated T^{a}s. Magnifications of the indicated nucleus are shown. (D) Fluorescence microscopy images of representative *wt*, *nup211ts*, and *alm1ts* cells expressing Nup211-GFP and Alm1-Tomato, at 25ºC and after 4 hours incubation at 36ºC. Magnifications of the indicated nucleus are shown (Insets). Arrowheads indicate perinuclear foci where Alm1 and Nup211

colocalize. (E) Fluorescence microscopy images of representative *wt* and *nup124Δ* cells expressing Alm1-Tomato (upper panels) and Nup211-GFP (lower panels), at 25ºC and 36ºC. (F) Fluorescence microscopy images of representative *wt* and *nup60Δ* cells expressing Alm1-Tomato (upper panels) and Nup211-GFP (lower panels), at 25ºC and 36ºC. Magnifications of the indicated nucleus are shown (Insets). Arrowheads indicate intranuclear Alm1/Nup211 foci. Quantification of Alm1-Tomato (upper panel) and Nup211-GFP (lower panel) levels in the indicated backgrounds and temperatures. Graph represents mean fluorescence intensity levels at the NE relative to the nucleoplasm and error bars represent SD. n= 30. ns= non-significant; *, $P < 0.05$; **, ***, $P < 0.001$. Maximal projections of three z-sections (step size 0.3 µm). Scale bars: 10 µm.

TPRs are the most peripheral nucleoporins at the nucleoplasmic side of the NPC and, therefore, they do not act as scaffold for other nucleoporins (Hase and Cordes, 2003). However, proper assembly of TPRs into the NPC requires other nuclear basket components. In *S. cerevisiae* Nup60 is responsible for the localization of Mlps into the NPC (Galy et al., 2004; Niepel et al., 2005; Palancade et al., 2005), while in humans Nup153 is the binding partner of TPRs (Hase and Cordes, 2003; Rajanala and Nandicoori, 2012). We found that deletion of *nup124*, the fission yeast ortholog of Nup153, does not alter the localization of Nup211 nor Alm1 (Fig. 2.1 E). However, *nup60* deletion resulted in the reduction of the NE/nucleoplasm signal of both TPR Nups, Alm1 and Nup211, and their mislocalization in nucleoplasmic foci (Fig. 2.1 F, arrowheads), especially at 36ºC (percentage of cells with NB nucleoplasmic foci: 3% at 25ºC (n=255), *vs* 39% at 36ºC (n=202)). This suggests that fission yeast nuclear basket component Nup60 could partially contribute to the proper stability or assembly of Alm1-Nup211 into the nuclear basket or, alternatively, it might be required for the localization of a specific subset of Alm1-Nup211 molecules into the nuclear pore.

2.2 The nuclear basket TPR nucleoporins are anchored to the NPC by Nup132.

It has been reported that the NPC outer ring Nup107-Nup160 subcomplex (also known as Y-subcomplex) acts as a keystone for the assembly into the NPC of other Nups, including the nuclear basket (Asakawa et al., 2019; Boehmer et al., 2003; Harel et al., 2003; Souquet et al., 2018). Given the synthetic lethality between *alm1Δ* and *nup132Δ* mutants, we next tested whether Nup132 is involved in the anchoring of the nuclear basket TPRs to the NPC. For that, we analyzed the distribution and total signal intensity of Alm1-Tomato and Nup211-GFP at NPCs in the *nup132Δ* background relative to control cells (Fig. 2.2 A and B). In the absence of Nup132, Alm1-Tomato mislocalizes to the nucleoplasm. This phenotype is exacerbated in the *nup132Δ alm1ts-Tomato* genetic background, in which Alm1ts-Tomato was also observed as isolated foci associated to the nuclear periphery (Fig. 2.2 A, arrowheads). Interestingly, Nup211 showed increased levels at the nuclear pore in the *nup132Δ* mutant, while its overall nuclear distribution and the NE/nucleoplasm ratio were mostly unaffected (Fig. 2.2 B), in agreement with previous results (Asakawa et al., 2019).

In view of the mislocalization of Alm1 in both *nup132Δ* and *nup211ts* strains, we wondered if *nup132Δ* and *nup211ts* mutants impact Alm1 localization synergistically or epistatically. However, the double mutant *nup132Δ nup211ts* is synthetically lethal, even a permissive temperature. This demonstrates that Nup132 also becomes essential for cell viability when the function of the TPR Nup211 is compromised. Since the lack of Nup132 impairs Alm1 localization to the nuclear pore and,

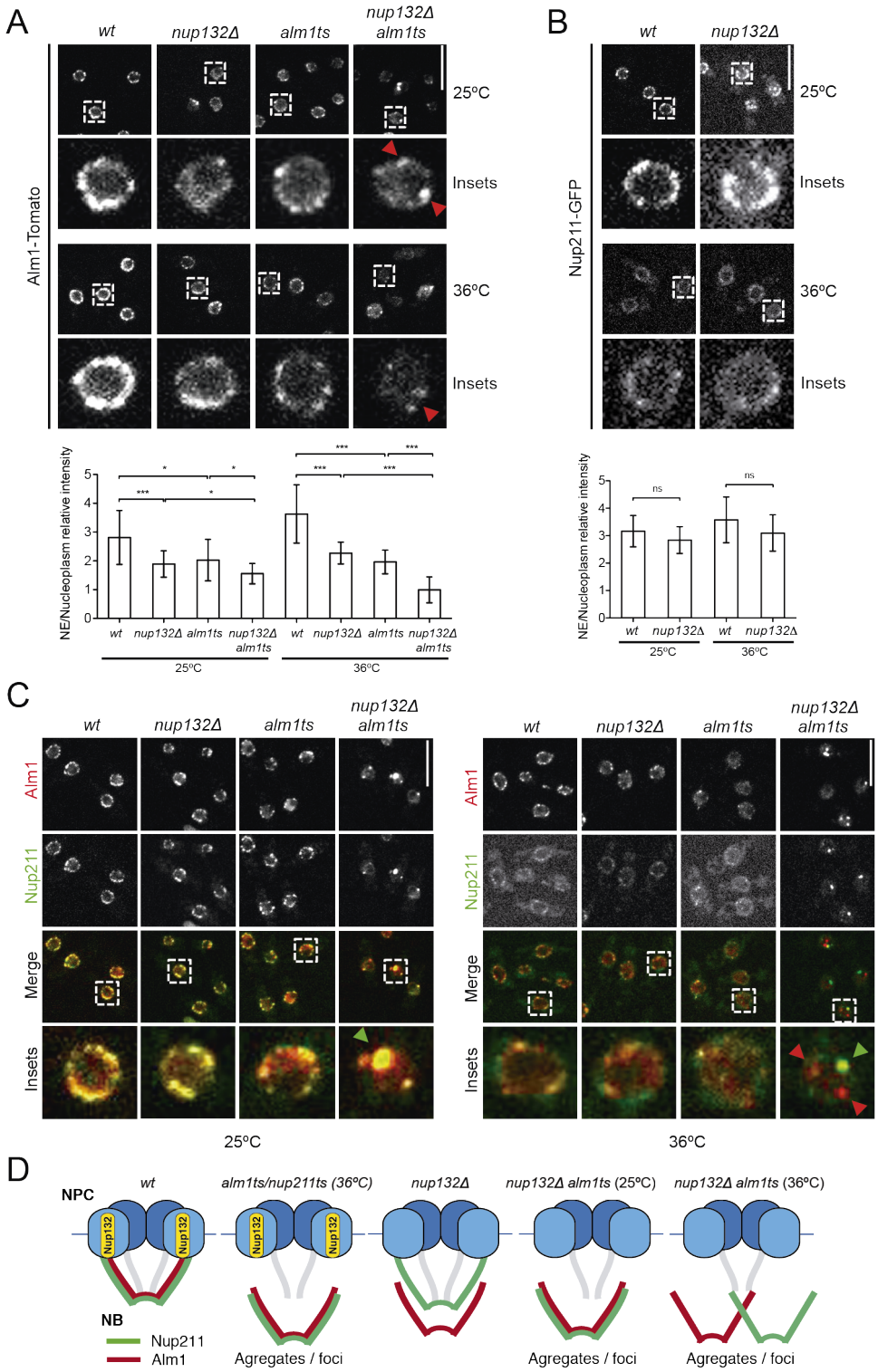

Figure 2.2. The nuclear basket TPRs are anchored to the NPC by Nup132. (A) Fluorescence microscopy images of representative *wt* and *nup132Δ* cells expressing Alm1-Tomato and Alm1ts-Tomato, at 25ºC and 36ºC. arrowheads point to Alm1 foci at the NP. Quantification of Alm1-Tomato levels in the indicated backgrounds and temperatures (lower panel). Graph represents mean fluorescence intensity levels at the NE relative to the nucleoplasm and error bars represent SD. n= 30. *, P < 0.05; ***, P < 0.001. (B) Fluorescence microscopy images of representative *wt* and *nup132Δ* cells expressing Nup211-GFP, at 25ºC and after 4 hours incubation at 36ºC. Quantification of Nup211-GFP levels in the indicated backgrounds and temperatures (lower panel). Graph represents mean fluorescence intensity levels at the NE relative to the nucleoplasm and error bars represent SD. n= 30. ns, non-significant. (C) Fluorescence microscopy images of representative *wt*, *nup132Δ*, *alm1ts* and *nup132Δ alm1ts* cells expressing Nup211-GFP and Alm1-Tomato, at 25ºC (left) and after 4 hours incubation at 36ºC (right). Magnifications of the indicated nucleus are shown (Insets). Arrowheads indicated the accumulation of NB TPRs in aberrant

perinuclear foci in which Alm1 and Nup211 do (green) or do not (red) colocalize. Maximal projections of three cental z sections (step size 0.3 µm). Scale bars: 10 µm. (D) Schematic model for TPR nucleoporins interaction and assembly into NPCs. In a *wt* background Nup211 and Alm1 interact directly with each other and are anchored to the NPC via Nup132. In the nuclear basket mutant backgrounds (*alm1ts* and *nup211ts*) TPR anchoring to the NPC is compromised, while Alm1-Nup211 interaction is maintained. In a *nup132Δ* background the localization of Alm1, but not Nup2111, is altered. In the *nup132Δ alm1ts* background the NB TPRs almost completely delocalize from the NPC at permissive Tª (25ºC) and their interaction is abrogated at restrictive Tª (36ºC).

in turn, Alm1 is required for the proper assembly of Nup211, we checked whether lack of both *nup132* and *alm1* resulted in a further delocalization of Nup211 from NPCs. *nup132Δ alm1ts* double mutant completely abrogates Nup211-GFP localization at the NPC; in the absence of Nup132, at permissive temperature Nup211-GFP mislocalizes from the NPC and appears as bright foci or aggregates that still colocalize with Alm1ts-Tomato (Fig. 2.2 C, green arrowhead), while at restrictive temperature the interaction between Alm1ts-Tomato and Nup211-GFP is disrupted (Fig. 2.2 C, red arrowheads). Altogether, these results demonstrate that Nup132 is critical for the interaction between Alm1 and Nup211, and for their anchoring to the NPC.

Importantly, budding yeast basketless cells (*nup60Δ* single mutant or *mlp1 mlp2* double mutant) are viable (Galy et al., 2004; Kosova et al., 2000; Niepel et al., 2005), whereas in fission yeast both *nup211ts* and *nup132Δ alm1ts* mutants are inviable (Fig. 2.1 A and B). The synthetic lethality between *nup132Δ* and *alm1ts* might be the result of impairment in the assembly of Nup211 into the NB, although other structural defects of the NPC in the *nup132Δ* genetic background might cause such lethality. This suggests that Nup211/Alm1 pair may have evolved new and essential functions not shared by Mlp proteins, which prompted us to dissect the roles of the nuclear basket TPR nucleoporins in *S. pombe*.

2.3 The nuclear basket TPR nucleoporins participate in mRNA docking and export.

In budding yeast the nuclear basket has been involved in the regulation of mRNA quality control just before NPC translocation; as a consecuence deregulation of Mlp1 causes altered poly(A)-RNA trafficking (Galy et al., 2004; Green et al., 2003; Kosova et al., 2000; Lewis et al., 2007; Palancade et al., 2005; Vinciguerra et al., 2005). Analogously, human TPR is required for regulating the nuclear export of intron containing mRNAs (Bangs et al., 1998; Coyle et al., 2011; Okamura et al., 2015; Rajanala and Nandicoori, 2012; Shibata et al., 2002; Umlauf et al., 2013). In the fission yeast, downregulation of *nup211*$^{+}$ expression leads to mRNA accumulation into the nucleus, which is likely due to defective mRNA export (Bae et al., 2009). Thus, in order to evaluate the contribution of the TPR nucleoporins to mRNA export, we performed fluorescence *in-situ* hybridization experiments using an oligo dT probe to stain the poly(A)-RNA, in each single mutant *nup211ts* and *alm1ts*. At permissive temperature, poly(A)-RNA was distributed throughout the cell in the control strains and in *nup211ts* and *alm1ts* mutants, with a two-fold enrichment of mRNA in the nucleus compared to the cytoplasm (Fig. 2.3 A). In contrast, after two hours at restrictive temperature (36ºC), *nup211ts* mutant cells significantly accumulated mRNA inside the nucleus, while cytoplasmic levels decreased (Fig. 2.3 A).

alm1ts mutant did not significantly accumulate bulk poly(A)-RNA neither at 25ºC nor at 36ºC, while the *alm1Δ* strain showed a slight nuclear increase of mRNA (Fig. 2.3 A). Given that the deletion of *nup132* impairs the proper assembly of the nuclear basket (Fig. 2.2 A-D), we next checked if *nup132Δ* mutant also displays mRNA export defects, as has been described for other nuclear pore components (Bai et al., 2004). *nup132Δ* mutant did not exhibit an increase in nuclear poly(A)-RNA *per se*, but has an additive effect to *alm1ts* in poly(A)-RNA accumulation (Fig. 2.3 B), which is consistent with the synthetic lethality that results when both genes are compromised (Fig. 2.1 B), and with the delocalization of Nup211 observed in this background (Fig. 2.2 C). These results demonstrate that Nup211 plays a critical role in mRNA export, similar to human TPR (Bangs et al., 1998; Coyle et al., 2011; Okamura et al., 2015; Rajanala and Nandicoori, 2012; Shibata et al., 2002; Umlauf et al., 2013). We hypothesize that the inhibition of poly(A)-RNA export observed in the *alm1* mutant is likely caused by the delocalization of Nup211 from NPCs in this genetic background, although an accessory function of Alm1 in mRNA export cannot be dismissed.

Several studies have shown that prior to export the nuclear basket contributes to the docking of mRNAs to the NPC through interaction with RNA-binding proteins (Bailer et al., 1998; Dimitrova et al., 2015; Jani et al., 2012; Saroufim et al., 2015; Strawn et al., 2001; Umlauf et al., 2013). In particular, the poly-A binding protein Nab2, which associates to mRNP during mRNA poly-adenilation, directly interacts with Mlp1 (Fasken et al., 2008; Grant et al., 2008; Green et al., 2003). To determine if this docking function is conserved in the fission yeast TPR nucleoporins, we examined the localization of Nab2 in the nuclear basket mutants. In wildtype cells Nab2 localizes at the nucleoplasm and at the nuclear periphery (Fig. 2.3 C), consistent with its mRNA binding activity. However, compromising the function of *alm1* and *nup211* resulted in increased nuclear levels of Nab2 (Fig. 2.3 C), although more prominently in the *nup211ts* mutant, in agreement with the FISH data (Fig. 2.3 A). Moreover, total Nab2 protein levels were slightly higher in these mutants than in wildtype cells (Fig. 2.3 D). Thus, this suggests that defective nuclear basket impairs nucleo-cytoplasmic trafficking of Nab2, leading to its accumulation in the nucleus, which in turn could affect protein stability.

Remarkably, we noticed that Nab2 formed discrete nuclear foci at the proximity of the nuclear periphery in both mutants, but especially in *alm1Δ* (Fig. 2.3 C, insets, arrowheads). Then, we analyzed by fluorescence microscopy the localization of Nab2 relative to Nup211 and Alm1. In control conditions, a fraction of Nab2 colocalized with these TPRs at the nuclear periphery, in agreement with its mRNA docking activity. After inactivation of *nup211ts*, which leads to nuclear basket dissociation from NPCs and its aggregation in foci at the vicinity of the NE (Fig. 2.1 D), Nab2 accumulated at these perinuclear foci containing both TPR Nups Nup211 and Alm1 (Fig. 2.3 E, arrowheads). Thus, the nuclear retention of poly(A)-RNAs and Nab2 in the absence of Nup211 and Alm1, and the colocalization of Nab2 with the TPR Nups, specially when they are not properly assembled at NPCs and mRNA export is impaired (*nup211ts*), suggest that fission yeast TPRs Nup211 and Alm1 provide indeed mRNPs docking activity to NPCs during mRNA export.

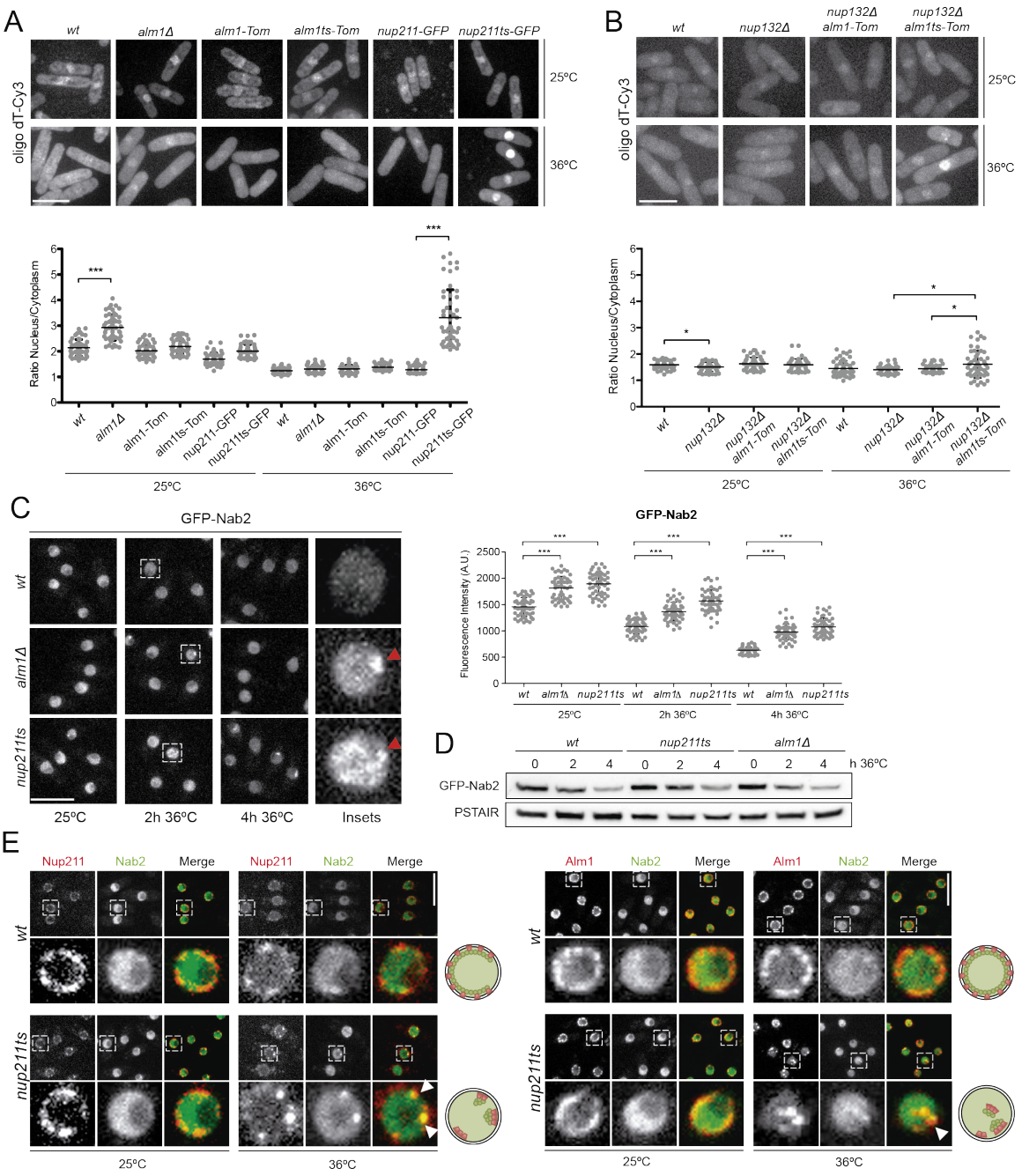

Figure 2.3. The nuclear basket participates in mRNA docking and export. (A, B) Fluorescence *In Situ* Hybridization (FISH) analysis of the indicated strains at 25ºC and after 2 hours incubation at 36ºC, using Cy3-labelled oligo (dT)50 probe to stain the RNA (upper panels). Maximal projections of 18 z sections (step size 0.3). Scale bar: 10 µm. Quantification of the Cy3-labelled oligo (dT) 50 probe fluorescence signal of the indicated strains (lower panels). Dot plots represent the ratio between the nucleus and the cytoplasm of individual cells. Error bars, SD. n=50. *, P < 0.05; ***, P < 0.001. (C) Fluorescence microscopy images of representative *wt*, *alm1Δ* and *nup211ts* cells expressing GFP-nab2 at the indicated conditions. Cells were cultured at 25ºC and shifted to 36ºC for 2h and 4h. Magnifications of the indicated nucleus are shown (Insets). Arrowheadd point to perinuclear Nab2 foci. Maximal projections of 18 sections (step size 0.3 µm). Scale bar: 10 µm. Quantification of nuclear GFP-Nab2 levels in the indicated backgrounds and T^{a}s (right). Dot plot represents mean fluorescence intensity levels (A.U.) and error bars represent SD. n= 30. ***, P < 0.001. (D) Western blot analysis of total GFP-Nab2 protein in the indicated strains and conditions, using anti-GFP mAb to detect GFP-Nab2 and PSTAIR as loading control. (E) Fluorescence microscopy images of representative *wt* and *nup211ts* cells coexpressing GFP-Nab2 and either Nup211-mCherry (left) or Alm1-Tomato (right). Magnifications of the indicated nucleus are shown (Insets). Arrowheads indicated Nab2 perinuclear foci that colocalize with NB TPRs. Scale bar: 10 µm. Schematic of the localization of nuclear basket TPR (red) and Nab2 (green).

2.4 The absence of Alm1 phenocopies exosome deficiency, while compromising Nup211 function leads to a block in mRNA export.

Previous work has shown that both human TPR and Mlps are part of a final QC mechanism that monitors the quality of the mRNPs prior to export. In this way, the nuclear basket either allows mRNA export or retains unspliced or defective mRNAs for degradation by the Rrp6-dependent exosome, preventing the synthesis of disfunctional proteins (Coyle et al., 2011; Galy et al., 2004; Green et al., 2003; Lewis et al., 2007; Palancade et al., 2005; Rajanala and Nandicoori, 2012; Vinciguerra et al., 2005). Rrp6-dependent QC mechanism is not essential under normal growth conditions; however, it becomes critical for cell survival in conditions of mRNA export impairment (Sugiyama et al., 2013). Consistently, double mutant between *rrp6Δ* and *rae1-167* (a *ts* allele of the mRNA export factor Rae1) is synthetically lethal, even at permissive temperature (Fig. 2.4 A). In the fission yeast two PABPs, Nab2 and Pab2, compete for binding to poly(A)-RNA tails and have been implicated in Rrp6-dependent QC. While Nab2 stabilizes unspliced pre-mRNAs and impedes their Pab2/Rrp6-mediated degradation, Pab2 targets hyperadenylated RNAs for degradation via the nuclear exosome (Grenier St-Sauveur et al., 2013; Lemieux et al., 2011). Importantly, *nup211ts* and *alm1Δ* mutants showed a strong negative genetic interaction with both *rrp6Δ* and *pab2Δ* mutants (Fig. 2.4 A), as has been previously described for budding yeast (Galy et al., 2004). In contrast, in the absence of *nab2*, *nup211ts* lethality is partially rescued, while *alm1Δ* mutant is not greatly affected (Fig. 2.4 B). These data show that Nup211 and Alm1 are required for survival in conditions of defective exosome activity, and suggest that mRNA export defects of *nup211ts*, but not *alm1Δ,* are partially alleviated when the Pab2/Rrp6-mediated degradation pathway prevails.

To get further insights into the functional connection between the TPR nucleoporins and mRNA QC, next, we examined the localization of Pab2, since this protein has been described as a component of the nuclear exosome machinery (Shichino et al., 2020; Sugiyama and Sugioka-Sugiyama, 2011; Sugiyama et al., 2013). In wildtype cells Pab2 localizes in the nucleoplasm, similarly to Nab2, although Pab2 is also enriched in nuclear exosome foci (Fig. 2.4 C, asterisks). Of note, after inactivation of *nup211ts*, Pab2 accumulated in aberrant foci at the nuclear periphery, colocalizing with both TPR proteins Nup211 and Alm1 (Fig. 2.4 C, arrowheads), similar to Nab2 (Fig. 2.3 E). This is consistent with a role of the nuclear basket in mRNP docking, probably through the interaction with both PABPs. In facts, in budding yeast the interaction of Mlp1 with the mRNA adaptor Nab2 is essential for coordinating the interplay between RNA export and QC mechanisms (Fasken et al., 2008; Grant et al., 2008; Green et al., 2003).

In order to dissect the functions of Nup211 and Alm1 in QC and export, and to discern between the phenotypes associated to defects in these processes, we used *rae1-167* as an example of mRNA export defective mutant (Bharathi et al., 1997; Brown et al., 1995; Murphy et al., 1996; Pritchard et al., 1999) and *rrp6Δ* as model for mRNA degradation deficient mutant (Fox and Mosley, 2016), and quantitated nuclear signal intensity of the Pab2-GFP. Impairment of exosome function (*i.e.* due to *rrp6* deletion) leads to the stabilization of pre-mRNAs and results in the drastic accumulation of poly(A)-

RNAs in nuclear foci, which are enriched in nuclear RNA decay proteins (Bousquet-Antonelli et al., 2000; Fan et al., 2018; Kadowaki et al., 1994; Shichino et al., 2020; Silla et al., 2018). Consistently, in *rrp6Δ* cells Pab2 formed very intense perinuclear foci that likely correspond to mRNPs intermediates accumulated as a result of deficient exosome activity (Fig. 2.4 D, arrowheads). In contrast, blocking the mRNA export pathway by inactivation of *rae1-167* leads to an overall increase in the nucleoplasmic Pab2-GFP signal (Fig. 2.4 D). Importantly, when the function of the nuclear basket was compromised using either *nup211ts* or *alm1Δ,* Pab2-GFP signal was increased in the nucleus and decreased in the cytoplasm. However, while in *alm1Δ* cells Pab2 was observed as intense perinuclear foci, similar to *rrp6Δ,* inactivation of *nup211ts* mainly results in the overall nuclear enrichment of Pab2, similar to *rae1-167* mutant, although less intense Pab2 perinuclear foci were also detected (Fig. 2.4 D, arrowheads). Therefore, the absence of the nuclear basket component Nup211, and to a less extent Alm1, leads to the nuclear accumulation of both PABPs Nab2 (Fig. 2.3 C) and Pab2 (Fig. 2.4 D). The nuclear accumulation of PABPs is consistent with the impairment of mRNA export (Fig. 2.3 A), as it is recapitulated by the inactivation of Rae1 export factor. Besides, in the *alm1Δ* mutant Pab2 further accumulates in bright foci at the nuclear periphery, similarly to deficient of exosome activity (*rrp6Δ*).

To further confirm this phenotype, we followed a biochemical approach and analyzed Pab2 protein levels in mutants defective either in mRNA export or in exosome activity, and compared them with those of TPR mutants. Importantly, in both *rrp6Δ* and *alm1Δ* strains, Pab2 protein levels were greatly decreased relative to wildtype cells (Fig. 2.4 E, asterisk). However, when the function of both Rae1 and Nup211 was compromised (by shifting the *ts* alleles from 25ºC to 36ºC), higher molecular weight bands of Pab2-GFP were observed at longer incubation times at the restrictive temperature (Fig. 2.4 E, asterisk), concomitantly with the decrease of 50kDa Pab2 protein band levels (Fig. 2.4 E, arrowheads). Interestingly, these higher molecular weight bands were also observed in wildtype cells after incubation at 36ºC for 2 hours, and likely reflects a change in mRNA export activity caused by the temperature shift. This suggested that Pab2 protein stability is altered, although differently, when the function of either the exosome or the mRNA export machinery is compromised. Together, these results point to Nup211 as an essential factor required mRNA export, while Alm1 may only play an accessory function. The increased accumulation of Pab2 in nuclear foci in *alm1Δ* cells, which phenocopies *rrp6* deletion, might suggest a possible functional connection between Alm1 and the nuclear exosome.

However, it has been described that both defects in mRNA processing/quality control and mRNA export result in the accumulation of PABPs in the nucleus (Brodsky and Silver, 2000; Fan et al., 2018; Hammell et al., 2002; Hilleren and Parker, 2001; Jensen et al., 2001; Paul and Montpetit, 2016; Tudek et al., 2018b; Zenklusen et al., 2002). Thus, we examined the exosome machinery itself, which at the cellular level is observed as nuclear foci. It has been reported that either an increase in nuclear mRNPs that are targeted for degradation or RNA exosome malfunction can be detected by changes in the number of exosome foci (Chen et al., 2011a; Shichino et al., 2020; Zhou et al., 2015). To further

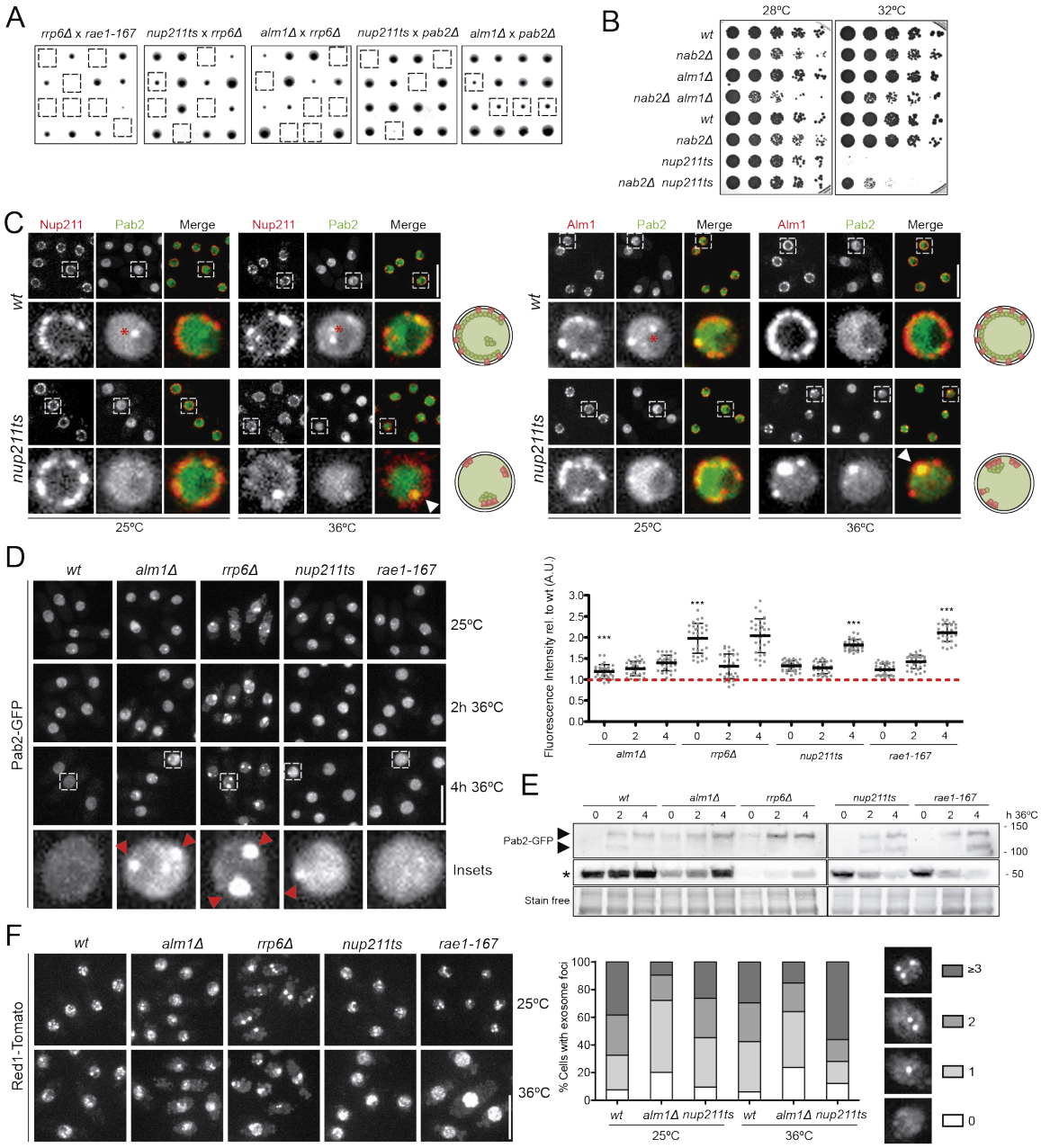

Figure 2.4. Nuclear basket Alm1 phenocopies exosome deficiency, while Nup211 has specialized in mRNA export. (A) Tetrad dissection analysis of crosses between *rrp6Δ* and *rae1-167* mutants, and *nup211ts* and *alm1Δ* strains with *rrp6Δ* and *pab2Δ*. Double mutants backgrounds are indicated with dashed squares. (B) Drop assay showing cell viability of *wt*, *nab2Δ*, *alm1Δ, nup211ts* single mutants, and the corresponding double mutants. Cells were grown at 25ºC, and plates were incubated at 28ºC and 32ºC. Cells spotted correspond to 5-fold dilutions with an initial O.D. of 0.3. (C) Fluorescence microscopy images of representative *wt* and *nup211ts* cells coexpressing Pab2-GFP and either Nup211-mCherry (left) or Alm1-Tomato (right). Maximal projections of three central z sections (step size 0.3 µm). Asterisks indicate Pab2 accumulation in exosome foci and arrowheads indicated Pab2 perinuclear foci that colocalize with NB TPRs. Scale bar: 10 µm. Schematic of the localization of TPR Nups (red) and Pab2 (green). (D) Fluorescence microscopy images of representative *wt*, *alm1Δ, rrp6Δ, nup211ts,* and *rae1-167* cells expressing Pab2-GFP (left). Cells were grown at 25ºC, and shifted to 36ºC for 2h and 4h. Maximal projections of 18 z sections (step size 0.3 µm). Magnifications of the indicated nucleus are shown (Insets). Arrowheads indicated Pab2 perinuclear foci. Scale bar: 10 µm. Quantification of nuclear Pab2-GFP levels in the indicated backgrounds and Tªs (right). Dot plot represents mean fluorescence intensity levels of each mutant relative to the *wt* strain at the same experimental conditions (red dashed line). Error bars represent SD. n= 30. ***, P < 0.001. (E) Western blot analysis of total Pab2-GFP protein from the indicated strains and Tªs. anti-GFP mAb was used to detect Pab2-GFP and stain free staining as loading control. Positions of molecular mass markers are indicated in kDa. Asterisk points to 50kDa Pab2-GFP protein band, and arrows point to higher Pab2-GFP protein bands (around 100 and 140 kDa). (F) Fluorescence microscopy images of representative *wt*, *alm1Δ, rrp6Δ, nup211ts* and *rae1-167* cells expressing Red1-Tomato at the indicated Tªs (left). Maximal projections of 18 z sections (step size 0.3 µm). Scale bar: 10 µm. Stacked column chart represents the quantification of the percentage of cells with 0, 1, 2 or ≥3 Red1 foci (right). n ≈ 200.

explore the hypothesis that the fission yeast nuclear basket is involved in mRNA QC, we measured the number of exosome foci in the two nuclear basket mutants, using the zinc-finger protein Red1 as exosome marker (Egan et al., 2014; Shichino et al., 2020; Sugiyama and Sugioka-Sugiyama, 2011). Whereas most wildtype cells showed three or more exosome foci, *alm1* deletion led to the formation of less but much brighter Red1 exosome foci, similar to the lack of exosome catalytic activity (*rrp6Δ*) (Fig. 2.4 F). Compromising the function of Nup211 or Rae1 results in both a drastic increase of Red1 overall nuclear signal and a larger number of nuclear exosome foci (Fig. 2.4 F). These experiments revealed that inactivation of *nup211ts* leads to overall nuclear accumulation of Pab2-Red1 and phenocopies mRNA export mutants, while *alm1Δ* presents less and brighter Pab2-containing exosome foci, which mimics lack of exosome activity.

Altogether, these results suggest that Alm1 might be involved in the mRNA QC pathway, while Nup211 primarily functions in the mRNA export pathway. However, given the interconnection between both processes and the interdependent localization of TPR nucleoporins, more experiment would be required to strengthen this hypothesis and clearly dissect the functions of the nuclear basket TPRs in mRNA QC and export.

2.5 mRNA export defects of *nup211ts* mutant are additive to *rae1* mutant and epistatic to *mex67* mutant.

Once mRNA processing and maturation are completed, mRNP are loaded with additional export factors to facilitate their translocation across the NPC (Bonnet and Palancade, 2014; Iglesias and Stutz, 2008; Stewart, 2010; Stutz and Izaurralde, 2003). Rae1 is a nuclear pore associated element in the fission yeast that is essential for the final step of mRNA export (Asakawa et al., 2014; Bharathi et al., 1997; Brown et al., 1995; Murphy et al., 1996; Pritchard et al., 1999). The interaction of Mex67 export factor with Rae1, through the mRNP adaptor Mlo3, as well as with FG nucleoporins of the NPC central channel, facilitates mRNP translocation through NPCs (Thakurta et al., 2005). *In S. pombe* Mex67 is not essential for cell viability; however, it is required in conditions of mRNA export impairment (Yoon et al., 2000). To get deeper insights into the function of the nuclear basket TPRs in mRNA export, we generated double mutants between deletions or termosensitive alleles of key factors required for mRNA export and the TPR mutants. This analysis revealed that the double mutants *rae1-167 nup211ts* and *mex67Δ nup211ts* showed a strong negative genetic interaction (Fig. 2.5 A and B). Importantly, *alm1Δ* presented a negative genetic interaction with *mex67Δ* (Fig. 2.5 B), but not with *rae1-167* mutant (Fig. 2.5 A). This, together with the accumulation of poly(A)-RNA (Fig. 2.3 A) and Nab2-GFP in the absence of Alm1 (Fig. 2.3 C), support the idea that Alm1 may directly or indirectly play in role in mRNA export, although this function would be considerably less critical than that of Nup211.

Based on these results, we next analyzed the efficiency of mRNA export in single and double mutants of *nup211ts* with *rae1-167* and *mex67Δ,* using the nuclear accumulation of the Nab2 as read-

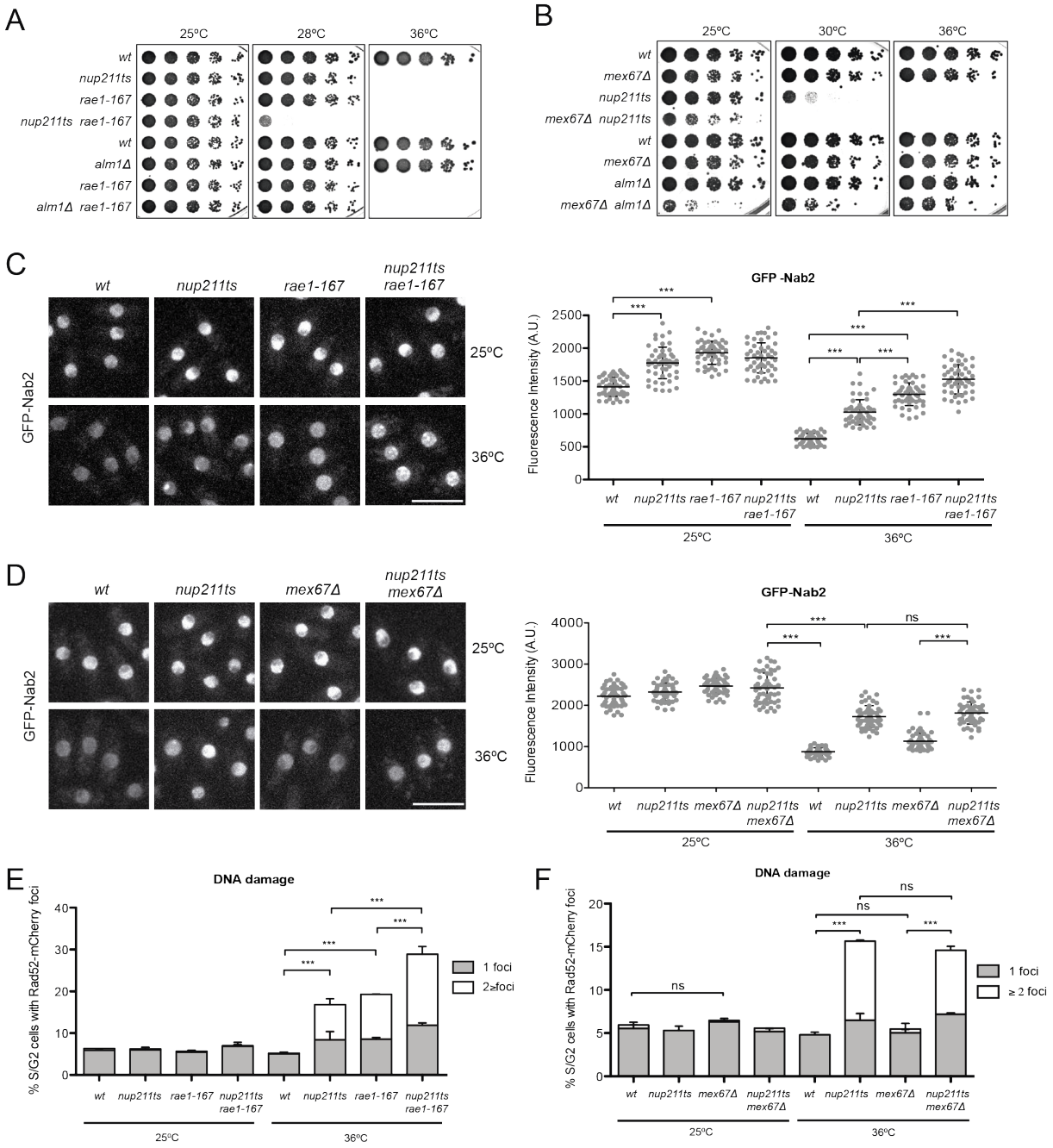

Figure 2.5. mRNA export defects of *nup211ts* mutant are additive to *rae1* mutant and epistatic to *mex67* mutant. (A, B) Drop assay showing cell viability of *wt*, *rae1-167*, *alm1Δ, nup211ts* single mutants, and the corresponding double mutants (A), and *wt*, *mex67Δ, nup211ts*, *alm1Δ* single mutants, and the corresponding double mutants (B). Cells were cultured at 25ºC, and plates were incubated at 25ºC, 28ºC and 36ºC. Spotted cells correspond to 5-fold dilutions with an initial O.D. of 0.25. (C, D) Fluorescence microscopy images of representative cells expressing GFP-nab2 in *wt*, *nup211ts* and *rae1-167* single mutants, and the corresponding double mutant (C), and *wt*, *nup211ts* and *mex67Δ* single mutants, and the corresponding double mutant (D). Cells were grown at 25ºC, and shifted to 36ºC for 4h. Maximal projections of 18 central z sections (step size 0.3 µm). Scale bar: 10 µm. Quantification of nuclear GFP-Nab2 fluorescence signal in the indicated strains and conditions (right). Dot plot represents fluorescence intensity (A.U.) of individual cell nuclei and error bars represent SD. n=50. ns, non-significant; ***, $P < 0.001$. (E, F) Quantification of DNA damage accumulation in the indicated strains and T^{a}s. Graph represents mean percentages of asynchronous S/G2 cells with Rad52-mCherry foci (1 focus in grey, 2 or more foci in white), of two independent experiments. Error bars represent SD. n=200. ns, non-significant; ***, $P < 0.001$ (% of cells with 2 or more Rad52 foci).

out. This assay revealed that the double mutant *rae1-167 nup211ts* has indeed an additive effect on mRNA export, as nuclear accumulation Nab2 was drastically increased in the double mutant compared to the single mutants (Fig. 2.5 C). However, the accumulation of Nab2 inside the nucleus of the double mutant *mex67Δ nup211ts* mutant was similar to the *nup211ts* single mutant (Fig. 2.5 D).

According to the *¨gene-gating¨* hypothesis, the topological proximity between mRNA transcription and the NPCs facilitates mRNA export and prevents the accumulation of R-loops. R-loops are the result of the hybridization of pre-mRNA molecules with their DNA template during transcription. R-loops formation interferes with DNA replication and, if not solved, they lead to DNA damage and genome instability (Castellano-Pozo et al., 2012; Dominguez-Sanchez et al., 2011; Huertas and Aguilera, 2003). Although R-loops may occurs during normal transcription, its frequency increases either in conditions of faulty mRNPs biogenesis (due to mutations in the THO or TREX-2 complexes), or by defective nuclear basket (Bhatia et al., 2014; Garcia-Benitez et al., 2017; Gavalda et al., 2016). Thus, we next examined whether a defective nuclear basket or compromising the function of mRNA export factors, such as Rae1 or Mex67, lead to DNA damage accumulation. To test this, as readout of DNA damage, we quantified by fluorescence microscopy the percentage of cells with Rad52 foci. Rad52 (RAD52 homolog) plays a central role in homologous recombination and DNA double-strand break repair, and is assembled in detectable nuclear foci during post-replication DNA repair and during the repair of induced DNA damage (Kim et al., 2000; Lisby et al., 2001; Meister et al., 2005; Ostermann et al., 1993). As expected, we observed that 6% of asynchronous wildtype cells showed Rad52-mCherry foci at both 25ºC and 36ºC, which represent cells undergoing post-replicative DNA repair (Fig. 2.5 E). *nup211ts* displayed a 3-fold increase in Rad52 foci in comparison to the wildtype background at restrictive temperature (Fig. 2.5 E), consistent DNA damage accumulation. In agreement with our previous results, the *nup211ts rae1-167* double mutant greatly increased DNA damage accumulation, as demonstrates the percentage of cells with Rad52 foci compared to single the mutants (Fig. 2.5 E), whereas DNA damage does not increase in the *mex67Δ nup211ts* double mutant compared to the single mutants (Fig. 2.5 F).

Together, these results point to a functional connection between Nup211 and the key mRNA export factors Rae1 and Mex67. The synthetic genetic interaction between *nup211ts* and *rae1-167* and the epistatic genetic interaction between *nup211ts* and *mex67Δ* in mRNA export and DNA damage accumulation suggest that Rae1 and Nup211 could function independently or at different steps of the mRNA export pathway, while Nup211 and Mex67 may work cooperatively or in the same mRNA export pathway.

2.6 Nup211 participates in the recruitment of Mex67.

During mRNA export in *S. pombe,* Mex67 interacts with Rae1 through the mRNP adaptor Mlo3 (Thakurta et al., 2005; Thakurta et al., 2007), although Mlo3 is released from the mRNA prior to mRNP translocation, while Mex67 and Rae1 act as shuttling proteins (Iglesias et al., 2010; Pritchard et al.,

1999). The genetic interaction with canonical mRNA export factors and the nuclear accumulation of mRNAs in the *nup211ts* mutant led us to investigate whether the involvement of the TPR nucleoporins, and mainly Nup211, in mRNA export could occur through the interaction with or the regulation of mRNA export factors. To do that, we analyzed by fluorescence microscopy the subnuclear localization of Rae1, Mlo3 and Mex67 in the TPR Nups mutants. While the distribution of Rae1 at the NPC was unaffected in the *nup211ts* mutant, its levels were slightly increased (Fig. 2.6 A), consistent with a block in mRNA export. In wildtype cells Mlo3-GFP shows a homogeneous nucleoplasmic distribution, excluded from the nucleolar region (Fig. 2.6 B). Interestingly, in the *nup211ts* mutant, Mlo3 accumulated in the nucleoplasm and was specially concentrated at the nuclear periphery. Remarkably, Mex67, which in wildtype cells is enriched at the nuclear periphery and at the nucleolar region (Yoon et al., 2000; Yoshida and Tani, 2005), completely mislocalized from the nuclear periphery in the *nup211ts* background at restrictive temperature, and in 37% of cases (n=219) Mex67 accumulated in abnormal perinuclear foci (Fig. 2.6 C, arrowhead). This was accompanied by an increase in total protein levels, which suggest that Mex67 protein stability might be conditioned in the *nup211ts* mutant (Fig. 2.6 C). We further confirmed that neither the localization of Rae1 nor Mex67 was significantly altered in *alm1*-deleted cells, whereas Mlo3 was enriched at the nucleoplasm (Fig. 2.6 A-C), which is consistent with the minor defects of mRNA export observed in this mutant (Fig. 2.3 A). Importantly, when the mRNA export pathway was blocked at the level of Rae1 (*rae1-167* background), both Mex67 and Mlo3 accumulated at NPCs (Fig. 2.6 D), which is indicative of defective mRNPs translocation through NPC (Brown et al., 1995). We hypothesize that when the function of Rae1 is impaired, Mex67-containing mRNPs cannot shuttle through the NPC and accumulate at the nuclear pore. However, the mislocalization of Mex67 from the nuclear periphery and its aggregation in abnormal perinuclear foci in the *nup211ts* background suggests a role of Nup211 in the recruitment or loading of Mex67 in a step that precedes Rae1 export function.

In *S. cerevisiae* adaptor proteins, such as Mlo3 and Nab2, mediate the recruitment of Mex67 into the mRNP (Hautbergue et al., 2008; Iglesias et al., 2010; Kohler and Hurt, 2007; Rougemaille et al., 2008; Strasser and Hurt, 2000; Strasser et al., 2002; Viphakone et al., 2012; Zenklusen et al., 2001). Given that Mex67 is no longer enriched at the nuclear periphery in the *nup211ts* mutant background (Fig. 2.6 C), we wondered if the absence of Nup211 could affect the docking of Mex67-containing mRNPs to the NPCs or the loading of Mex67 into the mRNPs. To discern between these two possibilities, we analyzed the colocalization of Mex67 with either the TPR Nups or mRNPs marked with Nab2/Pab2. In unperturbed conditions, Nup211 and Mex67 display a similar nuclear pore distribution. However, when the function of Nup211 is impaired, the colocalization of Mex67 with the nuclear basket TPRs is abolished in about 86% of cells (Fig. 2.6 E). Then, we checked if Nab2/Pab2-containing poly(A)-RNA foci colocalized with Mex67 in the *nup211ts* mutant. We found that although Mex67, Pab2 and Nab2 share a similar pattern at the nuclear periphery in control conditions, inactivation of Nup211 precluded the colocalization of Mex67 with both PABPs (Fig. 2.6 F). This data shows that when the function of Nup211 is impaired Nab2/Pab2-bound poly(A)-RNA foci are devoid of

Mex67 export factor and supports the hypothesis that Mex67 is not properly loaded into the mRNPs in the absence of Nup211.

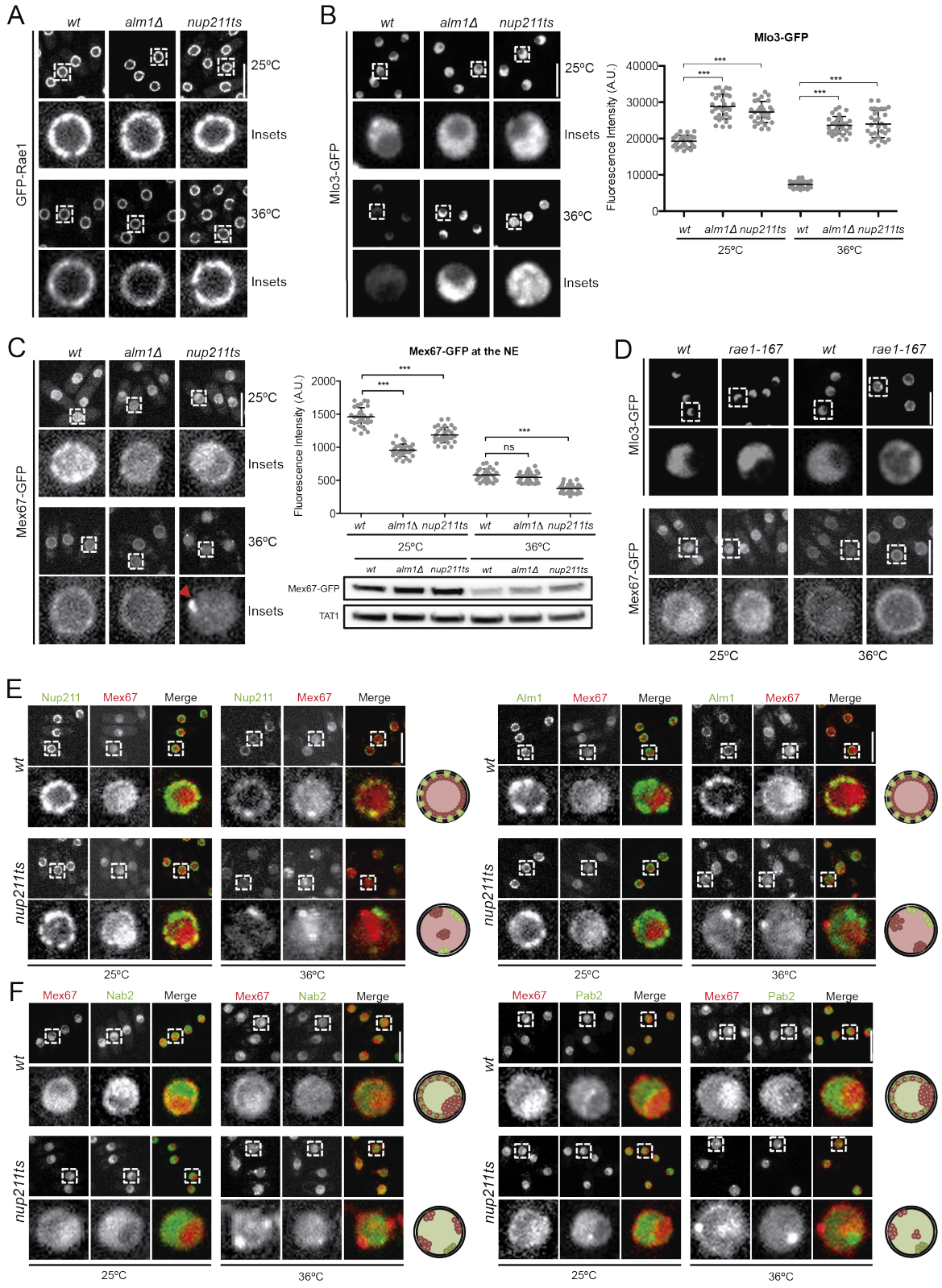

Figure 2.6. Nup211 participates in the recruitment of Mex67 to NPCs. (A, B) Fluorescence microscopy images of representative *wt*, *alm1Δ* and *nup211ts* cells expressing either GFP-rae1 (A) or mlo3-GFP (B) at the indicated T[a]s. Quantification of Mlo3-GFP levels (B, right panel) in the nucleoplasm, in the indicated backgrounds and T[a]s. Dot plot represents mean fluorescence intensity levels (A.U.) and error bars represent SD. n= 30. ***, P < 0.001. (C) Fluorescence microscopy images of

representative *wt*, *alm1Δ* and *nup211ts* cells expressing mex67-GFP at the indicated T^{a}s (left). Arrowhead indicates Mex67 perinuclear foci. Quantification of Mex67-GFP levels at the NE in the indicated backgrounds and T^{a}s (right). Dot plot represents mean fluorescence intensity levels (A.U.) and error bars represent SD. n= 30. ns, non-significant; ***, P < 0.001. Western blot analysis of total Mex67-GFP protein in the indicated strains and conditions, using anti-GFP mAb to detect Mex67-GFP and TAT1 as a loading control (right). (D) Fluorescence microscopy images of representative *wt* and *rae1-167* cells expressing either mlo3-GFP or mex67-GFP at the indicated T^{a}s. (E) Fluorescence microscopy images of representative *wt* and *nup211ts* cells coexpressing Mex67-mCherry and either Nup211-GFP (left) or Alm1-GFP (right). Schematic of the localization of nuclear basket TPR (green) and Mex67 (red). (F) Fluorescence microscopy images of representative *wt* and *nup211ts* cells coexpressing Mex67-mCherry and either GFP-Nab2 (left) or Pab2-GFP (right) at 25ºC and 36ºC. Schematic of the localization of Mex67 (red) and Nab2/Pab2 (green). Magnifications of the indicated nucleus are shown. Maximal projections of three central z sections (step size 0.3 µm). Scale bars: 10 µm.

Discussion

2.1 Nup211 and Alm1 interaction is required for their assembly at the nuclear basket.

Extending inwards into the nuclear interior, the NPC terminates in a flexible structure called nuclear basket. The main constituents of the nuclear basket are the TPR Nups in higher eukaryotes (Bangs et al., 1998; Cordes et al., 1997; Frosst et al., 2002; Hase et al., 2001; Krull et al., 2004), myosin-like proteins Mlp1 and Mlp2 in *Saccharomyces cerevisiae* (Galy et al., 2004; Kosova et al., 2000; Niepel et al., 2013; Strambio-de-Castillia et al., 1999), and Alm1 and Nup211 in the fission yeast (Asakawa et al., 2019; Salas-Pino et al., 2017). Besides, several studies have reported that TPR anchoring to the NPC depends on other nuclear basket nucleoporins as well as the core structure of the NPC (Asakawa et al., 2019; Boehmer et al., 2003; Feuerbach et al., 2002; Galy et al., 2004; Hase and Cordes, 2003; Palancade et al., 2005; Rajanala and Nandicoori, 2012; Souquet et al., 2018). However, in *S. pombe* it has never been addressed how the nuclear basket TPR Nups are assembled and anchored to the NPC. For that, we generated thermosensitive alleles of Alm1 and Nup211. We have observed Nup211 and Alm1 display a nearly identical distribution at the nuclear periphery (Fig. 2.1 D), and the absence of one TPR negatively affect the NPC localization of the other (Fig. 2.1 D). This data highlights that Nup211 and Alm1 display an interdependent localization and demonstrates that in the fission yeast TPR proteins interact directly to assemble at the nuclear basket.

Then, to assess how the nuclear basket TPRs are attached to the NPC in *S. pombe*, we have studied the effect of deleting several nuclear pore components over the localization of TPRs. Apart from TPR nucleoporins, the fission yeast nuclear basket is also composed by the FG-Nups Nup60, Nup61 and Nup124 (Asakawa et al., 2014). The nuclear outer ring of the NPC contains Nup132 and Nup107, while the cytoplasmic outer ring is formed by six different nucleoporins, Nup120, Nup131, Nup37, Nup96, Ely5 and Nup85 (Asakawa et al., 2019). Our results show that in the fission yeast Nup60 is partially responsible for TPR tethering to the NPC (Fig. 2.1 F), as happens for *S. cerevisiae* Mlps (Feuerbach et al., 2002; Galy et al., 2004; Palancade et al., 2005). In turn, deletion of Nup132 results in a major mislocalization of Alm1 to the nucleoplasm (Fig. 2.2 A). Moreover, when the function of Alm1 is compomised in the *nup132Δ* genetic background, both Alm1 and Nup211 delocalize from the NPC and form bright foci in what likely constitutes nuclear basket aggregates (Fig. 2.2 C). Remarkably, these nuclear basket aggregates contain both TPR proteins at permissive temperature,

whereas at restrictive conditions Alm1 and Nup211 interaction is disrupted (Fig. 2.2 C). Altogether, these results suggest that Alm1/Nup211 assembly into the nuclear basket mainly depends on their own interaction and their anchoring to the NPC via Nup132, although other Nups, such as Nup60, could also contribute to stabilize nuclear basket structure. Importantly, while in human cells the TPRs are anchored to the NPC by Nup153 (Hase and Cordes, 2003; Rajanala and Nandicoori, 2012), it has been recently described that in mouse embryonic stem cells the localization of Nup153 and TPRs is regulated by Nup133 (homolog of *Sp*Nup132), since in its absence 50% of the NPCs lack TPRs and appear as aggregates (Souquet et al., 2018). This suggests that the mechanism of nuclear basket assembly could be conserved. Indeed, the absence of Nup133, the *S. cerevisiae* ortholog of Nup132, destabilizes the entire Y-complex structure and leads to major NPC assembly defects (Doye et al., 1994; Pemberton et al., 1995; Walther et al., 2003). Similarly, in *S. pombe* loss of Nup132 induces significant nuclear NPC reorganization and NPCs tend to cluster (Asakawa et al., 2014; Bai et al., 2004). Importantly, Alm1 and Nup211 do not show a homogeneous pattern throughout nuclear periphery (Fig. 2.1 D), contrary to what happens for most nucleoporins, which show a continuous distribution along the NE surface (Asakawa et al., 2014). The fact that they only colocalize with a subset of nuclear pores could imply that there exists some kind of specialization regarding NPC functions, a hypothesis that has been proposed previously (Kosova et al., 2000; Niepel et al., 2013; Strambio-de-Castillia et al., 1999).

Based on sequence comparison, Nup211 and Alm1 proteins are equivalent to *S. cerevisiae* Mlp1 and Mlp2, respectively. However, phylogenetic analyses of *S. pombe* Nup211 and Alm1 and *S. cerevisiae* Mlp1 and Mlp2 have revealed that these proteins emerged by independent event of gene duplication and, therefore, they are not orthologs to each other (Field et al., 2014). Importantly, in relation to the essentiality of TPR nucleoporins for cell survival, in *S. cerevisiae* the double *mlp1 mlp2* deletion mutant is viable (Galy et al., 2004; Kosova et al., 2000; Niepel et al., 2005), whereas TPR is required for cell growth (David-Watine, 2011). *nup211*$^{+}$ is an essential gene (Bae et al., 2009), and we could not obtain the double mutants between *alm1Δ/alm1ts* and *nup211ts,* not even at permissive temperature. The fact that *alm1Δ nup211ts* double mutant is synthetically lethal could imply that, even though most of the roles of the TPR nucleoporins, such as SAC regulation (De Souza et al., 2009; Lee et al., 2008b; Rodriguez-Bravo et al., 2014; Schweizer et al., 2013), are conserved, in *S. pombe* they may have acquired additional or more prominent functions required for cell survival.

2.2 Alm1 and Nup211 particiate in mRNP docking to the NPC.

The different steps of mRNA biogenesis, from transcription to export, are highly coordinated and, therefore, the absence of any element involved in this pathway has negative consequences for mRNA metabolism (Katahira, 2015; Paul and Montpetit, 2016; Rodriguez-Navarro and Hurt, 2011; Stutz and Izaurralde, 2003; Tutucci and Stutz, 2011; Vinciguerra and Stutz, 2004). mRNP docking and export is a cooperative process in which the nuclear basket tethers mRNPs via the interaction with RNA-binding proteins, while nucleoporins of the central channel mediate the translocation towards the cytoplasm by

the interaction with mRNA export factors (Fig. I7 C) (Bonnet and Palancade, 2014; Carmody and Wente, 2009; Delaleau and Borden, 2015; Hocine et al., 2010; Katahira, 2015). The nuclear basket is part of a final quality control QC mechanism that monitors the quality of the mRNPs prior to export (Fig. I7 C). By interacting with mRNPs adaptor proteins either allows mRNA export or retain aberrantly processed or unspliced mRNAs, facilitating their degradation by the nuclear exosome (Bonnet et al., 2015; Coyle et al., 2011; Fasken et al., 2008; Galy et al., 2004; Green et al., 2003; Lewis et al., 2007; Palancade et al., 2005; Rajanala and Nandicoori, 2012; Vinciguerra et al., 2005). It was previously shown that both over-expression and repression of *S. pombe nup211*$^{+}$ causes defects in mRNA export (Bae et al., 2009). Despite this, it remains elusive the degree of conservation of these functions in *S. pombe*. In the second part of this study, we have performed a genetic and functional analysis to dissect the functions of the nuclear basket components Nup211 and Alm1 in mRNA docking, QC and export.

Our data demonstrate that interfering with the assembly of the nuclear basket leads to a massive nuclear accumulation of mRNAs and the two main PABPs in the fission yeast Nab2 and Pab2, which is more accentuated in the absence of Nup211 than in the *alm1*-deleted mutant (Fig. 2.3 A and C, Fig. 2.4 D). Moreover, the TPR nucleoporins colocalize with Nab2 and Pab2 in perinuclear foci, especially in conditions of mRNA export inhibition (Fig. 2.3 E and Fig. 2.4 C). Therefore, the docking activity of the nuclear basket seems to be conserved in the fission yeast. Nuclear basket docking is a rate-limiting step of the mRNA export pathways and not all the mRNPs that are docked at the nuclear basket are exported (Ben-Yishay et al., 2016; Grunwald and Singer, 2010; Mor et al., 2010; Oeffinger and Zenklusen, 2012; Saroufim et al., 2015; Siebrasse et al., 2012). It has been estimate that about three quarters of the total mRNAs that reach the nuclear basket return into the nucleoplasm and scan for another pore to exit (Kelich and Yang, 2014). This perinuclear scanning has been associated to the QC control funtion of the nuclear basket (Hessle et al., 2012; Soheilypour and Mofrad, 2016). In agreement with a functional connection between the nuclear basket and the exosome in fission yeast, the nuclear RNA silencing (NURS) complex (also known as MTREC, for Mtl1-Red1 core, composed of Red1, Mtl1, Red5, Ars2, Rmn1, and Iss10 proteins), involved in nuclear exosome recuitment and selective RNA elimination, physically interacts with the TPR Nups (Egan et al., 2014). Importantly, this complex as well as its functions seems to be conserved in human cells (Andersen et al., 2013b; Zhou et al., 2015). Indeed, Pab2, which accumulates in the nuclear periphery together with Nup211 and Alm1 (Fig. 2.4 C), is considered as part of the exosome machinery and physically associates with several exosome components, including Rrp6 and Red1 (Chen et al., 2011a; Egan et al., 2014; Grenier St-Sauveur et al., 2013; Lemieux et al., 2011; St-Andre et al., 2010; Yamanaka et al., 2010; Zhou et al., 2015).

We wondered whether the nuclear basket TPR nucleoporins could play a direct role in mRNA trafficking or whether, on the contrary, they would indirectly influence mRNA export through the exosome-dependent QC of mRNPs. To solve this question, we have used different approaches to compare the phenotypes of *alm1Δ* and *nup211ts* cells with canonical mutants defective in mRNA

export (*rae1-167*) and exosome-dependent degradation (*rrp6Δ*). Our results points to a main role of Nup211 in the regulation of mRNA export, while *alm1Δ* mimics an exosome deficient mutant (Fig. 2.4 D-F). However, mRNA degradation and export are interdependent processes (Andersen et al., 2013a; Hammell et al., 2002; Jensen et al., 2003; Luna et al., 2005; Saguez et al., 2005; Schmid and Jensen, 2008; Stutz and Izaurralde, 2003; Tutucci and Stutz, 2011). While an mRNA export block leads to the sequestration of newly synthesized transcripts at or near their transcription sites and to their rapid degradation by the exosome (Hilleren and Parker, 2001; Jensen et al., 2001; Tudek et al., 2018b), impairment of RNA exosome function results in the retention of poly(A)-RNA in nuclear foci (Bousquet-Antonelli et al., 2000; Fan et al., 2018; Kadowaki et al., 1994; Shichino et al., 2020; Silla et al., 2018). Consistently, Rrp6 becomes essential for cell survival in conditions of mRNA export impairment (Fig. 2.4 A) or defective mRNA processing (Sugiyama et al., 2013). Importantly, Nab2 and Pab2 compete for binding to poly(A)-RNA tails, stablishing an equilibrium between RNA processing and RNA decay: Pab2 targets hyperadenylated RNAs for degradation via the nuclear exosome (pre-mRNA decay pathway), whereas Nab2 stabilizes unspliced pre-mRNAs and impedes their Pab2/Rrp6-mediated degradation (Grenier St-Sauveur et al., 2013). Consistent with a main role of Nup211 in mRNA export, cell lethality of *nup211ts* exacerbates when the exosome function is impaired (in the absence of *rrp6* or *pab2*), whereas it is partially supressed when the exosome pathway is favoured (in the absence of *nab2*). On the other hand, *alm1Δ* displays a negative genetic interaction with *pab2* mutant, but not with *nab2* mutant. This points to a functional divergency of nuclear basket TPR nucleoporins in the RNA fate regulation.

Altogether, our results demonstrate that Nup211 is mainly involved in mRNA export. We hypothesize that the inhibition of poly(A)-RNA export in the *alm1* mutant could be due to the mislocalization of Nup211 from the nuclear periphery in this genetic background (Fig. 2.1 D) or to a less critical or indirect function of Alm1 in mRNA export through the mRNA QC degradation pathway. However, given the interdependent localization of TPR nucleoporins and the fact that all mRNA biogenesis steps are tightly coupled, further research would be needed to strengthen this hypothesis and to identify a direct role of the TPR nucleoporins in QC of mRNP prior to export.

2.3 Nup211 functions in mRNA export by recruiting Mex67.

To further characterize the role of the nuclear basket in mRNA export in *S. pombe*, we studied the functional connection between the nuclear basket TPRs and the mRNA export pathway. In fission yeast Mex67 and Rae1 are mRNA carrier factors that interact with nucleoporins of the NPC central channel (such as Nup159 and Nup98), and escort the mRNA molecules on their way through the NPC (Blevins et al., 2003; Pritchard et al., 1999; Strasser et al., 2000; Strawn et al., 2001; Thakurta et al., 2004). In fact, the genetic and biochemical interaction between Mex67 and Rae1 suggest that they participate together in mRNA export (Thakurta et al., 2005; Yoon et al., 2000). It has been described that the mRNA receptor Mex67 directly binds to the mRNA adaptor Mlo3 and, in turn, Mlo3 is linked to Rae1 (Thakurta et al., 2005; Thakurta et al., 2007). However, while Rae1 is essential for cell viability

(Brown et al., 1995; Murphy et al., 1996; Pritchard et al., 1999), Mex67 is not, although it becomes required when mRNA export is impaired, as demonstrates the synthetic lethality of *mex67*-deletion mutant with several export factors (*mlo3, elf1, dss1*) and nucleoporins (*npp106, nup97, nup184*) (Thakurta et al., 2005; Yoon, 2004; Yoon et al., 2000; Yoon et al., 1997). When we examined the genetic interaction between the nuclear basket mutants and these two mRNA export factors, we discovered that *nup211ts* have an additive genetic interaction with *rae1-167,* and an epistatic genetic interaction with *mex67*-deleted mutant in relation to mRNA export (Fig. 2.5). This suggests that Rae1 and Nup211 functions may occur at different steps of the mRNA export process, while Mex67 and Nup211 may work together in the mRNA export pathway. In agreement with this hypothesis, it has been shown that in metazoans TPRs participate in the regulation of mRNA trafficking through the NXF1 export pathway (Coyle et al., 2011).

Accordingly, impairment of Nup211 results in increased levels of Rae1 at the NPC (Fig. 2.6 A), while Mlo3 accumulates inside the nucleus (Fig. 2.6 B), consistent with the inhibition of mRNA export. Importantly, inactivation of *nup211ts* causes the delocalization of Mex67 from the nuclear periphery and its accumulation in aberrant nuclear foci (Fig. 2.6 C). Noteworthy, the localization of Mex67 is different between *nup211ts* and *rae1-167* cells. When the function of Rae1 is impaired, Mex67 accumulates at the nuclear periphery, as it cannot travel across the NPC (Fig. 2.6 D), whereas after Nup211 inactivation Mex67 delocalizes from nuclear basket and forms abnormal perinuclear foci (Fig. 2.6 C). Base on these data, we hypothesize that Nup211 could be involved in the recruitment or docking of Mex67 prior to export; then, Mex67 would be channelled from Nup211 to Rae1, to escort mRNPs through the NPC. But why does Mex67 mislocalize in *nup211ts* mutant?

Mex67 loading into the mRNP depends on adaptor proteins, such as Mlo3 and Nab2 (Hautbergue et al., 2008; Iglesias et al., 2010; Kohler and Hurt, 2007; Rougemaille et al., 2008; Strasser and Hurt, 2000; Strasser et al., 2002; Viphakone et al., 2012; Zenklusen et al., 2001). However, it has been recently suggested that in both budding yeast and mammalian cells Mex67/NXF1 acts as a mobile nucleoporin whose dynamic localization at the NPC is independent on mRNP interaction (Ben-Yishay et al., 2019; Derrer et al., 2019). According to these works, Mex67 export factor would bind to mature mRNP at the NPC before being translocated into the cytoplasm. Therefore, there exist two alternative hypotheses that could explain the phenotype of *nup211ts*. Mex67-containing mRNPs could be recruited to the nuclear basket via Nup211 interaction and, then, mRNPs would be channelled from the nuclear basket through the NPC central channel. Alternatively, Nup211 could facilitate the loading of Mex67 into mRNPs, once they have reached the nuclear basket and prior translocation through the NPC. Noteworthy, our results show that Mex67 foci formed after Nup211 inactivation do not colocalized with the TPR nucleoporins or with PABPs-mRNPs (Fig. 2.6 E and F), which supports the second hypothesis. Therefore, we propose that in the absence of Nup211, Mex67 export factor is not loaded into Pab2/Nab2-bound mRNPs, which become retained inside the nucleoplasm and trapped in disfunctional NB aggregates. But why Mex67 is not recruited to mRNPs after inactivation of Nup211?

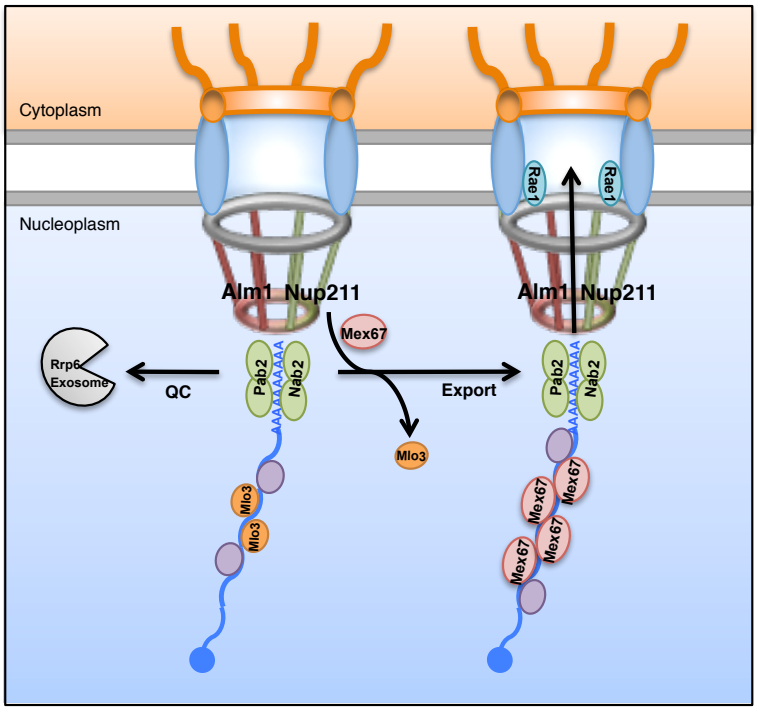

Figure 2.7. Working model depicting the roles of the nuclear basket TPRs Alm1 and Nup211 in mRNP docking, quality control and export. In the nucleus mRNAs are sequentially coated with different RNA binding proteins, such as Mlo3 adaptor, and the PABPs Nab2 and Pab2, generating mRNPs. Preceding translocation through the NPC central channel, mRNPs are docked to the nuclear basket via Alm1/Nup211 interaction with these RNA-binding proteins. Such targeting to the nuclear basket could contribute to quality control of mRNP, regulating the interplay between the degradation of faulty mRNPs (via the Rrp6-exosome) or the export of mature mRNPs. We hypothesize that Alm1 could be functionally related to this QC checkpoint at the nuclear basket, while Nup211 might play an essential role in mRNA export by recruiting Mex67 into export-competent mRNPs, licensing their translocation through the NPC by Rae1 export factor.

One possibility is that the docking of mRNPs to the nuclear basket might be necessary to assist the loading of Mex67; as a consequence of the deficient recruitment of Mex67, mRNPs would not be licensed to export. However, defective localization or activity of Mex67 cannot explain the cell lethality of *nup211ts* mutant, since *mex67*-deleted cells are viable, which might point to additional roles of Nup211. Another possibility is that the aberrant Pab2/Nab2-containing RNAs foci formed in conditions of Nup211 deficiency might correspond to abnormal mRNP molecules that are retained by the nuclear basket. In agreement with this, in metazoans association of NXF1 with mature mRNPs allows their docking to the nuclear basket, through TPR and Nup153, and then mRNPs are subsequently translocated across the central channel by RAE1 (Bachi et al., 2000; Matzat et al., 2008). Similarly, in yeast Mex67 loading into mRNPs chiefly occurs once the mRNPs have been quality-controlled, so that improperly processed or immatured mRNPs cannot be exported (Fasken and Corbett, 2009; Hackmann et al., 2014; Iglesias et al., 2010; Tudek et al., 2018b). According to the “hand-over” model, further loading of Mex67 into the export-competent mRNP is caused by the removal of Yra1 from the mRNP, as a result of Sub2/UAP56-dependent remodeling of the mRNPs, arginine methylation, and Tom1 E3 ligase-dependent ubiquitination (Hautbergue et al., 2008; Hung et al., 2010; Iglesias et al., 2010; Strasser and Hurt, 2001; Viphakone et al., 2012). Actually, Tom1 ubiquitinates Yra1 and promotes its dissociation from mRNPs, which acts as a signal of mRNP competency that elicits mRNA

export by allowing Mex67/Nab2-containing mRNPs to interact with nucleoporins to cross the NPC (Duncan et al., 2000; Iglesias et al., 2010). Tom1 is conserved in the fission yeast and, similar to his *S. cerevisiae* homolog, *ptr1-1* mutant functionally interacts with *rae1-167* and leads to mRNA export defects (Andoh et al., 2004). Given the different phenotypes over the localization of Mlo3 (Yra1) and Mex67 that triggers the inactivation of Nup211, it would be worth exploring whether the nuclear backet could be involved in the final remodeling of mRNPs to licence their export.

In conclusion, we propose that the nuclear basket contributes to the docking of mRNPs to the nuclear pore through interaction with PABPs (Fig. 2.7). On the one hand, this docking might assist RNA quality control, by retaining defective RNA or promoting their degradation by the nuclear exosome. On the other hand, nuclear basket docking could facilitate the loading of Mex67 into the mRNPs, in a Nup211-dependent manner, which is a prerequisite for their export.

Chapter 3

Dynamic and reversible aggregation of NPC components and mRNA machinery into nucleolar rings upon heat stress

3.1 The Nuclear Pore is remodeled upon heat shock.

Heat shock negatively affects the stability and function of cellular complexes and compromise cell viability, due to protein denaturation and aggregation. In order to cope with these harmful environmental conditions and ensure cell survival cells activate the evolutionary conserved HSR (Trott A., 2003; Verghese et al., 2012). Severe heat stress triggers profound changes in mRNA metabolism (Bond, 2006). In *S. cerevisiae* HS-dependent inhibition of mRNA export is achieved by changes in the composition of the mRNPs (Krebber et al., 1999; Zander et al., 2016) and the accumulation of the nuclear basket Mlp1 and Mlp2 in nuclear foci together with several mRNP factors (Carmody et al., 2010). The fact that in fission yeast the nuclear basket is required for mRNA export (Fig. 2.3) prompted us to analyze the localization of the nuclear basket nucleoporins during HS. For that, we compared the localization of all the described components of the nuclear basket in non-heat shock (25ºC) versus heat shock conditions (42ºC for 20 minutes). While in unperturbed conditions the two TPR nucleoporins of the nuclear basket, Alm1 and Nup211, show a punctuated pattern at the nuclear periphery, consistent with their NPC localization, surprisingly, we discovered that under heat stress Alm1 and Nup211 exhibited an atypical localization: they dissociated from the nuclear periphery and coalesced into a ring-like structure inside the nucleus (Fig. 3.1 A). However, the other described nuclear basket components, Nup60, Nup61 and Nup124 (Asakawa et al., 2019), maintained their normal localization at the nuclear pore (Fig. 3.1 A). Colocalization analyses between Alm1 and other NB nucleoporins (Nup60) confirmed this ring-like rearrangement of the nuclear basket TPR components with regard to the NPC (Fig. 3.1 B).

We have demonstrated previously that TPRs associate to the NPC through Nup132 (Fig. 2.2), a component of the NPC nucleoplasmic Y-subcomplex (Asakawa et al., 2014). Thus, we checked whether Nup132, as well as other components of the NPC Y-subcomplexes, suffer a similar spatial rearrangement as the nuclear basket TPRs in heat shock conditions. Intriguingly, we found that not all the nucleoporins conforming the Y-subcomplexes displayed the same behaviour. Nup132 and Nup85 mirrored the TPR localization and, almost completely, dissociated from NPCs to coalesce into a ring-like structure (Fig. 3.1 C). Notice that upon HS a fraction of Nup85 also accumulates in cytoplasmic stress granules, marked with the PABP Pab1, although most Nup85 fluorescence signal localized at this ring-like structure (Fig. 3.1 D). In turn, most of Y-components, including Nup107, Nup120, Nup96, Nup37, Ely5 and Seh1, remained at the nuclear periphery, except for Nup131, which disappeared from the nuclear pore to the cytoplasm (Fig. 3.1 C). This prompted us to analyze the other NPC subcomplexes, including nucleoporins of the inner ring (Nup155 and Nup40), the central channel (Nup44), and the cytoplasmic filaments (Nup82, Nup146 and Amo1) (Asakawa et al., 2014). The localization of none of these nucleoporins changed during a HS, with the exception of Amo1, which disappeared from the NPC and relocated to the cytoplasm (Fig. 3.1 E), similar to Nup131. Finally, we determined that the membrane ring nucleoporins Cut11 (West et al., 1998) and Tts1 (Zhang and Oliferenko, 2014), as well as the INM protein Ish1 (Taricani et al., 2002) did not reorganize upon HS (Fig. 3.1 E), which indicates that these rings are not the result of nuclear envelope invaginations.

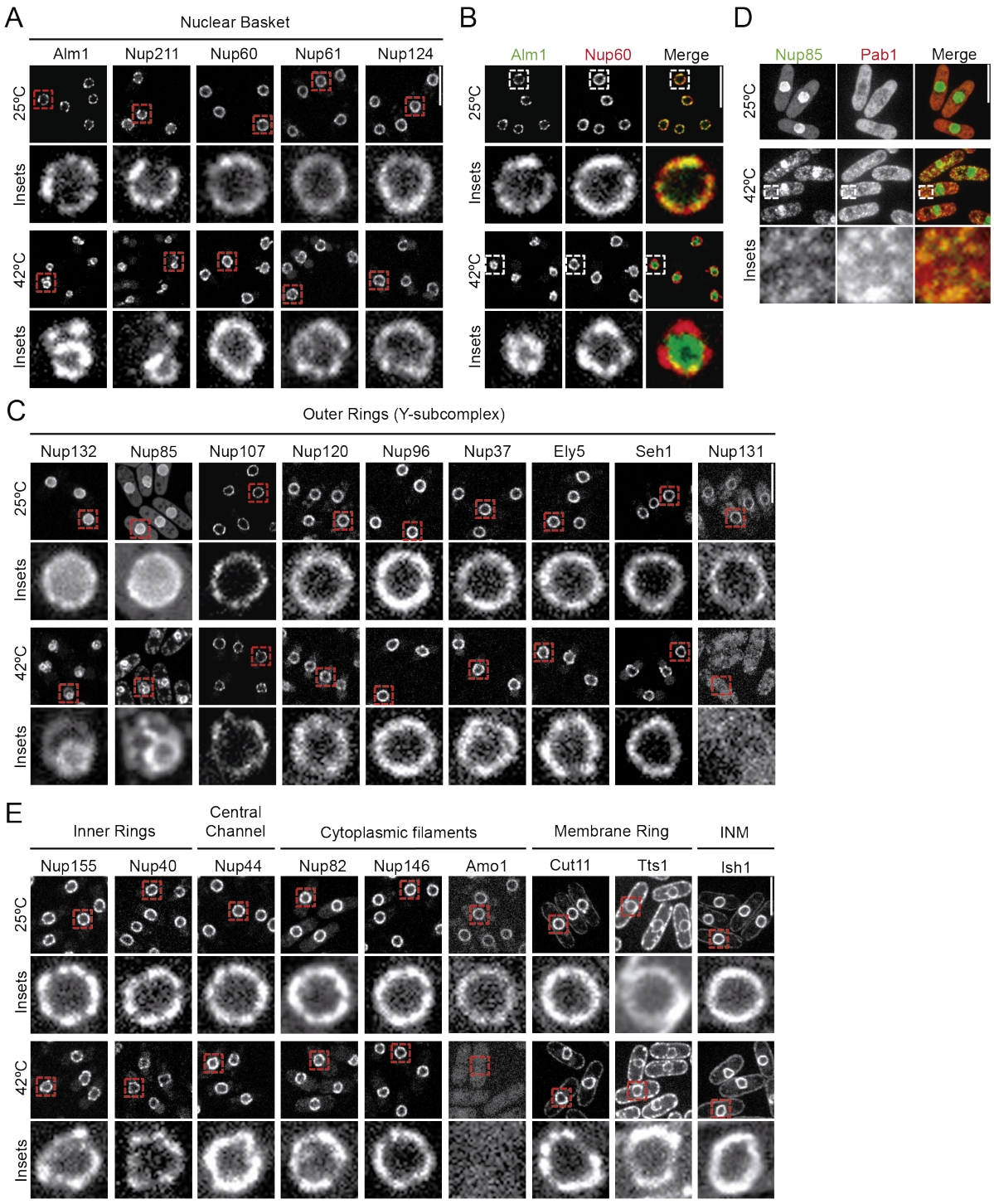

Figure 3.1. The Nuclear Pore is remodeled upon heat shock. (A) Fluorescence microscopy images of representative cells showing the nuclear basket components alm1-GFP, nup211-GFP, nup60-mCherry, GFP-nup61, and GFP-nup124 at 25ºC and after 42ºC heat shock treatment for 20 min. (B) Fluorescence microscopy images of representative cells expressing alm1-GFP (green) and nup60-mCherry (red) at 25ºC and 42ºC (20 min). (C) Fluorescence microscopy images of representative cells showing the NPC outer rings (Y-subcomplex) components GFP-nup132, GFP-nup85, nup107-GFP, nup120-GFP, nup96-GFP, nup37-GFP outer, ely5-GFP, seh1-GFP, and GFP-nup131 at 25ºC and 42ºC (20 min). (D) Fluorescence microscopy images of representative cells expressing GFP-nup85 (green) and pab1-mRFP (red) at 25ºC and 42ºC (20 min). (E) Fluorescence microscopy images of representative cells showing the NPC components of the inner rings (Nup155 and Nup40), the central channel (Nup44), cytoplasmic filaments (Nup82, Nup146 and Amo1), membrane ring (Cut11 and Tts1) and the INM protein Ish1 at 25ºC and 42ºC (20 min). Magnifications of the regions indicated by dashed boxes are shown (Insets). Maximal projections of three central z-sections (step size 0,3 μm). Scale bar: 10 µm.

Altogether, these results demonstrate that the structure of the NPC is reorganized upon HS. While the core of the NPC remains conventionally associated to the NE, the structural elements of the nuclear basket (Alm1 and Nup211), and the Y-subcomplex components Nup132 and Nup85 detach from the NPC and coalesce into a nuclear ring-like structure.

3.2 Heat shock induces the nucleolar accumulation of mRNAs and mRNA-related factors.

Previous studies have shown that the HSR provokes the inhibition of bulk mRNA export and the upregulation of stress responsive genes (Bond, 2006; Solis et al., 2016; Veri et al., 2018). As a consecuence, in yeasts HS leads to the nuclear accumulation of poly(A)-RNA, predominantly inside the nucleolus (Saavedra et al., 1996; Tani et al., 1996). To check that, we examined poly(A)-RNA distribution by fluorescence *in situ* hybridization (FISH) in cells grown at 25ºC and incubated at 42ºC for 20 minutes. Heat shocked cells chiefly concentrate poly(A)-RNA inside the nucleus, while cytoplasmic mRNA levels decrease, which is consistent with an inhibition of mRNA export (Fig. 3.2 A). Interestingly, under HS most of the stained RNA concentrated in the chromatin-free region of the nucleus, corresponding to the nucleolus, adopting a ring-like distribution, in close proximity to the rings marked with Nup85 (Fig. 3.2 A, insets). Thus, we named these structures as nucleolar rings (NuRs).

Under normal conditions, mRNAs are coated with mRNA binding proteins (RBPs), required for mRNA maturation, docking to the NPC and export (Kelly and Corbett, 2009; Rougemaille et al., 2008; Singh et al., 2015; Stewart, 2019). However, in *S. cerevisiae* the export inhibition of housekeeping transcripts has been attributed to the dissociation of mRNA adaptor and export factors from the mRNP particles, while selective transport of heat shock mRNAs involves the direct recruitment of Mex67 to such mRNAs (Fig. I9) (Krebber et al., 1999; Rollenhagen et al., 2007; Zander et al., 2016). In *S. pombe* it has been previously described that the export factor Mex67 relocates from the nuclear periphery to the nucleolus under heat stress, which correlates with the inhibition of mRNA export (Yoshida and Tani, 2005). Together, the drastic remodeling of the NPC and the NB during heat shock, and the fact that the nuclear basket participates in the docking and export of mRNPs, prompted us to examine the localization of the main players of the mRNA export pathway during heat stress. We observed that the mRNA export factor Mex67 delocalized from the nuclear periphery and adopted a ring-like distribution surrounding the nucleolus, marked with Gar2/nucleolin (Fig. 3.2 B-C) (Gulli et al., 1995; Sicard et al., 1998), analogously to the nuclear basket (Fig. 3.2 C) and Y-complex components Nup132 and Nup85. The poly(A)-binding protein Pab2 (Lemieux and Bachand, 2009; St-Andre et al., 2010) was similarly depleted from the NPCs and the nucleoplasm and, instead, was enriched in this ring-like structure at the nucleoplasm-nucleolar interface, colocalizing with the nuclear basket (Fig. 3.2 B-C). Most Nab2 maintained its nucleoplasmic localization, although it was also detected at NuRs (Figure 2 B-C). However, the RNA adaptor Mlo3 (Yra1/ALY/REF) (Thakurta et al., 2005) and the NPC-associated export factor Rae1 (Brown et al., 1995) maintained their normal respective localization at the nucleoplasm and the NPC upon HS (Fig. 3.2 B). These data show that mRNA receptor and

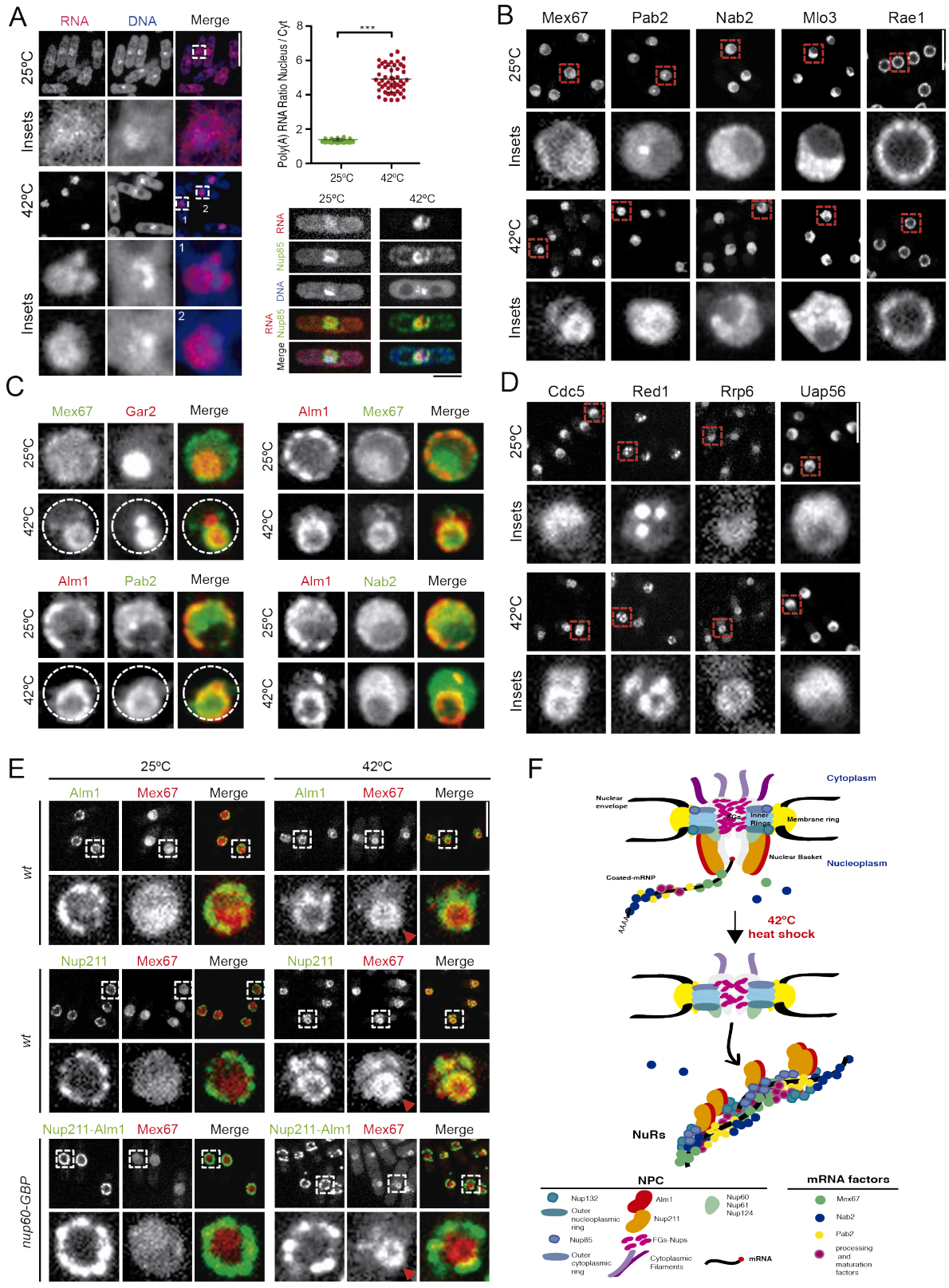

Figure 3.2. Heat shock induces nucleolar accumulation of mRNAs and mRNA binding factors. (A) FISH analysis of cells at 25ºC and after 42ºC heat shock treatment for 20 min, using Cy3-labelled oligo (dT)50 probe to stain RNA (red), DAPI to stain the DNA (blue) and Nup85 as NPC marker (green). Magnifications of the regions indicated by dashed boxes are shown (Insets). Quantification of nuclear Cy3-labelled oligo (dT) fluorescence signal in the indicated conditions is shown (right panel). Dot plot represents the ratio between the nucleus and the cytoplasm of individual cells. Error bars: SD. n=50. ***, P < 0.001. (B) Fluorescence microscopy images of representative cells expressing mex67-GFP, pab2-GFP, GFP-nab2, mlo3-GFP or GFP-rae1, at 25ºC and 42ºC (20 min). Magnifications of the indicated nucleus are shown (Insets). (C) Fluorescence microscopy

images of representative nuclei of cells expressing mex67-GFP and gar2-mCherry, or alm1-Tomato and either mex67-GFP, pab2-GFP or GFP-nab2 at 25ºC and 42ºC (20 min). Dashed lines outline the NE. (D) Fluorescence microscopy images of representative cells expressing Cdc5-GFP, Red1-tdTomato, Rrp6-GFP or Uap56-GFP at 25ºC and 42ºC (20 min). Magnifications of the regions indicated by dashed boxes are shown (Insets). (E) Fluorescence microscopy images of cells coexpressing Mex67-mCherry and either Alm1-GFP (upper panel) or Nup211-GFP (middle panel) in a *wt* background, or Nup211-GFP Alm1-GFP Mex67-mCherry in a *nup60-GBP* genetic background (lower panel), at 25ºC and 42ºC (20 min). Magnifications of the indicated nuclei are shown below. Arrowheads point to Mex67 localization at NuRs. Maximal projections of 3 central z-sections (step size 0,3 µm). Scale bars: 10 µm. (F) Cartoon depicting the components of NPC and the mRNA export machinery during normal growth conditions and upon 42ºC HS.

adaptors required for mRNA export also relocate to NuRs upon HS, which supports a role of these nuclear ring-like structures in the inhibition of mRNA export in these conditions.

The different stages of the nuclear mRNA metabolism, from transcription to export, are closely coordinated (see From transcription to mRNA export; Andersen et al., 2013a; Iglesias and Stutz, 2008; Katahira, 2015; Tutucci and Stutz, 2011). Apart from mRNA export, it has been reported that RNA processing and splicing are also inhibited during heat shock (Bond, 1988; Kay et al., 1987; Yost and Lindquist, 1986, 1991; Zander et al., 2016). Thus, we checked if the localization of other factors involved in nuclear mRNA metabolism, such as RNA processing and maturation, were also affected during an acute HS. We found that the spliceosome factor Cdc5 (McDonald et al., 1999), and the exosome components Red1 and Rrp6 (Sugiyama and Sugioka-Sugiyama, 2011) also redistribute to NuRs during HS, while other factors, such as the TREX complex RNA helicase Uap56 (Thakurta et al., 2005), did not change their localization (Fig. 3.2 D). This shows that NuRs not only contain mRNA export factors, but also specific factors required for mRNA maturation and decay and, therefore, they might facilitate as well the inhibition of mRNA processing and quality control during HS.

We reasoned that if the NB is essential for mRNA docking and export under normal growth conditions, the mRNA export inhibition induced upon HS could be a consequence of the redistribution of the NB components to NuRs, which would sequester mRNA export factors/adaptors. To test this, we expressed Alm1-GFP and Nup211-GFP in a strain harbouring Nup60 fused to the GFP-binding protein (GBP; Chen et al., 2017; Grallert et al., 2013), as Nup60 remains at NPC upon HS (Fig. 3.1 A), and confirmed that Nup60-GBP prevented the remodeling of the NB (Alm1 and Nup211) into NuRs (Fig. 3.2 E). However, even though Alm1-GFP and Nup211-GFP remained at the NPC and did not relocate to NuRs in the *nup60-GBP* background upon HS, the localization of the export factor Mex67 at NuRs was unaffected (Fig. 3.2 E, arrowheads). This result shows that avoiding the remodeling of the NB TPRs (Alm1-Nup211) into NuRs is not enough to restore mRNP export, and suggests that NuRs do not simply sequester the NPC and RBPs, but provides a robust mechanism for mRNA export inhibition during HS. Together, these data demonstrate that HS affects the nuclear distribution of several RNA-binding proteins, including mRNA adaptors, receptors, and processing factors, which relocate to NuRs upon HS, together with several nucleoporins (Fig. 3.2 F). Collaboratively, the accumulation of these factors at NuRs might contribute to the inhibition of mRNA processing, quality control and export, and to the retention of bulk mRNA in the nucleus.

3.3 Heat stress induces nucleolar reorganization and segregation.

The nucleolus is the subnuclear compartment responsible for the expression of rDNA genes and the preassembly of ribosomes. Pol I activity and ribosome biogenesis are finely regulated in response to environmental conditions. Consequently, the morphology, size and activity of the nucleolus reflect cell growth and metabolic status. From yeast to humans, it has been reported that HS results in changes in the nucleolar structure and in the segregation of nucleolar components (Grummt and Voit, 2010; Ju and Warner, 1994; Pederson and Politz, 2000; Russell and Zomerdijk, 2005; Stefanovsky et al., 2001; Tchelidze et al., 2017). To check whether NuR formation around the nucleolar region was accompanied by changes in the transcriptional activity and morphology of the nucleolus in fission yeast, we analyzed the localization of several factors associated to rDNA transcription and maintenance of nucleolar morphology upon HS. We found that during heat stress the RNA pol I largest subunit Nuc1 (Hirano et al., 1989) and the RNA pol I transcription initiation factor Acr1 (Nakazawa et al., 2008) appeared as intense nucleolar foci (Fig. 3.3 A), similar to the condensed nucleolar lobes formed by the rRNA-binding protein Gar2 (Fig. 3.2 C). In contrast, the rDNA-binding transcriptional regulator Reb1/TTF1 (Hirano et al., 1989; Zhao et al., 1997) changed from a diffuse distribution at the nucleolar region into NuRs, together with the NPC components (Fig. 3.3 A).

We further determined that the histone H3 (Hht2 in *S. pombe*), an structural component of chromatin (Matsumoto and Yanagida, 1985), also concentrated around the nucleolus upon HS (Fig. 3.3 B). Moreover, topoisomerase Top2, which is required for proper rDNA architecture (Yamagishi and Nomura, 1988), and Cnd1, part of the condensin complex involved in chromosome condensation during mitosis (Thadani et al., 2012), accumulated at NuRs as well (Fig. 3.3 B). This is consistent the HS-dependent size reduction of the nucleolar domain observed with Gar2/Nucleolin marker (Fig. 3.2 C and Fig. 3.3 B) and the described condensation of rDNA upon HS in *S. cerevisiae* (Matos-Perdomo and Machin, 2018).

In normal growth conditions, the nucleolus works as a sequestering center for transient inactivation of cell cycle regulators, such as p53 or Cdc14 phosphatase (Cueille et al., 2001; Trautmann et al., 2001). In particular, the activity of Cdc14, a conserved phosphatase that plays pleiotropic functions during cell cycle, is regulated by compartmentalization in the nucleus (Shou et al., 1999; Stegmeier and Amon, 2004; Visintin et al., 1999). Importantly, we found that upon HS, the Cdc14 phosphatase (Clp1) was also redistributed from its diffuse nucleolar localization into NuRs (Fig. 3.3 C). The mitotic kinases Aurora B (Ark1) (Petersen et al., 2001), and Polo (Plk1) (Ohkura et al., 1995), and the mitotic cyclin B (Cdc13) (Hagan et al., 1988) were also associated to NuRs upon HS (Fig. 3.3 C).

Therefore, the formation of NuRs is accompanied by changes in the morphology and size of the nucleolus, and by events of nucleolar segregation. The sequestration at NuRs of the machinery required for cell growth, including mRNA processing and export factors, as well as cell cycle regulators, raises the hypothesis that these structures might contribute to coordinate the inhibition of cell growth and division.

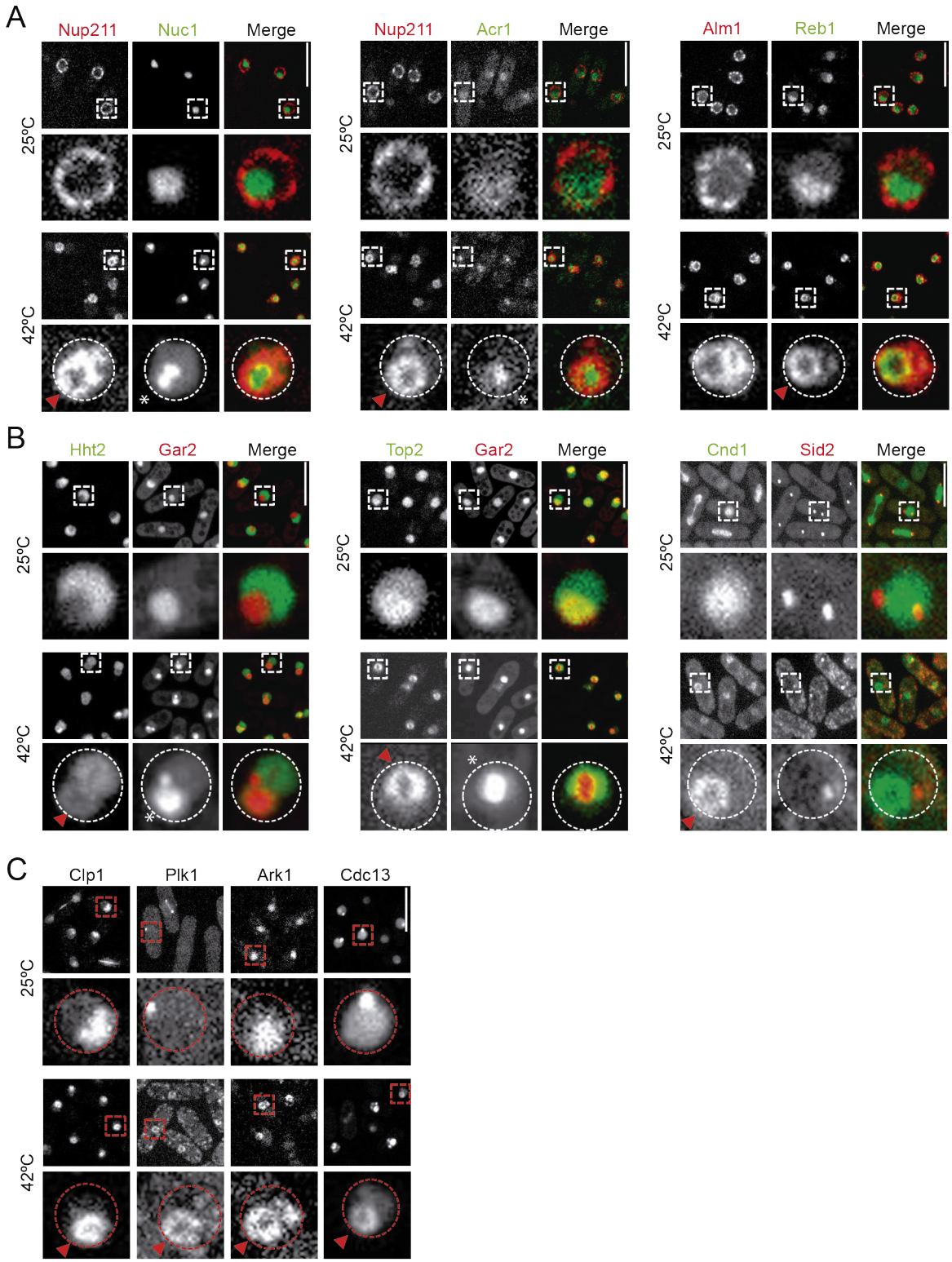

Figure 3.3. Nucleolar segregation and condensation upon HS. (A) Fluorescence microscopy images of representative cells coexpressing Nup211-mCherry and Nuc1-GFP (left panel), Nup211-mCherry and Acr1-GFP (middle panel), or Alm1-Tomato and Reb1-GFP (right panel), at 25ºC and 42ºC (20 min). (B) Fluorescence microscopy images of representative cells coexpressing Hht2-GFP and Gar2-mCherry (left panel), Top2-GFP and Gar2-mCherry (middle panel), or Cnd1-GFP and Sid2-Tomato (right panel), at 25ºC and 42ºC (20 min). (C) Fluorescence microscopy images of representative cells expressing either Clp1-Tomato, Plk1-GFP, Ark1-GFP or p41nmt:Cdc13-GFP, at 25ºC and 42ºC (20 min). Maximal projections of three z-sections (step size 0,3 µm). Scale bars: 10 µm. Magnifications of the indicated regions are shown below. Dashed lines outline the NE. Arrowheads point to NuRs and asterisks indicate condensation of nucleolar components.

3.4 Nucleolar rings are formed during HS-induced growth inhibition and their disassembly precedes the restoration of cell growth.

It has been shown that nuclear structure is dynamically and reversibly remodeled as a consequence of heat stress (Bond, 2006; Chowdhary et al., 2017; Jolly et al., 1999; Welch and Suhan, 1985). To get further insights into NuRs dynamics we characterized the kinetics of NuRs assembly and disassembly, using elements of the NPC (Nup132), the nuclear basket (Alm1) and mRNPs (Mex67). Firstly, we performed a time-course experiment to analyze the temporal order of aggregation of such elements into NuRs, using cell cultures grown at 25ºC and then shifted to 42ºC. Quantification of the percentage of cells with clearly defined NuRs at 5 minutes intervals revealed that just after 5 minutes at 42ºC more than 60% of cells present NuRs, reaching values over 90% after 10 minutes incubation (Fig. 3.4 A). Remarkably, Nup132, Alm1 and Mex67 rearranged into NuRs almost synchronously. Then, we imaged cells expressing GFP-nup85 (due to its low photobleaching) by *in vivo* fluorescence microscopy. This revealed that immediately after 42ºC incubation, Nup85 disappeared from its peripheral localization at the NPC and acquired a more diffuse nuclear pattern; then, it started to concentrate in foci that finally coalesce into NuRs. This structure is observed only 2-3 minutes after the shift to 42ºC (Fig. 3.4 B, arrows). Of note, NuRs remained assembled while the heat stress persists (Fig. 3.4 A and B).

Nuclear remodeling following heat shock has been described to be reversible, so when the temperature is restored to physiological growth conditions, those components that accumulated at NuRs should relocate to their normal localizations. Therefore, we analyzed the kinetics of NuR dissolution in cell cultures that were heat shocked for 40 minutes and, then, shifted back to 25ºC. We observed that 2 hours after the temperature shift to 25ºC ~90% of the cells still possessed visible NuRs; after 4 hours, the percentage of cells with NuRs went down to 60%, and dropped below 30% after 6 hours (Fig. 3.4 C). Interestingly, Nup132, Alm1 and Mex67 also showed a similar NuR disassembly kinetics, although Mex67 displayed a slightly faster relocalization. From these experiments we concluded that NuRs are dynamic structures that are rapidly formed after HS exposure, while their disassembly occurs significantly more slowly.

Cell growth inhibition upon a 10 min incubation at 42ºC occurs rapidly, and is not resumed until more than 3 hours after the shift to 25ºC (Fig. 3.4 D), similar to NuR formation and disassembly kinetics. Then, we reasoned that NuR formation should correlate with HS-induced cell growth arrest, and NuR disassembly should be required for cell growth resumption. Then, we further examined the correlation between NuR formation/dissolution and cell growth by monitoring the dynamics of NuRs disassembly by time-lapse microscopy, using GFP-Nup85 as NuR marker. We found that Nup85-NuRs dissolved on average 188.6 ± 31.5 minutes after the temperature shift to 25ºC. Importantly, cell growth resumed on average 200±27.3 min after the shift from 42ºC to 25ºC, only a few minutes after stress rings were dissolved (Fig. 3.4 E). It has been described that the length of the recovery period is variable depending on the level of heat stress and, in *S. cerevisiae*, it may last up to 3 hours in the most severe HS conditions (Muhlhofer et al., 2019; Vjestica et al., 2013; Yamamoto et al., 2008),

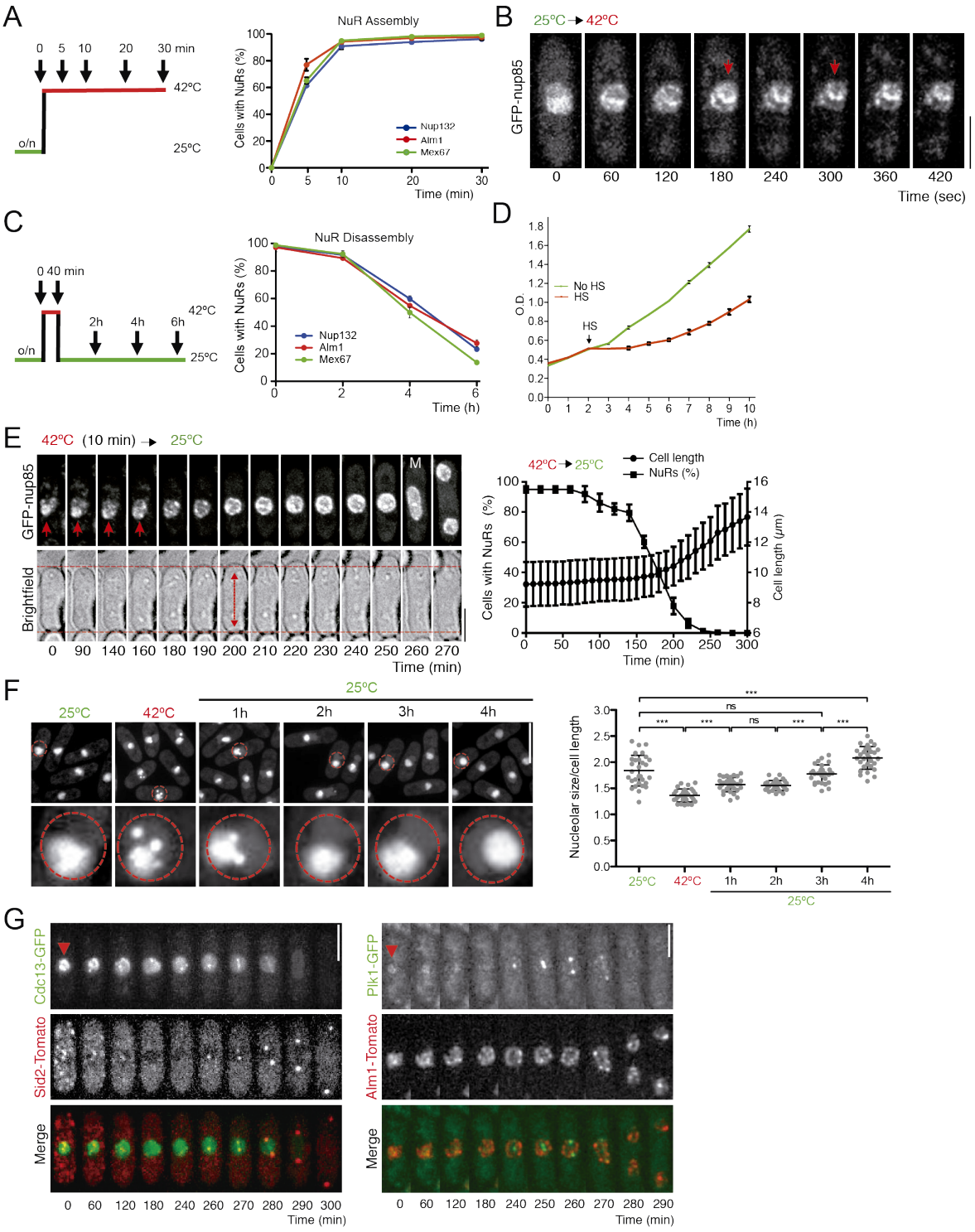

Figure 3.4. NuRs assembly and disassembly corralates with cell growth arrest and resumption. (A) Schematic representation of the experimental conditions tested to analyze NuR assembly. Graph showing the quantification of the percentage of cells in which GFP-Nup132 (NPC, blue), Alm1-Tomato (NB, red), or Mex67-GFP (mRNA export factor, green) localize at NuRs, at the indicated time points, after shifting cell cultures from 25ºC to 42ºC. Graph represents mean percentage and error bars represent SD, from two independent experiments. n= 200. (B) Time-lapse fluorescence images of a representative cell expressing GFP-Nup85 showing NuR assembly upon temperature shift from 25ºC to 42ºC. Maximal projections of 6 z-sections (step size 0,3 μm) are shown. Arrows indicate Nup85 aggregates coalescing into a NuR. Scale bar: 5 μm. (C) Schematic representation of the experimental conditions tested to analyze NuR disassembly. Graph showing quantification of the percentage of cells in which GFP-Nup132 (NPC, blue), Alm1-Tomato (NB, red), or Mex67-GFP (mRNA export factor, green) localize at NuRs, at the indicated time points. Cells were incubated at 42ºC for 40 minutes and then shifted to 25ºC. Graph represents mean percentage and error bars represent SD, from two independent experiments. n= 200. (D)

Graph showing the optical density (O.D.) *vs* time (hours) of cell cultures grown at 25ºC (green), heat shocked at 42ºC for 20 minutes and shifted back to 25ºC (red). Graph represents mean O.D. and error bars represent SD of three independent cell cultures. The timing of HS is indicated. (E) Time lapse brightfield and fluorescence images of cells expressing GFP-Nup85 as NuR marker incubated at 42ºC for 10 minutes and then shifted to 25ºC before imaging (left). Maximal projections of 6 z-sections (step size 0,3 µm) are shown. Double-headed arrow indicates the time of cell regrowth. Scale bar: 5 µm. M, mitosis. Graph showing the percentaje of cells with NuRs (left Y-axis) and the average cell length (right Y-axis) after shifting the cells from 25ºC to 42ºC (10 min), and then shifted to 25ºC (right). Graph represents mean and error bars represent SD from two independent experiments. n= 22. (F) Fluorescence microscopy images of representative cells expressing Gar2-mCherry as nucleolar marker. Nucleolar size was determined in cells grown at 25ºC, heat shocked (42ºC-10 min), and then shifted back to 25ºC. Maximal projections of 18 z-sections (step size 0,3 µm) are shown. Magnifications of the indicated nuclei are shown below. Dashed lines outline the NE. Scale bar: 10 µm. Graph showing the nucleolar size (Gar2-mCherry) relative to cell length. Dot plot represents mean and error bars represent SD. n= 30. ***, $P < 0.001$. (G) Time lapse fluorescence microscopy images of cells expressing either p41nmt:cdc13-GFP cyclin and sid2-Tomato (as SPB marker) or plo1-GFP and Alm1-Tomato, incubated at 42ºC for 20 minutes and then shifted to 25ºC. Maximal projections of 6 z-sections (step size 0,3 µm) are shown. Arrows indicate NuRs. Scale bar: 5 µm.

similar to our results. The differences in the timing of NuRs dissolution between the experiments shown in Fig. 3.4 C and E could be caused for the distinct durations of HS treatments, 40 min and 10 min, respectivelly, which support the notion that the length of the recovery period depends on the severity/duration of the stress.

The nucleolus is the site of highest RNA production and nucleolar size positively correlates with cell growth and RNA synthesis. Accordingly, rRNA transcription inhibition results in the gradual decrease of nucleolus size (Derenzini et al., 1998; Grummt and Voit, 2010; Ju and Warner, 1994; Pederson and Politz, 2000; Russell and Zomerdijk, 2005; Stefanovsky et al., 2001; Tchelidze et al., 2017). In agreement with that, we observed that during HS the nucleolar region (marked with Gar2) gets condensed and reduced its size, whereas during the recovery at 25ºC the nucleolus progressively turns back to its initial size and morphology (Fig. 3.4 F), coincident with the release of Cdc13/Cyclin B and Plo1 kinase from NuRs to the nucleoplasm and to the SPBs (Fig. 3.4 G). Together, these results suggest that NuRs are transient structures whose formation is associated to, or coordinated with, the inhibition of cell growth. When cells are allowed to recover at permissive temperature NuRs are disassembled and their components recycled prior to cell growth re-initiation.

3.5 Hsf1 delayed upregulation and Hsp104 activity are required for proper NuR dissolution and cell viability.

The HSR is mainly driven by the evolutionary conserved transcription factor Hsf1, which becomes activated, translocates into the nucleus and triggers the expression of HSR genes (Akerfelt et al., 2010; Gallo et al., 1993; Gallo et al., 1991; Richter et al., 2010). In *S. pombe*, Hsf1 is essential for growth and, therefore, is present in cells in unperturbed conditions; during heat shock its levels are upregulated and its activity is induced by posttranscriptional modifications, such as phosphorylation, in a similar mechanism than that operating in metazoans (Gallo et al., 1993; Gallo et al., 1991). Then, to test whether NuRs assembly is linked to the Hsf1-dependent HSR, we analyzed the kinetics of Hsf1 activation and accumulation inside the nucleus upon HS. As soon as 2.5 minutes after incubation at 42ºC, Hsf1 showed a sharp 5-fold increase in the nucleus/cytoplasm ratio, reaching a maximum ratio

of 6-fold after 15 minutes (Fig. 3.5 A). HS-dependent upregulation of Hsf1 is also observed at the protein level by western blot. Upon induction, we observed slow-migrating bands of Hsf1 (Fig. 3.5 B, asterisk) that likely correspond to hyper-phosphorylated forms of the protein, compared to non-phosphorylated or hypo-phosphorylated bands (Fig. 3.5 B, arrowhead). Noteworthy, Hsf1 levels peaked 3 hours after the shift to 25ºC and then gradually decreased, according with its nuclear accumulation kynetics (Fig. 3.5 B). This is in agreement with the transcriptional delayed upregulation of Hsf1 following a severe HS described for *S. cerevisiae* (Yamamoto et al., 2008).

To test whether Hsf1-dependent expression is required for NuR formation or dissolution during the recovery period, we used a strain in which the expression of *hsf1* is driven by the uracile-regulatable *Purg1* promoter (Vjestica et al., 2013; Watt et al., 2008), which in repressed conditions (in the absence of uracile), however, allows a basal Hsf1 expression enough to support cell growth (Vjestica et al., 2013). Hsf1 downregulation did not prevent Alm1 aggregation into NuRs (Fig. 3.5 C, asterisks), suggesting either that NuR formation is independent on Hsf1 or that the basal Hsf1 levels produced in the repressed conditions are enough to drive Alm1 accumulation into NuRs. Importantly, we found that NuRs dissolution during the recovery from HS was delayed in conditions of Hsf1 downregulation (Fig. 3.5 C, asterisks), suggesting that proper Hsf1 levels during the recovery after HS are required for timed dissolution of NuRs.

Hsf1 triggers the expression of HSR genes, mainly chaperones (Amoros and Estruch, 2001; Cotto and Morimoto, 1999; Hahn et al., 2004; Pincus, 2017; Solis et al., 2016; Trinklein et al., 2004). Thus, we next analyzed the accumulation of Hsf1 targets upon HS and their localization relative to NuRs. The chaperones of the Hsp70-Hsp40 family Ssa1 and Ssa2, ubiquitously located in the cell in unstressful conditions, were enriched at NuRs upon HS (Fig. 3.5 D). Moreover, the disagregasse Hsp104, which participates in aggregate solubilization and shows a nuclear localization in normal conditions, was also accumulated at NuRs during HS (Fig. 3.5 D). The presence of HSPs at NuRs suggests a protective function of these structures.

The HS-dependent relocation of chaperones into the nucleolus has been described for several organisms, where they have been proposed to promote the refolding and disaggregation of damaged proteins, enabling a faster cell recovery once the physiological conditions are restored (Deane and Brown, 2017; Glover and Lindquist, 1998; Nollen et al., 2001; Riezman, 2004; Vabulas et al., 2010; Vjestica et al., 2013; Voellmy and Boellmann, 2007). Then, we analyzed the timing of NuR dissolution in relation to Hsp104 accumulation and the involvement of Hsp104 in NuR formation and disaggregation. Upon HS, most cells showed NuRs containing Alm1 and Hsp104. During the recovery period at 25ºC, Alm1 is progressively recycled from NuR and relocates to the nuclear periphery after 2 hours (Fig. 3.5 E, arrowhead), while Hsp104 remain assembled at NuRs for more than 3 hours (Fig. 3.5 E, asterisk). Coincident with the relocalization of Alm1 to the nuclear periphery, Hsp104 starts to accumulate at cytoplasmic SGs, which coexist with NuRs until these are completely disassembled. Then, we tested whether the activity of Hsp104 is required for NuR formation and dissolution. For that, we used low concentrations of guanidinium hydrochloride (GH), an specific and reversible inhibitor of

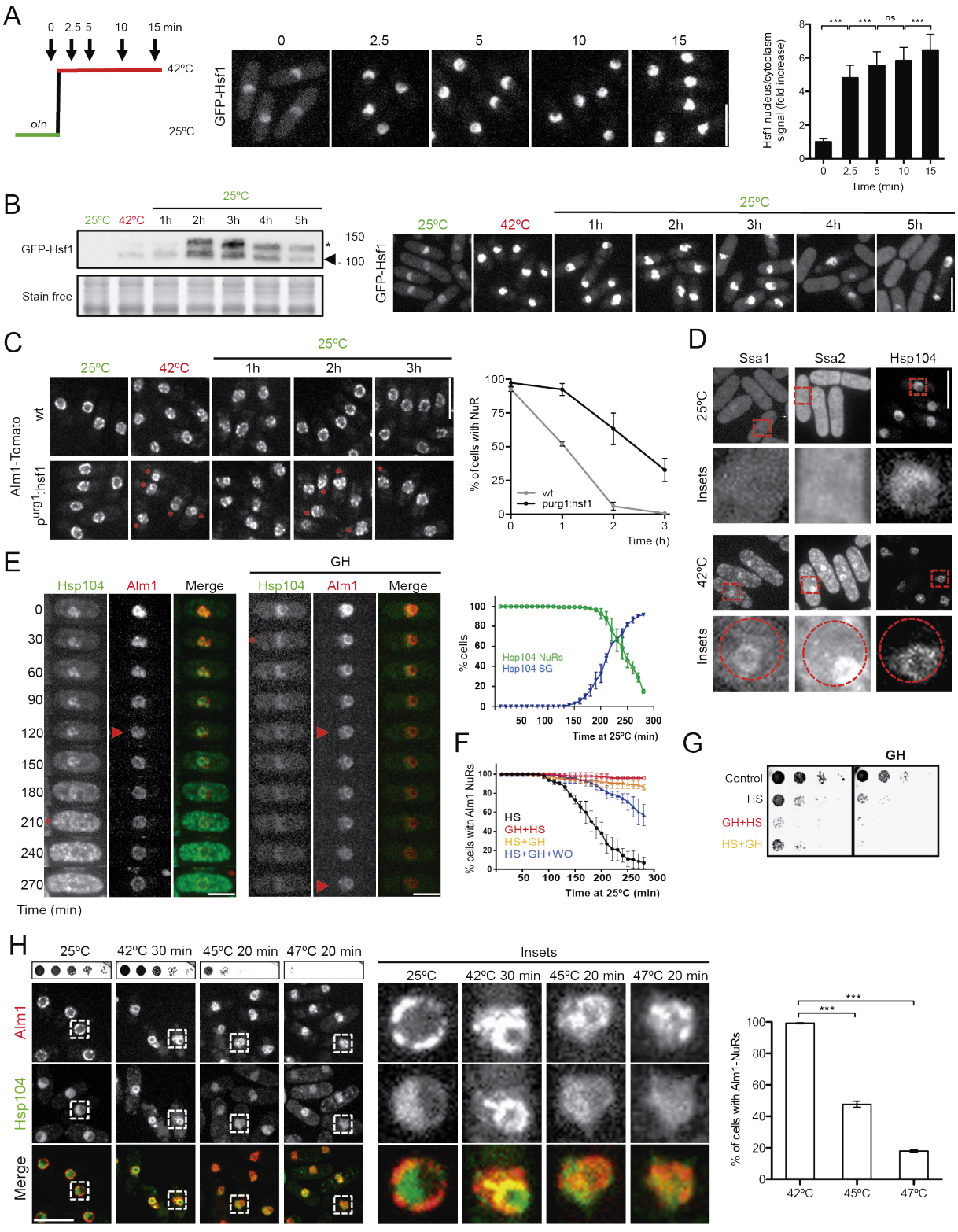

Figure 3.5. Hsf1 delayed upregulation and Hsp104 activity are required for proper NuR dissolution and cell viability after a HS. (A) Schematic representation of the experimental conditions tested to analyze Hsf1 activation upon incubation at 42ºC. Fluorescence microscopy images of representative cells expressing GFP-Hsf1, heat shocked for 2.5, 5, 10 and 15 minutes. Maximal projections of 18 z-sections (step size 0,3 µm) are shown. Scale bar: 10 µm. Graphs represent the nucleus/cytoplasm ratio of GFP-Hsf1 fluorescence intensity over time. Error bars: SD. n=50. ns, non-significant ; ***, $P < 0.001$. (B) Western blot analysis of total GFP-Hsf1 protein levels (left panel) of cells grown at 25ºC, incubated at 42ºC for 20 minutes and then shifted to 25ºC during 5 hours, using anti-GFP mAb to detect GFP-Hsf1 and stain free as loading control. Positions of molecular weight makers are indicated in kDa. Arrowhead points to non-phosphorylated or hypo-phosphorylated bands of Hsf1 and asterisk indicates hyper-phosphorylated bands of Hsf1. Fluorescence microscopy images of representative cells expressing

GFP-Hsf1, treated as explained before (right panel). Maximal projections of 18 z-sections (step size 0,3 µm) are shown. Scale bar: 10 µm. (C) Fluorescence microscopy images of representative cells expressing alm1-Tomato in a strain in which *hsf1* gene is expressed under the endogenous promoter or under the control of the regulatable promoter *purg1* in repressed conditions. Cells were grown in rich media and shifted to minimal media without uracile for 36 hours before the heat shock treatment. Aftewards, cells were shifted from 42ºC to 25ºC for 3 hours. Maximal projections of 3 z-sections (step size 0,3 µm) are shown. Asterisk indicate NuRs. Scale bar: 10 µm. Graph showing the percentage of cells with Alm1-NuRs, at the indicated time points. Graph represents mean and error bars represent SD, from two independent experiments. n= 200. (D) Fluorescence microscopy images of representative cells expressing Ssa1-YFP, GFP-Ssa2 and Hsp104-GFP at 25ºC and 42ºC (20 min). Maximal projections of 3 z-sections (step size 0,3 µm) are shown. Scale bar: 10 µm. Magnifications of the indicated nuclei are shown below. Dashed lines outline the NE. (E) Time-lapse images of representative cells coexpressing Hsp104-GFP and Alm1-Tomato. Cells were grown at 25ºC and incubated at 42ºC for 10 minutes. Immediately after the HS, the culture was split in two and 3 mM of guanidine hydrochloride (GH) was added to one of the cultures. Then, both cultures were shifted to 25ºC and filmed. Asterisks and arrowheads point to the localization of Hsp104 and Alm1, respectively. Maximal projections of 6 z-sections (step size 0,3 µm) are shown. Scale bar: 5 µm. Graph showing the percentage of untreated cells that show Hsp104 at NuRs (green), and cells with Hsp104 at cytoplasmic SG (blue), at the indicated time points after the HS. Graphs represents mean and error bars represent SD, from two independent experiments. n≥ 90. (F) Graph showing the percentage of cells with Alm1-NuRs at the indicated time points and conditions. Cells were grown at 25ºC and incubated at 42ºC for 10 minutes. 3mM GH was added either 10 minutes before the HS (red) or immediately after the HS (yellow). Blue represents cells in which GH was added immediately after the HS and washed out after 15 minutes. Black represent untreated cells. Graphs represents mean and error bars represent SD, from two independent experiments. n≥ 90 (G) Drop assay comparing cell survival in the indicated conditions. Cells were grown at 25ºC and incubated at 42ºC for 10 minutes. 3mM GH was added either 10 minutes before the HS (red) or immediately after the HS (yellow). Spotted cells correspond to 10-fold dilutions with an initial O.D of 0.3, on YES plates and GH-containing plates. (H) Drop assay comparing cell survival in the indicated conditions. Spotted cells correspond to 5-fold dilutions with an initial O.D of 0.3 on YES plates. Fluorescence microscopy images of representative cells coexpressing Alm1-Tomato and Hsp104-GFP at the indicated conditions. Maximal projections of three z-sections (step size 0,3 µm) are shown. Scale bar: 10 µm. Magnifications of the indicated nuclei are shown (Insets). Graph showing the percentage of cells with Alm1-NuRs, at the indicated conditions. Graph represents mean and error bars represent SD, from two independent experiments. n= 400.

the ATPase activity and function of Hsp104 (Grimminger et al., 2004; Jung et al., 2002). We added GH either 10 minutes before or immediately after the HS, and monitored the localization of Hsp104 and NuR dynamics by using Alm1 as marker (Fig. 3.5 E and F). In cells treated with GH before the HS, NuR formation and Hsp104 accumulation were not significantly affected, suggesting that NuR formation and Hsp104 recruitment to NuRs is independent on its ATPase activity. However, during the recovery period, Hsp104 is lost prematurely from NuRs, regardless whether GH was added before of after the HS (Fig. 3.5 E, asterisk), and, contrary to untreated cells, it does not localize to cytoplasmic SGs. In these conditions of Hsp104 inhibition, Alm1 NuR dissolution was abolished (Fig. 3.5 E, arrowhead), as 85% of GH-treated cells presented Alm1 NuRs after 270 min at 25ºC *versus* 6.95% of non-treated cells (Fig. 3.5 F). Furthermore, we found that a transient GH treatment of 20 minutes after a HS results in a delay in NuRs dissolution, consistent with a direct role of Hsp104 in NuR disaggregation (Fig. 3.5 F). Importantly, the defective NuR dissolution by Hsp104 impairment severely affected cell survival after the HS (Fig. 3.4 G), suggesting that proper NuR regulation provides cellular fitness. However, we cannot dismiss a further contribution of Hsp104 at SGs. These results show that Hsp104 is required for disaggregation of NuRs in order to resume growth after a HS.

We hypothesized that NuRs constitute a protective ¨emergency¨ response to the massive protein unfolding induced by a sudden acute HS. This is supported by the fact that wildtype cells survive after an acute stress (42ºC 10-30 min), without losing cell viability excessively (Fig. 3.5 H). However, incubation of wildtype cells at higher temperatures (45ºC-47ºC), which impinges higher proteotoxic damage, resulted in a major cell viability loss. Importantly, in cells incubated at 45ºC and 47ºC, NuR

formation is affected, as Alm1 accumulated as aggregates throughout the nucleus in a disorganized manner, and Hsp104 localization at Alm1 aggregates or in the nucleolar periphery was markedly decreased (Fig. 3.5 H). This suggests that Hsp104 activity is affected at these extreme temperatures and/or that the proteotoxic burden overcomes the chaperone system capacity. Together, these results support that NuRs are formed by the autonomous and ordered aggregation of nuclear proteins, and their disaggregation is likely controlled by molecular chaperones, which provides cellular fitness.

3.6 NuRs are not formed in conditions of acquired thermotolerance.

It has been described that when cells are subjected to a mild-heat pretreatment prior to a severe HS, mRNA splicing and export are not inhibited, both in *S. cerevisiae* and HeLa cells. Acquired thermotolerance has been attributed to the induction of HSPs, which buffer the effect of protein misfolding and aggregation (Bond, 2006; De Virgilio et al., 1991; Gross and Watson, 1998; Hahn et al., 2004; Parsell and Lindquist, 1993; Sanchez and Lindquist, 1990; Solis et al., 2016; Yost and Lindquist, 1986). Then, we analyzed the kinetics of Hsf1 nuclear accumulation when cells are directly shifted from 25ºC (1) to 42ºC (2), compared to cells pretreated with a mild heat during 45 min at 37ºC (3) prior to a severe 42ºC HS (4) (Yoshida and Tani, 2005). We observed that when cells are directly incubated at 42ºC Hsf1 rapidly disappeared from the cytoplasm and accumulated at the nucleus. This nuclear localization was sustained for 20 minutes, before Hsf1 levels started to drop significantly (Fig. 3.6 A). However, in mild-heat pretreated cells, Hsf1 nuclear accumulation upon HS was reduced and shortly sustained, since Hsf1 rapidly returned to the cytoplasm as soon as 10 minutes after incubation at 42ºC (Fig. 3.6 A). This demonstrates that mild heat shock (mild-HS) results in a reduced nuclear accumulation of Hsf1 and a faster inactivation kinetics after an acute heat stress.

This led us to investigate the impact of mild-heat pretreatment in the expression and nuclear accumulation of those HS-induced chaperones, including Hsp70 and Hsp104. For that, cells were similarly pretreated with a mild-HS (37ºC, 45 min) prior to the acute HS (42ºC, 20 min). As shown before (Fig. 3.5 D), Ssa1 and Ssa2 Hsp70 proteins and Hsp104 disaggregase were enriched at NuRs during HS (Fig. 3.6 B, 2). Importantly, these chaperones are overproduced during the mild-HS, especially Ssa1 and Hsp104, as evidenced by their massively accumulation in cytoplasmic stress granules and the increase in protein levels in this condition (Fig. 3.6 B and C, 3). However, when cells have been mild-heat pretreated prior to HS, Ssa1 and Hsp104 are not detected at NuRs (Fig. 3.6 B, 4). Interestingly, Ssa2 levels are reduced after incubation at 42ºC, consistent with its role in Hsf1 inactivation (Vjestica et al., 2013), and, contrary to Ssa1 and Hsp104, did not form cytoplasmic foci during the mild-HS. However, Ssa2 was observed at NuRs during the posterior HS, although its levels were drastically reduced (Fig. 3.6 B). The presence of Ssa2 at NuRs, although at low levels, shows that its localization is independent of other components and suggests that NuRs might have different composition depending on the level of stress.

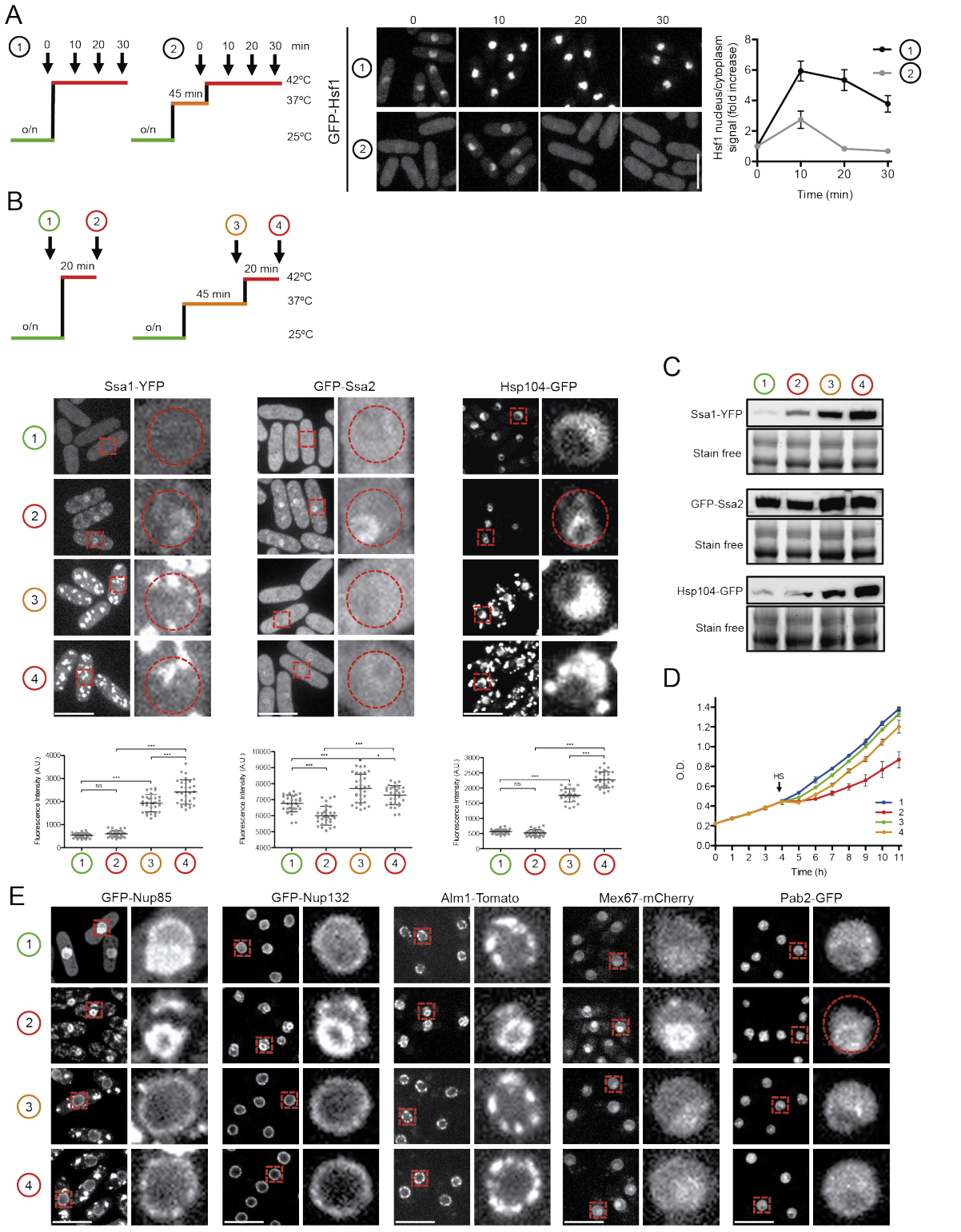

Figure 3.6. NuRs are not formed in conditions of acquired thermotolerance. (A) Schematic representation of the experimental conditions used to analyze Hsf1 activation. Cells were either cultured at 25ºC and heat shocked for 10, 20 and 30 minutes at 42ºC (1), or mild-heat pretreated at 37ºC for 45 min and then heat shocked for 10, 20 and 30 minutes at 42ºC (2). Fluorescence microscopy images of representative cells expressing GFP-Hsf1 in the experimental conditions described above. Maximal projections of 18 z-sections (step size 0,3 µm) are shown. Scale bar: 10 µm. Quantification of GFP-Hsf1 fluorescence intensity levels in the indicated conditions. Graph represents the fold increase of the nucleus/cytoplasm ratio of individual cells along time (minutes). Error bars: SD. n=35. (B) Schematic representation of the experimental conditions used to analyze chaperone accumulation (upper panel). Cells were either cultured at 25ºC (1) and heat shocked for 10 minutes at 42ºC (2), or mild-heat pretreated at 37ºC for 45 min (3) and then heat shocked for 10 minutes at 42ºC (4). Fluorescence microscopy images

of representative cells expressing Ssa1-YFP, GFP-Ssa2 and Hsp104-GFP in the described conditions (middle panel). Maximal projections of three z-sections (step size 0,3 µm) are shown. Scale bar, 10 µm. Magnifications of the regions indicated by dashed boxes are shown (insets). Dashed lines outline the NE. Quantification of Ssa1-YFP, GFP-Ssa2, and Hsp104-GFP fluorescence intensity levels in the whole cell area in the indicated conditions (lower panel). Graphs represent the mean values of individual cells. Error bars: SD. n=30. ns: non significant, $P < 0.05$ (*), $P < 0.001$ (***). (C) Western blot analysis of total Ssa1-YFP, GFP-Ssa2 and Hsp104-GFP protein levels in the indicated conditions, using anti-GFP mAb to detect chaperones (upper panels) and stain free as loading control (lower panels). (D) Graph showing the optical density of cell cultures treated as explained in B (1-4), and shifted back to 25ºC for 7 hours. Graph represents mean O.D. and error bars represent SD of three independent cell cultures. The timing of HS is indicated. (E) Fluorescence microscopy images of representative cells expressing GFP-Nup85, GFP-Nup132, Alm1-Tomato, Mex67-mCherrry, and Pab2-GFP, in the conditions indicated in B (1-4). Magnifications of the regions indicated by dashed boxes are shown. Dashed lines outline the NE. Maximal projections of 3 z-sections (step size 0,3 µm) are shown. Scale bar: 10 µm.

We reasoned that if NuR formation results directly or indirectly from protein misfolding and aggregation, then, increased levels of chaperones and disaggregases would prevent cell growth inhibition and NuRs formation upon HS. As expected, cell growth is resumed faster in conditions of thermotolerance (Fig. 3.6 D) and neither the NPC components Nup85, Nup132, Alm1 nor the RBPs Mex67 and Pab2 rearrange into NuRs under such conditions, and remained instead at their respective unperturbed locations (Fig. 3.6 E). Together, these data show that the aggregation of nuclrar proteins into NuRs is a consequence of acute HS, which is mostly prevented in conditions of thermotolerance.

3.7 The absence of Alm1 and proteasome disfunction result in acquired thermotolerance.

Even though cell viability is negatively affected by an acute heat shock (Fig. 3.7 A, 2: 10 min incubation at 47ºC), cell survival can be greatly increased if cells are in conditions of thermotolerance (Fig. 3.7 A, 3: 45 min at 37ºC) prior to an acute HS (Fig. 3.7 A, 4: 10 min at 47ºC), consistent with published data (Gross and Watson, 1998; Parsell et al., 1993; Riezman, 2004; Sanchez and Lindquist, 1990). Unexpectedly, we found that following a HS cell viability of *alm1*-deleted mutant is not reduced to the same extent than the wildtype (Fig. 3.7 A), suggesting that the absence of Alm1 induces a thermotolerant phenotype.

We have previously shown that when cells are mild-HS pretreated prior to a severe heat shock, the levels and timing of Hsf1 nuclear accumulation are greatly reduced (Fig. 3.6 A). Then, we wondered whether the thermotolerant phenotype observed in the absence of Alm1 could be due to an altered Hsf1 activation kinetics. We found that in *alm1*-deleted cells the dynamics of Hsf1 nuclear accumulation upon HS is similar to that of wildtype cells, although the nucleo-cytoplasmic ratio was reduced (Fig. 3.7 B). Then, we further analyzed the dynamics of Hsf1 during the recovery period in *alm1*-deleted cells compared to wildtype cells, by quantifying the percentage of cells along time in which the Hsf1 is still active, considering as so those cells in which the nucleus/cytoplasm ratio of Hsf1 is above control conditions (time 0: 42ºC). As shown before (Fig. 3.5 A), in wildtype cells Hsf1 nuclear levels peaked during the HS and the HSR is maintained for 3 hours, after which Hsf1 starts to relocate to the cytoplasm (Fig. 3.7 C and D). Remarkably, in the *alm1Δ* mutant, nuclear accumulation of Hsf1 was only maintained for 2 hours, after which most cells displayed a non-stressed Hsf1 distribution

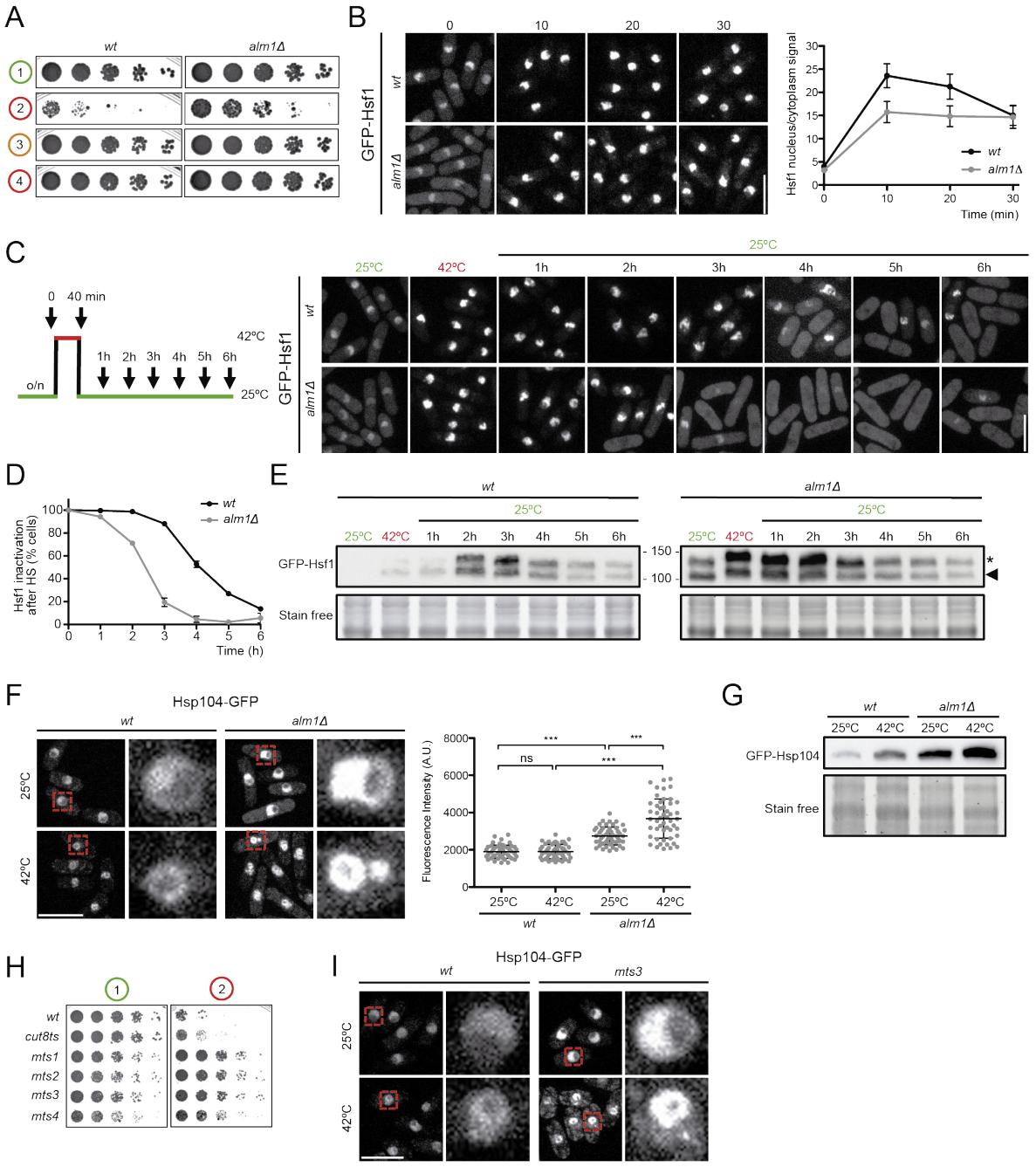

Figure 3.7. The absence of Alm1 and proteasome disfunction result in acquired thermotolerance. (A) Drop assay comparing cell viability of *wt* and *alm1Δ* cells in the following conditions: Cells were cultured at 25ºC (1), heat shocked for 10 minutes at 47ºC (2), mild heat pretreated at 37ºC for 45 min (3), or mild heat pretreated at 37ºC for 45 min followed by 47ºC incubation for 10 minutes. (1-4). Spotted cells correspond to 5-fold dilutions with an initial O.D of 0.3. (B) Fluorescence microscopy images of representative *wt* and *alm1Δ* cells expressing GFP-hsf1, grown at 25ºC and heat shocked for 10, 20 and 30 minutes (left panel). Scale bar: 10 µm. Graphs represent the nucleus/cytoplasmic ratio of GFP-Hsf1 fluorescence intensity over time. Error bars, SD. n=50. ***, $P < 0.001$. (C) Schematic representation of the experimental conditions tested to analyze Hsf1 inactivation after HS (left panel). Fluorescence microscopy images of representative *wt* and *alm1Δ* cells, expressing GFP-hsf1, incubated at 42ºC for 40 minutes and then shifted to 25ºC (right panel). Maximal projections of 18 z-sections (step size 0,3 µm) are shown. Scale bar: 10 µm. (D) Quantification of the percentage of cells with nuclear accumulation of Hsf1 as represented in C. Graphs represent mean and error bars represent SD from two independent experiments. n= 200. (E) Western blot analysis of total GFP-Hsf1 protein of *wt* and *alm1Δ* cells using anti-GFP mAb to detect GFP-Hsf1 (upper panel) and stain free as loading control (lower panel). Positions of molecular weight makers are indicated in kDa. Arrowhead points to non-phosphorylated or hypo-phosphorylated bands of Hsf1 and asterisk indicates hyper-phosphorylated bands of Hsf1. (F) Fluorescence microscopy images of representative *wt* and *alm1Δ* cells expressing Hsp104-GFP at 25ºC and 42ºC (20 min). Maximal projections of 3 z-sections (step size 0,3 µm) are shown. Scale bar: 10 µm. Dot plot represents the quantification

Hsp104-GFP nuclear fluorescence intensity levels of individual cells (right panel), and error bars represent SD. n=50. ***, P < 0.001. (G) Western blot analyses of total Hsp104-GFP proteins of *wt* and *alm1Δ* cells using anti-GFP mAb and stain free as loading control. (H) Drop assay comparing cell viability of the indicated proteasome mutants before (1) and after 10 minutes at 47ºC (2). Spotted cells correspond to 5-fold dilutions with an initial O.D of 0.3. (I) Fluorescence microscopy images of representative *wt* and *mts3* cells expressing Hsp104-GFP at 25ºC and 42ºC (20min). Magnifications of the regions indicated by dashed boxes are shown. Maximal projections of 3 z-sections (step size 0,3 µm) are shown. Scale bar: 10 µm.

(Fig. 3.7 C and D). Strikingly, western blot analysis revealed that in the absence of *alm1* Hsf1 protein levels are greatly increased both in non-stressful conditions and during HS, and Hsf1 mainly appears as slow-migrating band, which likely correspond with hyper-phosphorylated forms of active Hsf1 (Gallo et al., 1991; Yamamoto et al., 2008). Moreover, in this mutant background, Hsf1 activation peaked during the incubation at 42ºC and is maintained up to 2h of recovery, when it starts to decrease, contrary to the wildtype (Fig. 3.7 E). Altogether, these results show that in the absence of Alm1 cells possess a termotolerant phenotype, similar to the one acquired during mild-HS, and that the recovery period after a HS is shorter than in wildtype cells, which could be indicative of a constitutively active Hsf1. An abnormally increased activity of Hsf1 could have an impact on the amount of those HSPs whose expression is regulated by Hsf1. To check this, we examined the localization and total protein levels of those HS-induced chaperones in wildtype and *alm1Δ* cells. Notably, Hsp104 levels are greatly increased in *alm1*-deleted cells, both at normal growth conditions (25ºC) and upon heat stress (42ºC), compared to the wildtype cells (Fig. 3.6 F and G).

According to published data, the accumulation of misfolded proteins during HS is responsible for Hsf1 activation (Masser et al., 2019; Voellmy and Boellmann, 2007; Yamamoto et al., 2008). Consistently, chemical or genetic inhibition of the proteasome results in Hsf1 activation, due to the increase of misfolded and not-degraded proteins (Bush et al., 1997; Lee and Goldberg, 1998; Pirkkala et al., 2000; Pritts et al., 2002; Yamamoto et al., 2008). Given the described role of Alm1 in proteasome localization and function (Chapter 1), we hypothesized that the presence of a disfunctional proteasome in *alm1Δ* cells could be responsible for the thermotolerant phenotype of this mutant. In line with this, cell survival following a heat shock was increased in several proteasome defective mutants compared to a wildtype strain (Fig. 3.7 H). Consistently, a mutant in *mts3*, an essential catalytic subunit of the proteasome (Gordon et al., 1996), exhibited constitutive higher Hsp104 levels, even at permissive temperature (Fig. 3.7 I).

These results show that the absence of Alm1 results in a better adaptation to elevated temperatures, an altered kinetics of the HSR response, and abnormally increased levels of HS-induced chaperones. Altogether, these data point to the presence of a constitutively active HSR in *alm1Δ* cells, which might be consequence of deregulated proteasome activity.

Discussion

3.1 NPC, Nuclear Basket and mRNPs are remodeled during heat stress.

In unperturbed conditions different adaptor proteins are loaded into the pre-mRNA molecules at the distinct stages of mRNA processing. These proteins act as adaptors for the recruitment of mRNA export factors, responsible for the NPC docking and translocation of the mRNP from the nucleus to the cytoplasm (Kelly and Corbett, 2009; Rougemaille et al., 2008; Singh et al., 2015; Stewart, 2010, 2019). During heat shock, the inhibition of mRNA export results in poly(A)RNA accumulation predominantly in the nucleolar region, both in budding and fission yeasts (Saavedra et al., 1996; Tani et al., 1995). While in *S. cerevisiae* this has been attributed to the remodeling of mRNPs, as adaptor proteins are released from the mRNPs and impede their export from the nucleus (Bond, 1988; Carmody et al., 2010; Krebber et al., 1999; Mahl et al., 1989; Mayrand and Pederson, 1983; Rollenhagen et al., 2007; Yost and Lindquist, 1986; Zander et al., 2016), in *S. pombe* it has never been address the mechanism of mRNA export inhibition during HS. To gain knowledge on this process during heat shock, we examined the localization of RNA and several mRNA binding factors upon thermal stress. Interestingly, we observed that Poly(A)-RNAs, the mRNA export factor Mex67 and the PABP Pab2 adopted a ring-like distribution and concentrated at the nucleolar periphery, in a structure that we have named NuRs (for nucleolar rings). In turn, the PABP Nab2 enriched at the same localization, although was not completely depleted from the nucleoplasm, whereas the adaptor protein Mlo3 maintained its normal nucleoplasmic localization upon a heat shock (Fig. 3.2 A-C). In the simplest scenario, the fact that fission yeast RNA-binding proteins, such as Mlo3 and Nab2, stay in the nucleoplasm could imply that they are not inhibited upon thermal stress or that they are required for export of HS mRNA, while Mex67 and Pab2 localization at NuRs suggest that they are not working in such conditions. This is contrary to *S. cerevisiae*, in which direct recruitment of Mex67 to heat shock mRNAs, through the heat-responsive transcription factor Hsf1, promotes the selective export of HS mRNAs, while dissociation of mRNA adaptors, such as Nab2 and Yra1, from the mRNP particles is responsible for the block of normal mRNAs export (Carmody et al., 2010; Rollenhagen et al., 2007; Zander et al., 2016). Additionally, our results show that in *S. pombe* the nuclear pore-associated export factor Rae1 is kept at the NPC during heat shock (Fig. 3.2 B), while it has been described that its *S. cerevisiae* homolog Gle2 dissociates from the NPC under heat stress (Izawa et al., 2004). This may indicate that, contrary to budding yeast, Rae1 is required for mRNA export during a heat shock stress in fission yeast. This suggest that mRNA export pathways under stress and non-stress conditions share common elements. Besides, these data show that, even though mRNA export pathways are highly conserved among eukaryotes, some differences could have emerged along evolution, as the mechanism of mRNA export under heat shock conditions in fission yeast seems to differ from that of budding yeast.

We described earlier that the nuclear basket in involved in the NPC anchoring of mRNPs prior to export through the interaction with mRNA adaptor factors, such as Nab2 and Pab2, and that the loading of Mex67 into mRNPs is compromised in its absence (Chapter 2). Surprisingly, the nuclear

basket TPRs Alm1 and Nup211 also relocate to the nucleolar periphery during heat stress (Fig. 3.1 A-B). This shares similarities with the HS-induced rearrangement of Mlps, together with Nab2 and Yra1, in *S. cerevisiae* (Fig. I9). However, in this organism their retention in nuclear foci occurs a Mlp1-dependent manner (Carmody et al., 2010), which in different from what we observe in fission yeast. To check if the interaction between the nuclear basket and certain mRNA binding proteins at NuRs could contribute to the mRNA export inhibition, as happens in budding yeast, we artificially tethered Alm1 and Nup211 at the NPC during HS. However, we found that at least Mex67 still localizes at NuRs in these conditions, suggesting that RBP relocation into NuRs is independent on the nuclear basket TPRs or that additional factors could contribute to their anchoring. Therefore, NuRs do not simply sequester RBPs and NPC components, but provide a robust mechanism for mRNA export inhibition. Intriguingly, in human cells the interaction of the nuclear basket TPR with Hsf1 favors the export of heat shock mRNAs under stress (Skaggs et al., 2007). This could represent a new mechanism of gene gating operating under heat stress, in order to connect gene expression and export pathways and bypass the block of mRNA export induced by HS. It would be interesting to explore whether this gene-gating mechanism is conserved in yeast and, if so, which nuclear pore components could be involved.

On the other hand, during unperturbed conditions the competency of mRNPs is monitored by the QC surveillance mechanism in order to avoid the export of malformed or improperly processed mRNAs (reviewed in Fasken and Corbett, 2009; Schmid and Jensen, 2008; Soheilypour and Mofrad, 2018; Sommer and Nehrbass, 2005). From yeast to humans, it has been demonstrated that the TPR/Mlp nucleoporins operate in a final mRNP quality control at the NPC, facilitating mRNA degradation by the nuclear exosome by interacting with mRNPs adaptor proteins (Bonnet et al., 2015; Fasken and Corbett, 2009; Fasken et al., 2008; Saroufim et al., 2015; Soheilypour and Mofrad, 2016). Since in budding yeast the exosome preserves its catalytic activity during HS (Zander and Krebber, 2017), it has been proposed the retention of Nab2 and Yra1 in nuclear foci in a Mlp1-dependent manner is key to bypass the quality control of HS mRNA (Zander et al., 2016). Interestingly, we have discovered that several RNA processing factors (*e.g.* spliceosome component Cdc5) and components of the exosome machinery, including Red1, the exonuclease Rrp6 and Pab2, also coalesced into NuRs, together with the nuclear basket TPRs (Fig. 3.2 D). Thus, the retention of the exosome machinery at NuRs in *S. pombe* could contribute to keep the QC machinery away from HS transcripts in order to speed up their export, in an analogous mechanism than that of budding yeast. Together, our results show that under heat shock mRNA, RNA binding proteins and their associated nuclear basket components accumulate at the periphery of the nucleolus. We hypothesize that the structural modification of mRNP particles, together with their relocalization to this stress-induced NuRs could constitute mRNA reservoirs either to protect such mRNPs or to block mRNA export, providing a mechanism by which the general mRNA processing and export are inhibited.

When we studied how the NPC structure is remodeled under HS, we found that the majority of NPC components remained conventionally associated to NPCs (Fig. 3.1), although we discovered several

exceptions. Nup131 and Amo1, nucleoporins of the outer cytoplasmic ring and the cytoplasmic filaments, respectively, showed a unique pattern of localization, since they do localize neither at NuRs nor to the NE upon HS, but in a diffuse pattern in the cytoplasm (Fig. 3.1 C and E). Although the function of Nup131 has not been described yet, this Nup possesses several interacting partners, including Far8, a component of the striatin-interacting phosphatase and kinase (STRIPAK) complex that regulates the septation initiation network and participates in the regulation of the SPB (Asakawa et al., 2019; Frost et al., 2012; Goudreault et al., 2009; Singh et al., 2011). On the other hand, Amo1 is required for the organization of the microtubule cytoskeleton (Pardo and Nurse, 2005). The funtional implications of Nup131 and Amo1 delocalization would required further research. Importantly, Nup132, which in normal conditions is located at the nucleoplasmic outer ring of the NPC, delocalizes from NPCs and coalesce into NuRs upon severe thermal stress (Fig. 3.1 C). This is not surprising, since we have previously observed that Nup132 is required for NB anchoring to the NPC. However, the absence of Nup133 in *S. cerevisiae* and its *S. pombe* homolog Nup132 leads to defects in NPCs distribution and clustering (Bai et al., 2004; Doye et al., 1994; Pemberton et al., 1995). This begs the question of how are the integrity and the structure of the NPC maintained in such conditions.

While in yeast the NPCs are constitutively assembled, in higher eukaryotes NPCs are disassemble and reassemble every cell cycle due to NE breakdown during mitosis (Antonin et al., 2008; Clever et al., 2013). Moreover, different nucleoporins, apart from localizing at the NPC, can be found in the nucleoplasm together with other functional complexes, such as the transcription machinery (Capelson et al., 2010b; Kalverda et al., 2010) or the kinetochore during mitosis (Belgareh et al., 2001; Lince-Faria et al., 2009; Loiodice et al., 2004; Mishra et al., 2010; Orjalo et al., 2006; Zuccolo et al., 2007), to perform specific functions independently on the NPC (Chatel and Fahrenkrog, 2011). Interestingly, in human cells several Nups have been shown to be constituents of stress granules under stress induced by arsenite, sorbitol or tubercidin (Hochberg-Laufer et al., 2019; Youn et al., 2018; Zhang et al., 2018). However, to date it was not reported a similar phenomenon in fission yeast. Unexpectedly, Nup85, a nucleoporin of the cytoplasmic Y-subcomplex, did coalesce into NuRs (Fig. 3.1 C), but also in cytoplasmic stress granules (Fig. 3.1 D). Given the characterized role of Nup85 in mRNA export (Watanabe et al., 2012) and in the posttranscriptional silencing of stress-induced genes under normal growth conditions (Woolcock et al., 2012), it could be hypothesized that its aggregation into NuRs could contribute to mRNA export inhibition or the activation of stress-responsive genes.

Collaboratively, these results show that upon heat shock the NPCs are remodeled and spatially sorted into two distinct substructures; while the core of the NPC remains at the nuclear periphery, the NB TPRs, Nup211 and Alm1, and the Y-subcomplex components, Nup132 and Nup85, coalesce into NuRs (Fig. 3.2 F). This raises the question whether these nucleoporins are removed from their normal localization at NPC during HS to make specialized NPCs that might operate better during HS, or whether the dynamic changes of the NPC composition induced under heat shock could contribute to the inhibition of specific nucleoporin functions, such as gene expression, mRNA export, nucleo-cytoplasmic trafficking, or chromatin regulation. Further studies would be required to fully understand

the complexity of these NPC rearrangements and its functional relevance in canonical nuclear pore roles.

3.2 Protective functions of HSPs during heat shock.

Hsf1 trancription factor is the main player in the activation of the HSR (Akerfelt et al., 2010). In unperturbed conditions Hsf1 activity is regulated negatively by Hsp70-Hsp40 and Hsp90 chaperones, which keep it inactive in the cytoplasm. According to the "titration model", the accumulation of misfolded proteins upon a heat stress causes the release of these HSPs from Hsf1 and, as a consequence, Hsf1 is no longer repressed, initiating the HSR. This stress-induced situation is reversible, as the accumulation of these chaperones once the external insult is over reverts Hsf1 to its inhibited state (Cotto and Morimoto, 1999; Richter et al., 2010; Sorger, 1991; Verghese et al., 2012). Similarly, we have observed that NuR formation is a reversible process; when stressful conditions cease, NuRs components are disaggregated and relocate back to their functional compartments. Indeed, NuR formation and disassembly (Fig. 3.4 A-E) have similar kinetics to Hsf1 activation and inactivation (Fig. 3.5 A-B), and cell growth inhibition and resumption (Fig. 3.4 D and E), suggesting that NuR formation could be part of the HSR.

The accumulation at NuRs of chaperones, such as Hsp70 homologs Ssa1 and Ssa2 and Hsp104 (Fig. 3.5 D) is consistent with the observed protein aggregation under severe heat shock and shows that NuRs involve protein interactions that are not present under normal growth conditions. The relocation of chaperones to the nucleolus under stress seems to be a conserved mechanism. In metazoan, several HSPs, such as HSP70, DNAJB1 (*Sc*Hsp40, *Sp*Mas5), and the small heat shock protein HSPB1, translocate to the nucleolus during a heat shock (Azkanaz et al., 2019; Deane and Brown, 2017; Khalouei et al., 2014; Morcillo et al., 1997; Nollen et al., 2001; Pelham, 1984; Welch and Feramisco, 1984). But, which would be the advantage of such rearrangement? On the one hand, storage of misfolded proteins would prevent the interference with other nuclear components and macromolecular structures that remain active during heat stress. On the other hand, it has been proposed that Hsp70 drives injured proteins to the nucleolus, which is key to catalyze their refolding (Nollen et al., 2001; Pelham, 1984). In agreement, the accumulation of Hsp70 at the nucleolus is required for cell recovery once the unstressful conditions are restored (Azkanaz et al., 2019; Pelham, 1984; Shorbagi and Brown, 2016; Vjestica et al., 2013), and the reassembly of small nuclear RNPs after HS depends on the Hsp70/Ssa family of proteins and Hsp104 (Bracken and Bond, 1999). Our results show that the functions of these chaperones could be conserved in the fission yeast, as we found that Hsf1 as well as the activity the disaggregase Hsp104 are required for timed NuR dissolution and cell viability after heat shock (Fig. 3.5 C and G). In *S. pombe,* even under mild HS (37ºC), non-terminally unfolded proteins aggregate in cytosolic protein aggregate centers, named PACs, which might serve as nucleation sites for SGs formed at extreme temperatures (Cabrera et al., 2020). Our results show that during acute HS essential nuclear proteins aggregate and immobilize at NuRs. Interestingly, the fate of NuRs, as occur with PACs and SGs during the recovery from HS (Cabrera et

al., 2020), is not degradation, but instead they are mostly disaggregated by chaperones, recovering their native structure and activity to promote cell fitness and growth resumption after the HS. In conclusion, our study shows that NuRs are dynamic and reversible structures whose components are mostly recycled and not degraded, probably assisted by HS-induced chaperones, such as the disagregasse Hsp104.

It has been recently shown that the HSR is characterized by a modular behaviour both in time and with different levels of response, which depends on the severity of the stress. While during mild heat stress predominate the protection by molecular chaperones and increase protein synthesis and turnover, during extreme conditions protein aggregation has a prominent role and results in translation and cell growth inhibition (Muhlhofer et al., 2019). Thermotolerance is usually provided by the presence of heat shock proteins, especially Hsp104, whose expression is notably induced during heat shock (Bracken and Bond, 1999; Lindquist and Kim, 1996; Mosser et al., 2004; Sanchez and Lindquist, 1990; Yost and Lindquist, 1991). Indeed, the negative effects of elevated temperatures can be reduced if cells are transiently exposed to a mild heat prior to the acute HS (Fig. 3.6 D and Fig. 3.7 A), which allows the activation of HSR genes, including chaperones that prevent and reverse protein unfolding and aggregation (Fig. 3.6 B and C). Remarkably, under these conditions NuRs do not assemble (Fig. 3.6 E) and cell growth and viability are not compromise (Fig. 3.6 D, Fig. 3.7 A), suggesting that NuRs formation is not critical for survival when cells are previously protected by mild-HS. In this context, acquired thermotolerance produces a deep impact in the whole cell metabolism, preparing cells for a posterior and more detrimental conditions, without affecting cell growth, translation or protein aggregation (Bond, 2006; Bracken and Bond, 1999; Muhlhofer et al., 2019).

Unexpectedly, we discovered that *alm1*-deleted mutant possesses a thermotolerant phenotype. This is evidenced by its accelerated kinetics of Hsf1 inactivation after HS (Fig. 3.7 B-D), the constitutively hyperactivated state of Hsf1 (Fig. 3.7 E), and the abnormally high levels of chaperones, such as the disagregasse Hsp104 (Fig. 3.7 F-G), which results in a increased cell viability after a heat shock (Fig. 3.7 A). A similar phenotype is observed in proteasome mutants (Fig. 3.7 H-I), and in conditions of proteasome inhibition, which lead to HSR activation, chaperone induction and thermotolerance (Bush et al., 1997; Lee and Goldberg, 1998; Pritts et al., 2002; Yamamoto et al., 2008). Indeed, the accumulation of ubiquitinated proteins in proteasome mutants increases the Hsf1-dependent expression of HSPs (Pirkkala et al., 2000), conferring crossprotection. Given the previously characterized role of Alm1 in proteasome regulation (Chapter 1), we hypothesize that when the function of the proteasome is compromised, the accumulation of certain chaperones may counteract HS-induced damage and confer thermotolerance under HS conditions, resulting in increased cell survival rates after a heat shock, similar to a mild-heat pretreatment.

On the contrary, severe heat shock boosts protein denaturation and aggregation and strongly affects the stability of macromolecular complexes. As a consequence, heat shock affects negatively cell survival (Gross and Watson, 1998; Lindquist and Craig, 1988; Parsell and Lindquist, 1993; Pincus, 2017; Riezman, 2004; Sanchez and Lindquist, 1990; Verghese et al., 2012; Vogel et al., 1995). We

have observed that under a more severe HS treatment (45-47ºC) NuRs are not properly formed and cell viability is deeply compromise (Fig. 3.5 H). Therefore, our results show that NuRs represent a reversible state of protein aggregation that contribute to the cellular resilience and adaptation to acute temperature fluctuations and expand the view of HS-induced protein aggregation as a major threat for cellular homeostasis to an adaptive mechanism to maintain cell viability in stress conditions.

3.3 Heat shock induces nucleolar reorganization.

First studies described that heat shock drastically altered nuclear organization, including chromatin rearrangements and changes in the nucleolar morphology (Bond, 2006; Chowdhary et al., 2017; Jolly et al., 1999; Welch and Suhan, 1985). In fact, this seems to be a conserved process, caused by the reprogramming of the transcriptional programs, the disassembly of macromolecular complexes and the reversible aggregation of endogenous proteins in different cellular subcompartments (Boulon et al., 2010; Chowdhary et al., 2017; Chowdhary et al., 2019; Olson, 2004; Shav-Tal et al., 2005; Wallace et al., 2015). Analogously, the nucleolus is reorganized during stress, allegedly caused by the inhibition of rRNA transcription and the redistribution of many nuclear and nucleolar proteins into differentiated domains (Boisvert et al., 2007; Boulon et al., 2010; Grummt and Voit, 2010; Jacob et al., 2013; Liu et al., 1996; Mayer and Grummt, 2005; Nazer et al., 2011; Nemeth and Grummt, 2018; Shav-Tal et al., 2005; Yang et al., 2018). This process has been observed in several organisms (Bond, 2006; Boulon et al., 2010; Grummt, 2013; Hayashi and Matsunaga, 2019; Liu et al., 1996; Tani et al., 1996), and under different type of stresses, including transcription inhibition (Desnoyers et al., 1996; Shav-Tal et al., 2005; Yung et al., 1985), cytotoxic agents (Chan et al., 1999; Perlaky et al., 1997), UV radiation (Thielmann and Popanda, 1998), heat shock (Chan et al., 1999) or senescence (Kar et al., 2011). Accordingly, our study shows that in *S. pombe* heat stress also leads to changes in the nucleolar morphology and the reduction of the nucleolar size, as evidences Gar2 lob formation (Fig. 3.3 A-B and Fig. 3.4 F). Consistent with nucleolar contraction, topoisomerase Top2 and condensin complex subunit Cnd1, both involved in chromosome organization (Charbin et al., 2014; Hirano et al., 1989; Piskadlo et al., 2017; Tapia-Alveal et al., 2010), are also enriched at NuRs during HS (Fig. 3.3 B). Moreover, we observed events of nucleolar segregation, as the rDNA transcription factor Acr1 and the RNA polymerase Nuc1 appeared as intense nucleolar foci, and the transcriptional regulator Reb1 relocates at NuRs (Fig. 3.3 A), which might reflect the inhibition of rDNA transcription. Thus, under heat shock the fission yeast nucleolus is reorganized into two differentiated domains: a central condensed domain that contains the RNA pol I machinery (Nuc1, Acr1) and a peripheral domain that we named NuR, formed by aggregates of nuclear proteins whose functions seem to be inhibited in stress conditions (Fig. 3.8). Remarkably, NuR formation in response to HS correlates with nucleolar contraction, and its dissolution is accompanied by cell growth resumption and the recovery of the nucleolar morphology and size (Fig. 3.4). Further investigations will be required to fully characterize the nucleolar segregation occurring upon stress and to know its functional implications.

In yeast, the nucleolus is in contact with the nuclear envelope and, although it seems to be less complex, most of structural components are conserved with high eukaryotes. In higher eukaryotes the nucleolus is located more centrally in the nucleoplasm and has a tripartite structure with three specialized functional sub-compartments: the fibrillar center (FC), containing the RNAP I and cofactors; the dense fibrillar component (DFC), containing the rRNA; and the granular component (GC), the site of ribonucleoprotein processing and assembly (reviewed in Hayashi and Matsunaga, 2019; Hernandez-Verdun et al., 2010; Melese and Xue, 1995; Scheer and Hock, 1999; Schwarzacher and Wachtler, 1993; Sirri et al., 2008). During stress induced by transcriptional inhibition, nucleolar segregation results in the compaction and the separation of the FC and the GC, as well as the formation of nucleolar caps, which contain FCs and DFCs surrounding the GC (central body of the nucleolus). The nucleolus is not only considered a phase-separated quality control subcompartment in which heat shock-produced misfolded proteins accumulate in order to prevent protein degradation and irreversible aggregation and to assist protein refolding, but also a central hub for the coordination of the stress response. This is evidenced by the multiple nucleolar stress-induced pathways, including p53, mTOR, MAPK, and PI3K (phosphatidylinositol 3-kinase)-dependent pathways (Boulon et al., 2010; Latonen, 2019; Rekulapally and Suresh, 2019).

In mammalian cells during heat shock stress, the upregulation of intergenic spacers (IGSs), located between ribosomic genes, leads to the accumulation of such long noncoding transcripts at the center of the nucleolus to form a nucleolar aggregosome, also called “Detention Center”, which captures and immobilizes proteins whose functions are unrelated to ribosome biogenesis, including transcription factors, cell-cycle regulators, splicing factors and different RNA-binding proteins, as well as chaperones (Audas et al., 2012; Boisvert et al., 2007; Boulon et al., 2010; Jacob et al., 2013; Latonen, 2019; Nemeth and Grummt, 2018; Wang et al., 2018). Whether a similar mechanism exist in fission yeast and contribute to NuR formation remains to be explored. In *Tripanosoma,* a similar nucleolar rearrangement keeps proteins away from their canonical pathways and triggers the nucleolar accumulation of poly(A) RNAs (Nazer et al., 2011, 2012). Importantly, we found that in response to heat stress a wide range of proteins involved in several nuclear functions essential for life, including the mRNA export machinery (Fig. 3.2) or cell cycle regulators, such as Cdc14, Plo1, Ark1 and the mitotic cyclin Cdc13 (Fig. 3.3 C), accumulate at NuRs. The nucleolar accumulation of all these factors required for cell growth under normal condition, together with chaperones, might suggest that in the fission yeast NuRs act as “detention platform” for those activities that have to be inhibited and/or protected during HS in order to re-start cellular metabolism and growth when normal conditions are restored (Kuhl and Rensing, 2000).

In conclusion, this study shows that the nuclear basket TPRs and its associated nucleoporins relocate from the NPC to the interphase amid the nucleoplasm and the nucleolus, together with mRNA, RBPs, RNA processing factors, chaperones and cell cycle regulators (Fig. 3.8). These stress-induced structures, named NuRs, are rapidly formed upon acute HS and progressively disaggregate when growing conditions are restored. NuR dissolution depends on key HS response elements, such

as Hsf1 and Hsp104, and is coincident with the restoration of nucleolar morphology and with the release of cell growth inhibition. Our results suggest that spatially organized and reversible HS-induced protein aggregation leads to the transient inhibition of RNA-related nuclear activities, and functions as protective mechanism to resist acute HS conditions.

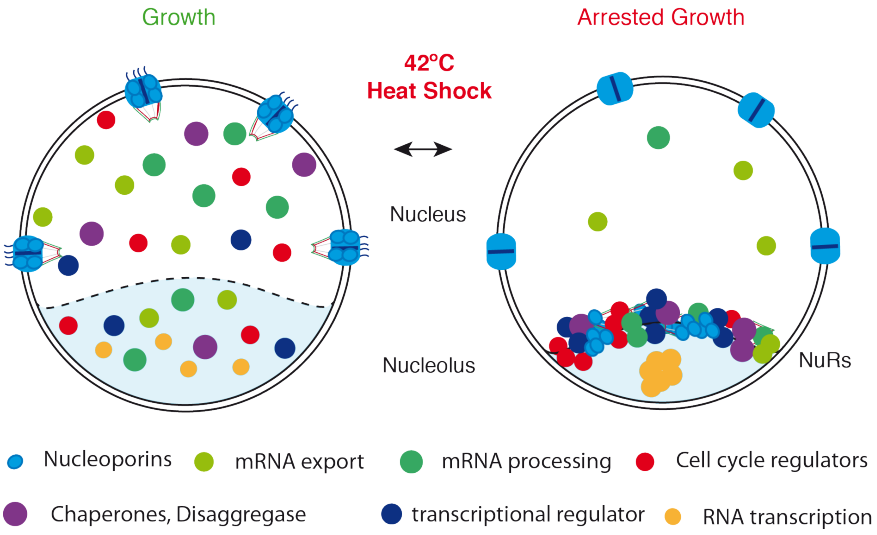

Figure 3.8. Cartoon depicting cell nucleus in normal growth conditions and during heat stress. HS leads to changes in NPC composition and nucleolar segregation, due to the rapid relocalization and aggregation of the nuclear basket TPRs and Nups of the Y-subcomplexes (blue), together with different nuclear components, such as transcriptional regulators (dark blue), processing and export factors (green), cell cycle regulators (red), chaperones and disaggregases (purple), in ring-like structures at the periphery of the nucleolar region, named nucleolar rings (NuRs). NuRs are transient structures formed concomitantly with the contraction of the nucleoli and the inhibiton of cell growth and mRNA export, and are disaggregated when normal conditions are restored.

Concluding Remarks

At the nucleoplasmic side of the NPCs, the large (~200kD) filamentous coiled-coil proteins TPR/Mlps converge in a distal ring, termed the nuclear basket. The nuclear basket forms a dynamic network that connects NPCs and acts as a platform for the anchoring of a wide range of nuclear components (Bangs et al., 1998; Cordes et al., 1997; Galy et al., 2004; Kosova et al., 2000; Krull et al., 2004; Niepel et al., 2013; Strambio-de-Castillia et al., 1999). Consequently, the nuclear basket is involved in the regulation of several nuclear functions, most of which have been conserved during evolution (Beck and Hurt, 2017; Capelson et al., 2010a; Grossman et al., 2012; Ibarra and Hetzer, 2015; Kabachinski and Schwartz, 2015). In this study, we aimed to perform a functional characterization of the nuclear basket TPR nucleoporins in *S. pombe*, including those that have been previously described in other systems and new roles that might have remained uncovered.

Our study revealed a new role of the nuclear basket TPR nucleoporin in the regulation of the spatial distribution of the proteasome within the fission yeast nucleus. We have shown that the TPR nucleoporin Alm1 is required for the localization of the proteasome and its NE anchor Cut8 at the nuclear periphery, which in turn regulate the proper balance of centromere/kinerochore proteins, contributing to the maintenance of genome integrity (Chapter 1). In *S. cerevisiae*, the Mlp interactome also includes the proteasome, via Esc1, a NE protein involved in telomere-NE anchoring and silencing, and Cdc31/centrin, which is linked to the mRNA export machinery (Niepel et al., 2013). Importantly, a later work using *Chlamydomonas reinhardtii* revealed that the proteasome is anchored to the INM surrounding the NPC and the nuclear basket itself (Albert et al., 2017). These works not only strengthen our results, but also go beyond and suggested that the localization of the proteasome inside the nucleus, and specifically its enrichment at the NE and the NPC, could represent a protein quality control system that acts as a degradation center for membrane and soluble proteins crossing the NPC (Boban and Foisner, 2016; Enenkel, 2014; Gardner et al., 2005; Prasad et al., 2010; Rosenbaum and Gardner, 2011; Smoyer and Jaspersen, 2019), including transcription factors (Lipford and Deshaies, 2003; Muratani and Tansey, 2003), DNA repair proteins (Bergink and Jentsch, 2009; Dantuma et al., 2009; Schauber et al., 1998), or the mRNA export machinery (Babour et al., 2012; Fischer et al., 2004).

Transcriptional regulation and mRNP processing and export are among the most studied functions of the TPR nucleoporins (Bonnet and Palancade, 2014; Brickner, 2009; Light and Brickner, 2013; Mendjan et al., 2006; Sood and Brickner, 2014; Stewart, 2019; Texari and Stutz, 2015; Tutucci and Stutz, 2011; Vinciguerra et al., 2005). In this work we have shown that interfering with nuclear basket assembly in the fission yeast impairs mRNA export and leads to the retention of Poly(A)-Binding Proteins (PABP) in aberrant perinuclear aggregates or foci, associated to the nuclear basket TPRs (Fig. 2.3-2.4). This is in agreement with previous studies showing that Mlp1 interaction with the PABP Nab2 is required for recognition and retention of unspliced or faulty mRNAs at the nuclear pore, which

are targeted to the nuclear exosome for degradation, a function that is also conserved in higher eukaryotes (Coyle et al., 2011; Doma and Parker, 2007; Fasken and Corbett, 2009; Galy et al., 2004; Green et al., 2003; Peck et al., 2019; Porrua and Libri, 2013; Rajanala and Nandicoori, 2012; Soheilypour and Mofrad, 2018). This mRNA QC pathway includes several nuclear basket associated partners, such as Pml39, Ulp1, Esc1, Swt1 or Nab2 (Lewis et al., 2007; Niepel et al., 2013; Palancade et al., 2005; Skruzny et al., 2009; Zhao et al., 2004).

Additionally, our results demonstrate that Nup211 is also required for the recruitment or loading of Mex67 export factors into mRNPs (Fig. 2.6). This direct function of the nuclear basket in mRNA export could be conserved in higher eukaryotes (Bachi et al., 2000; Matzat et al., 2008). Importantly, further loading of Mex67 into the export-competent mRNP is triggered by the removal of Yra1 from the mRNP due to the Tom1 E3 ligase-dependent ubiquitination (Hautbergue et al., 2008; Iglesias et al., 2010). Two ubiquitin ligases from the HECT family, Tom1 and Rsp5, have been shown to play a role in nuclear export of poly(A)-RNAs in *S. cerevisiae*. The yeast E3 ubiquitin ligase Rsp5 (whose targets include two RNA biogenesis/export machinery components Npl3 and Hpr1) participates in general as well as stress responsive transcripts export (Gupta et al., 2007; Gwizdek et al., 2005; Haitani and Takagi, 2008; Rodriguez et al., 2003). The ubiquitin E3 ligase Tom1 is required for export of Nab2-bound mRNPs through ubiquitination of Yra1, which promotes its dissociation from mRNPs and elecits mRNA export (Duncan et al., 2000; Iglesias et al., 2010). Ptr1, the fission yeast homolog of Tom1, is also involved in mRNA export (Andoh et al., 2004). Given the role of the nuclear basket Alm1 in the regulation of the proteasome, it would be worth exploring whether the nuclear basket could be involved in the final remodeling of mRNPs to licence their export through the ubiquitin proteasome pathway.

Nup211 and Nup85 are required for mRNA export (Bae et al., 2009; Watanabe et al., 2012) and Nup85 is also involved in the posttranscriptional silencing of stress-induced genes under normal growth conditions (Woolcock et al., 2012). Interestingly, upon heat shock the NPCs are remodeled and spatially sorted into two distinct substructures; while the core of the NPC remains at the nuclear periphery, the NB components Nup211 and Alm1 and components of the Y-suxcomplexes (Nup132 and Nup85) coalesce into NuRs (Fig. 3.1). This raises the question whether the TPR Nups and its NPC-associated components are removed from their normal locations during HS to be inhibited, to make specialized NPCs that might operate better during HS, or whether these NPC components could play new roles at NuRs. On the one hand, during HS transcription, processing, export and translation of housekeeping mRNAs is rapidly inhibited to favour the synthesis of HS factors (Zander et al., 2016). In *S. cerevisiae* HS-dependent inhibition of mRNA export is achieved by changes in the composition of the mRNPs (Krebber et al., 1999) and the accumulation of mRNP adaptors in nuclear foci in a Mlp1-dependent manner (Carmody et al., 2010), while the cytoplasmic fibrils of NPCs are remodeled to facilitate the export of HS transcripts (Izawa et al., 2004; Rollenhagen et al., 2007; Saavedra et al., 1997). In mammalian cells, some Nups relocate to cytoplasmic SGs under stress (Hochberg-Laufer et

al., 2019; Youn et al., 2018). This situation share similarities with our results in the fission yeast. Specifically, the sequestration of these Nups at NuRs under heat stress might contribute to release the posttranscriptional inhibition on stress-responsive genes or to inhibit bulk mRNA; although other explanations cannot be discarded. Future studies will focus on understanding the mechanisms of this NPC rearrangement and its biological implications.

On the other hand, proteotoxic stress leads to the organized accumulation of misfolded proteins that need to be refolded or degraded by the ubiquitin proteasome system to alleviate cell toxicity (Fang et al., 2016; Karmon and Ben Aroya, 2019; Malinovska et al., 2012; Miller et al., 2015). Indeed, chaperones aid in substrate recognition and degradation (Fang et al., 2014; Guerriero et al., 2013; Ho et al., 2019; McLoughlin et al., 2019). Intriguingly, the ubiquitin ligase Rsp5, involved in the regulation of mRNA export (Domanska and Kaminska, 2015; Gwizdek et al., 2005; Haitani and Takagi, 2008; Rodriguez et al., 2003), is the main ubiquitin ligase targeting cytosolic proteins for proteasome degradation upon HS (Fang et al., 2014). Interestingly, the SGA assay performed with the *alm1*-deleted mutant revealed an enrichment in synthetic factors involved in the regulation of stress-activated protein kinase signaling cascade, in the response to stress and in *de novo* protein folding. Given the role of Alm1 in the spatial regulation of the proteasome, and the hormetic effect of proteasome disfunction under HS, it would be interesting to investigate the interplay between proteasome distribution and function, and the HSR.

The nuclear basket components lack enzymatic activity and, therefore, their functions depends on the wide range of nuclear interacting partners that they possess (Niepel et al., 2013). However, TPR nucleoporins cannot be conceived as merely structural and static elements; the differential localization and function of TPRs is highly regulated by posttranslational modifications. For example, their phosphorylatation by ERK1/2, PKA, Mps1 and CDK1 kinases (Rajanala et al., 2014; Vomastek et al., 2008) has been linked to the regulation of NPC assembly and distribution (Fiserova et al., 2019; McCloskey et al., 2018), to the spatio-temporal regulation of SAC machinery during mitosis through the delivery of Mad1 from nuclear pores to kinetochores (Cunha-Silva et al., 2020; Lee et al., 2008b; Lince-Faria et al., 2009; Rajanala et al., 2014; Schweizer et al., 2013), or to the release of the ubiquitin E3 ligase COP1 from the nuclear envelope, promoting the degradation of its nuclear substrates, including c-Jun, a critical transcription factor that promotes cellular proliferation (Ouyang et al., 2020). Besides, several nucleoporins of the nuclear basket are regulated by other posttranslational modification, such as ubiquitination, SUMOylation or phosphorylation, which influences the plasticity of the NPC and DNA damage response (Nino et al., 2016), nuclear segregation (Hayakawa et al., 2012), sensing cellular stresses (Folz et al., 2019), or mRNA biogenesis of stress-responsive genes (Regot et al., 2013). Further studies will be required to fully uncover the multiple functions of the nuclear basket and how they are modulated.

CONCLUSIONS

1. *alm1Δ* mutant genetically interacts with chromatin, kinetochore and proteasome mutants.

2. Centromeric chromatin and stoichiometry of centromere–kinetochore proteins is altered in the absence of *alm1*.

3. Ectopic accumulation of Cnp3 at kinetochores impairs chromosome segregation.

4. Stoichiometric accumulation of Cnp3 at kinetochores is regulated by the localization and function of the proteasome.

5. Alm1 is required for proper localization of the 26S proteasome to the nuclear envelope.

6. Alm1-Nup211 interaction and anchoring to Nup132 are required for their assembly at the nuclear basket.

7. TPR nucleoporins Alm1 and Nup211 participate in mRNP docking to the nuclear basket through interaction with the PABPs Nab2 and Pab2.

8. *alm1Δ* is phenotipically more similar to an exosome deficient mutant, while *nup211ts* phenocopies mRNA export mutants, with which it genetically interacts.

9. mRNA export defects of *nup211ts* mutant are additive to *rae1* mutant and epistatic to *mex67* mutant.

10. Inactivation of Nup211 leads to the mislocalization of Mex67 from the nuclear pore and its accumulation in abnormal perinuclear foci, suggesting that Nup211 participates in the recruitment of Mex67.

11. Heat stress leads to the remodeling of the NPC and the aggregation of specific nucleoporins and mRNA-binding factors, involved in mRNA processing, quality control and export, in a ring-like structure at the nucleolar periphery, which we named nucleolar ring (NuR).

12. Heat stress induces changes the morphology, size and organization of the nucleolus, and the accumulation of RNA transcription factors, DNA associated factors, cell cycle regulators and chaperones at NuRs.

13. NuRs are dynamic structures formed by the aggregation of proteins during HS-induced growth inhibition and their disassembly precedes the restoration of cell growth.

14. NuR formation correlates with Hsf1 activation, and Hsf1 delayed upregulation and Hsp104 activity are required for proper disaggregation of NuRs and for cell viability.

15. Acquired thermotolerance prevents NuR formation and cell death upon heat shock.

16. The absence of *alm1* as well as proteasome disfunction result in acquired thermotolerance.

MATERIALS AND METHODS

MATERIALS

Strains

All *S. pombe* yeast strains used in this thesis are listed in Table S1.

Table S1. *S. pombe* strains used in this study.

Chapter 1		
Strain Name	**Genotype**	**Source**
RD312	h+ ade6-M210 ura4-D18 leu1-32	Lab collection
RD313	h- ade6-M210 ura4-D18 leu1-32	Lab collection
RD399	h+ alm1::ura4+ ura4-D18 leu1-32 ade6-M216	Lab collection
RD400	h- alm1::ura4+ ura4-D18 leu1-32 ade6-M216	Lab collection
RD4488	h- alm1::Nat ura4-D18 leu1-32	This study
RD3354	h clr4::kan leu1-32 ura4-D18 ade6-	Braun´s Lab
RD4097	h- SPSQ(cyhR) SPL42(CyhS) imr1L(NcoI)::Ura4 otr1R(Sph1)::ade6 hugR::cen1 leu1-32 ade6-210 ura4DS/E	Braun´s Lab
RD4098	h- SPSQ(cyhR) SPL42(CyhS) imr1L(NcoI)::Ura4 otr1R(Sph1)::ade6 hugR::cen1 clr4::Nat leu1-32 ade6-210 ura4DS/E	Braun´s Lab
RD4099	h- SPSQ(cyhR) SPL42(CyhS) imr1L(NcoI)::Ura4 otr1R(Sph1)::ade6 hugR::cen1 alm1::Nat leu1-32 ade6-210 ura4DS/E	Braun´s Lab
RD3081	h- cnp3::Kan leu1 ade6-M216	Watanabe´s lab
RD4476	h- mhf1::NatMX6	Moreno's Lab
RD5599	h- mis6-302 leu1-32	NBRP, Japan
RD5601	h- mis12-537 leu1-32	NBRP, Japan
RD4484	h- mis16-53 ade6-M210 his3D1 uraD18 argD leu1-32	Moreno's Lab
RD4485	h- mis18-262 ade6-M210 his3D1 arg3D4	Moreno's Lab
RD4483	h- sim1-139 ade6-M210 his3D1 ura4D18 argD leu1-32	Moreno's Lab
RD4482	h- sim3-143 ade6-M210 his3D1 ura4D18 argD leu1-32	Moreno's Lab
RD318	h+ ndc80-GFP(kanMX6) his- leu1-32 ade6- ura4-D18	Nurse´s Lab
RD284	h+ nuf2-GFP (kanMX6) ura4-D18	Nurse´s Lab
RD2963	h+ imrIL(NcoI)::ura4+ otr1R(SphI)::ade6+ ura4-DS/E leu1-32 ade6-M210	Ekwall´s Lab
RD2965	h+ imrIL(NcoI)::ura4+ otr1R(SphI)::ade6+ clr4::Kan ura4-DS/E leu1-32 ade6-M210	Ekwall´s Lab
RD3194	h+ imrIL(NcoI)::ura4+ otr1R(SphI)::ade6+ alm1::HphMX6 ura4-DS/E leu1-32 ade6-M210	This study
SB0071	cc2(SphI)::ura4+ ura4-DS/E leu1-32 ade6-M210	Allshire´s Lab
SB0091	cc2(SphI)::ura4+ clr4::Kan ura4-DS/E leu1-32 ade6-M210	Allshire´s Lab
	cc2(SphI)::ura4+ alm1::HphMX6 ura4-DS/E leu1-32 ade6-M210	This study
RD1409	h- cnp1-mCherry::kanMX6 ura4-D18 leu1-32	Lab collection
RD2314	h+ alm1::U cnp1-Cherry-K ura4-D18 leu1-32	This study
RD4124	h+ mhf1-GFP-Kan	Moreno's Lab
RD4141	h mhf1-GFP-Kan alm1::ura4+	This study
RD4479	h+ mhf2:eGFP:KanR	Moreno's Lab
RD4536	h mhf2:eGFP:KanR alm1::ura4+	This study
RD4434	h+ cnp20:GFP:Kan ura4-D18 leu1-32	Moreno´s Lab
RD4436	h+ cnp20:GFP:Kan alm1::ura4+ ura4-D18 leu1-32	This study
RD4157	h- pcs1:GFP-Leu2 ura4-D18 ade6-M216	Gregan´s Lab
RD4158	h- pcs1:GFP-Leu2 alm1::ura4+ ura4-D18 leu1-32	This study
RD4286	h- mde4:GFP:Kan ura4-D18 leu1-32	Gregan´s Lab
RD4383	h mde4:GFP:Kan alm1::ura4+	This study
RD4369	h- fta1:GFP:Hph ura4-	NBRP, Japan
RD4371	h- fta1:GFP:Hph alm1::ura4+ ura4-D18	This study
RD4373	h- sim4:Tomato:Kan ura4-D18	NBRP, Japan
RD4375	h- sim4:Tomato:Kan alm1::ura4+ ura4-D18	This study
RD3083	h- cnp3-tdTomato:kanMX6	Watanabe's Lab
RD3227	h cnp3:tdTomato:KanR alm1::ura4+	This study
RD4139	h- cnp3-GFP-Kan ura4-D18 leu1-32 ade6-M216	This study

RD4155	h- cnp3-GFP:Kan alm1::ura4 ura4-D18 leu1-32 ade6-M216	This study
RD4828	h- pINT-cnp3-GFP-NatR cnp3-GFP-Kan	This study
RD4830	h+ pINT-cnp3-GFP-NatR cnp3-GFP:Kan alm1::ura4+	This study
RD5768	h- nmt81-cnp3-GFP alm1::ura4+	This study
RD4463	h *mts4* cnp3:GFP:Kan	This study
RD4464	h *mts4* cnp3:GFP:Kan alm1::ura4+	This study
RD5034	h- mts4-GFP:Kan ura4-D18 leu1-32 ade6-M216	This study
RD5038	h mts4-GFP:Kan cut8-563 leu1-32	This study
RD3250	h+ rpn8-GFP:Nat ura4-D18 leu1-32 ade6-M216	This study
RD5558	h rpn8-GFP:Kan cut8-563 ura4-D18 leu1-32	This study
RD5006	h cut8-563 cnp3:tdTomato:Kan ura4-D18	This study
RD5008	h cut8-563 cnp3:tdTomato:Kan alm1::ura4+ ura4-D18	This study
RD5010	h cut8-563 cnp3:GFP:Kan ura4-D18	This study
RD4463	h *mts4* cnp3:GFP:Kan pINT-Cnp3:GFP:Nat	This study
RD4992	h alm1-tomato-Nat cut8-GFP-Leu2 ade6- leu1-32 ura4-D18	This study
RD4970	h- cut8:GFP-Leu2 ura4-D18 leu1-32 ade6-M216	NBRP, Japan
RD4845	h- cut8:GFP-Leu2 alm1::ura4+ ura4-D18 leu1-32 ade6-M216	This study
RD5681	h mts2-8myc	NBRP, Japan
RD5385	h alm::ura4+ mts2-8myc	This study
RD5684	h mts4-13-myc	NBRP, Japan
RD5689	h alm1::ura4+ mts4-13myc	This study

Chapter 2

Strain Name	**Genotype**	**Source**
RD312	h+ ade6-M210 ura4-D18 leu1-32	Lab collection
RD313	h- ade6-M210 ura4-D18 leu1-32	Lab collection
RD4508	h- nup211-GFP-Kan ura4-D18 leu1-32 ade6-M216	This study
RD5229	h+ nup211-GFP-Kan ura4-D18 leu1-32 ade6-M216	This study
RD5216	h+ nup211ts-GFP-Kan ura4-D18 leu1-32 ade6-M216	This study
RD5223	h- nup211ts-GFP-Kan ura4-D18 leu1-32 ade6-M216	This study
RD1117	h+ alm1-Tomato-Nat ura4-D18 leu1-32 ade6-M216	Lab collection
RD3637	h- alm1-Tomato-Nat ura4-D18 leu1-32 ade6-M216	Lab collection
RD5153	h^{90} alm1ts-Tomato-Nat ura4-D18 leu1-32 ade6-M216	This study
RD5585	h+ nup211ts-Hph ade6-M210 ura4-D18 leu1-32	This study
RD5586	h- nup211ts-Hph ade6-M210 ura4-D18 leu1-32	This study
RD5611	h^{+} alm1ts-Hph ade6-M210 ura4-D18 leu1-32	This study
RD5612	h^{90} alm1ts -Hph ade6-M210 ura4-D18 leu1-32	This study
RD399	h+ alm1::ura4+ ura4-D18 leu1-32 ade6-M216	Lab collection
RD400	h- alm1::ura4+ ura4-D18 leu1-32 ade6-M216	Lab collection
RD4217	h^{90} nup132::Kan ura4-D18 leu1-32 ade6-M216	NBRP, Japan
RD5230	h alm1-Tomato-Nat nup211-GFP-Kan ura4-D18 leu1-32	This study
RD5232	h alm1-Tomato-Nat nup211ts-GFP-Kan ura4-D18 leu1-32	This study
RD5178	h alm1ts-Tomato-Nat nup211-GFP-Kan ura4-D18 leu1-32	This study
RD5432	h+ nup60::Nat alm1-Tomato-Nat ura4-D18 leu1-32 ade6-M216	This study
RD5409	h nup60::Nat nup211-GFP-Kan ura4-D18 leu1-32 ade6-M216	This study
RD5587	h nup124::Kan alm1-Tomato-Nat ura4-D18 leu1-32 ade6-M216	This study
RD5782	h nup124::Kan nup211-GFP-Kan ura4-D18 leu1-32 ade6-M216	This study
RD4239	h- nup132::Kan alm1-Tomato-Nat ura4-D18 leu1-32 ade6-M216	Lab collection
RD5090	h^{90} nup132::Kan alm1ts-Tomato-Nat ura4-D18 leu1-32 ade6-M216	This study
RD5338	h+ nup132::Kan nup211-GFP-Kan ura4-D18 leu1-32 ade6-M216	This study
RD5340	h+ nup132::Kan alm1-Tomato-Nat nup211-GFP-Kan ura4-D18 leu1-32	This study
RD5279	h nup132::Kan alm1ts-Tomato-Nat nup211-GFP-Kan ura4-D18 leu1-32	This study
RD6405	h+ GFP-nab2-Kan ade6M210 leu1-32 ura418 his3A	NBRP, Japan
RD6408	h alm1::ura4+ GFP-nab2-Kan ade6M210 ura4-D18 leu1-32	This study
RD6410	h- nup211ts-Hph GFP-nab2-Kan ura4-D18 leu1-32	This study
RD6932	h nup211-mCherry-Nat GFP-nab2-Kan ura4-D18 leu1-32	This study
RD7013	h nup211ts-mCherry-Nat GFP-nab2-Kan ura4-D18 leu1-32	This study
RD6527	h alm1-Tomato-Nat GFP-nab2-Kan ura4-D18 leu1-32	This study
RD6529	h nup211ts-Hph alm1-Tomato GFP-nab2-Kan ura4-D18 leu1-32	This study
RD6491	h- rae1-167 lys1+::ura4-DSR::Kan leu1-32 ura4DS/E ade6-210/M216	NBRP, Japan

RD6566	h rae1-167 nup211ts-Hph leu1-32	This study
RD6584	h rae1-167 alm1::ura4+ leu1-32	This study
RD6258	h+ mex67::Nat ura4-D18 leu1-32 ade6-M216	This study
RD6268	h mex67::nat nup211-ts-Hph ura4-D18 leu1-32	This study
RD6270	h mex67::nat alm1::ura4+ ura4-D18 leu1-32	This study
RD6568	h rae1-167 GFP-nab2-Kan leu1-32	This study
RD6596	h rae1-167 nup211ts-Hph GFP-nab2-Kan leu1-32	This study
RD6412	h mex67::nat GFP-nab2-Kan ura4-D18 leu1-32	This study
RD6693	h mex67::nat nup211ts-Hph GFP-nab2-Kan ura4-D18 leu1-32	This study
RD2759	h rad52-mCherry-Nat ura4-D18 leu1-32	Lab collection
RD6253	h+ rad52-mcherry-nat nup211ts-Hph ura4-D18 leu1-32	This study
RD6570	h rae1-167 rad52-mCherry-Nat leu1-32	This study
RD6598	h rae1-167 nup211ts-Hph rad52-mCherry-Nat leu1-32	This study
RD6340	h mex67::nat rad52:mcherry:Nat ura4-D18 leu1-32	This study
RD6613	h mex67::Nat nup211ts-Hph rad52-mCherry-Nat ura4-D18 leu1-32	This study
RD7109	h nup211-mCherry-Nat pab2-GFP-Kan ura4-D18 leu1-32	This study
RD7111	h nup211ts-mCherry-Nat pab2-GFP-Kan ura4-D18 leu1-32	This study
RD7105	h alm1-Tomato pab2-GFP-Kan ura4-D18 leu1-32	This study
RD7107	h nup211ts-Hph alm1-Tomato pab2-GFP-Kan ura4-D18 leu1-32	This study
RD6494	h^{90} leu1-32 ura4D-18 ade6-M216 rrp6::KanR	NBRP, Japan
RD7033	h- pab2-GFP-Kan ura4-D18 leu1-32	This study
RD7045	h- alm1::ura4+ pab2-GFP-Kan ura4-D18 leu1-32	This study
RD7041	h- nup211ts-Hph pab2-GFP-Kan ura4-D18 leu1-32	This study
RD7118	h red1-Tomato-Kan pab2-GFP-Kan ura4-D18 leu1-32	This study
RD7143	h nup211ts-Hph red1-Tomato-Kan pab2-GFP-Kan ura4-D18 leu1-32	This study
RD7145	h alm1::ura4+ red1-Tomato-Kan pab2-GFP-Kan ura4-D18 leu1-32	This study
RD7097	h- rae1-167 pab2-GFP-Kan red1-Tomato-Kan ura4-D18 leu1-32	This study
RD7095	h- rrp6::Kan pab2-GFP-Kan red1-Tomato-Kan ura4-D18 leu1-32	This study
RD6518	h^{90} GFP-rae1-KanR ade6-216 ura4 leu1-32 lys1-131	Hiraoka's Lab
RD6588	h alm1::ura4+ GFP-rae1-Kan ade6-M210 ura4-D18 leu1-32	This study
RD6564	h nup211ts-Hph GFP-rae1-Kan ade6-M210 ura4-D18 leu1-32	This study
RD6020	h mlo3-GFP-Kan ura4-D18 leu1-32	This study
RD6024	h alm1::ura4+ mlo3-GFP-Kan ura4-D18 leu1-32	This study
RD6022	h nup211ts-Hph mlo3-GFP-Kan ura4-D18 leu1-32	This study
RD6000	h- mex67-GFP-Kan ura4-D18 leu1-32	This study
RD6001	h+ alm1::ura4+ mex67-GFP-Kan ura4-D18 leu1-32	This study
RD6003	h+ nup211ts-Hph mex67-GFP-Kan ura4-D18 leu1-32	This study
RD6000	h- mex67-GFP-Kan ura4-D18 leu1-32	This study
RD6001	h+ mex67-GFP-Kan nup211ts-Hph ura4-D18 leu1-32	This study
RD6003	h+ mex67-GFP-Kan alm1::ura4+ ura4-D18 leu1-32	This study
RD6594	h rae1-167 mex67-GFP-Kan leu1-32	This study
RD6688	h mlo3-GFP-Kan rae1-167 leu1-32	This study
RD6313	h nup211-GFP-Kan mex67-mCherry-Nat ura4-D18 leu1-32	This study
RD6338	h nup211ts-GFP-Kan mex67-mCherry-Nat ura4-D18 leu1-32	This study
RD6309	h- alm1-GFP-Kan mex67-mCherry-Nat ura4-D18 leu1-32	This study
RD6336	h nup211ts-Hph alm1-GFP-Kan mex67-mCherry-Nat ura4-D18 leu1-32	This study
RD6487	h mex67-mCherry-Nat GFP-nab2-Kan ura4-D18 leu1-32	This study
RD6488	h nup211ts-Hph mex67-mCherry-Nat GFP-nab2-Kan ura4-D18 leu1-32	This study
RD7120	h mex67-mCherry-Nat pab2-GFP-Kan ura4-D18 leu1-32	This study
RD7124	h nup211ts-Hph mex67-mCherry-Nat pab2-GFP-Kan ura4-D18 leu1-32	This study

Chapter 3		
Strain Name	**Genotype**	**Source**
RD401	h+ alm1-GFP-kanMX6 ura4-D18 leu1-32 ade6-M216	Lab collection
RD4508	h- nup211-GFP-Kan ura4-D18 leu1-32 ade6-M216	This study
RD5285	h nup60-mCherry-Nat ura4-D18 leu1-32	This study
RD6520	h^{90} lys1+::Pnup61-GFP-nup161 nup61::ura4+ ade6-216 ura4 leu1-32	Hiraoka's Lab
RD6522	h^{90} lys1+::Pnup124-GFP-nup124 ade6-216 ura4 leu1-32	Hiraoka's Lab
RD5551	h nup60-mCherry-nat alm1-GFP-Kan ade6-216 ura4 leu1-32	This study
RD3203	h gar2-mcherry-Kan alm1-GFP-Kan leu1-32 ura4D-18 ade6-M216	This study
RD4202	h nup107-GFP-Kan alm1-Tomato-Nat ura4-D18 leu1-32 ade6-M216	This study

RD6524	h^{90} lys1+::Pnup132-GFP-nup132 nup132:ura4+ ade6-216 ura4 leu-32	Hiraoka's Lab
RD3338	h GFP-nup85-Kan ura4-D18 leu1-32 ade6-M216	Doye's Lab
RD4221	h^{90} nup120::nup120-GFP-HA-Kan ade6-216 leu1-32 lys1-131 ura4-D18	Hiraoka's Lab
RD7486	h- nup96-GFP-Kan ade6-216 ura4 leu-32	This study
RD7484	h- nup37-GFP-Kan ade6-216 ura4 leu-32	This study
RD7488	h- ely5-GFP-Kan ade6-216 ura4 leu-32	This study
RD6519	h^{90} seh1-GFP-HA-KanR ade6-216 ura4 leu-32 lys1-131	Hiraoka's Lab
RD6523	h^{90} lys1+::Pnup131-GFP-nup131 nup131::ura4+ ade6-216 ura4 leu-32	Hiraoka's Lab
RD7884	h GFP-nup85- Kan pab1-mRFP-Hph ura4-D18 leu1-32 ade6-M216	This study
RD6521	h^{90} ade6-216 ura4 leu-32 lys1 nup155+-GFP-KanR	Hiraoka's Lab
RD4218	h^{90} nup40::nup40-GFP-HA-Kan ade6-216 leu1-32 lys1-131 ura4-D18	NBRP, Japan
RD4220	h^{90} SPBC13A2.02::SPBC13A2.02 (nup82)-GFP-HA-Kan ade6-216 leu1-32 lys1-131 ura4-D18	NBRP, Japan
RD4224	h^{90} nup146::nup146-GFP-HA-Kanr ade6-216 leu1-32 lys1-131 ura4-D18	NBRP, Japan
RD334	h- amo1-GFP-Kan	Lab collection
RD4235	h^{90} nup44-GFP-HA-Kan ade6-216 leu1-32 lys1-131 ura4-D18	NBRP, Japan
RD14	h cut11-GFP-ura4+ leu1-32	Lab collection
RD3646	h- tts1-mCherry:ura+ ade6- leu1-32 ura4D18	Lab collection
RD6919	h ish1-GFP-Kan nup211-mCherry-Nat	This study
RD6000	h- mex67-GFP-Kan ura4-D18 leu1-32	This study
RD7033	h- pab2-GFP-Kan ura4-D18 leu1-32	This study
RD6405	h^{+} GFP-nab2-Kan ade6M210 leu1-32 ura418 his3A	NBRP, Japan
RD6020	h mlo3-GFP-Kan ura4-D18 leu1-32	This study
RD6518	h^{90} GFP-rae1-KanR ade6-216 ura4 leu-32 lys1-131	Hiraoka's Lab
RD6066	h gar2-mcherry-Kan mex67-GFP-Kan leu1-32 ura4D-18 ade6-M216	This study
RD6820	h alm1-Tomato-Nat mex67-GFP-Kan ura4-D18 leu1-32	This study
RD6527	h alm1-Tomato-Nat GFP-nab2-Kan ura4-D18 leu1-32	This study
RD7105	h alm1-Tomato pab2-GFP-Kan ura4-D18 leu1-32	This study
RD7587	h cdc5-GFP-Kan ura4-D18 leu1-32	V.A. Tallada
RD6495	h^{90} red1-tdtomato-KanR rrp6-GFP-Kan leu1-32 ura4D-18 ade6-M216	This study
RD6696	h^{90} uap56-GFP-Kan ura4-D18 leu1-32	This study
RD6309	h- alm1-GFP-Kan mex67-mCherry-Nat ura4-D18 leu1-32	This study
RD6541	h^{+} nup60-GBP-13myc-Kan alm1-GFP-Kan mex67-mCherry-Nat ura4-D18 leu1-32	This study
RD6313	h nup211-GFP-Kan mex67-mCherry-Nat ura4-D18 leu1-32	This study
RD6544	h nup60-GBP-13myc-K nup211-GFP-Kan mex67-mCherry-Nat ura4-D18 leu1-32	This study
RD6967	h nuc1-GFP-3HA-Kan nup211-mcherry-Nat	Lab collection
RD6967	h acr1-GFP-leu nup211-mcherry-Nat ura4-D18 leu1-32	Lab collection
RD6224	h alm1-Tomato-Nat reb1-GFP-Kan ura4-D18 leu1-32	This study
RD7588	h hht2-GFP-Ura4+ gar2-mcherry-Kan ura4-D18 leu1-32	Lab collection
RD3150	h top2-GFP-Ura4+ gar2-mCherry-Kan ura4-D18 leu1-32 his-	Lab collection
RD2604	h sid2-Tomato::natMX6 cnd1-GFP: ura4 ura4-D18 leu1-32	Lab collection
RD2921	h ark1-GFP-Kan clp1-Tomato-Nat ura4-D18 leu1-32	Lab collection
RD6394	h plo1-GFP-Kan alm1-Tomato-Nat	Lab collection
RD4131	h- p41nmt:cdc13-GFP-ura sid2-Tomato-natMX6	Lab collection
RD1937	h- ura4-D18 leu1-32	Lab collection
RD7343	h- GFP-hsf1-ura4+ ura4-D18 leu1-32 ade6-M216	Oliferenko's Lab
RD7466	h purg1-hsf1 alm1-Tomato-Nat GFP-Nup85-Kan	This study
RD6	h- ssa1-YFP-Kan ura4-D18 leu1-32 ade6-M216	Lab collection
RD7341	h+ GFP-ssa2-ura4+ ura4-D18 leu1-32 ade6-M216	Oliferenko's Lab
RD7441	h+ hsp104-GFP-ura4+ ura4-D18 leu1-32 ade6-M216	Oliferenko's Lab
RD7443	h+ hsp104-GFP-ura4+ alm1-Tomato-Nat ura4-D18 leu1-32 ade6-M216	This study
RD399	h+ alm1::ura4+ ura4-D18 leu1-32 ade6-M216	Lab collection
RD7435	h alm1::ura4+ GFP-hsf1-ura4+ ura4-D18 leu1-32 ade6-M216	This study
RD7447	h alm1::ura4+ hsp104-GFP-ura4+ ura4-D18 leu1-32 ade6-M216	This study
RD4760	h cut8-563 leu1-32 his2	NBRP, Japan
RD4407	h- *mts1*	Lab collection
RD4409	h- *mts2*	Lab collection
RD4412	h- *mts3*	Lab collection
RD4415	h+ *mts4*	Lab collection
RD7525	h *mts3* hsp104-GFP-ura4+	This study

Plasmids

Table S2. Plasmids used in this study.

Name	Application	Source
pFA6a-GFP(S65t)-kanMX6	Gene C-terminal tagging	J. Bahler
pFA6a:tdTomato-HphMx6	Gene C-terminal tagging	JQ Wu
pFA6a-mCherry-natMx6	Gene C-terminal tagging	JQ Wu
pRA6a-GBP-HphMX6	Gene C-terminal tagging	I. Hagan
pFA6a-kanMX6	Gene deletion	J. Bahler
pFA6a-natMx6	Gene deletion	AC. Carr
pFA6a-hphMx6	Gene deletion	AC. Carr
pFA6a-3HA-kanMX6	Gene C-terminal tagging	J. Bahler
pFA6a–13Myc–kanMX6	Gene C-terminal tagging	J. Bahler
pINTH41EGFPC	Genomic integration and expression	J. Bahler
pREP1-His_6–Ubi	His_6-ubiquitin expression	H. Seino
pGEM®-T	Clonning	Promega

Primers

Oligonucleotides for tagging or deleting genes were designed according to Bahler et al., 1998. All primers were purchased at Sigma Aldrich and stored at a concentration of 100uM at -20ºC.

Antibiotics

- **Ampicillin (Amp):** ß-lactam antibiotic that inhibits bacterial cell-wall synthesis used for selection of plasmid-bearing *E. coli*. Concentration: 10mg/mL. Sigma-Aldrich.
- **Geneticin (G418):** aminoglycoside antibiotic used for yeast strain selection. Concentration: 100 µg/ml. Invitrogen
- **Hygromycin B (Hyg):** aminoglycosidic antibiotic that inhibits protein synthesis, used for yeast strain selection. Concentration: 50 µg/ml. Invitrogen.
- **Nourseothricin (Clon-Nat):** aminoglycosidic antibiotic that inhibits protein biosynthesis by inducing miscoding, used for yeast strain selection. Concentration: 100 µg/ml. Werner BioAgents.

Antibodies

The following antibodies, listed in **Table S3**, have been used at the indicated concentrations for Western blot analysis (WB), immunofluorescence (IF) or protein immunoprecipitation (IP).

Table S3. Antibodies used in this study.

Antibody (organism)	Dilution/application	Supplier/Source
anti-Myc (mouse)	1:2000 / WB	9E10, Santa Cruz Biotechnology
anti-GFP (mouse)	1:2000 / WB-IP	11814460001, Roche
anti-ubiquitin (rabbit)	1:200 / WB-IP	sc-9133 Santa Cruz Biotechnology
anti–α-tubulin TAT1 (mouse)	1:2000 / WB	K. Gull, University of Oxford
anti-PSTAIR (mouse)	1:2000 / WB	P7962, Sigma-Aldrich
anti–mouse IgG (goat)	1:2000/ WB	A3562, Sigma-Aldrich
anti–rabbit IgG (goat)	1:2000/ WB	A0545, Sigma-Aldrich
anti-Myc (mouse)	1:100-200 /IF	9E10, Santa Cruz Biotechnology
anti-mouse Alexa488 (goat)	1:1000/IF	A11029, Invitrogen

Secondary antibodies anti–mouse IgG and anti–rabbit IgG are conjugated with Horseradish Peroxidase (HRP), which allow chemiluminescence detection using SuperSignal West Femto Maximum Sensitivity Substrate (34095, Thermo Fisher) or Clarity Western ECL Substrate (170, 5060, BioRad).

Commercial kits

Table S4. Commercial kits used in this study.

Commercial kits	Application	Supplier
QIAamp DNA Mini Kit	Plasmid DNA extraction	Qiagen
QIAquick Gel Extraction Kit	DNA purification from enzymatic reactions and agarose gels	Qiagen
RNeasy Mini Kit	RNA extraction	Qiagen
SuperScript III First-Strand Synthesis SuperMix	cDNA synthesis from RNA	Life Technologies
TURBO DNA-free™ Kit	Removal of DNA from RNA samples	Applied Biosystems
iTaq™ Universal SYBR® Green One-Step Kit	RT-qPCR.	Bio-Rad
Light Cycler 480 Sybr-Green Master Mix	RT-qPCR	Roche
RC DC protein Assay kit	Protein quantification	Bio-Rad
TGX-Fast Cast acrylamide gels	Polyacrylamide gel electrophoresis for protein separation	Bio-Rad
Trans-Blot Turbo Transfer System	Nitrocelullose membrane transfer in western blot	Bio-Rad
Clarity Western ECL Substrate	Protein detection by western blot	Bio-Rad
Supersignal West Femto	Protein detection by western blot	Thermo Fisher

All commercial kits were used following the manufacturer's instructions.

Chemicals, drugs and inhibitors

- **1 kB plus DNA ladder:** DNA size markers for nucleic acid electrophoresis. 10787018, Invitrogen.
- **5-fluoroorotic acid (FOA):** toxic analog of uracil that in the presence of URA4 gene product is converted to fluorodeoxyuridine, which inhibits cell growth, used for yeast strain selection and silencing asays. Concentration: 1 mg/ml. F9001-5, Zymo Research.
- **Acetone (≥99.9%):** used for removal of TCA after protein extraction and precipitation. 179124, Sigma-Aldrich.
- **Agarose-NTA-Ni^{2+}:** nickel-charged affinity resin used for the purification of histidine-tagged proteins. Proteins bound to the resin may be eluted with either low pH buffer or by competition with imidazole or histidine. P6611, Sigma-Aldrich.
- **Anti-Mouse IgG-coated magnetic beads:** superparamagnetic polystyrene beads (4.5 µm diameter) coated with polyclonal goat anti-mouse IgG antibodies, used for purification of protein-bound mouse IgG primary antibodies. 11201D, ThermoFisher.

- **Bicinchoninic acid (BCA):** reagent that promote copper binding to proteins and reduction, forming a color complex proportional to the concentration of the proteins, used for protein quantification. B9643, Sigma-Aldrich.
- **cOmplete Mini EDTA-free:** cocktail that inhibit a broad spectrum of serine and cysteine proteases, used in protein sample extraction. 11836170001, Roche.
- **Cycloheximide (CHX):** protein synthesis inhibitor. Concentration: 100 µg/ml. 01810, Sigma-Aldrich.
- **DMSO (Dimethyl sulfoxide):** organosulfor compound used as solvent. 276855, Sigma-Aldrich
- **Ethidium bromide (EtBr):** intercalating agent that binds to nucleic acids, used for visualization of DNA and RNA in gel electrophoresis. E1510, Sigma-Aldrich
- **Formamide (≥99.5%):** amide that destibilizes nucleic acids, used in hybridization buffers for RNA and DNA applications, such as FISH. F9037, Sigma-Aldrich.
- **Guanidinium hydrochloride (GH):** reversible and specific inhibitor of Hsp104 activity. Concentration: 3 mM. G3272, Sigma-Aldrich.
- **Herring sperm:** Deoxyribonucleic acid from herring sperm used as blocking agent in FISH protocol. D7290, Sigma-Aldrich.
- **Imidazole:** organic compound used to elute tagged proteins bound to nickel ions attached to the surface of beads in the chromatography column. 56750, Sigma-Aldrich.
- **N-ethylmaleimide (NEM)**: inhibitor of cystein peptidases, used for inhibition of de-ubiquitinating enzymes, used in protein sample extraction. Concentration: 5mM. E3876, Sigma-Aldrich.
- **Paraformaldehyde (pFA):** agent that depolymerize to formaldehyde in solution and cross-link molecules, used for cell fixation. Concentration: 4% (w/v). 158127, Sigma-Aldrich.
- **Phenylmethylsulfonyl fluoride (PMSF):** Inhibitor of serine proteases (chymotrypsin, trypsin, and cysteine), used in protein sample extraction. Concentration: 10mM. P7626, Sigma-Aldrich.
- **Precision Plus Protein™ WesternC™ Blotting Standards:** standard marker ladder used for molecular weight sizing of proteins in western blotting. 1610376, Bio-Rad.
- **Ribonucleoside vanadyl complexes (VRC):** transition state analogs that bind to active sites and inhibits many Rnases, used to protect RNA from degradation in the FISH protocol. R3380, Sigma-Aldrich.
- **RNaseOUT:** recombinant ribonuclease inhibitor that protects mRNA and improves total cDNA yields. 10154652, Invitrogen.
- **Sodium borohydride ($NaBH_4$):** reducing agent used in Paraformaldehyde cell fixation. Concentration: 1%. 213462, Sigma-Aldrich.
- **Thiabendazole (TBZ):** broad-spectrum antihelminthic drug that, along other effects, depolymerize microtubules; used for sensitivity assays. Concentration: 10-15µg/ml. T8904, Sigma-Aldrich.
- **Transfer RNAs (tRNA) from *E. coli*:** act as a competitor to hybridization solutions to prevent nonspecific binding of the probe durning FISH protocol. TRNAMRE-RO Roche, Sigma-Aldrich.
- **Trichloroacetic acid (TCA, ≥99.0%):** denaturing reagent used for protein extraction and precipitatios. T6399, Sigma-Aldrich.

- **Triton™ X-100:** non-ionic surfactant and emulsifier that is often used in biochemical applications, used as detergent to permeabilize cell membranes. T8787, Sigma-Aldrich.
- **Trizol Reagent:** solution of phenol, guanidine isothiocyanate and other components that disrupts cells and dissolves cell components during sample homogenization while facilitate the isolation of RNA. 15596026, Life Technologies.

Enzymes

- **BioTaq**: DNA polymerase used for low fidelity PCRs and mutagenic PCRs. BIO-21040, Bioline.
- **Q5® High-Fidelity DNA Polymerase:** DNA polymerase used for high fidelity PCRs. M0491L, NEB.
- **Restriction Enzymes**: DNA endonucleases used for sequence-specific digestions. NEB.
- **T4 DNA ligase:** for join blunt end and cohesive end termini. 15224090, ThermoFisher.
- **Zymolyase (20T-100T):** lytic enzyme from *Arthrobacter luteus* used for cell wall digestion. Concentration: 1-5mg/ml. ThermoFisher.

All enzymes were used following the manufacturer's instructions.

METHODS

Cell biology methods

E. coli cultivation and transformation

E. coli DH5α strain (dlacZΔM15 Δ(lacZYA-argF) U169 recA1 endA1 hsdR17(rK-mK+) supE44 thi-1 gyrA96 relA1) and stardard procedures were used (Sambrook, 1989; Sambrook, 2001). Cells were cultured in LB medium at 37ºC with the corresponding antibiotic, if required. *E. coli* transformation were performed according to stardard procedures (Inoue et al., 1990). In short, competent DH5α *E. coli* cellls were added an alicuot of the respective plasmid or DNA fragments, incubated for 30 min on ice, heat shocked for 1.5 min at 42ºC, incubated in SOC medium for 1h at 37ºC and plated onto the corresponding selective medium plates.

- **LB medium:** 1% Tryptone (w/v), 0.5% Bacto-yeast extract (w/v), 1% NaCl, pH : 7.0. When required, LB is supplemented with 10mg/mL ampicillin.
- **SOC medium (Super Optimal broth with Catabolite repression):** 2% Bacto-tryptone, 0.5% Bacto-yeast extract, 10mM NaCl, 2.5mM KCl, 20mM glucose, 10mM $MgSO_4$ 10mM final MgCl2, pH7.0.

S. pombe cultivation

Standard media and cell culture protocols were used (Hagan, 2016; Moreno et al., 1991). Unless otherwise stated, cells were cultured in rich media (YES) at 25ºC and grown to exponential mid-log phase, monitoring optical density (O.D. A_{595}). Strains containing plasmids were grown in selective medium. Strains containing a selective marker were plated onto the corresponding selective medium plates. For experiments performed with thermosensitive mutants, cells were cultured at the permissive temperature of 25ºC, and shifted to 36ºC for 2h and/or 4h. For experiments with the *mts4* thermosensitive mutant, cells were grown at the permissive temperature of 25ºC and shifted to 34ºC for 1h, unless otherwise stated. For experiments with the *cut8-563* thermosensitive mutant, cells were grown at the permissive temperature of 25ºC and shifted to 36ºC for 3h. For Cnp3-GFP downregulation experiments, cells expressing Cnp3-GFP under the control of the weak *nmt81* promoter were grown in EMM at 25ºC and then 15µM thiamine (T4625, Sigma-Aldrich) was added to the culture medium. Cells were further grown for 3 generations in the presence of thiamine.

- **YES medium:** 0.5% (w/v) yeast extract, (3.0% w/v) glucose, supplements: 300 mg/L adenine, histidine, leucine, uridine and lysine.
- **EMM medium:** 14.7mM potassium hydrogen phthallate, 15.5 mM Na_2HPO_4, 93.5 mM, NH_4Cl, 2% (w/v) glucose, salts, vitamins, minerals.

- **EMM2 medium:** 14.7mM potassium hydrogen phthallate, 15.5 mM Na_2HPO_4, 93.5 mM, NH_4Cl, 2% (w/v) glucose, salts, vitamins, minerals, supplements: 300 mg/L adenine, histidine, leucine, uridine and lysine. If required, the absence of one aminoacid is specified, *e.g.* MM-Uracile.
- Solid media is made by adding 2% peptone.

S. pombe transformation

Yeast transformation was performed by the Lithium Acetate (LiAc) method as described earlier (Hagan, 2016; Moreno et al., 1991). Mid-log phase cells were harvest, washed once with water and once with LiAc. 100 ul of cells resuspended in LiAc-TE were added 4ul of salmon sperm carrier DNA and 10ul of the DNA/plasmid. After incubation for 10min at RT, cells were added 260 ul of PEG-LiAc-TE, incubated for 30-60 min at 30ºC, added DMSO (dimethyl sulfoxide, Sigma-Aldrich) and heat shocked for 5min at 42ºC. Cells were plated onto non-selective medium, and after 1 day plates were replicated in selective media.

- **TE:** 10mM Tris-Cl**,** 1mM EDTA.
- **LiAc-TE:** 100mM LiAc (Fluka ref. 62393), 10uM Tris-Hcl, 1uM M EDTA, pH 7’5.
- **PEG-LiAc-TE:** 50% PEG 3350 (P4338, Sigma-Aldrich), 100mM LiAc (62393, Sigma-Aldrich), 10uM Tris-Hcl, 1uM M EDTA, pH 7’5

S. pombe genetic cross and tetrad isolation

Mating of strains was performed in sporulation agar (SPA) medium plates, incubated at 25ºC for 2-3 days. Tetrad dissection was performed in YES plates, using a dissection microscope (MSM 400; Singer Instruments).

- **SPA:** 1% (w/v) glucose, 7.3mM KH_2PO_4, supplements (1/5): 45 mg/l adenine, histidine, leucine, uracil and lysine hydrochloride.

Drop assays

For drop assays, strains were grown in YES media at 25ºC to exponential mid-log phase, equalized to an O.D. of 0.2-0.3, serially five-fold diluted, and spotted onto YES plates, unless otherwise stated.

For TBZ sensitivity assay, cells were spotted onto YES plates containing DMSO (Sigma-Aldrich) or YES plates containing 15 μg/ml thiabendazole (TBZ, Sigma-Aldrich), and grown at 25ºC and 30ºC. Pictures were taken after incubation for 3-6 days.

For silencing assays, cultures were grown in non-selective (N/S) media to exponential mid-log phase and diluted to an O.D. of 0.2. An aliquot of each cell suspension and serial 5-fold dilutions were spotted in EMM, EMM-Ura, and EMM+FOA (1 mg/ml) plates. Pictures were taken after incubation at 25ºC and 30ºC, for 3-6 days.

SGA assay

Synthetic genetic array (SGA) assay based on TBZ sensitivity was performed as described previously (Barrales et al., 2016; Dixon et al., 2008; Roguev et al., 2007; Verrier et al., 2015), with minor modifications. Query strains (wildtype and *alm1Δ* mutant bearing the *IRC1L*:*ura4*$^{+}$ reporter) were crossed with single gene deletion mutants (*Bioneer* haploid deletion mutant library, v. 3.0) in SPA plates, using the Singer RoToR HDA (Singer Instruments). Plates were incubated at 42ºC for 3 days to eliminate unmated haploids and diploids. Spores were germinted in YES plates. After haploid selection, two additional steps of double mutants selection were performed, spotting onto EMM-Ura (ForMedium, PMD0410) and YES supplemented with G418 (100 µg/ml. Invitrogen) for selection of deletion mutants, Hygromycin (100 µg/ml, Invitrogen) for selection of marker next to centromere, and ClonNat (100 µg/ml, Werner Bioreagents) for selection of *alm1Δ* mutant. Finally, cells were spotted on YES plates containing TBZ (Sigma-Aldrich) at a final concentration of 10 *µ*g/ml, and YES with DMSO as control. After plate incubation for 3-4 days at 25ºC, pictures were taken and sizes of individual colonies were obtained using the HT-colony-grid-analyzer software. The growth of the single and double mutants was quantified on both control and TBZ-contaiing media, and normalized to the median ratio. *R-Studio* software was used for data processing and analysis, *Cluster v. 3.0* software was used for clustering analysis, *TreeView* software was used for data visualization, to identify and select those genes that showed a negative genetic interaction with *alm1*-deleted mutant, and AmiGO browser was used for Gene Ontology Enrichment analysis to find which GO terms are over-represented based on biological function.

Heat shock experiments

Cells were growth in rich media (YES) at 25ºC to exponential mid-log phase. For fluorescence microscopy experiments, cells were heat shocked at 42ºC for 20 minutes in a water bath, unless otherwise stated. For analyzing the recovery after heat shock, cells were grown at 25ºC, incubated for 20 minutes at 42ºC and shifted back to 25ºC. To assay acquired thermotolerance, prior to heat shock, cells were incubated for 45 minutes at 37ºC, and then subjected to heat shock treatment (42ºC 20 min). For cell survival and viability experiments, cell were grown at 25ºC and heat shocked during 10 minutes at 47ºC, unless otherwise stated. For *in vivo* fluorescence microscopy experiments to observe NuRs formation, cells were grown at 25ºC to exponential mid-log phase, and filmed in the microscope using 42ºC preheated chamber and objective. For the experiments in wich the expression of *hsf1*$^{+}$ is repressed, we used a strain containing the uracile-regulatable Purg1 promoter upstream the *hsf1*$^{+}$ gene (Vjestica et al., 2013; Watt et al., 2008). For that, cells were grown at 25ºC in rich media (YES), washed and shifted to minimal media without uracile for 36 hours before peforming the experiment. For the experiments in wich the activity of Hsp104 is inhibited, we used Guanidinium hydrochloride (GH, Sigma-Aldrich) at a final concentration of 3 mM (Grimminger et al., 2004; Jung et al., 2002). For that cells were grown in rich media at 25ºC and either incubated at 42ºC for 20 minutes without GH,

adding GH 10 minutes before the HS, adding the GH 20 minutes after the HS, or incubated for 20 minutes with the GH (added 20 minutes after the HS) and washed out.

In vivo fluorescence microscopy

Preparation of cell cultures for microscopy was performed as follows: mid-log phase cultures were collected by centrifugation (2500 rpm), resuspended in the same growth liquid medium and placed in microscope slides or µ-Slide 8-well dishes (80827; Ibidi), previously coated with soybean lectin (L1395; Sigma-Aldrich). Conditioned media was used to maintain cells during filming.

Live-cell imaging was performed with a spinning-disk confocal microscope (IX-81; Olympus; Evolve camera, Plan Apochromat 100Å~, 1.4 NA objective; Roper Scientific). Images were acquired with Metamorph software (Molecular Devices) and analyzed with ImageJ (National Institutes of Health). Unless otherwise stated, images were obtained in z-stacks of 18 slices 0.3 µm intervals.

Cell fixation and immunoblotting

Immunofluorescence microscopy was essentially performed as described previously (Hagan and Hyams, 1988; Hagan, 2016), using paraformaldehyde for cell fixation. In short, mid-log phase cultures were added 0.125 volumes of 30% w/v of paraformaldehyde and 0.2% v/v of glutaraldehyde, and were incubated 60 minutes shaking. Cells were recovered by centrifugation, whased three times with PEM buffer and cell wall was digested with PEMS buffer + 0.5mg/ml zymolyase 100T (ThermoFisher) 70 min at 37ºC. Cell membranes were permeabilized with PEMS + 1% Triton X-100, washed three times with PEM buffer, and incubated with PEM with sodium borohydride for quenching. Then, cell pellet were washed twice with PEM and resuspended in PEMBAL buffer before antibody incubation. Primary antibody was mouse anti-Myc (Santa Cruz Biotechnology), used at a dilution of 1:100 for mts2-8Myc, and 1:200 for mts4-13Myc. Secondary antibody was goat Alexa488-tagged anti-mouse (Invitrogen), used at a dilution of 1:1000. For DAPI staining, cells were fixed with 70% cold ethanol, washed with PBS, resuspended in PBS + 0.2µg/ml DAPI (4′,6-diamidino-2-phenylindole, Sigma-Aldrich), and added mounting media.

- **PEM buffer:** 100 mM PIPES [piperazine-N,N-bis(2-ethanesulfonic acid)], 1 mM EGTA, 1 mM $MgSO_4$.
- **PEMS buffer:** PEM buffer, 1.2M sorbitol.
- **PEMBAL buffer:** PEM buffer, 1% BSA (bovine serum albumin), 100 mM lysine hydrochloride, 0,1% NaN_3.
- **PBS buffer:** 137 mM NaCl**,** 2.7 mM Kcl, 8 mM Na_2HPO_4**,** 2 mM KH_2PO_4.
- **Mounting media:** 38 ul glycerol 50%, 10 ul antifade (p-Phenylenediamine, 10mg/mL), 52ul H_2O.

Fluorescence *in situ* hybridization (FISH)

Cells were grown in YES media at 25°C and shifted for 2 hours to 36ºC for thermosensitive mutant inactivation, before fixation with paraformaldehyde. Fluorescence in situ hybridization of poly(A)-RNA was performed with Cy3-labeled oligo-dT(50) probe (provided by A. Aguilera, CABIMER), following an adaptation of a method previously described (Croft et al., 1999), as well as the hybridization method (Trcek et al., 2012). In short, mid-log phase cultures were incubated 5 min at 30ºC with 1 volume of YES 2.4 sorbitol. Cells were fixed with paraformaldehyde, incubating 30 min at 30ºC in shaking. Cell pellets were washed with PEMS buffer and incubated in PEMS with 1mg/ml zymolyase 100T (ThermoFisher) 90 min at 37ºC shaking. After centrifugation, cells were incubated in PEMS with 1% Triton X-100 for 5 min, washed twice with PEM buffer, and incubated with PEM with sodium borohydride. After 5 min incubation, cells were resuspended in PEMBAL buffer. Then, cells were washed once with 0.1M NaOH, once with ice-cold buffer B and PBS. Cell suspension was added to slices coated with poly-L-lysine (P8920, Sigma-Aldrich), incubated 30 min at 4ºC and washed with buffer B. Slices were incubated overnight with 70% ethanol. After overnight incubation, slices were washed twice with SSC buffer and incubated in hybridization solution for 15 min. Cells attached to the slice were incubated 3 hours with 20ul of hybridization mix. Slice were washed twice with hybridization solution, once with 2X SSC with 0.1% Triton X-100, twice with 1X SSC and once with PBS before DAPI staining and observation. FISH experiments were performed in colaboration with P. Real-Calderón.

- **PEM buffer:** 100 mM PIPES [piperazine-N,N-bis(2-ethanesulfonic acid)], 1 mM EGTA, 1 mM $MgSO_4$.
- **PEMS buffer:** PEM buffer, 1.2M sorbitol.
- **PEMBAL buffer:** PEM buffer, 1% BSA (bovine serum albumin), 100 mM lysine hydrochloride, 0,1% NaN_3.
- **B buffer:** 1.2 M sorbitol, 100 mM potassium phosphate buffer (K_2HPO_4 and KH2PO4, pH 7.5).
- **PBS buffer:** 137 mM NaCl**,** 2.7 mM Kcl, 8 mM Na_2HPO_4**,** 2 mM KH_2PO_4.
- **SSC (Saline-sodium citrate, 20X) buffer:** 3M NaCl, 300 mM NaCit (trisodium citrate), pH 7.0.
- **Hybridization solution**: 2X SSC, 10% formamide (Sigma-Aldrich).
- **Hybridization mix**: 2X SSC buffer, 10% formamide, 2.5mg/ml BSA (UltraPure™ BSA (50 mg/mL), AM2616, ThermoFisher), 10mM VRC (Ribonucleoside vanadyl complexes, Sigma-Aldrich), containing 100 ng Cy3-labeled oligo-dT(50) probes, 100ug herring sperm DNA (Sigma-Aldrich) and 100 ug *E. coli* tRNA (TRNAMRE-RO Roche, Sigma-Aldrich).
- **Mounting media:** 38 ul glycerol 50%, 10 ul antifade, 52ul H_2O.

Molecular biology methods

Plasmid DNA isolation from *E. coli*

Unless otherwise stated, standard *E. coli* genome engineering methods were used as described (Sambrook, 1989). Plasmid DNA extraction from *E. coli* was performed using the Qiagen commercial kit (51304).

Genomic DNA isolation from *S. pombe*

Unless otherwise stated, standard fission yeast genome engineering methods were used as described (Hagan, 2016; Moreno et al., 1991). Briefly, 10 ml of exponentially growing cells were collected, washed with H_2O, resuspended in lysis buffer, and lysed with acid-washed glass beads (G9268, Sigma-Aldrich), using a FastPrep (MP Biomedicals). After centrifugation, supernatant was transferred to a fresh microcentrifuge tube and the DNA was extracted by isopropanol and 70% ethanol precipitation.

- **Lysis Buffer:** 10 mM Tris (pH 8.0)**,** 2% Triton X-100**,** 1% SDS, 100 mM NaCl, 1 mM EDTA (pH 8.0).

Polymerase Chain Reaction (PCR)

Amplification of DNA fragments by PCR was performed using the corresponding primers, templates and polymerases, BioTaq (BIO-21040) or Q5® High-Fidelity DNA Polymerase (M0491S), following manufacturer's intructions, or Q5 polymerase provided by the CABD Proteomic service. Annealling temperature and time of extension were adjusted depending on the primers and the product size. DNA concentration was estimated with the NanoDrop spectrophotometer, which measures absorbance at 260nm.

Gene deletion and protein tagging

Strains expressing GFP, mCherry, tdTomato, 3HA, 13-Myc, and GBP -tagged proteins and deletion strains were constructed using PCR-based methods and homologous recombination as described previously, using *ura4*$^+$, *kanMX6* (kanR), *hphMX6* (hygR), and *natMX6* (natR) genes as selection markers (Bahler et al., 1998; Fennessy et al., 2014; Sato et al., 2005; Shaner et al., 2004).

Cloning using restriction enzymes: digestion and ligation

For DNA cloning, DNA purification, digestion with restriction enzymes and ligation standard methods were used, following manufacturer's instructions.

Agarose gel electrophoresis

Agaroses gel electrophoresis was used to analyze PCR products or purify DNA fragments. Electrophoresis was performed in agarose (A1015.250, Biomol) gels, prepared at a concentration of 1% (w/v) in 1XTBE using ethidium bromide to stain the DNA, and run in 1XTBE at 120V, using a 1 kB plus DNA ladder (Invitrogen) as DNA size markers. DNA was visualized using UV-light.

- **TBE:** 100 mM Tris base, 100 mM Boric acid, 2uM EDTA.
- **6X DNA loading dye:** 30% (v/v) glycerol, 0.25% (w/v) bromophenol blue.

Random mutagenesis

For *nup211* mutagenesis, *nup211* was tagged at the C-terminus using the pFA6a-GFP(S65t)-kanMX6 plasmid and the nup211_Ctag_FW and nup211_Ctag_RV primers (**Table S5**). To obtain the nup211-GFP-Kan DNA fragment, genomic DNA extraction from the RD4508 strain and Q5® High-Fidelity DNA Polymerase (M0491) PCR protocol were performed, using the Nup211_FW and Nup211_RV primers. The reactions were prepared in 50 µl total volume with 10 µl of 5X Q5 Reaction Buffer, 1 µl of dNTP mix 40 µM, 10 pmol of each primer and 1 U of Q5 High-Fidelity DNA Polymerase. PCR products were cloned in pGEM®-T vector according to pGEM®-T and pGEM®-T Easy Vector Systems protocol (A-tailing, Ligation & Transformation, A1360, Promega). *E. coli* DH5α strain positive colonies from the transformation were selected and plasmid DNA was subjected to digestion using *Eco*RI, *Hin*dIII and *Nde*I to check positive clones. nup211-GFP-Kan DNA fragments cloned in the pGEMT plasmid were subjected to Taq PCR-based mutagenesis following the BioTaq protocol by Bioline and the Biotaq protocol modified with reduced dATP concentration, respectively. The reactions were prepared up to 50 µl of total volume as follows:

Standard PCR reaction conditions		Mutagenic PCR reaction conditions	
10X NH_4 Reaction Buffer	5 µl	10X NH_4 Reaction Buffer	5 µl
50 mM $MgCl_2$	2 µl	50 mM $MgCl_2$	2 µl
Primers	10 pmol each	Primers	10 pmol each
2.5 U of BioTaq	1 µl	2.5 U of BioTaq	1 µl
40 µM dNTP mix	0.5 µl	40 µM dNTP mix	0.25 µl of each dNTP except for dATP
ddH_2O	Up to 50 ul	ddH_2O	Up to 50 ul

The samples were subjected to heating at 94°C for 5 min followed by 35 PCR cycles (15 s at 94ºC, 30 s at 64ºC, 5 min at 72ºC) and finished at 72°C for 10 min.

Mutagenized PCR products were transformed in a *wt* strain (RD1936). Selected candidates were those that grew at 25ºC but not at 36ºC. From the transformation, 19 candidates were selected: 3 with a penetrating phenotype (*nup211 1.3, nup211 8.2, nup211 17.1*) and 15 with a less penetrating phenotype. Experiments were performed with the mutant *nup211 1.3-GFP*, remaned *nup211ts-GFP*.

For alm1 mutagenesis, the same protocol as explained before was performed, using alm1-Tomato-Nat strain (RD3637) as template and the primers listed in **Table S5.** Transformation of the mutagenized

alm1-Tomato-Nat DNA fragments was performed in a strain lacking nup132 (RD4217). We selected one candidate that grew at 25ºC, but not a 36ºC in this genetic background, named *alm1ts-Tomato.* GFP and Tomato tags from *nup211ts* and *alm1ts* were removed using nup211FW-untag/nup211RV-untag and alm1FW-untag/ alm1RV-untag primers, respectively. Sequencing of mutant clones was performed by Sequgen service, following standard instructions, using the primers listed in **Table S6**. Generation of thermosensitive mutants by random mutagenesis was performed by P. Real-Calderón and I. Flor-Parra.

Table S5. List of primers for *nup211* and *alm1* tagging, amplification and mutagenesis.

Name	Sequence	Source
Nup211_Ctag_FW	CTGCTAAATCCGGCTCCCTTAAAAGACAACGTGACGATG CGAACAAAGGAGGATCCAGTTCGAACCAAAAGAAAGCAA AACGGATCCCCGGGTTAATTAA	This study
Nup211_Ctag_RV	TTTACTCATGTCATTATTATAAATCATGTTAACTAAATATGA ATAGTCCTAAGAGTGATTTATGAACCATATGAAAACATGA ATTCGAGCTCGTTTAAAC	This study
Nup211_FW	GTATCAACTACCTCGTCGCTACACACC	This study
Nup211_RV	TGCAAAATCAAGAAATAGCAAAAACC	This study
nup211FW-untag	ACAAGTATGTAGTTTACCTAGTGAACG170	This study
nup211RV-untag	TCACTCACTTCCGACCTTATTTGTTCC170	This study
Alm1-GFP.a(Ctag-FW)	AATTAAAGTCGTTTTTTTTATTGGAAACCAGAAATAATAAT TATGCAGCTAACCTATTTTATTATCTGTTTACAAACTCTGA ATTCGAGCTCGTTTAAAC	(Salas-Pino et al., 2017)
Alm1-GFP.a (Ctag-RV)	ACACTAATTCTCCTCCTAAACGGTCCAGTTCAGACGCTGG TATGGATGTTTCCAATGATGTTAAGAAAGCCAAACCCGGA CGGATCCCCGGGTTAATTAA	(Salas-Pino et al., 2017)
Alm1_FW	GACGTTCCAGTATTTGCATTGTTGTTGG170	This study
Alm1_RV	TACACTACGCTATGATACACTACGTTGC170	This study
alm1FW-untag	TATTTTGATATTTTTTGAAGAGCTATAGATATTTTGCGCAA CTAATGTCCTTATTCAGATATGTAAGCTACGCAGTTTGGC GGATCCCCGGGTTAATTAA	This study
alm1RV-untag	CTATATTAGTGATAGGTAACATTATAACCCAGTTAATACAA TACCTATACTCAGTTGCTACTTATACAACCTGTGTATTGGA ATTCGAGCTCGTTTAAAC	This study

Table S6. List of primers for sequencing *nup211* and *alm1*.

	Primer Name	Sequence	Source
Nup211 Sequencing	TS_0	GTATCAACTACCTCGTCGCTACACACC	This study
	TS_1	GATCTAAAGGATGCCCTTGC	
	TS_2	TGAGGATTGCTCTTTACGGC	
	TS_3	TTGGAAGACTGTCAGAAAGC	
	TS_4	CGCCTGCAACTCCTAATTCC	
	TS_5	CCTGCAGCAGGATAATTTCC	
	TS_6	GATGAATGAAACCCATGAGC	
	TS_7	GGAATATTCAGCGGAAAGCC	
	TS_8	CTTAAGGCAGAAATAGGCGC	
	TS_9	TGCTGAACAGATCACGAAGG	

	TS_10	GCAGCAGGTTGAAGAAAAGC	
	TS_11	GGCTCCCTTAAAAGACAACG	
	TS_12	CAACATTGAAGATGGAAGCG	
Alm1 Sequencing	alm1.sec1.sense	AAGGAAGAGATACTCGTTCAGGAG	(Salas-Pino et al., 2017)
	alm1.sec2.sense	CTCCAACAGAAGGTTTCTAGC	
	alm1.sec3.sense	TGTTAGCTACTTCTCGAAGCAG	
	alm1.sec4.sense	GGAATTGAGTACTCCAGCAGG	
	alm1.sec5.sense	GATAGCGAAACAAGAGTTGC	
	alm1.sec6.sense	AGCAGTACTTCTGAATCCGTTG	
	alm1.sec7.sense	CTCAACAAACCTTCTGCAACC	
	alm1.sec8.sense	AACTTAGCTAGAGTGCGAGCAG	

RNA extraction from *S. pombe* and quantitative RT-PCR

For the measurement of coding-genes transcriptional levels, cells were grown in liquid YES medium at 25ºC to exponential mid-log phase and total RNA was obtained by using RNeasy spin column (RNeasy Mini Kit, Qiagen) following the manufacturer instructions. Transcriptional levels of act1, cnp1, cnp20, and cnp3 were measured by RT-qPCR using iTaq™ Universal SYBR® Green One-Step Kit as indicated (Bio-Rad) in 10 µl of final volume with 5µl of iTaq™ Universal SYBR® Green Reaction Mix, 0.125µl of iScript reverse transcriptase, a mixture of forward and reverse primers (final concentration of 300nM each) and 500 ng of RNA. Transcript levels of *cnp1*, *cnp20*, and *cnp3* were obtained from three independent experiments, and normalized to the internal reference gene *act1*. The primers used for qPCR are listed in **Table S7**. Primers used in RT-qPCRs were designed with a Tm close to 60 °C and an amplicon size between 100-180 bp, according to the recommendations given by Light Cycler 480 Real-Time PCR System.

Table S7. List of primers for RT-qPCR.

Locus	Primer name	Primer	Source
cnp1	cnp1 Forward	GTTTGCGCTGGCAATCTACG	This study
	cnp1 Reverse	CCTGGCTAATTGCATGTCTCG	
cnp3	cnp3 Forward	CGTTGAAATGCCAGCAGGAG	This study
	cnp3 Reverse	ACTGTGACCTCGATCTTTCCC	
cnp20	cnp2 Forward	CCAGCCGATCCAATTCAGGA	This study
	cnp20 Reverse	TGGGGAATTGACAGCTTCGT	
act1	act1 Forward	AAGTACCCCATTGAGCACGG	This study
	act1 Reverse	CAGTCAACAAGCAAGGGTGC	

For the RT-qPCR of the transcriptional levels of heterochromatin domains, total RNA was isolated from cells grown to exponential mid-log phase in YES at 25ºC or 30ºC using a Trizol Reagent (Life Technologies) and 0.55 mm zirconia/silica beads. After removing DNA contamination from the total RNA with TURBO DNA-free™ (Applied Biosystems), samples were subjected to RT-PCR using the SuperScript III First-Strand Synthesis SuperMix (Life Technologies) for cDNA synthesis and treated with Rnase (RNaseOUT, Invitrogen). Quantitative PCR reactions were carried out in 15 µl of volume, with 7.5 µl Light Cycler 480 Sybr-Green Master Mix (Roche), 2.5µl of a mixture of forward and reverse primers (1.5µM) and 5µl of cDNA, previously diluted. Transcript levels of were obtained from five

independent experiments, and normalized to the internal reference gene *act1*. The primers used for qPCR are listed in **Table S8**.

Table S8. List of primers for RT-qPCR.

Locus	Primer name	Primer	Source
act1$^+$	act1-4 FOR	GATTCTCATGGAGCGTGGTT	(Braun et al., 2011)
	act1-4 REV	CGCTCGTTTCCGATAGTGAT	
cen-dh	cen-dh FOR	TGAATCGTGTCACTCAACCC	(Buhler et al., 2007)
	cen-dh REV	TGAATCGTGTCATTCAACCC	
cen-dg	cen-dg-1 FOR	TGCTCTGACTTGGCTTGTCTT	(Braun et al., 2011)
	cen-dg-1 REV	CCCTAACTTGGAAAGGCACA	
cnt1	SG1953 FOR	TCGCCGGTAACAAAAGGATCA	(Braun et al., 2011)
	SG1954 REV	GCATTAGACAACTCGTTCGATC	
imr	imr_(MR35) FOR	GAGCATGGTGGTGGTTATGGA	(Braun et al., 2011)
	imr_(MR36) REV	CGACTAAACCGAAAGCCTCGA	
tlh1+/ tlh2+	tlh1- mb274 FOR	ATGGTCGTCGCTTCAGAAATTGC	(Buhler et al., 2007)
	tlh1- mb276 REV	CTCCTTGGAAGAATTGCAAGCCTC	
TERRA	Sg1038/1039	GAAGTTCACTCAGTCATAATTAATTGGAAC	(Bah et al., 2012)2
	Sg1039 REV	GGGCCCAATAGTGGGGGCATTGTAT TTGTG	

Biochemical methods

Protein extraction from *S. pombe* lysates

Protein extracts for western blotting were prepared by using either the trichloroacetic acid (TCA) precipitation protocol or the RIPA protocol. For TCA extraction, 45 ml of mig-log phase asynchronous cultures were quenched by the addition of 5 ml of ice-cold ≥99.0% TCA (Sigma-Aldrich). After 30minutes incubation on ice, cells were pelleted by centrifugation and washed with 10 ml of ice-cold ≥99.9% acetone (Sigma-Aldrich). After removing acetone, cell pellets were washed with beating buffer with protease inhibitors (cOmplete Mini EDTA-free, Roche) and lysed with acid-washed glass beads (G9268, Sigma-Aldrich), using a FastPrep (MP Biomedicals). Cell extracts were cleared by centrifugation. For RIPA extraction, 50-100 ml of mig-log phase asynchronous cultures were collected and washed with STOP buffer. Cells were pelleted by centrifugation, washed with RIPA buffer with protease inhibitors (cOmplete Mini EDTA-free, Roche), and lysed with acid-washed glass beads (G9268, Sigma-Aldrich), using a FastPrep (MP Biomedicals). Cell extracts were cleared by 15 min 13000 rpm centrifugation.

- **Beating Buffer:** 8 M urea**,** 50 mM ammonium bicarbonate**,** 5 mM EDTA.
- **STOP Buffer:** 10 mM EDTA**,** 150 mM NaCl**,** 50 mM NaF**,** 1 mM NaN_3, pH 8.0.
- **RIPA:** 50 mM Tris-Hcl (pH7.5), 1% SDS, 150mM NaCl, 0.5% sodium deoxycholate, 1% NP-40, 1mM EDTA.

Western Blot analysis

Protein concentracion was measured using RC DC protein Assay kit (Bio-Rad) or 4% (w/v) cooper sulfate-BCA (bicinchoninic acid, Sigma-Aldrich) assay. Protein samples were adjusted to the same total protein concentration, resuspended in 5 µl of 5X sample buffer and boiled. Protein samples were loaded on 7,5/10% TGX-Fast Cast acrylamide gels (161-0183; Bio-Rad) and blotted on nitrocellulose membranes (Trans-Blot Turbo Transfer System, Bio-Rad). Membranes were blocked with PBS + 0.1% Triton + 5% (w/v) milk. Unless otherwise stated, blots were probed o/n with the corresponding primary antibody, followed by the appropriate secondary antibody, as indicated in **Table S3**. As loading control we used mouse anti–α-tubulin mAb (TAT1; K. Gull, University of Oxford, Oxford, England, UK), anti-PSTAIR mAb (Sigma-Aldrich), or stain free stainning. Antibody dilutions were prepared in PBS + 0.1% Triton + 5% (w/v) milk. Precision Plus Protein™ WesternC™ Blotting Standards (Bio-Rad) was used as marker ladder for molecular weight sizing of proteins in western blotting. Protein detection was performed using ECL (170-5060, Bio-Rad) or Supersignal West Femto (34095, Thermo Fisher) and Chemidoc XRS+ (Bio-Rad).

- **5X sample loading buffer:** 3.3mM Tris-HCl (pH 6.8), 50% glycerol**,** 10% SDS, 0.05% blue bromophenol, 5% beta-mercaptoethanol.
- **PBS buffer:** 137 mM NaCl**,** 2.7 mM Kcl, 8 mM Na_2HPO_4**,** 2 mM KH_2PO_4.

Measurement of protein stability

For the analysis of Cnp3 half-life, wildtype and *alm1Δ* cells were grown in YES at 25ªC to mid-log phase, and then 100 µg/ml Cycloheximide (CHX, Sigma-Aldrich) was added to the cultures. Cells were harvested at the indicated time points, and whole cell extracts were prepared for immunoblotting using mouse anti-GFP mAb (11814460001; Roche) to detect Cnp3-GFP, and mouse anti-PSTAIR mAb (P7962; Sigma-Aldrich) as a loading control. ImageJ software (version 1.5; National Institutes of Health) was used to quantify Cnp3-GFP protein levels. Experiments to measure protein stability were performed by S. Salas-Pino.

Protein immunoprecipitation

For immunoprecipitation of Cnp3 protein, *mts4* mutant cells expressing cnp3-GFP were grown in YES to mid-log phase at 25ºC and then shifted to 36 ºC for 3 hours. 45 min before harvesting 5mM of N-ethylmaleimide (NEM, Sigma-Aldrich) was added to the culture media to inhibit de-ubiquitinating enzymes. Cells were harvested by centrifugation and the pellets were washed with ice-cold STOP buffer and snap-frozen in liquid nitrogen. Native extracts were prepared in Phosphate-Buffer-Saline with protease inhibitor cocktail (cOmplete Mini EDTA-free, Roche) and PMSF (phenylmethylsulfonyl fluoride, 10mM). Anti-mouse IgG-coated magnetic beads (Dynabeads, Thermofisher) were incubated with 1 µg of mouse anti-GFP mAb, following by incubation with 6 mg of total protein extracts for 1 hour at 4 ºC. Beads were washed three times with PBS with protease inhibitors, resuspended in 50 µl of

SDS-PAGE sample loading buffer and boiled for 5 minutes. Samples were clarified by centrifugation at 13000 rpm for 10 minutes. 20 µ pf protein samples were loaded on 7,5/10% TGX-Fast Cast acrylamide gels (Bio-Rad) and blotted on nitrocellulose membranes (Bio-Rad), using mouse anti-GFP mAb (Roche) to detect Cnp3-GFP and rabbit anti-ubiquitin mAb (sc-9133; Santa Cruz; provided by J.A. Sanchez Alcazar, CABD/UPO) to detect ubiquitinated proteins. The secondary antibody were anti–mouse IgG (Sigma-Aldrich) and anti–rabbit IgG (Sigma-Aldrich) at a 1:2.000 dilution. Protein immunoprecipitation experiments were performed by S. Salas-Pino

- **Phosphate-Buffered-Saline:** 20 mM Tris-HCl**:** 150 mM NaCl**,** 5 mM MgCl2**,** 0.2% Triton X-100**,** 10% Glycerol.
- **SDS-PAGE sample loading buffer**: 0.25M Tris-HCL (pH 6.8), 8% (w/v) SDS, 0.004% (w/v) bromphenol blue, 20% (v/v) 2-mercaptoethanol.

Ubiquitin pull down assay

Polyubiquitination analysis was performed as previously described (Shiozaki et al., 1997). Cells expressing the endogenous *cnp3* tagged with GFP and overexpressing *cnp3-GFP* from the medium-strength *nmt41* promoter in a single copy (pINT-Cnp3-GFP) were transformed with the pREP1-His_6–Ubi plasmid (provided by Dr. H. Seino). Cells were grown in EMM at 25ºC in the absence of thiamine for 22 hours and then shifted to 36ºC for 3 hours. 45 min before harvesting 5mM of N-ethylmaleimide (NEM, Sigma-Aldrich) was added to the culture media to inhibit de-ubiquitinating enzymes. Cells were harvested by centrifugation, washed once with ice-cold STOP buffer, and whole cell extract were prepared in Buffer G. 6mg of total protein extract (input) was incubated for 1 hour with agarose-NTA-Ni^{2+} (Sigma-Aldrich) at room temperature. The beads were then washed three times with Buffer U and once with Buffer U with 10mM Imidazole (Sigma Aldrich). 50ul of SDS-PAGE sample loading buffer was added to the beads and incubated 5 min at 100ºC. Protein samples were loaded on 7,5/10% TGX-Fast Cast acrylamide gels (Bio-Rad) and blotted on nitrocellulose membranes (Bio-Rad). 20 ul of samples were immunoblotted with anti-GFP antibody (Roche) and rabbit anti-Ubiquitin mAb (Santa Cruz). Inputs with the same amount of total protein were immunoblotted with mouse anti-GFP mAb (Roche) to detect Cnp3-GFP and mouse anti–α-tubulin mAb (TAT1; K. Gull, University of Oxford, Oxford, England, UK) as loading control. The secondary antibody were anti–mouse IgG (Sigma-Aldrich) and anti–rabbit IgG (Sigma-Aldrich) at a 1:2.000 dilution. Ubiquitin pull down assays were performed by S. Salas-Pino

- **STOP Buffer:** 10 mM EDTA**,** 150 mM NaCl**,** 50 mM NaF**,** 1 mM NaN_3, pH 8.0.
- **Buffer G**: 50 mM Tris-HCl, 6M guanidine HCl, 0.1 M sodium phosphate, pH8.0.
- **Buffer U**: 50mM Tris-HCl, 8M urea, 0.1M sodium phosphate, pH8.0.
- **SDS-PAGE sample loading buffer**: 0.25M Tris-HCL (pH 6.8), 8% (w/v) SDS, 0.004% (w/v) bromphenol blue, 20% (v/v) 2-mercaptoethanol.

Statistical and data analysis

Fluorescence microscopy quantification

Quantification of fluorescence signal at the nuclear periphery was performed on maximal projections of 3 z-sections (step size 0,3 μm). Quantification of fluorescence signal at the nuclear interior was performed over the whole nuclear area, substracting the cytoplasmic background, in maximal projections of 18 z-sections (step size 0,3 μm). Quantification of RNA fluorescence signal was performed on maximal projections of 18 z-sections (step size 0,3 μm). Quantification of nuclear GFP-Hsf1 was performed on the whole nuclear area, relative to the cytoplasmic signal, on maximal projections of 18 z-sections (step size 0,3 μm). Quantification of chaperones levels was performed on the whole cell area, on maximal projections of 18 z-sections (step size 0,3 μm). Quantification of nucleolar size was performed using Gar2 as nucleolar marker, measuring the nucleolar area relative to cell length, on maximal projections of 18 z-sections (step size 0,3 μm). In every case, background signal intensity in every region of interest was substracted.

Statistical analysis

Graphs and statistical analyses were performed using Excel (Microsoft) and with Prism 5.0 (GraphPad) softwares. Unless otherwise stated, graphs represent the mean, and error bars represent Standard Deviation (SD). n is the total number of cells analyzed from at least three independent experiments. Statistical comparisons between two groups were performed by Chi-square or unpaired Student's t test, considering two-tailed p-values exceeding 0.05 to be non-significant (ns). Pvalues are represented as follows: $P < 0.05$ (*), $P < 0.001$ (**), $P < 0.001$ (***). Data distribution was assumed to be normal, but this was not formally tested.

BIBLIOGRAPHY

Abruzzi, K.C., Belostotsky, D.A., Chekanova, J.A., Dower, K., and Rosbash, M. (2006). 3'-end formation signals modulate the association of genes with the nuclear periphery as well as mRNP dot formation. EMBO J *25*, 4253-4262.

Abruzzi, K.C., Lacadie, S., and Rosbash, M. (2004). Biochemical analysis of TREX complex recruitment to intronless and intron-containing yeast genes. EMBO J *23*, 2620-2631.

Ahmed, S., and Brickner, J.H. (2010). A role for DNA sequence in controlling the spatial organization of the genome. Nucleus *1*, 402-406.

Aibara, S., Gordon, J.M., Riesterer, A.S., McLaughlin, S.H., and Stewart, M. (2017). Structural basis for the dimerization of Nab2 generated by RNA binding provides insight into its contribution to both poly(A) tail length determination and transcript compaction in Saccharomyces cerevisiae. Nucleic Acids Res *45*, 1529-1538.

Aiken, C.T., Kaake, R.M., Wang, X., and Huang, L. (2011). Oxidative stress-mediated regulation of proteasome complexes. Mol Cell Proteomics *10*, R110 006924.

Akerfelt, M., Morimoto, R.I., and Sistonen, L. (2010). Heat shock factors: integrators of cell stress, development and lifespan. Nat Rev Mol Cell Biol *11*, 545-555.

Akhtar, A., and Gasser, S.M. (2007). The nuclear envelope and transcriptional control. Nature reviews Genetics *8*, 507-517.

Alber, F., Dokudovskaya, S., Veenhoff, L.M., Zhang, W., Kipper, J., Devos, D., Suprapto, A., Karni-Schmidt, O., Williams, R., Chait, B.T.*, et al.* (2007). The molecular architecture of the nuclear pore complex. Nature *450*, 695-701.

Albert, S., Schaffer, M., Beck, F., Mosalaganti, S., Asano, S., Thomas, H.F., Plitzko, J.M., Beck, M., Baumeister, W., and Engel, B.D. (2017). Proteasomes tether to two distinct sites at the nuclear pore complex. Proc Natl Acad Sci U S A *114*, 13726-13731.

Alcazar-Roman, A.R., Tran, E.J., Guo, S., and Wente, S.R. (2006). Inositol hexakisphosphate and Gle1 activate the DEAD-box protein Dbp5 for nuclear mRNA export. Nat Cell Biol *8*, 711-716.

Alfredsson-Timmins, J., Henningson, F., and Bjerling, P. (2007). The Clr4 methyltransferase determines the subnuclear localization of the mating-type region in fission yeast. J Cell Sci *120*, 1935-1943.

Allard, S., Utley, R.T., Savard, J., Clarke, A., Grant, P., Brandl, C.J., Pillus, L., Workman, J.L., and Cote, J. (1999). NuA4, an essential transcription adaptor/histone H4 acetyltransferase complex containing Esa1p and the ATM-related cofactor Tra1p. EMBO J *18*, 5108-5119.

Allen, N.P., Huang, L., Burlingame, A., and Rexach, M. (2001). Proteomic analysis of nucleoporin interacting proteins. J Biol Chem *276*, 29268-29274.

Allshire, R.C., and Ekwall, K. (2015). Epigenetic Regulation of Chromatin States in Schizosaccharomyces pombe. Cold Spring Harb Perspect Biol *7*, a018770.

Allshire, R.C., Nimmo, E.R., Ekwall, K., Javerzat, J.P., and Cranston, G. (1995). Mutations derepressing silent centromeric domains in fission yeast disrupt chromosome segregation. Genes Dev *9*, 218-233.

Altaf, M., Auger, A., Monnet-Saksouk, J., Brodeur, J., Piquet, S., Cramet, M., Bouchard, N., Lacoste, N., Utley, R.T., Gaudreau, L.*, et al.* (2010). NuA4-dependent acetylation of nucleosomal histones H4 and H2A directly stimulates incorporation of H2A.Z by the SWR1 complex. J Biol Chem *285*, 15966-15977.

Amano, M., Suzuki, A., Hori, T., Backer, C., Okawa, K., Cheeseman, I.M., and Fukagawa, T. (2009). The CENP-S complex is essential for the stable assembly of outer kinetochore structure. J Cell Biol *186*, 173-182.

Amoros, M., and Estruch, F. (2001). Hsf1p and Msn2/4p cooperate in the expression of Saccharomyces cerevisiae genes HSP26 and HSP104 in a gene- and stress type-dependent manner. Molecular microbiology *39*, 1523-1532.

Amsterdam, A., Pitzer, F., and Baumeister, W. (1993). Changes in intracellular localization of proteasomes in immortalized ovarian granulosa cells during mitosis associated with a role in cell cycle control. Proc Natl Acad Sci U S A *90*, 99-103.

Andersen, J.S., Lam, Y.W., Leung, A.K., Ong, S.E., Lyon, C.E., Lamond, A.I., and Mann, M. (2005). Nucleolar proteome dynamics. Nature *433*, 77-83.

Andersen, P.K., Jensen, T.H., and Lykke-Andersen, S. (2013a). Making ends meet: coordination between RNA 3'-end processing and transcription initiation. Wiley interdisciplinary reviews RNA *4*, 233-246.

Andersen, P.R., Domanski, M., Kristiansen, M.S., Storvall, H., Ntini, E., Verheggen, C., Schein, A., Bunkenborg, J., Poser, I., Hallais, M.*, et al.* (2013b). The human cap-binding complex is functionally connected to the nuclear RNA exosome. Nat Struct Mol Biol *20*, 1367-1376.

Anderson, P., and Kedersha, N. (2006). RNA granules. J Cell Biol *172*, 803-808.

Ando, Y., Tomaru, Y., Morinaga, A., Burroughs, A.M., Kawaji, H., Kubosaki, A., Kimura, R., Tagata, M., Ino, Y., Hirano, H.*, et al.* (2011). Nuclear pore complex protein mediated nuclear localization of dicer protein in human cells. PLoS One *6*, e23385.

Andoh, T., Azad, A.K., Shigematsu, A., Ohshima, Y., and Tani, T. (2004). The fission yeast ptr1+ gene involved in nuclear mRNA export encodes a putative ubiquitin ligase. Biochemical and biophysical research communications *317*, 1138-1143.

Antonin, W., Ellenberg, J., and Dultz, E. (2008). Nuclear pore complex assembly through the cell cycle: regulation and membrane organization. FEBS letters *582*, 2004-2016.

Appelgren, H., Kniola, B., and Ekwall, K. (2003). Distinct centromere domain structures with separate functions demonstrated in live fission yeast cells. J Cell Sci *116*, 4035-4042.

Asakawa, H., Kojidani, T., Yang, H.J., Ohtsuki, C., Osakada, H., Matsuda, A., Iwamoto, M., Chikashige, Y., Nagao, K., Obuse, C.*, et al.* (2019). Asymmetrical localization of Nup107-160 subcomplex components within the nuclear pore complex in fission yeast. PLoS Genet *15*, e1008061.

Asakawa, H., Yang, H.J., Yamamoto, T.G., Ohtsuki, C., Chikashige, Y., Sakata-Sogawa, K., Tokunaga, M., Iwamoto, M., Hiraoka, Y., and Haraguchi, T. (2014). Characterization of nuclear pore complex components in fission yeast Schizosaccharomyces pombe. Nucleus *5*, 149-162.

Audas, T.E., Jacob, M.D., and Lee, S. (2012). Immobilization of proteins in the nucleolus by ribosomal intergenic spacer noncoding RNA. Mol Cell *45*, 147-157.

Azkanaz, M., Rodriguez Lopez, A., de Boer, B., Huiting, W., Angrand, P.O., Vellenga, E., Kampinga, H.H., Bergink, S., Martens, J.H., Schuringa, J.J.*, et al.* (2019). Protein quality control in the nucleolus safeguards recovery of epigenetic regulators after heat shock. eLife *8*.

Babour, A., Dargemont, C., and Stutz, F. (2012). Ubiquitin and assembly of export competent mRNP. Biochim Biophys Acta *1819*, 521-530.

Bachi, A., Braun, I.C., Rodrigues, J.P., Pante, N., Ribbeck, K., von Kobbe, C., Kutay, U., Wilm, M., Gorlich, D., Carmo-Fonseca, M.*, et al.* (2000). The C-terminal domain of TAP interacts with the nuclear pore complex and promotes export of specific CTE-bearing RNA substrates. RNA *6*, 136-158.

Bader, N., Jung, T., and Grune, T. (2007). The proteasome and its role in nuclear protein maintenance. Exp Gerontol *42*, 864-870.

Bae, J.A., Moon, D., and Yoon, J.H. (2009). Nup211, the fission yeast homolog of Mlp1/Tpr, is involved in mRNA export. Journal of microbiology *47*, 337-343.

Baejen, C., Torkler, P., Gressel, S., Essig, K., Soding, J., and Cramer, P. (2014). Transcriptome maps of mRNP biogenesis factors define pre-mRNA recognition. Mol Cell *55*, 745-757.

Bah, A., Wischnewski, H., Shchepachev, V., and Azzalin, C.M. (2012). The telomeric transcriptome of Schizosaccharomyces pombe. Nucleic Acids Res *40*, 2995-3005.

Bahler, J., Wu, J.Q., Longtine, M.S., Shah, N.G., McKenzie, A., 3rd, Steever, A.B., Wach, A., Philippsen, P., and Pringle, J.R. (1998). Heterologous modules for efficient and versatile PCR-based gene targeting in Schizosaccharomyces pombe. Yeast *14*, 943-951.

Bahn, Y.S., Xue, C., Idnurm, A., Rutherford, J.C., Heitman, J., and Cardenas, M.E. (2007). Sensing the environment: lessons from fungi. Nat Rev Microbiol *5*, 57-69.

Bai, S.W., Rouquette, J., Umeda, M., Faigle, W., Loew, D., Sazer, S., and Doye, V. (2004). The fission yeast Nup107-120 complex functionally interacts with the small GTPase Ran/Spi1 and is required for mRNA export, nuclear pore distribution, and proper cell division. Mol Cell Biol *24*, 6379-6392.

Bailer, S.M., Siniossoglou, S., Podtelejnikov, A., Hellwig, A., Mann, M., and Hurt, E. (1998). Nup116p and nup100p are interchangeable through a conserved motif which constitutes a docking site for the mRNA transport factor gle2p. EMBO J *17*, 1107-1119.

Baler, R., Dahl, G., and Voellmy, R. (1993). Activation of human heat shock genes is accompanied by oligomerization, modification, and rapid translocation of heat shock transcription factor HSF1. Mol Cell Biol *13*, 2486-2496.

Bangs, P., Burke, B., Powers, C., Craig, R., Purohit, A., and Doxsey, S. (1998). Functional analysis of Tpr: identification of nuclear pore complex association and nuclear localization domains and a role in mRNA export. J Cell Biol *143*, 1801-1812.

Barkess, G., and West, A.G. (2012). Chromatin insulator elements: establishing barriers to set heterochromatin boundaries. Epigenomics *4*, 67-80.

Barrales, R.R., Forn, M., Georgescu, P.R., Sarkadi, Z., and Braun, S. (2016). Control of heterochromatin localization and silencing by the nuclear membrane protein Lem2. Genes Dev *30*, 133-148.

Basilico, F., Maffini, S., Weir, J.R., Prumbaum, D., Rojas, A.M., Zimniak, T., De Antoni, A., Jeganathan, S., Voss, B., van Gerwen, S.*, et al.* (2014). The pseudo GTPase CENP-M drives human kinetochore assembly. eLife *3*, e02978.

Becerra, M., Lombardia, L.J., Gonzalez-Siso, M.I., Rodriguez-Belmonte, E., Hauser, N.C., and Cerdan, M.E. (2003). Genome-wide analysis of the yeast transcriptome upon heat and cold shock. Comp Funct Genomics *4*, 366-375.

Beck, M., and Hurt, E. (2017). The nuclear pore complex: understanding its function through structural insight. Nat Rev Mol Cell Biol *18*, 73-89.

Belgareh, N., Rabut, G., Bai, S.W., van Overbeek, M., Beaudouin, J., Daigle, N., Zatsepina, O.V., Pasteau, F., Labas, V., Fromont-Racine, M.*, et al.* (2001). An evolutionarily conserved NPC subcomplex, which redistributes in part to kinetochores in mammalian cells. J Cell Biol *154*, 1147-1160.

Ben-Efraim, I., Frosst, P.D., and Gerace, L. (2009). Karyopherin binding interactions and nuclear import mechanism of nuclear pore complex protein Tpr. BMC Cell Biol *10*, 74.

Ben-Yishay, R., Ashkenazy, A.J., and Shav-Tal, Y. (2016). Dynamic Encounters of Genes and Transcripts with the Nuclear Pore. Trends Genet *32*, 419-431.

Ben-Yishay, R., Mor, A., Shraga, A., Ashkenazy-Titelman, A., Kinor, N., Schwed-Gross, A., Jacob, A., Kozer, N., Kumar, P., Garini, Y.*, et al.* (2019). Imaging within single NPCs reveals NXF1's role in mRNA export on the cytoplasmic side of the pore. J Cell Biol *218*, 2962-2981.

Bergink, S., and Jentsch, S. (2009). Principles of ubiquitin and SUMO modifications in DNA repair. Nature *458*, 461-467.

Bernard, P., Maure, J.F., Partridge, J.F., Genier, S., Javerzat, J.P., and Allshire, R.C. (2001). Requirement of heterochromatin for cohesion at centromeres. Science *294*, 2539-2542.

Bersaglieri, C., and Santoro, R. (2019). Genome Organization in and around the Nucleolus. Cells *8*.

Bharathi, A., Ghosh, A., Whalen, W.A., Yoon, J.H., Pu, R., Dasso, M., and Dhar, R. (1997). The human RAE1 gene is a functional homologue of Schizosaccharomyces pombe rae1 gene involved in nuclear export of Poly(A)+ RNA. Gene *198*, 251-258.

Bhatia, V., Barroso, S.I., Garcia-Rubio, M.L., Tumini, E., Herrera-Moyano, E., and Aguilera, A. (2014). BRCA2 prevents R-loop accumulation and associates with TREX-2 mRNA export factor PCID2. Nature *511*, 362-365.

Bjork, P., and Wieslander, L. (2017). Integration of mRNP formation and export. Cell Mol Life Sci *74*, 2875-2897.

Blevins, M.B., Smith, A.M., Phillips, E.M., and Powers, M.A. (2003). Complex formation among the RNA export proteins Nup98, Rae1/Gle2, and TAP. J Biol Chem *278*, 20979-20988.

Blobel, G. (1985). Gene gating: a hypothesis. Proc Natl Acad Sci U S A *82*, 8527-8529.

Boban, M., and Foisner, R. (2016). Degradation-mediated protein quality control at the inner nuclear membrane. Nucleus *7*, 41-49.

Boehmer, T., Enninga, J., Dales, S., Blobel, G., and Zhong, H. (2003). Depletion of a single nucleoporin, Nup107, prevents the assembly of a subset of nucleoporins into the nuclear pore complex. Proc Natl Acad Sci U S A *100*, 981-985.

Boeke, J.D., LaCroute, F., and Fink, G.R. (1984). A positive selection for mutants lacking orotidine-5'-phosphate decarboxylase activity in yeast: 5-fluoro-orotic acid resistance. Molecular & general genetics : MGG *197*, 345-346.

Boeke, J.D., Trueheart, J., Natsoulis, G., and Fink, G.R. (1987). 5-Fluoroorotic acid as a selective agent in yeast molecular genetics. Methods in enzymology *154*, 164-175.

Boisvert, F.M., van Koningsbruggen, S., Navascues, J., and Lamond, A.I. (2007). The multifunctional nucleolus. Nat Rev Mol Cell Biol *8*, 574-585.

Bond, U. (1988). Heat shock but not other stress inducers leads to the disruption of a sub-set of snRNPs and inhibition of in vitro splicing in HeLa cells. EMBO J *7*, 3509-3518.

Bond, U. (2006). Stressed out! Effects of environmental stress on mRNA metabolism. FEMS yeast research *6*, 160-170.

Bonnet, A., Bretes, H., and Palancade, B. (2015). Nuclear pore components affect distinct stages of intron-containing gene expression. Nucleic Acids Res *43*, 4249-4261.

Bonnet, A., and Palancade, B. (2014). Regulation of mRNA trafficking by nuclear pore complexes. Genes (Basel) *5*, 767-791.

Bosl, B., Grimminger, V., and Walter, S. (2006). The molecular chaperone Hsp104--a molecular machine for protein disaggregation. J Struct Biol *156*, 139-148.

Boulon, S., Westman, B.J., Hutten, S., Boisvert, F.M., and Lamond, A.I. (2010). The nucleolus under stress. Mol Cell *40*, 216-227.

Bousquet-Antonelli, C., Presutti, C., and Tollervey, D. (2000). Identification of a regulated pathway for nuclear pre-mRNA turnover. Cell *102*, 765-775.

Boy-Marcotte, E., Garmendia, C., Garreau, H., Lallet, S., Mallet, L., and Jacquet, M. (2006). The transcriptional activation region of Msn2p, in Saccharomyces cerevisiae, is regulated by stress but is insensitive to the cAMP signalling pathway. Mol Genet Genomics *275*, 277-287.

Bracken, A.P., and Bond, U. (1999). Reassembly and protection of small nuclear ribonucleoprotein particles by heat shock proteins in yeast cells. RNA *5*, 1586-1596.

Braun, S., Garcia, J.F., Rowley, M., Rougemaille, M., Shankar, S., and Madhani, H.D. (2011). The Cul4-Ddb1(Cdt)(2) ubiquitin ligase inhibits invasion of a boundary-associated antisilencing factor into heterochromatin. Cell *144*, 41-54.

Bresch, C., Muller, G., and Egel, R. (1968). Genes involved in meiosis and sporulation of a yeast. Molecular & general genetics : MGG *102*, 301-306.

Brickner, D.G., Ahmed, S., Meldi, L., Thompson, A., Light, W., Young, M., Hickman, T.L., Chu, F., Fabre, E., and Brickner, J.H. (2012). Transcription factor binding to a DNA zip code controls interchromosomal clustering at the nuclear periphery. Dev Cell *22*, 1234-1246.

Brickner, D.G., and Brickner, J.H. (2012). Interchromosomal clustering of active genes at the nuclear pore complex. Nucleus *3*, 487-492.

Brickner, D.G., Cajigas, I., Fondufe-Mittendorf, Y., Ahmed, S., Lee, P.C., Widom, J., and Brickner, J.H. (2007). H2A.Z-mediated localization of genes at the nuclear periphery confers epigenetic memory of previous transcriptional state. PLoS Biol *5*, e81.

Brickner, D.G., Randise-Hinchliff, C., Lebrun Corbin, M., Liang, J.M., Kim, S., Sump, B., D'Urso, A., Kim, S.H., Satomura, A., Schmit, H.*, et al.* (2019). The Role of Transcription Factors and Nuclear Pore Proteins in Controlling the Spatial Organization of the Yeast Genome. Dev Cell *49*, 936-947 e934.

Brickner, J.H. (2009). Transcriptional memory at the nuclear periphery. Curr Opin Cell Biol *21*, 127-133.

Brickner, J.H., and Walter, P. (2004). Gene recruitment of the activated INO1 locus to the nuclear membrane. PLoS Biol *2*, e342.

Brodsky, A.S., and Silver, P.A. (2000). Pre-mRNA processing factors are required for nuclear export. RNA *6*, 1737-1749.

Brooks, P., Fuertes, G., Murray, R.Z., Bose, S., Knecht, E., Rechsteiner, M.C., Hendil, K.B., Tanaka, K., Dyson, J., and Rivett, J. (2000). Subcellular localization of proteasomes and their regulatory complexes in mammalian cells. Biochem J *346 Pt 1*, 155-161.

Brown, C.R., Kennedy, C.J., Delmar, V.A., Forbes, D.J., and Silver, P.A. (2008). Global histone acetylation induces functional genomic reorganization at mammalian nuclear pore complexes. Genes Dev *22*, 627-639.

Brown, J.A., Bharathi, A., Ghosh, A., Whalen, W., Fitzgerald, E., and Dhar, R. (1995). A mutation in the Schizosaccharomyces pombe rae1 gene causes defects in poly(A)+ RNA export and in the cytoskeleton. J Biol Chem *270*, 7411-7419.

Brune, C., Munchel, S.E., Fischer, N., Podtelejnikov, A.V., and Weis, K. (2005). Yeast poly(A)-binding protein Pab1 shuttles between the nucleus and the cytoplasm and functions in mRNA export. RNA *11*, 517-531.

Brunquell, J., Morris, S., Lu, Y., Cheng, F., and Westerheide, S.D. (2016). The genome-wide role of HSF-1 in the regulation of gene expression in Caenorhabditis elegans. BMC Genomics *17*, 559.

Buchan, J.R., and Parker, R. (2009). Eukaryotic stress granules: the ins and outs of translation. Mol Cell *36*, 932-941.

Budenholzer, L., Cheng, C.L., Li, Y., and Hochstrasser, M. (2017). Proteasome Structure and Assembly. J Mol Biol *429*, 3500-3524.

Buhler, M., and Gasser, S.M. (2009). Silent chromatin at the middle and ends: lessons from yeasts. EMBO J *28*, 2149-2161.

Buhler, M., Haas, W., Gygi, S.P., and Moazed, D. (2007). RNAi-dependent and -independent RNA turnover mechanisms contribute to heterochromatic gene silencing. Cell *129*, 707-721.

Bui, K.H., von Appen, A., DiGuilio, A.L., Ori, A., Sparks, L., Mackmull, M.T., Bock, T., Hagen, W., Andres-Pons, A., Glavy, J.S.*, et al.* (2013). Integrated structural analysis of the human nuclear pore complex scaffold. Cell *155*, 1233-1243.

Burns, L.T., and Wente, S.R. (2014). From hypothesis to mechanism: uncovering nuclear pore complex links to gene expression. Mol Cell Biol *34*, 2114-2120.

Bush, K.T., Goldberg, A.L., and Nigam, S.K. (1997). Proteasome inhibition leads to a heat-shock response, induction of endoplasmic reticulum chaperones, and thermotolerance. J Biol Chem *272*, 9086-9092.

Buttrick, G.J., and Millar, J.B. (2011). Ringing the changes: emerging roles for DASH at the kinetochore-microtubule Interface. Chromosome research : an international journal on the molecular, supramolecular and evolutionary aspects of chromosome biology *19*, 393-407.

Cabal, G.G., Genovesio, A., Rodriguez-Navarro, S., Zimmer, C., Gadal, O., Lesne, A., Buc, H., Feuerbach-Fournier, F., Olivo-Marin, J.C., Hurt, E.C.*, et al.* (2006). SAGA interacting factors confine sub-diffusion of transcribed genes to the nuclear envelope. Nature *441*, 770-773.

Cabrera, M., Boronat, S., Marte, L., Vega, M., Perez, P., Ayte, J., and Hidalgo, E. (2020). Chaperone-Facilitated Aggregation of Thermo-Sensitive Proteins Shields Them from Degradation during Heat Stress. Cell Rep *30*, 2430-2443 e2434.

Callan, H.G., Randall, J.T., and Tomlin, S.G. (1949). An electron microscope study of the nuclear membrane. Nature *163*, 280.

Cam, H., and Grewal, S.I. (2004). RNA interference and epigenetic control of heterochromatin assembly in fission yeast. Cold Spring Harb Symp Quant Biol *69*, 419-427.

Cam, H.P., Sugiyama, T., Chen, E.S., Chen, X., FitzGerald, P.C., and Grewal, S.I. (2005). Comprehensive analysis of heterochromatin- and RNAi-mediated epigenetic control of the fission yeast genome. Nat Genet *37*, 809-819.

Cam, H.P., and Whitehall, S. (2016). Analysis of Heterochromatin in Schizosaccharomyces pombe. Cold Spring Harb Protoc *2016*.

Capelson, M., Doucet, C., and Hetzer, M.W. (2010a). Nuclear pore complexes: guardians of the nuclear genome. Cold Spring Harb Symp Quant Biol *75*, 585-597.

Capelson, M., Liang, Y., Schulte, R., Mair, W., Wagner, U., and Hetzer, M.W. (2010b). Chromatin-bound nuclear pore components regulate gene expression in higher eukaryotes. Cell *140*, 372-383.

Carmody, S.R., Tran, E.J., Apponi, L.H., Corbett, A.H., and Wente, S.R. (2010). The mitogen-activated protein kinase Slt2 regulates nuclear retention of non-heat shock mRNAs during heat shock-induced stress. Mol Cell Biol *30*, 5168-5179.

Carmody, S.R., and Wente, S.R. (2009). mRNA nuclear export at a glance. J Cell Sci *122*, 1933-1937.

Carpy, A., Krug, K., Graf, S., Koch, A., Popic, S., Hauf, S., and Macek, B. (2014). Absolute proteome and phosphoproteome dynamics during the cell cycle of Schizosaccharomyces pombe (Fission Yeast). Mol Cell Proteomics *13*, 1925-1936.

Carroll, C.W., Milks, K.J., and Straight, A.F. (2010). Dual recognition of CENP-A nucleosomes is required for centromere assembly. In J Cell Biol, pp. 1143-1155.

Casanal, A., Kumar, A., Hill, C.H., Easter, A.D., Emsley, P., Degliesposti, G., Gordiyenko, Y., Santhanam, B., Wolf, J., Wiederhold, K.*, et al.* (2017). Architecture of eukaryotic mRNA 3'-end processing machinery. Science *358*, 1056-1059.

Casolari, J.M., Brown, C.R., Drubin, D.A., Rando, O.J., and Silver, P.A. (2005). Developmentally induced changes in transcriptional program alter spatial organization across chromosomes. Genes Dev *19*, 1188-1198.

Casolari, J.M., Brown, C.R., Komili, S., West, J., Hieronymus, H., and Silver, P.A. (2004). Genome-wide localization of the nuclear transport machinery couples transcriptional status and nuclear organization. Cell *117*, 427-439.

Castellano-Pozo, M., Garcia-Muse, T., and Aguilera, A. (2012). R-loops cause replication impairment and genome instability during meiosis. EMBO reports *13*, 923-929.

Castells-Roca, L., Garcia-Martinez, J., Moreno, J., Herrero, E., Belli, G., and Perez-Ortin, J.E. (2011). Heat shock response in yeast involves changes in both transcription rates and mRNA stabilities. PLoS One *6*, e17272.

Castillo, A.G., Mellone, B.G., Partridge, J.F., Richardson, W., Hamilton, G.L., Allshire, R.C., and Pidoux, A.L. (2007). Plasticity of fission yeast CENP-A chromatin driven by relative levels of histone H3 and H4. PLoS Genet *3*, e121.

Castillo, A.G., Pidoux, A.L., Catania, S., Durand-Dubief, M., Choi, E.S., Hamilton, G., Ekwall, K., and Allshire, R.C. (2013). Telomeric repeats facilitate CENP-A(Cnp1) incorporation via telomere binding proteins. PLoS One *8*, e69673.

Catania, S., and Allshire, R.C. (2014). Anarchic centromeres: deciphering order from apparent chaos. Curr Opin Cell Biol *26*, 41-50.

Catania, S., Pidoux, A.L., and Allshire, R.C. (2015). Sequence features and transcriptional stalling within centromere DNA promote establishment of CENP-A chromatin. PLoS Genet *11*, e1004986.

Causton, H.C., Ren, B., Koh, S.S., Harbison, C.T., Kanin, E., Jennings, E.G., Lee, T.I., True, H.L., Lander, E.S., and Young, R.A. (2001). Remodeling of yeast genome expression in response to environmental changes. Mol Biol Cell *12*, 323-337.

Cernilogar, F.M., Onorati, M.C., Kothe, G.O., Burroughs, A.M., Parsi, K.M., Breiling, A., Lo Sardo, F., Saxena, A., Miyoshi, K., Siomi, H.*, et al.* (2011). Chromatin-associated RNA interference components contribute to transcriptional regulation in Drosophila. Nature *480*, 391-395.

Chadrin, A., Hess, B., San Roman, M., Gatti, X., Lombard, B., Loew, D., Barral, Y., Palancade, B., and Doye, V. (2010). Pom33, a novel transmembrane nucleoporin required for proper nuclear pore complex distribution. J Cell Biol *189*, 795-811.

Chan, G.K., Liu, S.T., and Yen, T.J. (2005). Kinetochore structure and function. Trends Cell Biol *15*, 589-598.

Chan, P.K., Bloom, D.A., and Hoang, T.T. (1999). The N-terminal half of NPM dissociates from nucleoli of HeLa cells after anticancer drug treatments. Biochemical and biophysical research communications *264*, 305-309.

Chan, S., Choi, E.A., and Shi, Y. (2011). Pre-mRNA 3'-end processing complex assembly and function. Wiley interdisciplinary reviews RNA *2*, 321-335.

Charbin, A., Bouchoux, C., and Uhlmann, F. (2014). Condensin aids sister chromatid decatenation by topoisomerase II. Nucleic Acids Res *42*, 340-348.

Chatel, G., and Fahrenkrog, B. (2011). Nucleoporins: leaving the nuclear pore complex for a successful mitosis. Cell Signal *23*, 1555-1562.

Cheeseman, I.M. (2014). The kinetochore. Cold Spring Harb Perspect Biol *6*, a015826.

Cheeseman, I.M., Brew, C., Wolyniak, M., Desai, A., Anderson, S., Muster, N., Yates, J.R., Huffaker, T.C., Drubin, D.G., and Barnes, G. (2001). Implication of a novel multiprotein Dam1p complex in outer kinetochore function. J Cell Biol *155*, 1137-1145.

Cheeseman, I.M., Chappie, J.S., Wilson-Kubalek, E.M., and Desai, A. (2006). The conserved KMN network constitutes the core microtubule-binding site of the kinetochore. Cell *127*, 983-997.

Cheeseman, I.M., and Desai, A. (2008). Molecular architecture of the kinetochore-microtubule interface. Nat Rev Mol Cell Biol *9*, 33-46.

Chekanova, J.A., Abruzzi, K.C., Rosbash, M., and Belostotsky, D.A. (2008). Sus1, Sac3, and Thp1 mediate post-transcriptional tethering of active genes to the nuclear rim as well as to non-nascent mRNP. RNA *14*, 66-77.

Chen, B.R., and Runge, K.W. (2009). A new Schizosaccharomyces pombe chronological lifespan assay reveals that caloric restriction promotes efficient cell cycle exit and extends longevity. Exp Gerontol *44*, 493-502.

Chen, D., Toone, W.M., Mata, J., Lyne, R., Burns, G., Kivinen, K., Brazma, A., Jones, N., and Bahler, J. (2003). Global transcriptional responses of fission yeast to environmental stress. Mol Biol Cell *14*, 214-229.

Chen, E.S., Zhang, K., Nicolas, E., Cam, H.P., Zofall, M., and Grewal, S.I. (2008). Cell cycle control of centromeric repeat transcription and heterochromatin assembly. Nature *451*, 734-737.

Chen, H.M., Futcher, B., and Leatherwood, J. (2011a). The fission yeast RNA binding protein Mmi1 regulates meiotic genes by controlling intron specific splicing and polyadenylation coupled RNA turnover. PLoS One *6*, e26804.

Chen, L., and Madura, K. (2014). Degradation of specific nuclear proteins occurs in the cytoplasm in Saccharomyces cerevisiae. Genetics *197*, 193-197.

Chen, L., Romero, L., Chuang, S.M., Tournier, V., Joshi, K.K., Lee, J.A., Kovvali, G., and Madura, K. (2011b). Sts1 plays a key role in targeting proteasomes to the nucleus. J Biol Chem *286*, 3104-3118.

Chen, X.Q., Du, X., Liu, J., Balasubramanian, M.K., and Balasundaram, D. (2004). Identification of genes encoding putative nucleoporins and transport factors in the fission yeast Schizosaccharomyces pombe: a deletion analysis. Yeast *21*, 495-509.

Chen, Y.H., Wang, G.Y., Hao, H.C., Chao, C.J., Wang, Y., and Jin, Q.W. (2017). Facile manipulation of protein localization in fission yeast through binding of GFP-binding protein to GFP. J Cell Sci *130*, 1003-1015.

Cheng, H., Dufu, K., Lee, C.S., Hsu, J.L., Dias, A., and Reed, R. (2006). Human mRNA export machinery recruited to the 5' end of mRNA. Cell *127*, 1389-1400.

Chi, B., Wang, Q., Wu, G., Tan, M., Wang, L., Shi, M., Chang, X., and Cheng, H. (2013). Aly and THO are required for assembly of the human TREX complex and association of TREX components with the spliced mRNA. Nucleic Acids Res *41*, 1294-1306.

Chikashige, Y., Ding, D.Q., Imai, Y., Yamamoto, M., Haraguchi, T., and Hiraoka, Y. (1997). Meiotic nuclear reorganization: switching the position of centromeres and telomeres in the fission yeast Schizosaccharomyces pombe. EMBO J *16*, 193-202.

Chiodi, I., Biggiogera, M., Denegri, M., Corioni, M., Weighardt, F., Cobianchi, F., Riva, S., and Biamonti, G. (2000). Structure and dynamics of hnRNP-labelled nuclear bodies induced by stress treatments. J Cell Sci *113 (Pt 22)*, 4043-4053.

Choi, E.S., Stralfors, A., Catania, S., Castillo, A.G., Svensson, J.P., Pidoux, A.L., Ekwall, K., and Allshire, R.C. (2012). Factors that promote H3 chromatin integrity during transcription prevent promiscuous deposition of CENP-A(Cnp1) in fission yeast. PLoS Genet *8*, e1002985.

Chopra, K., Bawaria, S., and Chauhan, R. (2019). Evolutionary divergence of the nuclear pore complex from fungi to metazoans. Protein Sci *28*, 571-586.

Chowdhary, S., Kainth, A.S., and Gross, D.S. (2017). Heat Shock Protein Genes Undergo Dynamic Alteration in Their Three-Dimensional Structure and Genome Organization in Response to Thermal Stress. Mol Cell Biol *37*.

Chowdhary, S., Kainth, A.S., Pincus, D., and Gross, D.S. (2019). Heat Shock Factor 1 Drives Intergenic Association of Its Target Gene Loci upon Heat Shock. Cell Rep *26*, 18-28 e15.

Chowdhury, M., and Enenkel, C. (2015). Intracellular Dynamics of the Ubiquitin-Proteasome-System. F1000Res *4*, 367.

Chun, Y., Kim, R., and Lee, S. (2016). Centromere Protein (CENP)-W Interacts with Heterogeneous Nuclear Ribonucleoprotein (hnRNP) U and May Contribute to Kinetochore-Microtubule Attachment in Mitotic Cells. PLoS One *11*, e0149127.

Chun, Y., Lee, M., Park, B., and Lee, S. (2013). CSN5/JAB1 interacts with the centromeric components CENP-T and CENP-W and regulates their proteasome-mediated degradation. J Biol Chem *288*, 27208-27219.

Cleveland, D.W., Mao, Y., and Sullivan, K.F. (2003). Centromeres and kinetochores: from epigenetics to mitotic checkpoint signaling. Cell *112*, 407-421.

Clever, M., Mimura, Y., Funakoshi, T., and Imamoto, N. (2013). Regulation and coordination of nuclear envelope and nuclear pore complex assembly. Nucleus *4*, 105-114.

Cohen, R.L., Espelin, C.W., De Wulf, P., Sorger, P.K., Harrison, S.C., and Simons, K.T. (2008). Structural and functional dissection of Mif2p, a conserved DNA-binding kinetochore protein. Mol Biol Cell *19*, 4480-4491.

Collins, K.A., Castillo, A.R., Tatsutani, S.Y., and Biggins, S. (2005). De novo kinetochore assembly requires the centromeric histone H3 variant. Mol Biol Cell *16*, 5649-5660.

Collins, K.A., Furuyama, S., and Biggins, S. (2004). Proteolysis contributes to the exclusive centromere localization of the yeast Cse4/CENP-A histone H3 variant. Curr Biol *14*, 1968-1972.

Conlin, L.K., and Nelson, H.C. (2007). The natural osmolyte trehalose is a positive regulator of the heat-induced activity of yeast heat shock transcription factor. Mol Cell Biol *27*, 1505-1515.

Cook, A., Bono, F., Jinek, M., and Conti, E. (2007). Structural biology of nucleocytoplasmic transport. Annu Rev Biochem *76*, 647-671.

Corbett, K.D. (2017). Molecular Mechanisms of Spindle Assembly Checkpoint Activation and Silencing. Prog Mol Subcell Biol *56*, 429-455.

Corbett, K.D., Yip, C.K., Ee, L.S., Walz, T., Amon, A., and Harrison, S.C. (2010). The monopolin complex crosslinks kinetochore components to regulate chromosome-microtubule attachments. Cell *142*, 556-567.

Cordes, V.C., Hase, M.E., and Muller, L. (1998). Molecular segments of protein Tpr that confer nuclear targeting and association with the nuclear pore complex. Exp Cell Res *245*, 43-56.

Cordes, V.C., Reidenbach, S., Rackwitz, H.R., and Franke, W.W. (1997). Identification of protein p270/Tpr as a constitutive component of the nuclear pore complex-attached intranuclear filaments. J Cell Biol *136*, 515-529.

Cotto, J.J., and Morimoto, R.I. (1999). Stress-induced activation of the heat-shock response: cell and molecular biology of heat-shock factors. Biochem Soc Symp *64*, 105-118.

Coux, O., Tanaka, K., and Goldberg, A.L. (1996). Structure and functions of the 20S and 26S proteasomes. Annu Rev Biochem *65*, 801-847.

Coyle, J.H., Bor, Y.C., Rekosh, D., and Hammarskjold, M.L. (2011). The Tpr protein regulates export of mRNAs with retained introns that traffic through the Nxf1 pathway. RNA *17*, 1344-1356.

Craig, E.A. (1985). The stress response: changes in eukaryotic gene expression in response to environmental stress. Science *230*, 800-801.

Croft, J.A., Bridger, J.M., Boyle, S., Perry, P., Teague, P., and Bickmore, W.A. (1999). Differences in the localization and morphology of chromosomes in the human nucleus. J Cell Biol *145*, 1119-1131.

Cronshaw, J.M., Krutchinsky, A.N., Zhang, W., Chait, B.T., and Matunis, M.J. (2002). Proteomic analysis of the mammalian nuclear pore complex. J Cell Biol *158*, 915-927.

Cueille, N., Salimova, E., Esteban, V., Blanco, M., Moreno, S., Bueno, A., and Simanis, V. (2001). Flp1, a fission yeast orthologue of the s. cerevisiae CDC14 gene, is not required for cyclin degradation or rum1p stabilisation at the end of mitosis. J Cell Sci *114*, 2649-2664.

Cunha-Silva, S., Osswald, M., Goemann, J., Barbosa, J., Santos, L.M., Resende, P., Bange, T., Ferras, C., Sunkel, C.E., and Conde, C. (2020). Mps1-mediated release of Mad1 from nuclear pores ensures the fidelity of chromosome segregation. J Cell Biol *219*.

D'Angelo, M.A., Gomez-Cavazos, J.S., Mei, A., Lackner, D.H., and Hetzer, M.W. (2012). A change in nuclear pore complex composition regulates cell differentiation. Dev Cell *22*, 446-458.

D'Angelo, M.A., Raices, M., Panowski, S.H., and Hetzer, M.W. (2009). Age-dependent deterioration of nuclear pore complexes causes a loss of nuclear integrity in postmitotic cells. Cell *136*, 284-295.

D'Urso, A., and Brickner, J.H. (2014). Mechanisms of epigenetic memory. Trends Genet *30*, 230-236.

D'Urso, A., and Brickner, J.H. (2017). Epigenetic transcriptional memory. Curr Genet *63*, 435-439.

Dahlmann, B., Kopp, F., Kuehn, L., Niedel, B., Pfeifer, G., Hegerl, R., and Baumeister, W. (1989). The multicatalytic proteinase (prosome) is ubiquitous from eukaryotes to archaebacteria. FEBS letters *251*, 125-131.

Dan, J., Liu, Y., Liu, N., Chiourea, M., Okuka, M., Wu, T., Ye, X., Mou, C., Wang, L., Wang, L.*, et al.* (2014). Rif1 maintains telomere length homeostasis of ESCs by mediating heterochromatin silencing. Dev Cell *29*, 7-19.

Dantuma, N.P., Heinen, C., and Hoogstraten, D. (2009). The ubiquitin receptor Rad23: at the crossroads of nucleotide excision repair and proteasomal degradation. DNA Repair (Amst) *8*, 449-460.

Das, R., Yu, J., Zhang, Z., Gygi, M.P., Krainer, A.R., Gygi, S.P., and Reed, R. (2007). SR proteins function in coupling RNAP II transcription to pre-mRNA splicing. Mol Cell *26*, 867-881.

David-Watine, B. (2011). Silencing nuclear pore protein Tpr elicits a senescent-like phenotype in cancer cells. PLoS One *6*, e22423.

Davis, L.I. (1995). The nuclear pore complex. Annu Rev Biochem *64*, 865-896.

De Souza, C.P., Hashmi, S.B., Nayak, T., Oakley, B., and Osmani, S.A. (2009). Mlp1 acts as a mitotic scaffold to spatially regulate spindle assembly checkpoint proteins in Aspergillus nidulans. Mol Biol Cell *20*, 2146-2159.

De Souza, C.P., and Osmani, S.A. (2007). Mitosis, not just open or closed. Eukaryot Cell *6*, 1521-1527.

De Virgilio, C., Piper, P., Boller, T., and Wiemken, A. (1991). Acquisition of thermotolerance in Saccharomyces cerevisiae without heat shock protein hsp 104 and in the absence of protein synthesis. FEBS letters *288*, 86-90.

De Virgilio, C., Simmen, U., Hottiger, T., Boller, T., and Wiemken, A. (1990). Heat shock induces enzymes of trehalose metabolism, trehalose accumulation, and thermotolerance in Schizosaccharomyces pombe, even in the presence of cycloheximide. FEBS letters *273*, 107-110.

Deane, C.A.S., and Brown, I.R. (2017). Differential Targeting of Hsp70 Heat Shock Proteins HSPA6 and HSPA1A with Components of a Protein Disaggregation/Refolding Machine in Differentiated Human Neuronal Cells following Thermal Stress. Frontiers in neuroscience *11*, 227.

Degols, G., Shiozaki, K., and Russell, P. (1996). Activation and regulation of the Spc1 stress-activated protein kinase in Schizosaccharomyces pombe. Mol Cell Biol *16*, 2870-2877.

DeGrasse, J.A., DuBois, K.N., Devos, D., Siegel, T.N., Sali, A., Field, M.C., Rout, M.P., and Chait, B.T. (2009). Evidence for a shared nuclear pore complex architecture that is conserved from the last common eukaryotic ancestor. Mol Cell Proteomics *8*, 2119-2130.

Delaleau, M., and Borden, K.L. (2015). Multiple Export Mechanisms for mRNAs. Cells *4*, 452-473.

Denegri, M., Chiodi, I., Corioni, M., Cobianchi, F., Riva, S., and Biamonti, G. (2001). Stress-induced nuclear bodies are sites of accumulation of pre-mRNA processing factors. Mol Biol Cell *12*, 3502-3514.

Denning, D., Mykytka, B., Allen, N.P., Huang, L., Al, B., and Rexach, M. (2001). The nucleoporin Nup60p functions as a Gsp1p-GTP-sensitive tether for Nup2p at the nuclear pore complex. J Cell Biol *154*, 937-950.

Denning, D.P., Patel, S.S., Uversky, V., Fink, A.L., and Rexach, M. (2003). Disorder in the nuclear pore complex: the FG repeat regions of nucleoporins are natively unfolded. Proc Natl Acad Sci U S A *100*, 2450-2455.

Derenzini, M., Trere, D., Pession, A., Montanaro, L., Sirri, V., and Ochs, R.L. (1998). Nucleolar function and size in cancer cells. The American journal of pathology *152*, 1291-1297.

Derrer, C.P., Mancini, R., Vallotton, P., Huet, S., Weis, K., and Dultz, E. (2019). The RNA export factor Mex67 functions as a mobile nucleoporin. J Cell Biol *218*, 3967-3976.

Desnoyers, S., Kaufmann, S.H., and Poirier, G.G. (1996). Alteration of the nucleolar localization of poly(ADP-ribose) polymerase upon treatment with transcription inhibitors. Exp Cell Res *227*, 146-153.

Di Giammartino, D.C., and Manley, J.L. (2014). New links between mRNA polyadenylation and diverse nuclear pathways. Mol Cells *37*, 644-649.

Dieppois, G., Iglesias, N., and Stutz, F. (2006). Cotranscriptional recruitment to the mRNA export receptor Mex67p contributes to nuclear pore anchoring of activated genes. Mol Cell Biol *26*, 7858-7870.

Dilworth, D.J., Tackett, A.J., Rogers, R.S., Yi, E.C., Christmas, R.H., Smith, J.J., Siegel, A.F., Chait, B.T., Wozniak, R.W., and Aitchison, J.D. (2005). The mobile nucleoporin Nup2p and chromatin-bound Prp20p function in endogenous NPC-mediated transcriptional control. J Cell Biol *171*, 955-965.

Dimaano, C., and Ullman, K.S. (2004). Nucleocytoplasmic transport: integrating mRNA production and turnover with export through the nuclear pore. Mol Cell Biol *24*, 3069-3076.

Dimitrova, L., Valkov, E., Aibara, S., Flemming, D., McLaughlin, S.H., Hurt, E., and Stewart, M. (2015). Structural Characterization of the Chaetomium thermophilum TREX-2 Complex and its Interaction with the mRNA Nuclear Export Factor Mex67:Mtr2. Structure *23*, 1246-1257.

Ding, D., Muthuswamy, S., and Meier, I. (2012). Functional interaction between the Arabidopsis orthologs of spindle assembly checkpoint proteins MAD1 and MAD2 and the nucleoporin NUA. Plant Mol Biol *79*, 203-216.

Ding, R., West, R.R., Morphew, D.M., Oakley, B.R., and McIntosh, J.R. (1997). The spindle pole body of Schizosaccharomyces pombe enters and leaves the nuclear envelope as the cell cycle proceeds. Mol Biol Cell *8*, 1461-1479.

Dingwall, C., and Laskey, R.A. (1991). Nuclear targeting sequences--a consensus? Trends Biochem Sci *16*, 478-481.

Dixon, S.J., Fedyshyn, Y., Koh, J.L., Prasad, T.S., Chahwan, C., Chua, G., Toufighi, K., Baryshnikova, A., Hayles, J., Hoe, K.L.*, et al.* (2008). Significant conservation of synthetic lethal genetic interaction networks between distantly related eukaryotes. Proc Natl Acad Sci U S A *105*, 16653-16658.

Doma, M.K., and Parker, R. (2007). RNA quality control in eukaryotes. Cell *131*, 660-668.

Domanska, A., and Kaminska, J. (2015). Role of Rsp5 ubiquitin ligase in biogenesis of rRNA, mRNA and tRNA in yeast. RNA Biol *12*, 1265-1274.

Dominguez-Sanchez, M.S., Barroso, S., Gomez-Gonzalez, B., Luna, R., and Aguilera, A. (2011). Genome instability and transcription elongation impairment in human cells depleted of THO/TREX. PLoS Genet *7*, e1002386.

Doye, V., Wepf, R., and Hurt, E.C. (1994). A novel nuclear pore protein Nup133p with distinct roles in poly(A)+ RNA transport and nuclear pore distribution. EMBO J *13*, 6062-6075.

Doyon, Y., and Cote, J. (2004). The highly conserved and multifunctional NuA4 HAT complex. Curr Opin Genet Dev *14*, 147-154.

Duncan, K., Umen, J.G., and Guthrie, C. (2000). A putative ubiquitin ligase required for efficient mRNA export differentially affects hnRNP transport. Curr Biol *10*, 687-696.

Dunn, E.F., Hammell, C.M., Hodge, C.A., and Cole, C.N. (2005). Yeast poly(A)-binding protein, Pab1, and PAN, a poly(A) nuclease complex recruited by Pab1, connect mRNA biogenesis to export. Genes Dev *19*, 90-103.

Earnshaw, W.C., Allshire, R.C., Black, B.E., Bloom, K., Brinkley, B.R., Brown, W., Cheeseman, I.M., Choo, K.H., Copenhaver, G.P., Deluca, J.G*., et al.* (2013). Esperanto for histones: CENP-A, not CenH3, is the centromeric histone H3 variant. Chromosome research : an international journal on the molecular, supramolecular and evolutionary aspects of chromosome biology *21*, 101-106.

Eckmann, C.R., Rammelt, C., and Wahle, E. (2011). Control of poly(A) tail length. Wiley interdisciplinary reviews RNA *2*, 348-361.

Egan, E.D., Braun, C.R., Gygi, S.P., and Moazed, D. (2014). Post-transcriptional regulation of meiotic genes by a nuclear RNA silencing complex. RNA *20*, 867-881.

Egel, R. (1973). Commitment to meiosis in fission yeast. Molecular and General Genetics *121*, 277–284.

Egel, R. (1989). Molecular Biology of the Fission Yeast (Academic Press, San Diego).

Egel, R. (2004). The Molecular Biology of Schizosaccharomyces pombe: Genetics, Genomics, and Beyond (Springer, Berlin, Heidelberg).

Eisenhardt, N., Redolfi, J., and Antonin, W. (2014). Interaction of Nup53 with Ndc1 and Nup155 is required for nuclear pore complex assembly. J Cell Sci *127*, 908-921.

Ekwall, K., Cranston, G., and Allshire, R.C. (1999). Fission yeast mutants that alleviate transcriptional silencing in centromeric flanking repeats and disrupt chromosome segregation. Genetics *153*, 1153-1169.

Emmerth, S., Schober, H., Gaidatzis, D., Roloff, T., Jacobeit, K., and Buhler, M. (2010). Nuclear retention of fission yeast dicer is a prerequisite for RNAi-mediated heterochromatin assembly. Dev Cell *18*, 102-113.

Enenkel, C. (2014). Proteasome dynamics. Biochim Biophys Acta *1843*, 39-46.

Enenkel, C., Lehmann, A., and Kloetzel, P.M. (1998). Subcellular distribution of proteasomes implicates a major location of protein degradation in the nuclear envelope-ER network in yeast. EMBO J *17*, 6144-6154.

Enquist-Newman, M., Cheeseman, I.M., Van Goor, D., Drubin, D.G., Meluh, P.B., and Barnes, G. (2001). Dad1p, third component of the Duo1p/Dam1p complex involved in kinetochore function and mitotic spindle integrity. Mol Biol Cell *12*, 2601-2613.

Eytan, E., Ganoth, D., Armon, T., and Hershko, A. (1989). ATP-dependent incorporation of 20S protease into the 26S complex that degrades proteins conjugated to ubiquitin. Proc Natl Acad Sci U S A *86*, 7751-7755.

Fan, J., Kuai, B., Wang, K., Wang, L., Wang, Y., Wu, X., Chi, B., Li, G., and Cheng, H. (2018). mRNAs are sorted for export or degradation before passing through nuclear speckles. Nucleic Acids Res *46*, 8404-8416.

Fang, N.N., Chan, G.T., Zhu, M., Comyn, S.A., Persaud, A., Deshaies, R.J., Rotin, D., Gsponer, J., and Mayor, T. (2014). Rsp5/Nedd4 is the main ubiquitin ligase that targets cytosolic misfolded proteins following heat stress. Nat Cell Biol *16*, 1227-1237.

Fang, N.N., Zhu, M., Rose, A., Wu, K.P., and Mayor, T. (2016). Deubiquitinase activity is required for the proteasomal degradation of misfolded cytosolic proteins upon heat-stress. Nat Commun *7*, 12907.

Fantes, P.A., and Hoffman, C.S. (2016). A Brief History of Schizosaccharomyces pombe Research: A Perspective Over the Past 70 Years. Genetics *203*, 621-629.

Fasken, M.B., and Corbett, A.H. (2005). Process or perish: quality control in mRNA biogenesis. Nat Struct Mol Biol *12*, 482-488.

Fasken, M.B., and Corbett, A.H. (2009). Mechanisms of nuclear mRNA quality control. RNA Biol *6*, 237-241.

Fasken, M.B., Corbett, A.H., and Stewart, M. (2019). Structure-function relationships in the Nab2 polyadenosine-RNA binding Zn finger protein family. Protein Sci *28*, 513-523.

Fasken, M.B., Stewart, M., and Corbett, A.H. (2008). Functional significance of the interaction between the mRNA-binding protein, Nab2, and the nuclear pore-associated protein, Mlp1, in mRNA export. J Biol Chem *283*, 27130-27143.

Fennessy, D., Grallert, A., Krapp, A., Cokoja, A., Bridge, A.J., Petersen, J., Patel, A., Tallada, V.A., Boke, E., Hodgson, B*., et al.* (2014). Extending the Schizosaccharomyces pombe molecular genetic toolbox. PLoS One *9*, e97683.

Ferguson, S.B., Anderson, E.S., Harshaw, R.B., Thate, T., Craig, N.L., and Nelson, H.C. (2005). Protein kinase A regulates constitutive expression of small heat-shock genes in an Msn2/4p-independent and Hsf1p-dependent manner in Saccharomyces cerevisiae. Genetics *169*, 1203-1214.

Fernandez-Martinez, J., Kim, S.J., Shi, Y., Upla, P., Pellarin, R., Gagnon, M., Chemmama, I.E., Wang, J., Nudelman, I., Zhang, W*., et al.* (2016). Structure and Function of the Nuclear Pore Complex Cytoplasmic mRNA Export Platform. Cell *167*, 1215-1228 e1225.

Fernandez-Martinez, J., and Rout, M.P. (2009). Nuclear pore complex biogenesis. Curr Opin Cell Biol *21*, 603-612.

Feuerbach, F., Galy, V., Trelles-Sticken, E., Fromont-Racine, M., Jacquier, A., Gilson, E., Olivo-Marin, J.C., Scherthan, H., and Nehrbass, U. (2002). Nuclear architecture and spatial positioning help establish transcriptional states of telomeres in yeast. Nat Cell Biol *4*, 214-221.

Fica, S.M., and Nagai, K. (2017). Cryo-electron microscopy snapshots of the spliceosome: structural insights into a dynamic ribonucleoprotein machine. Nat Struct Mol Biol *24*, 791-799.

Field, M.C., Koreny, L., and Rout, M.P. (2014). Enriching the pore: splendid complexity from humble origins. Traffic *15*, 141-156.

Finley, D. (2009). Recognition and processing of ubiquitin-protein conjugates by the proteasome. Annu Rev Biochem *78*, 477-513.

Finley, D., Ulrich, H.D., Sommer, T., and Kaiser, P. (2012). The ubiquitin-proteasome system of Saccharomyces cerevisiae. Genetics *192*, 319-360.

Fischer, J., Teimer, R., Amlacher, S., Kunze, R., and Hurt, E. (2015). Linker Nups connect the nuclear pore complex inner ring with the outer ring and transport channel. Nat Struct Mol Biol *22*, 774-781.

Fischer, T., Cui, B., Dhakshnamoorthy, J., Zhou, M., Rubin, C., Zofall, M., Veenstra, T.D., and Grewal, S.I. (2009). Diverse roles of HP1 proteins in heterochromatin assembly and functions in fission yeast. Proc Natl Acad Sci U S A *106*, 8998-9003.

Fischer, T., Rodriguez-Navarro, S., Pereira, G., Racz, A., Schiebel, E., and Hurt, E. (2004). Yeast centrin Cdc31 is linked to the nuclear mRNA export machinery. Nat Cell Biol *6*, 840-848.

Fischer, T., Strasser, K., Racz, A., Rodriguez-Navarro, S., Oppizzi, M., Ihrig, P., Lechner, J., and Hurt, E. (2002). The mRNA export machinery requires the novel Sac3p-Thp1p complex to dock at the nucleoplasmic entrance of the nuclear pores. EMBO J *21*, 5843-5852.

Fiserova, J., Efenberkova, M., Sieger, T., Maninova, M., Uhlirova, J., and Hozak, P. (2017). Chromatin organization at the nuclear periphery as revealed by image analysis of structured illumination microscopy data. J Cell Sci *130*, 2066-2077.

Fiserova, J., Maninova, M., Sieger, T., Uhlirova, J., Sebestova, L., Efenberkova, M., Capek, M., Fiser, K., and Hozak, P. (2019). Nuclear pore protein TPR associates with lamin B1 and affects nuclear lamina organization and nuclear pore distribution. Cell Mol Life Sci *76*, 2199-2216.

Folco, H.D., Campbell, C.S., May, K.M., Espinoza, C.A., Oegema, K., Hardwick, K.G., Grewal, S.I., and Desai, A. (2015). The CENP-A N-tail confers epigenetic stability to centromeres via the CENP-T branch of the CCAN in fission yeast. Curr Biol *25*, 348-356.

Folco, H.D., Pidoux, A.L., Urano, T., and Allshire, R.C. (2008). Heterochromatin and RNAi are required to establish CENP-A chromatin at centromeres. Science *319*, 94-97.

Folz, H., Nino, C.A., Taranum, S., Caesar, S., Latta, L., Waharte, F., Salamero, J., Schlenstedt, G., and Dargemont, C. (2019). SUMOylation of the nuclear pore complex basket is involved in sensing cellular stresses. J Cell Sci *132*.

Foster, S.A., and Morgan, D.O. (2012). The APC/C subunit Mnd2/Apc15 promotes Cdc20 autoubiquitination and spindle assembly checkpoint inactivation. Mol Cell *47*, 921-932.

Fox, M.J., and Mosley, A.L. (2016). Rrp6: Integrated roles in nuclear RNA metabolism and transcription termination. Wiley interdisciplinary reviews RNA *7*, 91-104.

Frey, S., and Gorlich, D. (2009). FG/FxFG as well as GLFG repeats form a selective permeability barrier with self-healing properties. EMBO J *28*, 2554-2567.

Frosst, P., Guan, T., Subauste, C., Hahn, K., and Gerace, L. (2002). Tpr is localized within the nuclear basket of the pore complex and has a role in nuclear protein export. J Cell Biol *156*, 617-630.

Frost, A., Elgort, M.G., Brandman, O., Ives, C., Collins, S.R., Miller-Vedam, L., Weibezahn, J., Hein, M.Y., Poser, I., Mann, M.*, et al.* (2012). Functional repurposing revealed by comparing S. pombe and S. cerevisiae genetic interactions. Cell *149*, 1339-1352.

Funabiki, H., Hagan, I., Uzawa, S., and Yanagida, M. (1993). Cell cycle-dependent specific positioning and clustering of centromeres and telomeres in fission yeast. J Cell Biol *121*, 961-976.

Gachet, Y., Reyes, C., Courtheoux, T., Goldstone, S., Gay, G., Serrurier, C., and Tournier, S. (2008). Sister kinetochore recapture in fission yeast occurs by two distinct mechanisms, both requiring Dam1 and Klp2. Mol Biol Cell *19*, 1646-1662.

Gaik, M., Flemming, D., von Appen, A., Kastritis, P., Mucke, N., Fischer, J., Stelter, P., Ori, A., Bui, K.H., Bassler, J.*, et al.* (2015). Structural basis for assembly and function of the Nup82 complex in the nuclear pore scaffold. J Cell Biol *208*, 283-297.

Gaits, F., Shiozaki, K., and Russell, P. (1997). Protein phosphatase 2C acts independently of stress-activated kinase cascade to regulate the stress response in fission yeast. J Biol Chem *272*, 17873-17879.

Gallo, G.J., Prentice, H., and Kingston, R.E. (1993). Heat shock factor is required for growth at normal temperatures in the fission yeast Schizosaccharomyces pombe. Mol Cell Biol *13*, 749-761.

Gallo, G.J., Schuetz, T.J., and Kingston, R.E. (1991). Regulation of heat shock factor in Schizosaccharomyces pombe more closely resembles regulation in mammals than in Saccharomyces cerevisiae. Mol Cell Biol *11*, 281-288.

Galy, V., Gadal, O., Fromont-Racine, M., Romano, A., Jacquier, A., and Nehrbass, U. (2004). Nuclear retention of unspliced mRNAs in yeast is mediated by perinuclear Mlp1. Cell *116*, 63-73.

Garcia-Benitez, F., Gaillard, H., and Aguilera, A. (2017). Physical proximity of chromatin to nuclear pores prevents harmful R loop accumulation contributing to maintain genome stability. Proc Natl Acad Sci U S A *114*, 10942-10947.

Garcia-Oliver, E., Garcia-Molinero, V., and Rodriguez-Navarro, S. (2012). mRNA export and gene expression: the SAGA-TREX-2 connection. Biochim Biophys Acta *1819*, 555-565.

Gardner, R.G., Nelson, Z.W., and Gottschling, D.E. (2005). Degradation-mediated protein quality control in the nucleus. Cell *120*, 803-815.

Gasch, A.P., Spellman, P.T., Kao, C.M., Carmel-Harel, O., Eisen, M.B., Storz, G., Botstein, D., and Brown, P.O. (2000). Genomic expression programs in the response of yeast cells to environmental changes. Mol Biol Cell *11*, 4241-4257.

Gascoigne, K.E., Takeuchi, K., Suzuki, A., Hori, T., Fukagawa, T., and Cheeseman, I.M. (2011). Induced ectopic kinetochore assembly bypasses the requirement for CENP-A nucleosomes. Cell *145*, 410-422.

Gavalda, S., Santos-Pereira, J.M., Garcia-Rubio, M.L., Luna, R., and Aguilera, A. (2016). Excess of Yra1 RNA-Binding Factor Causes Transcription-Dependent Genome Instability, Replication Impairment and Telomere Shortening. PLoS Genet *12*, e1005966.

Gialitakis, M., Arampatzi, P., Makatounakis, T., and Papamatheakis, J. (2010). Gamma interferon-dependent transcriptional memory via relocalization of a gene locus to PML nuclear bodies. Mol Cell Biol *30*, 2046-2056.

Gilbert, W., and Guthrie, C. (2004). The Glc7p nuclear phosphatase promotes mRNA export by facilitating association of Mex67p with mRNA. Mol Cell *13*, 201-212.

Gilchrist, D., Mykytka, B., and Rexach, M. (2002). Accelerating the rate of disassembly of karyopherin.cargo complexes. J Biol Chem *277*, 18161-18172.

Glickman, M.H., Rubin, D.M., Fried, V.A., and Finley, D. (1998). The regulatory particle of the Saccharomyces cerevisiae proteasome. Mol Cell Biol *18*, 3149-3162.

Glover, J.R., and Lindquist, S. (1998). Hsp104, Hsp70, and Hsp40: a novel chaperone system that rescues previously aggregated proteins. Cell *94*, 73-82.

Glover, J.R., and Lum, R. (2009). Remodeling of protein aggregates by Hsp104. Protein Pept Lett *16*, 587-597.

Gonzalez, M., He, H., Dong, Q., Sun, S., and Li, F. (2014). Ectopic centromere nucleation by CENP--a in fission yeast. Genetics *198*, 1433-1446.

Gordon, C., McGurk, G., Wallace, M., and Hastie, N.D. (1996). A conditional lethal mutant in the fission yeast 26 S protease subunit mts3+ is defective in metaphase to anaphase transition. J Biol Chem *271*, 5704-5711.

Goshima, G., Saitoh, S., and Yanagida, M. (1999). Proper metaphase spindle length is determined by centromere proteins Mis12 and Mis6 required for faithful chromosome segregation. Genes Dev *13*, 1664-1677.

Goudreault, M., D'Ambrosio, L.M., Kean, M.J., Mullin, M.J., Larsen, B.G., Sanchez, A., Chaudhry, S., Chen, G.I., Sicheri, F., Nesvizhskii, A.I*., et al*. (2009). A PP2A phosphatase high density interaction network identifies a novel striatin-interacting phosphatase and kinase complex linked to the cerebral cavernous malformation 3 (CCM3) protein. Mol Cell Proteomics *8*, 157-171.

Gozalo, A., Duke, A., Lan, Y., Pascual-Garcia, P., Talamas, J.A., Nguyen, S.C., Shah, P.P., Jain, R., Joyce, E.F., and Capelson, M. (2020). Core Components of the Nuclear Pore Bind Distinct States of Chromatin and Contribute to Polycomb Repression. Mol Cell *77*, 67-81 e67.

Grallert, A., Patel, A., Tallada, V.A., Chan, K.Y., Bagley, S., Krapp, A., Simanis, V., and Hagan, I.M. (2013). Centrosomal MPF triggers the mitotic and morphogenetic switches of fission yeast. Nat Cell Biol *15*, 88-95.

Grandi, P., Dang, T., Pane, N., Shevchenko, A., Mann, M., Forbes, D., and Hurt, E. (1997). Nup93, a vertebrate homologue of yeast Nic96p, forms a complex with a novel 205-kDa protein and is required for correct nuclear pore assembly. Mol Biol Cell *8*, 2017-2038.

Grant, R.P., Marshall, N.J., Yang, J.C., Fasken, M.B., Kelly, S.M., Harreman, M.T., Neuhaus, D., Corbett, A.H., and Stewart, M. (2008). Structure of the N-terminal Mlp1-binding domain of the Saccharomyces cerevisiae mRNA-binding protein, Nab2. J Mol Biol *376*, 1048-1059.

Green, D.M., Johnson, C.P., Hagan, H., and Corbett, A.H. (2003). The C-terminal domain of myosin-like protein 1 (Mlp1p) is a docking site for heterogeneous nuclear ribonucleoproteins that are required for mRNA export. Proc Natl Acad Sci U S A *100*, 1010-1015.

Green, E.M., Jiang, Y., Joyner, R., and Weis, K. (2012). A negative feedback loop at the nuclear periphery regulates GAL gene expression. Mol Biol Cell *23*, 1367-1375.

Gregan, J., Riedel, C.G., Pidoux, A.L., Katou, Y., Rumpf, C., Schleiffer, A., Kearsey, S.E., Shirahige, K., Allshire, R.C., and Nasmyth, K. (2007). The kinetochore proteins Pcs1 and Mde4 and heterochromatin are required to prevent merotelic orientation. Curr Biol *17*, 1190-1200.

Grenier St-Sauveur, V., Soucek, S., Corbett, A.H., and Bachand, F. (2013). Poly(A) tail-mediated gene regulation by opposing roles of Nab2 and Pab2 nuclear poly(A)-binding proteins in pre-mRNA decay. Mol Cell Biol *33*, 4718-4731.

Grewal, S.I., and Moazed, D. (2003). Heterochromatin and epigenetic control of gene expression. Science *301*, 798-802.

Grimminger, V., Richter, K., Imhof, A., Buchner, J., and Walter, S. (2004). The prion curing agent guanidinium chloride specifically inhibits ATP hydrolysis by Hsp104. J Biol Chem *279*, 7378-7383.

Groll, M., Bajorek, M., Kohler, A., Moroder, L., Rubin, D.M., Huber, R., Glickman, M.H., and Finley, D. (2000). A gated channel into the proteasome core particle. Nat Struct Biol *7*, 1062-1067.

Gross, C., and Watson, K. (1998). De novo protein synthesis is essential for thermotolerance acquisition in a Saccharomyces cerevisiae trehalose synthase mutant. Biochem Mol Biol Int *45*, 663-671.

Grossman, E., Medalia, O., and Zwerger, M. (2012). Functional architecture of the nuclear pore complex. Annu Rev Biophys *41*, 557-584.

Grummt, I. (2013). The nucleolus-guardian of cellular homeostasis and genome integrity. Chromosoma *122*, 487-497.

Grummt, I., and Voit, R. (2010). Linking rDNA transcription to the cellular energy supply. Cell Cycle *9*, 225-226.

Grunwald, D., and Singer, R.H. (2010). In vivo imaging of labelled endogenous beta-actin mRNA during nucleocytoplasmic transport. Nature *467*, 604-607.

Grunwald, D., Singer, R.H., and Rout, M. (2011). Nuclear export dynamics of RNA-protein complexes. Nature *475*, 333-341.

Gruter, P., Tabernero, C., von Kobbe, C., Schmitt, C., Saavedra, C., Bachi, A., Wilm, M., Felber, B.K., and Izaurralde, E. (1998). TAP, the human homolog of Mex67p, mediates CTE-dependent RNA export from the nucleus. Mol Cell *1*, 649-659.

Gu, Y., Yam, C., and Oliferenko, S. (2012). Divergence of mitotic strategies in fission yeasts. Nucleus *3*, 220-225.

Guerriero, C.J., Weiberth, K.F., and Brodsky, J.L. (2013). Hsp70 targets a cytoplasmic quality control substrate to the San1p ubiquitin ligase. J Biol Chem *288*, 18506-18520.

Guettouche, T., Boellmann, F., Lane, W.S., and Voellmy, R. (2005). Analysis of phosphorylation of human heat shock factor 1 in cells experiencing a stress. BMC Biochem *6*, 4.

Gulli, M.P., Girard, J.P., Zabetakis, D., Lapeyre, B., Melese, T., and Caizergues-Ferrer, M. (1995). gar2 is a nucleolar protein from Schizosaccharomyces pombe required for 18S rRNA and 40S ribosomal subunit accumulation. Nucleic Acids Res *23*, 1912-1918.

Gumeni, S., Evangelakou, Z., Gorgoulis, V.G., and Trougakos, I.P. (2017). Proteome Stability as a Key Factor of Genome Integrity. Int J Mol Sci *18*.

Gupta, R., Kus, B., Fladd, C., Wasmuth, J., Tonikian, R., Sidhu, S., Krogan, N.J., Parkinson, J., and Rotin, D. (2007). Ubiquitination screen using protein microarrays for comprehensive identification of Rsp5 substrates in yeast. Mol Syst Biol *3*, 116.

Guttinger, S., Laurell, E., and Kutay, U. (2009). Orchestrating nuclear envelope disassembly and reassembly during mitosis. Nat Rev Mol Cell Biol *10*, 178-191.

Gwizdek, C., Hobeika, M., Kus, B., Ossareh-Nazari, B., Dargemont, C., and Rodriguez, M.S. (2005). The mRNA nuclear export factor Hpr1 is regulated by Rsp5-mediated ubiquitylation. J Biol Chem *280*, 13401-13405.

Gwizdek, C., Iglesias, N., Rodriguez, M.S., Ossareh-Nazari, B., Hobeika, M., Divita, G., Stutz, F., and Dargemont, C. (2006). Ubiquitin-associated domain of Mex67 synchronizes recruitment of the mRNA export machinery with transcription. Proc Natl Acad Sci U S A *103*, 16376-16381.

Hackmann, A., Wu, H., Schneider, U.M., Meyer, K., Jung, K., and Krebber, H. (2014). Quality control of spliced mRNAs requires the shuttling SR proteins Gbp2 and Hrb1. Nat Commun *5*, 3123.

Hagan, I., Hayles, J., and Nurse, P. (1988). Cloning and sequencing of the cyclin-related cdc13+ gene and a cytological study of its role in fission yeast mitosis. J Cell Sci *91 (Pt 4)*, 587-595.

Hagan, I.M., and Hyams, J.S. (1988). The use of cell division cycle mutants to investigate the control of microtubule distribution in the fission yeast Schizosaccharomyces pombe. J Cell Sci *89 (Pt 3)*, 343-357.

Hagan, I.M.C., A.M.; Grallert, A.; Nurse, P. (2016). Fission Yeast: A Laboratory Manual (Cold Spring Harbor Laboratory Press).

Hahn, J.S., Hu, Z., Thiele, D.J., and Iyer, V.R. (2004). Genome-wide analysis of the biology of stress responses through heat shock transcription factor. Mol Cell Biol *24*, 5249-5256.

Hahn, J.S., Neef, D.W., and Thiele, D.J. (2006). A stress regulatory network for co-ordinated activation of proteasome expression mediated by yeast heat shock transcription factor. Molecular microbiology *60*, 240-251.

Haitani, Y., and Takagi, H. (2008). Rsp5 is required for the nuclear export of mRNA of HSF1 and MSN2/4 under stress conditions in Saccharomyces cerevisiae. Genes to cells : devoted to molecular & cellular mechanisms *13*, 105-116.

Hall, I.M., Noma, K., and Grewal, S.I. (2003). RNA interference machinery regulates chromosome dynamics during mitosis and meiosis in fission yeast. Proc Natl Acad Sci U S A *100*, 193-198.

Hall, I.M., Shankaranarayana, G.D., Noma, K., Ayoub, N., Cohen, A., and Grewal, S.I. (2002). Establishment and maintenance of a heterochromatin domain. Science *297*, 2232-2237.

Hammell, C.M., Gross, S., Zenklusen, D., Heath, C.V., Stutz, F., Moore, C., and Cole, C.N. (2002). Coupling of termination, 3' processing, and mRNA export. Mol Cell Biol *22*, 6441-6457.

Hara, M., and Fukagawa, T. (2017). Critical Foundation of the Kinetochore: The Constitutive Centromere-Associated Network (CCAN). Prog Mol Subcell Biol *56*, 29-57.

Harel, A., Orjalo, A.V., Vincent, T., Lachish-Zalait, A., Vasu, S., Shah, S., Zimmerman, E., Elbaum, M., and Forbes, D.J. (2003). Removal of a single pore subcomplex results in vertebrate nuclei devoid of nuclear pores. Mol Cell *11*, 853-864.

Hase, M.E., and Cordes, V.C. (2003). Direct interaction with nup153 mediates binding of Tpr to the periphery of the nuclear pore complex. Mol Biol Cell *14*, 1923-1940.

Hase, M.E., Kuznetsov, N.V., and Cordes, V.C. (2001). Amino acid substitutions of coiled-coil protein Tpr abrogate anchorage to the nuclear pore complex but not parallel, in-register homodimerization. Mol Biol Cell *12*, 2433-2452.

Hashikawa, N., Mizukami, Y., Imazu, H., and Sakurai, H. (2006). Mutated yeast heat shock transcription factor activates transcription independently of hyperphosphorylation. J Biol Chem *281*, 3936-3942.

Hashikawa, N., Yamamoto, N., and Sakurai, H. (2007). Different mechanisms are involved in the transcriptional activation by yeast heat shock transcription factor through two different types of heat shock elements. J Biol Chem *282*, 10333-10340.

Hasin, N., Cusack, S.A., Ali, S.S., Fitzpatrick, D.A., and Jones, G.W. (2014). Global transcript and phenotypic analysis of yeast cells expressing Ssa1, Ssa2, Ssa3 or Ssa4 as sole source of cytosolic Hsp70-Ssa chaperone activity. BMC Genomics *15*, 194.

Haslbeck, M., Braun, N., Stromer, T., Richter, B., Model, N., Weinkauf, S., and Buchner, J. (2004). Hsp42 is the general small heat shock protein in the cytosol of Saccharomyces cerevisiae. EMBO J *23*, 638-649.

Haslbeck, M., Miess, A., Stromer, T., Walter, S., and Buchner, J. (2005). Disassembling protein aggregates in the yeast cytosol. The cooperation of Hsp26 with Ssa1 and Hsp104. J Biol Chem *280*, 23861-23868.

Haslbeck, M., Walke, S., Stromer, T., Ehrnsperger, M., White, H.E., Chen, S., Saibil, H.R., and Buchner, J. (1999). Hsp26: a temperature-regulated chaperone. EMBO J *18*, 6744-6751.

Hautbergue, G.M., Hung, M.L., Golovanov, A.P., Lian, L.Y., and Wilson, S.A. (2008). Mutually exclusive interactions drive handover of mRNA from export adaptors to TAP. Proc Natl Acad Sci U S A *105*, 5154-5159.

Hayakawa, A., Babour, A., Sengmanivong, L., and Dargemont, C. (2012). Ubiquitylation of the nuclear pore complex controls nuclear migration during mitosis in S. cerevisiae. J Cell Biol *196*, 19-27.

Hayama, R., Rout, M.P., and Fernandez-Martinez, J. (2017). The nuclear pore complex core scaffold and permeability barrier: variations of a common theme. Curr Opin Cell Biol *46*, 110-118.

Hayashi, A., Asakawa, H., Haraguchi, T., and Hiraoka, Y. (2006). Reconstruction of the kinetochore during meiosis in fission yeast Schizosaccharomyces pombe. Mol Biol Cell *17*, 5173-5184.

Hayashi, K., and Matsunaga, S. (2019). Heat and chilling stress induce nucleolus morphological changes. Journal of plant research *132*, 395-403.

Hayashi, T., Ebe, M., Nagao, K., Kokubu, A., Sajiki, K., and Yanagida, M. (2014). Schizosaccharomyces pombe centromere protein Mis19 links Mis16 and Mis18 to recruit CENP-A through interacting with NMD factors and the SWI/SNF complex. Genes to cells : devoted to molecular & cellular mechanisms *19*, 541-554.

Hayashi, T., Fujita, Y., Iwasaki, O., Adachi, Y., Takahashi, K., and Yanagida, M. (2004). Mis16 and Mis18 are required for CENP-A loading and histone deacetylation at centromeres. Cell *118*, 715-729.

Hayles, J., Wood, V., Jeffery, L., Hoe, K.L., Kim, D.U., Park, H.O., Salas-Pino, S., Heichinger, C., and Nurse, P. (2013). A genome-wide resource of cell cycle and cell shape genes of fission yeast. Open Biol *3*, 130053.

Hector, R.E., Nykamp, K.R., Dheur, S., Anderson, J.T., Non, P.J., Urbinati, C.R., Wilson, S.M., Minvielle-Sebastia, L., and Swanson, M.S. (2002). Dual requirement for yeast hnRNP Nab2p in mRNA poly(A) tail length control and nuclear export. EMBO J *21*, 1800-1810.

Hediger, F., Dubrana, K., and Gasser, S.M. (2002a). Myosin-like proteins 1 and 2 are not required for silencing or telomere anchoring, but act in the Tel1 pathway of telomere length control. J Struct Biol *140*, 79-91.

Hediger, F., Neumann, F.R., Van Houwe, G., Dubrana, K., and Gasser, S.M. (2002b). Live imaging of telomeres: yKu and Sir proteins define redundant telomere-anchoring pathways in yeast. Curr Biol *12*, 2076-2089.

Helmlinger, D., Marguerat, S., Villen, J., Gygi, S.P., Bahler, J., and Winston, F. (2008). The S. pombe SAGA complex controls the switch from proliferation to sexual differentiation through the opposing roles of its subunits Gcn5 and Spt8. Genes Dev *22*, 3184-3195.

Herbomel, G., Kloster-Landsberg, M., Folco, E.G., Col, E., Usson, Y., Vourc'h, C., Delon, A., and Souchier, C. (2013). Dynamics of the full length and mutated heat shock factor 1 in human cells. PLoS One *8*, e67566.

Hernandez-Verdun, D., Roussel, P., Thiry, M., Sirri, V., and Lafontaine, D.L. (2010). The nucleolus: structure/function relationship in RNA metabolism. Wiley interdisciplinary reviews RNA *1*, 415-431.

Herrero, E., and Thorpe, P.H. (2016). Synergistic Control of Kinetochore Protein Levels by Psh1 and Ubr2. PLoS Genet *12*, e1005855.

Hessle, V., von Euler, A., Gonzalez de Valdivia, E., and Visa, N. (2012). Rrp6 is recruited to transcribed genes and accompanies the spliced mRNA to the nuclear pore. RNA *18*, 1466-1474.

Hewawasam, G., Shivaraju, M., Mattingly, M., Venkatesh, S., Martin-Brown, S., Florens, L., Workman, J.L., and Gerton, J.L. (2010). Psh1 is an E3 ubiquitin ligase that targets the centromeric histone variant Cse4. Mol Cell *40*, 444-454.

Hilleren, P., and Parker, R. (2001). Defects in the mRNA export factors Rat7p, Gle1p, Mex67p, and Rat8p cause hyperadenylation during 3'-end formation of nascent transcripts. RNA *7*, 753-764.

Hinshaw, S.M., and Harrison, S.C. (2018). Kinetochore Function from the Bottom Up. Trends Cell Biol *28*, 22-33.

Hirai, H., Arai, K., Kariyazono, R., Yamamoto, M., and Sato, M. (2014). The kinetochore protein Kis1/Eic1/Mis19 ensures the integrity of mitotic spindles through maintenance of kinetochore factors Mis6/CENP-I and CENP-A. PLoS One *9*, e111905.

Hirano, T., Konoha, G., Toda, T., and Yanagida, M. (1989). Essential roles of the RNA polymerase I largest subunit and DNA topoisomerases in the formation of fission yeast nucleolus. J Cell Biol *108*, 243-253.

Ho, C.T., Grousl, T., Shatz, O., Jawed, A., Ruger-Herreros, C., Semmelink, M., Zahn, R., Richter, K., Bukau, B., and Mogk, A. (2019). Cellular sequestrases maintain basal Hsp70 capacity ensuring balanced proteostasis. Nat Commun *10*, 4851.

Hochberg-Laufer, H., Schwed-Gross, A., Neugebauer, K.M., and Shav-Tal, Y. (2019). Uncoupling of nucleo-cytoplasmic RNA export and localization during stress. Nucleic Acids Res *47*, 4778-4797.

Hocine, S., Singer, R.H., and Grunwald, D. (2010). RNA processing and export. Cold Spring Harb Perspect Biol *2*, a000752.

Hodge, C.A., Tran, E.J., Noble, K.N., Alcazar-Roman, A.R., Ben-Yishay, R., Scarcelli, J.J., Folkmann, A.W., Shav-Tal, Y., Wente, S.R., and Cole, C.N. (2011). The Dbp5 cycle at the nuclear pore complex during mRNA export I: dbp5 mutants with defects in RNA binding and ATP hydrolysis define key steps for Nup159 and Gle1. Genes Dev *25*, 1052-1064.

Hodges, A.J., Plummer, D.A., and Wyrick, J.J. (2019). NuA4 acetyltransferase is required for efficient nucleotide excision repair in yeast. DNA Repair (Amst) *73*, 91-98.

Hoffman, C.S., Wood, V., and Fantes, P.A. (2015). An Ancient Yeast for Young Geneticists: A Primer on the Schizosaccharomyces pombe Model System. Genetics *201*, 403-423.

Hofmann, C., Cheeseman, I.M., Goode, B.L., McDonald, K.L., Barnes, G., and Drubin, D.G. (1998). Saccharomyces cerevisiae Duo1p and Dam1p, novel proteins involved in mitotic spindle function. J Cell Biol *143*, 1029-1040.

Hohmann, S.M., W. H. (2003). Yeast Stress Responses.

Holzer, G., and Antonin, W. (2018). Nuclear Pore Complexes: Global Conservation and Local Variation. Curr Biol *28*, R674-R677.

Holzer, G., and Antonin, W. (2019). Breaking the Y. PLoS Genet *15*, e1008109.

Hong, Y., Rogers, R., Matunis, M.J., Mayhew, C.N., Goodson, M.L., Park-Sarge, O.K., and Sarge, K.D. (2001). Regulation of heat shock transcription factor 1 by stress-induced SUMO-1 modification. J Biol Chem *276*, 40263-40267.

Hori, T., Amano, M., Suzuki, A., Backer, C.B., Welburn, J.P., Dong, Y., McEwen, B.F., Shang, W.H., Suzuki, E., Okawa, K.*, et al.* (2008). CCAN makes multiple contacts with centromeric DNA to provide distinct pathways to the outer kinetochore. Cell *135*, 1039-1052.

Hori, T., Shang, W.H., Takeuchi, K., and Fukagawa, T. (2013). The CCAN recruits CENP-A to the centromere and forms the structural core for kinetochore assembly. J Cell Biol *200*, 45-60.

Horton, L.E., James, P., Craig, E.A., and Hensold, J.O. (2001). The yeast hsp70 homologue Ssa is required for translation and interacts with Sis1 and Pab1 on translating ribosomes. J Biol Chem *276*, 14426-14433.

Hottiger, T., De Virgilio, C., Hall, M.N., Boller, T., and Wiemken, A. (1994). The role of trehalose synthesis for the acquisition of thermotolerance in yeast. II. Physiological concentrations of trehalose increase the thermal stability of proteins in vitro. European journal of biochemistry *219*, 187-193.

Hou, H., Zhou, Z., Wang, Y., Wang, J., Kallgren, S.P., Kurchuk, T., Miller, E.A., Chang, F., and Jia, S. (2012). Csi1 links centromeres to the nuclear envelope for centromere clustering. J Cell Biol *199*, 735-744.

Houseley, J., LaCava, J., and Tollervey, D. (2006). RNA-quality control by the exosome. Nat Rev Mol Cell Biol *7*, 529-539.

Hsin, J.P., Xiang, K., and Manley, J.L. (2014). Function and control of RNA polymerase II C-terminal domain phosphorylation in vertebrate transcription and RNA processing. Mol Cell Biol *34*, 2488-2498.

Huertas, P., and Aguilera, A. (2003). Cotranscriptionally formed DNA:RNA hybrids mediate transcription elongation impairment and transcription-associated recombination. Mol Cell *12*, 711-721.

Hugle, B., Kleinschmidt, J.A., and Franke, W.W. (1983). The 22 S cylinder particles of Xenopus laevis. II. Immunological characterization and localization of their proteins in tissues and cultured cells. Eur J Cell Biol *32*, 157-163.

Huis In 't Veld, P.J., Jeganathan, S., Petrovic, A., Singh, P., John, J., Krenn, V., Weissmann, F., Bange, T., and Musacchio, A. (2016). Molecular basis of outer kinetochore assembly on CENP-T. eLife *5*.

Huisinga, K.L., Brower-Toland, B., and Elgin, S.C. (2006). The contradictory definitions of heterochromatin: transcription and silencing. Chromosoma *115*, 110-122.

Hung, M.L., Hautbergue, G.M., Snijders, A.P., Dickman, M.J., and Wilson, S.A. (2010). Arginine methylation of REF/ALY promotes efficient handover of mRNA to TAP/NXF1. Nucleic Acids Res *38*, 3351-3361.

Hurt, E., Luo, M.J., Rother, S., Reed, R., and Strasser, K. (2004). Cotranscriptional recruitment of the serine-arginine-rich (SR)-like proteins Gbp2 and Hrb1 to nascent mRNA via the TREX complex. Proc Natl Acad Sci U S A *101*, 1858-1862.

Hurt, E., Strasser, K., Segref, A., Bailer, S., Schlaich, N., Presutti, C., Tollervey, D., and Jansen, R. (2000). Mex67p mediates nuclear export of a variety of RNA polymerase II transcripts. J Biol Chem *275*, 8361-8368.

Ibarra, A., Benner, C., Tyagi, S., Cool, J., and Hetzer, M.W. (2016). Nucleoporin-mediated regulation of cell identity genes. Genes Dev *30*, 2253-2258.

Ibarra, A., and Hetzer, M.W. (2015). Nuclear pore proteins and the control of genome functions. Genes Dev *29*, 337-349.

Iglesias, N., Paulo, J.A., Tatarakis, A., Wang, X., Edwards, A.L., Bhanu, N.V., Garcia, B.A., Haas, W., Gygi, S.P., and Moazed, D. (2020). Native Chromatin Proteomics Reveals a Role for Specific Nucleoporins in Heterochromatin Organization and Maintenance. Mol Cell *77*, 51-66 e58.

Iglesias, N., and Stutz, F. (2008). Regulation of mRNP dynamics along the export pathway. FEBS letters *582*, 1987-1996.

Iglesias, N., Tutucci, E., Gwizdek, C., Vinciguerra, P., Von Dach, E., Corbett, A.H., Dargemont, C., and Stutz, F. (2010). Ubiquitin-mediated mRNP dynamics and surveillance prior to budding yeast mRNA export. Genes Dev *24*, 1927-1938.

Imazu, H., and Sakurai, H. (2005). Saccharomyces cerevisiae heat shock transcription factor regulates cell wall remodeling in response to heat shock. Eukaryot Cell *4*, 1050-1056.

Inoue, H., Nojima, H., and Okayama, H. (1990). High efficiency transformation of Escherichia coli with plasmids. Gene *96*, 23-28.

Isaac, S., Walfridsson, J., Zohar, T., Lazar, D., Kahan, T., Ekwall, K., and Cohen, A. (2007). Interaction of Epe1 with the heterochromatin assembly pathway in Schizosaccharomyces pombe. Genetics *175*, 1549-1560.

Ishii, K., Arib, G., Lin, C., Van Houwe, G., and Laemmli, U.K. (2002). Chromatin boundaries in budding yeast: the nuclear pore connection. Cell *109*, 551-562.

Iwasaki, O., and Noma, K. (2012). Global genome organization mediated by RNA polymerase III-transcribed genes in fission yeast. Gene *493*, 195-200.

Izawa, S., Takemura, R., and Inoue, Y. (2004). Gle2p is essential to induce adaptation of the export of bulk poly(A)+ mRNA to heat shock in Saccharomyces cerevisiae. J Biol Chem *279*, 35469-35478.

Jacinto, F.V., Benner, C., and Hetzer, M.W. (2015). The nucleoporin Nup153 regulates embryonic stem cell pluripotency through gene silencing. Genes Dev *29*, 1224-1238.

Jacob, M.D., Audas, T.E., Uniacke, J., Trinkle-Mulcahy, L., and Lee, S. (2013). Environmental cues induce a long noncoding RNA-dependent remodeling of the nucleolus. Mol Biol Cell *24*, 2943-2953.

Jacob, S.T. (1995). Regulation of ribosomal gene transcription. Biochem J *306 (Pt 3)*, 617-626.

Jacquet, M., Renault, G., Lallet, S., De Mey, J., and Goldbeter, A. (2003). Oscillatory nucleocytoplasmic shuttling of the general stress response transcriptional activators Msn2 and Msn4 in Saccharomyces cerevisiae. J Cell Biol *161*, 497-505.

Jakobsen, B.K., and Pelham, H.R. (1988). Constitutive binding of yeast heat shock factor to DNA in vivo. Mol Cell Biol *8*, 5040-5042.

Jani, D., Lutz, S., Hurt, E., Laskey, R.A., Stewart, M., and Wickramasinghe, V.O. (2012). Functional and structural characterization of the mammalian TREX-2 complex that links transcription with nuclear messenger RNA export. Nucleic Acids Res *40*, 4562-4573.

Jani, D., Valkov, E., and Stewart, M. (2014). Structural basis for binding the TREX2 complex to nuclear pores, GAL1 localisation and mRNA export. Nucleic Acids Res *42*, 6686-6697.

Jaspersen, S.L., and Ghosh, S. (2012). Nuclear envelope insertion of spindle pole bodies and nuclear pore complexes. Nucleus *3*, 226-236.

Jensen, T.H., Dower, K., Libri, D., and Rosbash, M. (2003). Early formation of mRNP: license for export or quality control? Mol Cell *11*, 1129-1138.

Jensen, T.H., Patricio, K., McCarthy, T., and Rosbash, M. (2001). A block to mRNA nuclear export in S. cerevisiae leads to hyperadenylation of transcripts that accumulate at the site of transcription. Mol Cell *7*, 887-898.

Jia, S., Noma, K., and Grewal, S.I. (2004). RNAi-independent heterochromatin nucleation by the stress-activated ATF/CREB family proteins. Science *304*, 1971-1976.

Jimeno, S., Rondon, A.G., Luna, R., and Aguilera, A. (2002). The yeast THO complex and mRNA export factors link RNA metabolism with transcription and genome instability. EMBO J *21*, 3526-3535.

Johnson, S.A., Cubberley, G., and Bentley, D.L. (2009). Cotranscriptional recruitment of the mRNA export factor Yra1 by direct interaction with the 3' end processing factor Pcf11. Mol Cell *33*, 215-226.

Jolly, C., Usson, Y., and Morimoto, R.I. (1999). Rapid and reversible relocalization of heat shock factor 1 within seconds to nuclear stress granules. Proc Natl Acad Sci U S A *96*, 6769-6774.

Josse, L., Harley, M.E., Pires, I.M., and Hughes, D.A. (2006). Fission yeast Dss1 associates with the proteasome and is required for efficient ubiquitin-dependent proteolysis. Biochem J *393*, 303-309.

Ju, Q., and Warner, J.R. (1994). Ribosome synthesis during the growth cycle of Saccharomyces cerevisiae. Yeast *10*, 151-157.

Jung, G., Jones, G., and Masison, D.C. (2002). Amino acid residue 184 of yeast Hsp104 chaperone is critical for prion-curing by guanidine, prion propagation, and thermotolerance. Proc Natl Acad Sci U S A *99*, 9936-9941.

Kabachinski, G., and Schwartz, T.U. (2015). The nuclear pore complex--structure and function at a glance. J Cell Sci *128*, 423-429.

Kadowaki, T., Chen, S., Hitomi, M., Jacobs, E., Kumagai, C., Liang, S., Schneiter, R., Singleton, D., Wisniewska, J., and Tartakoff, A.M. (1994). Isolation and characterization of Saccharomyces cerevisiae mRNA transport-defective (mtr) mutants. J Cell Biol *126*, 649-659.

Kaimal, J.M., Kandasamy, G., Gasser, F., and Andreasson, C. (2017). Coordinated Hsp110 and Hsp104 Activities Power Protein Disaggregation in Saccharomyces cerevisiae. Mol Cell Biol *37*.

Kalverda, B., and Fornerod, M. (2010). Characterization of genome-nucleoporin interactions in Drosophila links chromatin insulators to the nuclear pore complex. Cell Cycle *9*, 4812-4817.

Kalverda, B., Pickersgill, H., Shloma, V.V., and Fornerod, M. (2010). Nucleoporins directly stimulate expression of developmental and cell-cycle genes inside the nucleoplasm. Cell *140*, 360-371.

Kanoh, J., and Ishikawa, F. (2001). spRap1 and spRif1, recruited to telomeres by Taz1, are essential for telomere function in fission yeast. Curr Biol *11*, 1624-1630.

Kanoh, J., Sadaie, M., Urano, T., and Ishikawa, F. (2005). Telomere binding protein Taz1 establishes Swi6 heterochromatin independently of RNAi at telomeres. Curr Biol *15*, 1808-1819.

Kar, B., Liu, B., Zhou, Z., and Lam, Y.W. (2011). Quantitative nucleolar proteomics reveals nuclear re-organization during stress- induced senescence in mouse fibroblast. BMC Cell Biol *12*, 33.

Karmon, O., and Ben Aroya, S. (2019). Spatial Organization of Proteasome Aggregates in the Regulation of Proteasome Homeostasis. Front Mol Biosci *6*, 150.

Katahira, J. (2012). mRNA export and the TREX complex. Biochim Biophys Acta *1819*, 507-513.

Katahira, J. (2015). Nuclear export of messenger RNA. Genes (Basel) *6*, 163-184.

Katahira, J., Strasser, K., Podtelejnikov, A., Mann, M., Jung, J.U., and Hurt, E. (1999). The Mex67p-mediated nuclear mRNA export pathway is conserved from yeast to human. EMBO J *18*, 2593-2609.

Kato, H., Jiang, J., Zhou, B.R., Rozendaal, M., Feng, H., Ghirlando, R., Xiao, T.S., Straight, A.F., and Bai, Y. (2013). A conserved mechanism for centromeric nucleosome recognition by centromere protein CENP-C. Science *340*, 1110-1113.

Kay, R.J., Russnak, R.H., Jones, D., Mathias, C., and Candido, E.P. (1987). Expression of intron-containing C. elegans heat shock genes in mouse cells demonstrates divergence of 3' splice site recognition sequences between nematodes and vertebrates, and an inhibitory effect of heat shock on the mammalian splicing apparatus. Nucleic Acids Res *15*, 3723-3741.

Kearsey, S.E., Stevenson, A.L., Toda, T., and Wang, S.W. (2007). Fission yeast Cut8 is required for the repair of DNA double-strand breaks, ribosomal DNA maintenance, and cell survival in the absence of Rqh1 helicase. Mol Cell Biol *27*, 1558-1567.

Kedersha, N., Stoecklin, G., Ayodele, M., Yacono, P., Lykke-Andersen, J., Fritzler, M.J., Scheuner, D., Kaufman, R.J., Golan, D.E., and Anderson, P. (2005). Stress granules and processing bodies are dynamically linked sites of mRNP remodeling. J Cell Biol *169*, 871-884.

Kelich, J.M., and Yang, W. (2014). High-resolution imaging reveals new features of nuclear export of mRNA through the nuclear pore complexes. Int J Mol Sci *15*, 14492-14504.

Keller, C., Adaixo, R., Stunnenberg, R., Woolcock, K.J., Hiller, S., and Buhler, M. (2012). HP1(Swi6) mediates the recognition and destruction of heterochromatic RNA transcripts. Mol Cell *47*, 215-227.

Kelly, S.M., and Corbett, A.H. (2009). Messenger RNA export from the nucleus: a series of molecular wardrobe changes. Traffic *10*, 1199-1208.

Kelly, S.M., Leung, S.W., Pak, C., Banerjee, A., Moberg, K.H., and Corbett, A.H. (2014). A conserved role for the zinc finger polyadenosine RNA binding protein, ZC3H14, in control of poly(A) tail length. RNA *20*, 681-688.

Kendirgi, F., Rexer, D.J., Alcazar-Roman, A.R., Onishko, H.M., and Wente, S.R. (2005). Interaction between the shuttling mRNA export factor Gle1 and the nucleoporin hCG1: a conserved mechanism in the export of Hsp70 mRNA. Mol Biol Cell *16*, 4304-4315.

Kerres, A., Jakopec, V., Beuter, C., Karig, I., Pohlmann, J., Pidoux, A., Allshire, R., and Fleig, U. (2006). Fta2, an essential fission yeast kinetochore component, interacts closely with the conserved Mal2 protein. Mol Biol Cell *17*, 4167-4178.

Khalouei, S., Chow, A.M., and Brown, I.R. (2014). Localization of heat shock protein HSPA6 (HSP70B') to sites of transcription in cultured differentiated human neuronal cells following thermal stress. J Neurochem *131*, 743-754.

Kim, D.I., Birendra, K.C., and Roux, K.J. (2015). Making the LINC: SUN and KASH protein interactions. Biol Chem *396*, 295-310.

Kim, D.U., Hayles, J., Kim, D., Wood, V., Park, H.O., Won, M., Yoo, H.S., Duhig, T., Nam, M., Palmer, G.*, et al.* (2010). Analysis of a genome-wide set of gene deletions in the fission yeast Schizosaccharomyces pombe. Nat Biotechnol *28*, 617-623.

Kim, S.A., Yoon, J.H., Lee, S.H., and Ahn, S.G. (2005). Polo-like kinase 1 phosphorylates heat shock transcription factor 1 and mediates its nuclear translocation during heat stress. J Biol Chem *280*, 12653-12657.

Kim, S.J., Fernandez-Martinez, J., Nudelman, I., Shi, Y., Zhang, W., Raveh, B., Herricks, T., Slaughter, B.D., Hogan, J.A., Upla, P.*, et al.* (2018). Integrative structure and functional anatomy of a nuclear pore complex. Nature *555*, 475-482.

Kim, S.J., Fernandez-Martinez, J., Sampathkumar, P., Martel, A., Matsui, T., Tsuruta, H., Weiss, T.M., Shi, Y., Markina-Inarrairaegui, A., Bonanno, J.B.*, et al.* (2014). Integrative structure-function mapping of the nucleoporin Nup133 suggests a conserved mechanism for membrane anchoring of the nuclear pore complex. Mol Cell Proteomics *13*, 2911-2926.

Kim, W.J., Lee, S., Park, M.S., Jang, Y.K., Kim, J.B., and Park, S.D. (2000). Rad22 protein, a rad52 homologue in Schizosaccharomyces pombe, binds to DNA double-strand breaks. J Biol Chem *275*, 35607-35611.

King, M.C., Drivas, T.G., and Blobel, G. (2008). A network of nuclear envelope membrane proteins linking centromeres to microtubules. Cell *134*, 427-438.

Kirstein, J., Arnsburg, K., Scior, A., Szlachcic, A., Guilbride, D.L., Morimoto, R.I., Bukau, B., and Nillegoda, N.B. (2017). In vivo properties of the disaggregase function of J-proteins and Hsc70 in Caenorhabditis elegans stress and aging. Aging Cell *16*, 1414-1424.

Kiseleva, E., Allen, T.D., Rutherford, S., Bucci, M., Wente, S.R., and Goldberg, M.W. (2004). Yeast nuclear pore complexes have a cytoplasmic ring and internal filaments. J Struct Biol *145*, 272-288.

Kitagawa, T., Ishii, K., Takeda, K., and Matsumoto, T. (2014). The 19S proteasome subunit Rpt3 regulates distribution of CENP-A by associating with centromeric chromatin. Nat Commun *5*, 3597.

Kitamura, E., Tanaka, K., Kitamura, Y., and Tanaka, T.U. (2007). Kinetochore microtubule interaction during S phase in Saccharomyces cerevisiae. Genes Dev *21*, 3319-3330.

Klare, K., Weir, J.R., Basilico, F., Zimniak, T., Massimiliano, L., Ludwigs, N., Herzog, F., and Musacchio, A. (2015). CENP-C is a blueprint for constitutive centromere-associated network assembly within human kinetochores. J Cell Biol *210*, 11-22.

Kniola, B., O'Toole, E., McIntosh, J.R., Mellone, B., Allshire, R., Mengarelli, S., Hultenby, K., and Ekwall, K. (2001). The domain structure of centromeres is conserved from fission yeast to humans. Mol Biol Cell *12*, 2767-2775.

Knockenhauer, K.E., and Schwartz, T.U. (2016). The Nuclear Pore Complex as a Flexible and Dynamic Gate. Cell *164*, 1162-1171.

Kohler, A., and Hurt, E. (2007). Exporting RNA from the nucleus to the cytoplasm. Nat Rev Mol Cell Biol *8*, 761-773.

Komarnitsky, P., Cho, E.J., and Buratowski, S. (2000). Different phosphorylated forms of RNA polymerase II and associated mRNA processing factors during transcription. Genes Dev *14*, 2452-2460.

Kops, G.J., and Shah, J.V. (2012). Connecting up and clearing out: how kinetochore attachment silences the spindle assembly checkpoint. Chromosoma *121*, 509-525.

Korntner-Vetter, M., Lefevre, S., Hu, X.W., George, R., and Singleton, M.R. (2019). Subunit interactions and arrangements in the fission yeast Mis16-Mis18-Mis19 complex. Life Sci Alliance *2*.

Kosinski, J., Mosalaganti, S., von Appen, A., Teimer, R., DiGuilio, A.L., Wan, W., Bui, K.H., Hagen, W.J., Briggs, J.A., Glavy, J.S.*, et al.* (2016). Molecular architecture of the inner ring scaffold of the human nuclear pore complex. Science *352*, 363-365.

Kosova, B., Pante, N., Rollenhagen, C., Podtelejnikov, A., Mann, M., Aebi, U., and Hurt, E. (2000). Mlp2p, a component of nuclear pore attached intranuclear filaments, associates with nic96p. J Biol Chem *275*, 343-350.

Kraemer, D.M., Strambio-de-Castillia, C., Blobel, G., and Rout, M.P. (1995). The essential yeast nucleoporin NUP159 is located on the cytoplasmic side of the nuclear pore complex and serves in karyopherin-mediated binding of transport substrate. J Biol Chem *270*, 19017-19021.

Krakowiak, J., Zheng, X., Patel, N., Feder, Z.A., Anandhakumar, J., Valerius, K., Gross, D.S., Khalil, A.S., and Pincus, D. (2018). Hsf1 and Hsp70 constitute a two-component feedback loop that regulates the yeast heat shock response. eLife *7*.

Krebber, H., Taura, T., Lee, M.S., and Silver, P.A. (1999). Uncoupling of the hnRNP Npl3p from mRNAs during the stress-induced block in mRNA export. Genes Dev *13*, 1994-2004.

Kress, T.L., Krogan, N.J., and Guthrie, C. (2008). A single SR-like protein, Npl3, promotes pre-mRNA splicing in budding yeast. Mol Cell *32*, 727-734.

Kriegenburg, F., Jakopec, V., Poulsen, E.G., Nielsen, S.V., Roguev, A., Krogan, N., Gordon, C., Fleig, U., and Hartmann-Petersen, R. (2014). A chaperone-assisted degradation pathway targets kinetochore proteins to ensure genome stability. PLoS Genet *10*, e1004140.

Krull, S., Dorries, J., Boysen, B., Reidenbach, S., Magnius, L., Norder, H., Thyberg, J., and Cordes, V.C. (2010). Protein Tpr is required for establishing nuclear pore-associated zones of heterochromatin exclusion. EMBO J *29*, 1659-1673.

Krull, S., Thyberg, J., Bjorkroth, B., Rackwitz, H.R., and Cordes, V.C. (2004). Nucleoporins as components of the nuclear pore complex core structure and Tpr as the architectural element of the nuclear basket. Mol Biol Cell *15*, 4261-4277.

Kudo, N., Taoka, H., Toda, T., Yoshida, M., and Horinouchi, S. (1999). A novel nuclear export signal sensitive to oxidative stress in the fission yeast transcription factor Pap1. J Biol Chem *274*, 15151-15158.

Kuhl, N.M., and Rensing, L. (2000). Heat shock effects on cell cycle progression. Cell Mol Life Sci *57*, 450-463.

Kuhn, T.M., and Capelson, M. (2019). Nuclear Pore Proteins in Regulation of Chromatin State. Cells *8*.

Kuhn, U., Buschmann, J., and Wahle, E. (2017). The nuclear poly(A) binding protein of mammals, but not of fission yeast, participates in mRNA polyadenylation. RNA *23*, 473-482.

Kundu, S., and Peterson, C.L. (2009). Role of chromatin states in transcriptional memory. Biochim Biophys Acta *1790*, 445-455.

Kurshakova, M.M., Krasnov, A.N., Kopytova, D.V., Shidlovskii, Y.V., Nikolenko, J.V., Nabirochkina, E.N., Spehner, D., Schultz, P., Tora, L., and Georgieva, S.G. (2007). SAGA and a novel Drosophila export complex anchor efficient transcription and mRNA export to NPC. EMBO J *26*, 4956-4965.

Kwak, J., Workman, J.L., and Lee, D. (2011). The proteasome and its regulatory roles in gene expression. Biochim Biophys Acta *1809*, 88-96.

Kylberg, K., Bjork, P., Fomproix, N., Ivarsson, B., Wieslander, L., and Daneholt, B. (2010). Exclusion of mRNPs and ribosomal particles from a thin zone beneath the nuclear envelope revealed upon inhibition of transport. Exp Cell Res *316*, 1028-1038.

la Cour, T., Kiemer, L., Molgaard, A., Gupta, R., Skriver, K., and Brunak, S. (2004). Analysis and prediction of leucine-rich nuclear export signals. Protein Eng Des Sel *17*, 527-536.

Labade, A.S., Karmodiya, K., and Sengupta, K. (2016). HOXA repression is mediated by nucleoporin Nup93 assisted by its interactors Nup188 and Nup205. Epigenetics Chromatin *9*, 54.

Lafarga, M., Fernandez, R., Mayo, I., Berciano, M.T., and Castano, J.G. (2002). Proteasome dynamics during cell cycle in rat Schwann cells. Glia *38*, 313-328.

Laine, J.P., Singh, B.N., Krishnamurthy, S., and Hampsey, M. (2009). A physiological role for gene loops in yeast. Genes Dev *23*, 2604-2609.

Lamke, J., Brzezinka, K., and Baurle, I. (2016). HSFA2 orchestrates transcriptional dynamics after heat stress in Arabidopsis thaliana. Transcription *7*, 111-114.

Lapetina, D.L., Ptak, C., Roesner, U.K., and Wozniak, R.W. (2017). Yeast silencing factor Sir4 and a subset of nucleoporins form a complex distinct from nuclear pore complexes. J Cell Biol *216*, 3145-3159.

Laporte, D., Salin, B., Daignan-Fornier, B., and Sagot, I. (2008). Reversible cytoplasmic localization of the proteasome in quiescent yeast cells. J Cell Biol *181*, 737-745.

Lara-Gonzalez, P., Westhorpe, F.G., and Taylor, S.S. (2012). The spindle assembly checkpoint. Curr Biol *22*, R966-980.

Latonen, L. (2019). Phase-to-Phase With Nucleoli - Stress Responses, Protein Aggregation and Novel Roles of RNA. Frontiers in cellular neuroscience *13*, 151.

Lee, D.H., and Goldberg, A.L. (1998). Proteasome inhibitors: valuable new tools for cell biologists. Trends Cell Biol *8*, 397-403.

Lee, P., Cho, B.R., Joo, H.S., and Hahn, J.S. (2008a). Yeast Yak1 kinase, a bridge between PKA and stress-responsive transcription factors, Hsf1 and Msn2/Msn4. Molecular microbiology *70*, 882-895.

Lee, S.H., Sterling, H., Burlingame, A., and McCormick, F. (2008b). Tpr directly binds to Mad1 and Mad2 and is important for the Mad1-Mad2-mediated mitotic spindle checkpoint. Genes Dev *22*, 2926-2931.

Lelandais, G., and Devaux, F. (2010). Comparative functional genomics of stress responses in yeasts. OMICS *14*, 501-515.

Lemaitre, C., and Bickmore, W.A. (2015). Chromatin at the nuclear periphery and the regulation of genome functions. Histochemistry and cell biology *144*, 111-122.

Lemieux, C., and Bachand, F. (2009). Cotranscriptional recruitment of the nuclear poly(A)-binding protein Pab2 to nascent transcripts and association with translating mRNPs. Nucleic Acids Res *37*, 3418-3430.

Lemieux, C., Marguerat, S., Lafontaine, J., Barbezier, N., Bahler, J., and Bachand, F. (2011). A Pre-mRNA degradation pathway that selectively targets intron-containing genes requires the nuclear poly(A)-binding protein. Mol Cell *44*, 108-119.

Leung, S.W., Apponi, L.H., Cornejo, O.E., Kitchen, C.M., Valentini, S.R., Pavlath, G.K., Dunham, C.M., and Corbett, A.H. (2009). Splice variants of the human ZC3H14 gene generate multiple isoforms of a zinc finger polyadenosine RNA binding protein. Gene *439*, 71-78.

Levin, D.E. (2005). Cell wall integrity signaling in Saccharomyces cerevisiae. Microbiol Mol Biol Rev *69*, 262-291.

Lewis, A., Felberbaum, R., and Hochstrasser, M. (2007). A nuclear envelope protein linking nuclear pore basket assembly, SUMO protease regulation, and mRNA surveillance. J Cell Biol *178*, 813-827.

Li, C., Goryaynov, A., and Yang, W. (2016). The selective permeability barrier in the nuclear pore complex. Nucleus *7*, 430-446.

Li, Y., Bachant, J., Alcasabas, A.A., Wang, Y., Qin, J., and Elledge, S.J. (2002). The mitotic spindle is required for loading of the DASH complex onto the kinetochore. Genes Dev *16*, 183-197.

Liang, Y., Franks, T.M., Marchetto, M.C., Gage, F.H., and Hetzer, M.W. (2013). Dynamic association of NUP98 with the human genome. PLoS Genet *9*, e1003308.

Light, W.H., Brickner, D.G., Brand, V.R., and Brickner, J.H. (2010). Interaction of a DNA zip code with the nuclear pore complex promotes H2A.Z incorporation and INO1 transcriptional memory. Mol Cell *40*, 112-125.

Light, W.H., and Brickner, J.H. (2013). Nuclear pore proteins regulate chromatin structure and transcriptional memory by a conserved mechanism. Nucleus *4*, 357-360.

Light, W.H., Freaney, J., Sood, V., Thompson, A., D'Urso, A., Horvath, C.M., and Brickner, J.H. (2013). A conserved role for human Nup98 in altering chromatin structure and promoting epigenetic transcriptional memory. PLoS Biol *11*, e1001524.

Lim, R.Y., Huang, N.P., Koser, J., Deng, J., Lau, K.H., Schwarz-Herion, K., Fahrenkrog, B., and Aebi, U. (2006). Flexible phenylalanine-glycine nucleoporins as entropic barriers to nucleocytoplasmic transport. Proc Natl Acad Sci U S A *103*, 9512-9517.

Lin, D.H., Stuwe, T., Schilbach, S., Rundlet, E.J., Perriches, T., Mobbs, G., Fan, Y., Thierbach, K., Huber, F.M., Collins, L.N.*, et al.* (2016). Architecture of the symmetric core of the nuclear pore. Science *352*, aaf1015.

Lince-Faria, M., Maffini, S., Orr, B., Ding, Y., Claudia, F., Sunkel, C.E., Tavares, A., Johansen, J., Johansen, K.M., and Maiato, H. (2009). Spatiotemporal control of mitosis by the conserved spindle matrix protein Megator. J Cell Biol *184*, 647-657.

Lindquist, S., and Craig, E.A. (1988). The heat-shock proteins. Annu Rev Genet *22*, 631-677.

Lindquist, S., and Kim, G. (1996). Heat-shock protein 104 expression is sufficient for thermotolerance in yeast. Proc Natl Acad Sci U S A *93*, 5301-5306.

Lindsay, M.E., Plafker, K., Smith, A.E., Clurman, B.E., and Macara, I.G. (2002). Npap60/Nup50 is a tri-stable switch that stimulates importin-alpha:beta-mediated nuclear protein import. Cell *110*, 349-360.

Lipford, J.R., and Deshaies, R.J. (2003). Diverse roles for ubiquitin-dependent proteolysis in transcriptional activation. Nat Cell Biol *5*, 845-850.

Lisby, M., Rothstein, R., and Mortensen, U.H. (2001). Rad52 forms DNA repair and recombination centers during S phase. Proc Natl Acad Sci U S A *98*, 8276-8282.

Liu, S.M., and Stewart, M. (2005). Structural basis for the high-affinity binding of nucleoporin Nup1p to the Saccharomyces cerevisiae importin-beta homologue, Kap95p. J Mol Biol *349*, 515-525.

Liu, X., McLeod, I., Anderson, S., Yates, J.R., 3rd, and He, X. (2005). Molecular analysis of kinetochore architecture in fission yeast. EMBO J *24*, 2919-2930.

Liu, X.D., Liu, P.C., Santoro, N., and Thiele, D.J. (1997). Conservation of a stress response: human heat shock transcription factors functionally substitute for yeast HSF. EMBO J *16*, 6466-6477.

Liu, Y., Liang, S., and Tartakoff, A.M. (1996). Heat shock disassembles the nucleolus and inhibits nuclear protein import and poly(A)+ RNA export. EMBO J *15*, 6750-6757.

Liu, Z., Yan, M., Liang, Y., Liu, M., Zhang, K., Shao, D., Jiang, R., Li, L., Wang, C., Nussenzveig, D.R.*, et al.* (2019). Nucleoporin Seh1 Interacts with Olig2/Brd7 to Promote Oligodendrocyte Differentiation and Myelination. Neuron *102*, 587-601 e587.

Lock, A., Rutherford, K., Harris, M.A., and Wood, V. (2018). PomBase: The Scientific Resource for Fission Yeast. Methods in molecular biology *1757*, 49-68.

Logsdon, G.A., Barrey, E.J., Bassett, E.A., DeNizio, J.E., Guo, L.Y., Panchenko, T., Dawicki-McKenna, J.M., Heun, P., and Black, B.E. (2015). Both tails and the centromere targeting domain of CENP-A are required for centromere establishment. J Cell Biol *208*, 521-531.

Loiodice, I., Alves, A., Rabut, G., Van Overbeek, M., Ellenberg, J., Sibarita, J.B., and Doye, V. (2004). The entire Nup107-160 complex, including three new members, is targeted as one entity to kinetochores in mitosis. Mol Biol Cell *15*, 3333-3344.

Lotz, S.K., Knighton, L.E., Nitika, Jones, G.W., and Truman, A.W. (2019). Not quite the SSAme: unique roles for the yeast cytosolic Hsp70s. Curr Genet *65*, 1127-1134.

Lu, P.Y., Levesque, N., and Kobor, M.S. (2009). NuA4 and SWR1-C: two chromatin-modifying complexes with overlapping functions and components. Biochem Cell Biol *87*, 799-815.

Luger, K., Mader, A.W., Richmond, R.K., Sargent, D.F., and Richmond, T.J. (1997). Crystal structure of the nucleosome core particle at 2.8 A resolution. Nature *389*, 251-260.

Luke, B., and Lingner, J. (2009). TERRA: telomeric repeat-containing RNA. EMBO J *28*, 2503-2510.

Luna, R., Jimeno, S., Marin, M., Huertas, P., Garcia-Rubio, M., and Aguilera, A. (2005). Interdependence between transcription and mRNP processing and export, and its impact on genetic stability. Mol Cell *18*, 711-722.

Luo, M.L., Zhou, Z., Magni, K., Christoforides, C., Rappsilber, J., Mann, M., and Reed, R. (2001). Pre-mRNA splicing and mRNA export linked by direct interactions between UAP56 and Aly. Nature *413*, 644-647.

Luthra, R., Kerr, S.C., Harreman, M.T., Apponi, L.H., Fasken, M.B., Ramineni, S., Chaurasia, S., Valentini, S.R., and Corbett, A.H. (2007). Actively transcribed GAL genes can be physically linked to the nuclear pore by the SAGA chromatin modifying complex. J Biol Chem *282*, 3042-3049.

Lutz, Y., Jacob, M., and Fuchs, J.P. (1988). The distribution of two hnRNP-associated proteins defined by a monoclonal antibody is altered in heat-shocked HeLa cells. Exp Cell Res *175*, 109-124.

Lutzmann, M., Kunze, R., Buerer, A., Aebi, U., and Hurt, E. (2002). Modular self-assembly of a Y-shaped multiprotein complex from seven nucleoporins. EMBO J *21*, 387-397.

Ma, J., Kelich, J.M., Junod, S.L., and Yang, W. (2017). Super-resolution mapping of scaffold nucleoporins in the nuclear pore complex. J Cell Sci *130*, 1299-1306.

Ma, J., and Yang, W. (2010). Three-dimensional distribution of transient interactions in the nuclear pore complex obtained from single-molecule snapshots. Proc Natl Acad Sci U S A *107*, 7305-7310.

Macara, I.G. (2001). Transport into and out of the nucleus. Microbiol Mol Biol Rev *65*, 570-594, table of contents.

Mahl, P., Lutz, Y., Puvion, E., and Fuchs, J.P. (1989). Rapid effect of heat shock on two heterogeneous nuclear ribonucleoprotein-associated antigens in HeLa cells. J Cell Biol *109*, 1921-1935.

Maiato, H., DeLuca, J., Salmon, E.D., and Earnshaw, W.C. (2004). The dynamic kinetochore-microtubule interface. J Cell Sci *117*, 5461-5477.

Makise, M., Mackay, D.R., Elgort, S., Shankaran, S.S., Adam, S.A., and Ullman, K.S. (2012). The Nup153-Nup50 protein interface and its role in nuclear import. J Biol Chem *287*, 38515-38522.

Maksimov, V., Oya, E., Tanaka, M., Kawaguchi, T., Hachisuka, A., Ekwall, K., Bjerling, P., and Nakayama, J.I. (2018). The binding of Chp2's chromodomain to methylated H3K9 is essential for Chp2's role in heterochromatin assembly in fission yeast. PLoS One *13*, e0201101.

Malinovska, L., Kroschwald, S., Munder, M.C., Richter, D., and Alberti, S. (2012). Molecular chaperones and stress-inducible protein-sorting factors coordinate the spatiotemporal distribution of protein aggregates. Mol Biol Cell *23*, 3041-3056.

Mandell, J.G., Bahler, J., Volpe, T.A., Martienssen, R.A., and Cech, T.R. (2005). Global expression changes resulting from loss of telomeric DNA in fission yeast. Genome Biol *6*, R1.

Mannen, T., Andoh, T., and Tani, T. (2008). Dss1 associating with the proteasome functions in selective nuclear mRNA export in yeast. Biochemical and biophysical research communications *365*, 664-671.

Marguerat, S., Schmidt, A., Codlin, S., Chen, W., Aebersold, R., and Bahler, J. (2012). Quantitative analysis of fission yeast transcriptomes and proteomes in proliferating and quiescent cells. Cell *151*, 671-683.

Marks, J., Hagan, I.M., and Hyams, J.S. (1986). Growth polarity and cytokinesis in fission yeast: the role of the cytoskeleton. J Cell Sci Suppl *5*, 229-241.

Martienssen, R., and Moazed, D. (2015). RNAi and heterochromatin assembly. Cold Spring Harb Perspect Biol *7*, a019323.

Martinez-Pastor, M.T., Marchler, G., Schuller, C., Marchler-Bauer, A., Ruis, H., and Estruch, F. (1996). The Saccharomyces cerevisiae zinc finger proteins Msn2p and Msn4p are required for transcriptional induction through the stress response element (STRE). EMBO J *15*, 2227-2235.

Masser, A.E., Kang, W., Roy, J., Mohanakrishnan Kaimal, J., Quintana-Cordero, J., Friedlander, M.R., and Andreasson, C. (2019). Cytoplasmic protein misfolding titrates Hsp70 to activate nuclear Hsf1. eLife *8*.

Masuda, S., Das, R., Cheng, H., Hurt, E., Dorman, N., and Reed, R. (2005). Recruitment of the human TREX complex to mRNA during splicing. Genes Dev *19*, 1512-1517.

Matos-Perdomo, E., and Machin, F. (2018). The ribosomal DNA metaphase loop of Saccharomyces cerevisiae gets condensed upon heat stress in a Cdc14-independent TORC1-dependent manner. Cell Cycle *17*, 200-215.

Matsuda, A., Asakawa, H., Haraguchi, T., and Hiraoka, Y. (2017). Spatial organization of the Schizosaccharomyces pombe genome within the nucleus. Yeast *34*, 55-66.

Matsumoto, S., and Yanagida, M. (1985). Histone gene organization of fission yeast: a common upstream sequence. EMBO J *4*, 3531-3538.

Matsuyama, A., Arai, R., Yashiroda, Y., Shirai, A., Kamata, A., Sekido, S., Kobayashi, Y., Hashimoto, A., Hamamoto, M., Hiraoka, Y*., et al.* (2006). ORFeome cloning and global analysis of protein localization in the fission yeast Schizosaccharomyces pombe. Nat Biotechnol *24*, 841-847.

Matzat, L.H., Berberoglu, S., and Levesque, L. (2008). Formation of a Tap/NXF1 homotypic complex is mediated through the amino-terminal domain of Tap and enhances interaction with nucleoporins. Mol Biol Cell *19*, 327-338.

Maul, G.G., Maul, H.M., Scogna, J.E., Lieberman, M.W., Stein, G.S., Hsu, B.Y., and Borun, T.W. (1972). Time sequence of nuclear pore formation in phytohemagglutinin-stimulated lymphocytes and in HeLa cells during the cell cycle. J Cell Biol *55*, 433-447.

Mayer, C., and Grummt, I. (2005). Cellular stress and nucleolar function. Cell Cycle *4*, 1036-1038.

Mayrand, S., and Pederson, T. (1983). Heat shock alters nuclear ribonucleoprotein assembly in Drosophila cells. Mol Cell Biol *3*, 161-171.

McAinsh, A.D., and Meraldi, P. (2011). The CCAN complex: linking centromere specification to control of kinetochore-microtubule dynamics. Semin Cell Dev Biol *22*, 946-952.

McCleland, M.L., Gardner, R.D., Kallio, M.J., Daum, J.R., Gorbsky, G.J., Burke, D.J., and Stukenberg, P.T. (2003). The highly conserved Ndc80 complex is required for kinetochore assembly, chromosome congression, and spindle checkpoint activity. Genes Dev *17*, 101-114.

McCloskey, A., Ibarra, A., and Hetzer, M.W. (2018). Tpr regulates the total number of nuclear pore complexes per cell nucleus. Genes Dev *32*, 1321-1331.

McDonald, H.B., and Byers, B. (1997). A proteasome cap subunit required for spindle pole body duplication in yeast. J Cell Biol *137*, 539-553.

McDonald, W.H., Ohi, R., Smelkova, N., Frendewey, D., and Gould, K.L. (1999). Myb-related fission yeast cdc5p is a component of a 40S snRNP-containing complex and is essential for pre-mRNA splicing. Mol Cell Biol *19*, 5352-5362.

McDowall, M.D., Harris, M.A., Lock, A., Rutherford, K., Staines, D.M., Bahler, J., Kersey, P.J., Oliver, S.G., and Wood, V. (2015). PomBase 2015: updates to the fission yeast database. Nucleic Acids Res *43*, D656-661.

McLoughlin, F., Kim, M., Marshall, R.S., Vierstra, R.D., and Vierling, E. (2019). HSP101 Interacts with the Proteasome and Promotes the Clearance of Ubiquitylated Protein Aggregates. Plant Physiol *180*, 1829-1847.

Meinel, D.M., Burkert-Kautzsch, C., Kieser, A., O'Duibhir, E., Siebert, M., Mayer, A., Cramer, P., Soding, J., Holstege, F.C., and Strasser, K. (2013). Recruitment of TREX to the transcription machinery by its direct binding to the phospho-CTD of RNA polymerase II. PLoS Genet *9*, e1003914.

Meister, P., Taddei, A., Vernis, L., Poidevin, M., Gasser, S.M., and Baldacci, G. (2005). Temporal separation of replication and recombination requires the intra-S checkpoint. J Cell Biol *168*, 537-544.

Mekhail, K., and Moazed, D. (2010). The nuclear envelope in genome organization, expression and stability. Nat Rev Mol Cell Biol *11*, 317-328.

Melese, T., and Xue, Z. (1995). The nucleolus: an organelle formed by the act of building a ribosome. Curr Opin Cell Biol *7*, 319-324.

Meluh, P.B., Yang, P., Glowczewski, L., Koshland, D., and Smith, M.M. (1998). Cse4p is a component of the core centromere of Saccharomyces cerevisiae. Cell *94*, 607-613.

Mendjan, S., Taipale, M., Kind, J., Holz, H., Gebhardt, P., Schelder, M., Vermeulen, M., Buscaino, A., Duncan, K., Mueller, J.*, et al.* (2006). Nuclear pore components are involved in the transcriptional regulation of dosage compensation in Drosophila. Mol Cell *21*, 811-823.

Meszaros, N., Cibulka, J., Mendiburo, M.J., Romanauska, A., Schneider, M., and Kohler, A. (2015). Nuclear pore basket proteins are tethered to the nuclear envelope and can regulate membrane curvature. Dev Cell *33*, 285-298.

Milks, K.J., Moree, B., and Straight, A.F. (2009). Dissection of CENP-C-directed centromere and kinetochore assembly. Mol Biol Cell *20*, 4246-4255.

Miller, S.B., Mogk, A., and Bukau, B. (2015). Spatially organized aggregation of misfolded proteins as cellular stress defense strategy. J Mol Biol *427*, 1564-1574.

Mishra, R.K., Chakraborty, P., Arnaoutov, A., Fontoura, B.M., and Dasso, M. (2010). The Nup107-160 complex and gamma-TuRC regulate microtubule polymerization at kinetochores. Nat Cell Biol *12*, 164-169.

Mitchell, J.M., Mansfeld, J., Capitanio, J., Kutay, U., and Wozniak, R.W. (2010). Pom121 links two essential subcomplexes of the nuclear pore complex core to the membrane. J Cell Biol *191*, 505-521.

Mitchison, J.M. (1971). The Biology of the Cell Cycle.

Mitchison, J.M. (1990). The fission yeast, Schizosaccharomyces pombe. Bioessays *12*, 189-191.

Mizuguchi, T., Barrowman, J., and Grewal, S.I. (2015). Chromosome domain architecture and dynamic organization of the fission yeast genome. FEBS letters *589*, 2975-2986.

Moazed, D., Buhler, M., Buker, S.M., Colmenares, S.U., Gerace, E.L., Gerber, S.A., Hong, E.J., Motamedi, M.R., Verdel, A., Villen, J.*, et al.* (2006). Studies on the mechanism of RNAi-dependent heterochromatin assembly. Cold Spring Harb Symp Quant Biol *71*, 461-471.

Mojardin, L., Vazquez, E., and Antequera, F. (2013). Specification of DNA replication origins and genomic base composition in fission yeasts. J Mol Biol *425*, 4706-4713.

Montpetit, B., Thomsen, N.D., Helmke, K.J., Seeliger, M.A., Berger, J.M., and Weis, K. (2011). A conserved mechanism of DEAD-box ATPase activation by nucleoporins and InsP6 in mRNA export. Nature *472*, 238-242.

Mor, A., Suliman, S., Ben-Yishay, R., Yunger, S., Brody, Y., and Shav-Tal, Y. (2010). Dynamics of single mRNP nucleocytoplasmic transport and export through the nuclear pore in living cells. Nat Cell Biol *12*, 543-552.

Morano, K.A., Grant, C.M., and Moye-Rowley, W.S. (2012). The response to heat shock and oxidative stress in Saccharomyces cerevisiae. Genetics *190*, 1157-1195.

Morcillo, G., Gorab, E., Tanguay, R.M., and Diez, J.L. (1997). Specific intranucleolar distribution of Hsp70 during heat shock in polytene cells. Exp Cell Res *236*, 361-370.

Moreno, S., Klar, A., and Nurse, P. (1991). Molecular genetic analysis of fission yeast Schizosaccharomyces pombe. Methods in enzymology *194*, 795-823.

Moreno-Moreno, O., Torras-Llort, M., and Azorin, F. (2006). Proteolysis restricts localization of CID, the centromere-specific histone H3 variant of Drosophila, to centromeres. Nucleic Acids Res *34*, 6247-6255.

Moris, N., Shrivastava, J., Jeffery, L., Li, J.J., Hayles, J., and Nurse, P. (2016). A genome-wide screen to identify genes controlling the rate of entry into mitosis in fission yeast. Cell Cycle *15*, 3121-3130.

Mosalaganti, S., Kosinski, J., Albert, S., Schaffer, M., Strenkert, D., Salome, P.A., Merchant, S.S., Plitzko, J.M., Baumeister, W., Engel, B.D.*, et al.* (2018). In situ architecture of the algal nuclear pore complex. Nat Commun *9*, 2361.

Mosammaparast, N., and Pemberton, L.F. (2004). Karyopherins: from nuclear-transport mediators to nuclear-function regulators. Trends Cell Biol *14*, 547-556.

Moser, B.A., and Nakamura, T.M. (2009). Protection and replication of telomeres in fission yeast. Biochem Cell Biol *87*, 747-758.

Mosser, D.D., Ho, S., and Glover, J.R. (2004). Saccharomyces cerevisiae Hsp104 enhances the chaperone capacity of human cells and inhibits heat stress-induced proapoptotic signaling. Biochemistry *43*, 8107-8115.

Motamedi, M.R., Verdel, A., Colmenares, S.U., Gerber, S.A., Gygi, S.P., and Moazed, D. (2004). Two RNAi complexes, RITS and RDRC, physically interact and localize to noncoding centromeric RNAs. Cell *119*, 789-802.

Muhlhofer, M., Berchtold, E., Stratil, C.G., Csaba, G., Kunold, E., Bach, N.C., Sieber, S.A., Haslbeck, M., Zimmer, R., and Buchner, J. (2019). The Heat Shock Response in Yeast Maintains Protein Homeostasis by Chaperoning and Replenishing Proteins. Cell Rep *29*, 4593-4607 e4598.

Muller-McNicoll, M., Botti, V., de Jesus Domingues, A.M., Brandl, H., Schwich, O.D., Steiner, M.C., Curk, T., Poser, I., Zarnack, K., and Neugebauer, K.M. (2016). SR proteins are NXF1 adaptors that link alternative RNA processing to mRNA export. Genes Dev *30*, 553-566.

Muniz, L., Davidson, L., and West, S. (2015). Poly(A) Polymerase and the Nuclear Poly(A) Binding Protein, PABPN1, Coordinate the Splicing and Degradation of a Subset of Human Pre-mRNAs. Mol Cell Biol *35*, 2218-2230.

Muratani, M., and Tansey, W.P. (2003). How the ubiquitin-proteasome system controls transcription. Nat Rev Mol Cell Biol *4*, 192-201.

Murphy, R., Watkins, J.L., and Wente, S.R. (1996). GLE2, a Saccharomyces cerevisiae homologue of the Schizosaccharomyces pombe export factor RAE1, is required for nuclear pore complex structure and function. Mol Biol Cell *7*, 1921-1937.

Musacchio, A., and Desai, A. (2017). A Molecular View of Kinetochore Assembly and Function. Biology (Basel) *6*.

Musacchio, A., and Hardwick, K.G. (2002). The spindle checkpoint: structural insights into dynamic signalling. Nat Rev Mol Cell Biol *3*, 731-741.

Musacchio, A., and Salmon, E.D. (2007). The spindle-assembly checkpoint in space and time. Nat Rev Mol Cell Biol *8*, 379-393.

Nagpal, H., and Fukagawa, T. (2016). Kinetochore assembly and function through the cell cycle. Chromosoma *125*, 645-659.

Nakayama, J., Rice, J.C., Strahl, B.D., Allis, C.D., and Grewal, S.I. (2001). Role of histone H3 lysine 9 methylation in epigenetic control of heterochromatin assembly. Science *292*, 110-113.

Nakazawa, N., Nakamura, T., Kokubu, A., Ebe, M., Nagao, K., and Yanagida, M. (2008). Dissection of the essential steps for condensin accumulation at kinetochores and rDNAs during fission yeast mitosis. J Cell Biol *180*, 1115-1131.

Nandi, D., Tahiliani, P., Kumar, A., and Chandu, D. (2006). The ubiquitin-proteasome system. J Biosci *31*, 137-155.

Nathan, D.F., Vos, M.H., and Lindquist, S. (1997). In vivo functions of the Saccharomyces cerevisiae Hsp90 chaperone. Proc Natl Acad Sci U S A *94*, 12949-12956.

Nazer, E., Verdun, R.E., and Sanchez, D.O. (2011). Nucleolar localization of RNA binding proteins induced by actinomycin D and heat shock in Trypanosoma cruzi. PLoS One *6*, e19920.

Nazer, E., Verdun, R.E., and Sanchez, D.O. (2012). Severe heat shock induces nucleolar accumulation of mRNAs in Trypanosoma cruzi. PLoS One *7*, e43715.

Nemeth, A., and Grummt, I. (2018). Dynamic regulation of nucleolar architecture. Curr Opin Cell Biol *52*, 105-111.

Neumann, N., Lundin, D., and Poole, A.M. (2010). Comparative genomic evidence for a complete nuclear pore complex in the last eukaryotic common ancestor. PLoS One *5*, e13241.

Nguyen, A.N., and Shiozaki, K. (1999). Heat-shock-induced activation of stress MAP kinase is regulated by threonine- and tyrosine-specific phosphatases. Genes Dev *13*, 1653-1663.

Nielsen, S.V., Poulsen, E.G., Rebula, C.A., and Hartmann-Petersen, R. (2014). Protein quality control in the nucleus. Biomolecules *4*, 646-661.

Niepel, M., Molloy, K.R., Williams, R., Farr, J.C., Meinema, A.C., Vecchietti, N., Cristea, I.M., Chait, B.T., Rout, M.P., and Strambio-De-Castillia, C. (2013). The nuclear basket proteins Mlp1p and Mlp2p are part of a dynamic interactome including Esc1p and the proteasome. Mol Biol Cell *24*, 3920-3938.

Niepel, M., Strambio-de-Castillia, C., Fasolo, J., Chait, B.T., and Rout, M.P. (2005). The nuclear pore complex-associated protein, Mlp2p, binds to the yeast spindle pole body and promotes its efficient assembly. J Cell Biol *170*, 225-235.

Nino, C.A., Guet, D., Gay, A., Brutus, S., Jourquin, F., Mendiratta, S., Salamero, J., Geli, V., and Dargemont, C. (2016). Posttranslational marks control architectural and functional plasticity of the nuclear pore complex basket. J Cell Biol *212*, 167-180.

Ninomiya, K., Adachi, S., Natsume, T., Iwakiri, J., Terai, G., Asai, K., and Hirose, T. (2020). LncRNA-dependent nuclear stress bodies promote intron retention through SR protein phosphorylation. EMBO J *39*, e102729.

Nishino, T., Rago, F., Hori, T., Tomii, K., Cheeseman, I.M., and Fukagawa, T. (2013). CENP-T provides a structural platform for outer kinetochore assembly. EMBO J *32*, 424-436.

Nollen, E.A., Salomons, F.A., Brunsting, J.F., van der Want, J.J., Sibon, O.C., and Kampinga, H.H. (2001). Dynamic changes in the localization of thermally unfolded nuclear proteins associated with chaperone-dependent protection. Proc Natl Acad Sci U S A *98*, 12038-12043.

Noma, K., Cam, H.P., Maraia, R.J., and Grewal, S.I. (2006). A role for TFIIIC transcription factor complex in genome organization. Cell *125*, 859-872.

Noma, K., Sugiyama, T., Cam, H., Verdel, A., Zofall, M., Jia, S., Moazed, D., and Grewal, S.I. (2004). RITS acts in cis to promote RNA interference-mediated transcriptional and post-transcriptional silencing. Nat Genet *36*, 1174-1180.

Noma, K.I. (2017). The Yeast Genomes in Three Dimensions: Mechanisms and Functions. Annu Rev Genet *51*, 23-44.

Nonaka, N., Kitajima, T., Yokobayashi, S., Xiao, G., Yamamoto, M., Grewal, S.I., and Watanabe, Y. (2002). Recruitment of cohesin to heterochromatic regions by Swi6/HP1 in fission yeast. Nat Cell Biol *4*, 89-93.

Obado, S.O., Brillantes, M., Uryu, K., Zhang, W., Ketaren, N.E., Chait, B.T., Field, M.C., and Rout, M.P. (2016). Interactome Mapping Reveals the Evolutionary History of the Nuclear Pore Complex. PLoS Biol *14*, e1002365.

Oda, Y., Kimura, M., Kose, S., Fasken, M.B., Corbett, A.H., and Imamoto, N. (2014). The Schizosaccharomyces pombe Hikeshi/Opi10 protein has similar biochemical functions to its human homolog but acts in different physiological contexts. FEBS letters *588*, 1899-1905.

Oeffinger, M., and Zenklusen, D. (2012). To the pore and through the pore: a story of mRNA export kinetics. Biochim Biophys Acta *1819*, 494-506.

Ohkura, H., Hagan, I.M., and Glover, D.M. (1995). The conserved Schizosaccharomyces pombe kinase plo1, required to form a bipolar spindle, the actin ring, and septum, can drive septum formation in G1 and G2 cells. Genes Dev *9*, 1059-1073.

Okada, M., Cheeseman, I.M., Hori, T., Okawa, K., McLeod, I.X., Yates, J.R., 3rd, Desai, A., and Fukagawa, T. (2006). The CENP-H-I complex is required for the efficient incorporation of newly synthesized CENP-A into centromeres. Nat Cell Biol *8*, 446-457.

Okamura, M., Inose, H., and Masuda, S. (2015). RNA Export through the NPC in Eukaryotes. Genes (Basel) *6*, 124-149.

Olson, M.O. (2004). Sensing cellular stress: another new function for the nucleolus? Sci STKE *2004*, pe10.

Olson, M.O., Hingorani, K., and Szebeni, A. (2002). Conventional and nonconventional roles of the nucleolus. Int Rev Cytol *219*, 199-266.

Olsson, I., and Bjerling, P. (2011). Advancing our understanding of functional genome organisation through studies in the fission yeast. Curr Genet *57*, 1-12.

Onischenko, E., Stanton, L.H., Madrid, A.S., Kieselbach, T., and Weis, K. (2009). Role of the Ndc1 interaction network in yeast nuclear pore complex assembly and maintenance. J Cell Biol *185*, 475-491.

Onischenko, E., Tang, J.H., Andersen, K.R., Knockenhauer, K.E., Vallotton, P., Derrer, C.P., Kralt, A., Mugler, C.F., Chan, L.Y., Schwartz, T.U.*, et al.* (2017). Natively Unfolded FG Repeats Stabilize the Structure of the Nuclear Pore Complex. Cell *171*, 904-917 e919.

Orjalo, A.V., Arnaoutov, A., Shen, Z., Boyarchuk, Y., Zeitlin, S.G., Fontoura, B., Briggs, S., Dasso, M., and Forbes, D.J. (2006). The Nup107-160 nucleoporin complex is required for correct bipolar spindle assembly. Mol Biol Cell *17*, 3806-3818.

Ostermann, K., Lorentz, A., and Schmidt, H. (1993). The fission yeast rad22 gene, having a function in mating-type switching and repair of DNA damages, encodes a protein homolog to Rad52 of Saccharomyces cerevisiae. Nucleic Acids Res *21*, 5940-5944.

Ouyang, W., Guo, P., Takeda, K., Fu, Q., Fang, H., and Frucht, D.M. (2020). Erk1/2 inactivation promotes a rapid redistribution of COP1 and degradation of COP1 substrates. Proc Natl Acad Sci U S A.

Paeschke, K., McDonald, K.R., and Zakian, V.A. (2010). Telomeres: structures in need of unwinding. FEBS letters *584*, 3760-3772.

Palancade, B., Zuccolo, M., Loeillet, S., Nicolas, A., and Doye, V. (2005). Pml39, a novel protein of the nuclear periphery required for nuclear retention of improper messenger ribonucleoparticles. Mol Biol Cell *16*, 5258-5268.

Palmer, A., Mason, G.G., Paramio, J.M., Knecht, E., and Rivett, A.J. (1994). Changes in proteasome localization during the cell cycle. Eur J Cell Biol *64*, 163-175.

Palmer, D.K., O'Day, K., Wener, M.H., Andrews, B.S., and Margolis, R.L. (1987). A 17-kD centromere protein (CENP-A) copurifies with nucleosome core particles and with histones. J Cell Biol *104*, 805-815.

Pante, N., and Aebi, U. (1996). Molecular dissection of the nuclear pore complex. Crit Rev Biochem Mol Biol *31*, 153-199.

Paraskevopoulos, K., Kriegenburg, F., Tatham, M.H., Rosner, H.I., Medina, B., Larsen, I.B., Brandstrup, R., Hardwick, K.G., Hay, R.T., Kragelund, B.B.*, et al.* (2014). Dss1 is a 26S proteasome ubiquitin receptor. Mol Cell *56*, 453-461.

Pardo, M., and Nurse, P. (2005). The nuclear rim protein Amo1 is required for proper microtubule cytoskeleton organisation in fission yeast. J Cell Sci *118*, 1705-1714.

Paredes, V., Franco, A., Madrid, M., Soto, T., Vicente-Soler, J., Gacto, M., and Cansado, J. (2004). Transcriptional and post-translational regulation of neutral trehalase in Schizosaccharomyces pombe during thermal stress. Yeast *21*, 593-603.

Park, S.H., Kukushkin, Y., Gupta, R., Chen, T., Konagai, A., Hipp, M.S., Hayer-Hartl, M., and Hartl, F.U. (2013). PolyQ proteins interfere with nuclear degradation of cytosolic proteins by sequestering the Sis1p chaperone. Cell *154*, 134-145.

Parker, R., and Sheth, U. (2007). P bodies and the control of mRNA translation and degradation. Mol Cell *25*, 635-646.

Parsell, D.A., Kowal, A.S., Singer, M.A., and Lindquist, S. (1994). Protein disaggregation mediated by heat-shock protein Hsp104. Nature *372*, 475-478.

Parsell, D.A., and Lindquist, S. (1993). The function of heat-shock proteins in stress tolerance: degradation and reactivation of damaged proteins. Annu Rev Genet *27*, 437-496.

Parsell, D.A., Taulien, J., and Lindquist, S. (1993). The role of heat-shock proteins in thermotolerance. Philosophical transactions of the Royal Society of London Series B, Biological sciences *339*, 279-285; discussion 285-276.

Partridge, J.F., Borgstrom, B., and Allshire, R.C. (2000). Distinct protein interaction domains and protein spreading in a complex centromere. Genes Dev *14*, 783-791.

Pascual-Garcia, P., Debo, B., Aleman, J.R., Talamas, J.A., Lan, Y., Nguyen, N.H., Won, K.J., and Capelson, M. (2017). Metazoan Nuclear Pores Provide a Scaffold for Poised Genes and Mediate Induced Enhancer-Promoter Contacts. Mol Cell *66*, 63-76 e66.

Pascual-Garcia, P., Govind, C.K., Queralt, E., Cuenca-Bono, B., Llopis, A., Chavez, S., Hinnebusch, A.G., and Rodriguez-Navarro, S. (2008). Sus1 is recruited to coding regions and functions during transcription elongation in association with SAGA and TREX2. Genes Dev *22*, 2811-2822.

Patel, S.S., Belmont, B.J., Sante, J.M., and Rexach, M.F. (2007). Natively unfolded nucleoporins gate protein diffusion across the nuclear pore complex. Cell *129*, 83-96.

Paul, B., and Montpetit, B. (2016). Altered RNA processing and export lead to retention of mRNAs near transcription sites and nuclear pore complexes or within the nucleolus. Mol Biol Cell *27*, 2742-2756.

Pearl, L.H., and Prodromou, C. (2006). Structure and mechanism of the Hsp90 molecular chaperone machinery. Annu Rev Biochem *75*, 271-294.

Peck, S.A., Hughes, K.D., Victorino, J.F., and Mosley, A.L. (2019). Writing a wrong: Coupled RNA polymerase II transcription and RNA quality control. Wiley interdisciplinary reviews RNA *10*, e1529.

Pederson, T., and Politz, J.C. (2000). The nucleolus and the four ribonucleoproteins of translation. J Cell Biol *148*, 1091-1095.

Peffer, S., Goncalves, D., and Morano, K.A. (2019). Regulation of the Hsf1-dependent transcriptome via conserved bipartite contacts with Hsp70 promotes survival in yeast. J Biol Chem *294*, 12191-12202.

Pelham, H., Lewis, M., and Lindquist, S. (1984). Expression of a Drosophila heat shock protein in mammalian cells: transient association with nucleoli after heat shock. Philosophical transactions of the Royal Society of London Series B, Biological sciences *307*, 301-307.

Pelham, H.R. (1984). Hsp70 accelerates the recovery of nucleolar morphology after heat shock. EMBO J *3*, 3095-3100.

Pemberton, L.F., and Paschal, B.M. (2005). Mechanisms of receptor-mediated nuclear import and nuclear export. Traffic *6*, 187-198.

Pemberton, L.F., Rout, M.P., and Blobel, G. (1995). Disruption of the nucleoporin gene NUP133 results in clustering of nuclear pore complexes. Proc Natl Acad Sci U S A *92*, 1187-1191.

Perlaky, L., Valdez, B.C., and Busch, H. (1997). Effects of cytotoxic drugs on translocation of nucleolar RNA helicase RH-II/Gu. Exp Cell Res *235*, 413-420.

Perpelescu, M., and Fukagawa, T. (2011). The ABCs of CENPs. Chromosoma *120*, 425-446.

Petersen, J., Paris, J., Willer, M., Philippe, M., and Hagan, I.M. (2001). The S. pombe aurora-related kinase Ark1 associates with mitotic structures in a stage dependent manner and is required for chromosome segregation. J Cell Sci *114*, 4371-4384.

Petrovic, A., Keller, J., Liu, Y., Overlack, K., John, J., Dimitrova, Y.N., Jenni, S., van Gerwen, S., Stege, P., Wohlgemuth, S.*, et al.* (2016). Structure of the MIS12 Complex and Molecular Basis of Its Interaction with CENP-C at Human Kinetochores. Cell *167*, 1028-1040 e1015.

Pidoux, A.L., and Allshire, R.C. (2004). Kinetochore and heterochromatin domains of the fission yeast centromere. Chromosome research : an international journal on the molecular, supramolecular and evolutionary aspects of chromosome biology *12*, 521-534.

Pidoux, A.L., and Allshire, R.C. (2005). The role of heterochromatin in centromere function. Philosophical transactions of the Royal Society of London Series B, Biological sciences *360*, 569-579.

Pidoux, A.L., Choi, E.S., Abbott, J.K., Liu, X., Kagansky, A., Castillo, A.G., Hamilton, G.L., Richardson, W., Rappsilber, J., He, X.*, et al.* (2009). Fission yeast Scm3: A CENP-A receptor required for integrity of subkinetochore chromatin. Mol Cell *33*, 299-311.

Pidoux, A.L., Richardson, W., and Allshire, R.C. (2003). Sim4: a novel fission yeast kinetochore protein required for centromeric silencing and chromosome segregation. J Cell Biol *161*, 295-307.

Pincus, D. (2017). Size doesn't matter in the heat shock response. Curr Genet *63*, 175-178.

Piper, P. (1998). Differential role of Hsps and trehalose in stress tolerance. Trends in microbiology *6*, 43-44.

Piper, P.W. (1995). The heat shock and ethanol stress responses of yeast exhibit extensive similarity and functional overlap. FEMS Microbiol Lett *134*, 121-127.

Pirkkala, L., Alastalo, T.P., Zuo, X., Benjamin, I.J., and Sistonen, L. (2000). Disruption of heat shock factor 1 reveals an essential role in the ubiquitin proteolytic pathway. Mol Cell Biol *20*, 2670-2675.

Piskadlo, E., Tavares, A., and Oliveira, R.A. (2017). Metaphase chromosome structure is dynamically maintained by condensin I-directed DNA (de)catenation. eLife *6*.

Porrua, O., and Libri, D. (2013). RNA quality control in the nucleus: the Angels' share of RNA. Biochim Biophys Acta *1829*, 604-611.

Prasad, R., Kawaguchi, S., and Ng, D.T. (2010). A nucleus-based quality control mechanism for cytosolic proteins. Mol Biol Cell *21*, 2117-2127.

Pritchard, C.E., Fornerod, M., Kasper, L.H., and van Deursen, J.M. (1999). RAE1 is a shuttling mRNA export factor that binds to a GLEBS-like NUP98 motif at the nuclear pore complex through multiple domains. J Cell Biol *145*, 237-254.

Pritts, T.A., Hungness, E.S., Hershko, D.D., Robb, B.W., Sun, X., Luo, G.J., Fischer, J.E., Wong, H.R., and Hasselgren, P.O. (2002). Proteasome inhibitors induce heat shock response and increase IL-6 expression in human intestinal epithelial cells. Am J Physiol Regul Integr Comp Physiol *282*, R1016-1026.

Protter, D.S.W., and Parker, R. (2016). Principles and Properties of Stress Granules. Trends Cell Biol *26*, 668-679.

Przewloka, M.R., Venkei, Z., Bolanos-Garcia, V.M., Debski, J., Dadlez, M., and Glover, D.M. (2011). CENP-C is a structural platform for kinetochore assembly. Curr Biol *21*, 399-405.

Ptak, C., Aitchison, J.D., and Wozniak, R.W. (2014). The multifunctional nuclear pore complex: a platform for controlling gene expression. Curr Opin Cell Biol *28*, 46-53.

Ptak, C., and Wozniak, R.W. (2016). Nucleoporins and chromatin metabolism. Curr Opin Cell Biol *40*, 153-160.

Pyhtila, B., and Rexach, M. (2003). A gradient of affinity for the karyopherin Kap95p along the yeast nuclear pore complex. J Biol Chem *278*, 42699-42709.

Rabut, G., Doye, V., and Ellenberg, J. (2004). Mapping the dynamic organization of the nuclear pore complex inside single living cells. Nat Cell Biol *6*, 1114-1121.

Rago, F., Gascoigne, K.E., and Cheeseman, I.M. (2015). Distinct organization and regulation of the outer kinetochore KMN network downstream of CENP-C and CENP-T. Curr Biol *25*, 671-677.

Raices, M., Bukata, L., Sakuma, S., Borlido, J., Hernandez, L.S., Hart, D.O., and D'Angelo, M.A. (2017). Nuclear Pores Regulate Muscle Development and Maintenance by Assembling a Localized Mef2C Complex. Dev Cell *41*, 540-554 e547.

Raices, M., and D'Angelo, M.A. (2017). Nuclear pore complexes and regulation of gene expression. Curr Opin Cell Biol *46*, 26-32.

Rajanala, K., and Nandicoori, V.K. (2012). Localization of nucleoporin Tpr to the nuclear pore complex is essential for Tpr mediated regulation of the export of unspliced RNA. PLoS One *7*, e29921.

Rajanala, K., Sarkar, A., Jhingan, G.D., Priyadarshini, R., Jalan, M., Sengupta, S., and Nandicoori, V.K. (2014). Phosphorylation of nucleoporin Tpr governs its differential localization and is required for its mitotic function. J Cell Sci *127*, 3505-3520.

Rajoo, S., Vallotton, P., Onischenko, E., and Weis, K. (2018). Stoichiometry and compositional plasticity of the yeast nuclear pore complex revealed by quantitative fluorescence microscopy. Proc Natl Acad Sci U S A *115*, E3969-E3977.

Rallis, C., and Bahler, J. (2016). Cell-based screens and phenomics with fission yeast. Crit Rev Biochem Mol Biol *51*, 86-95.

Randise-Hinchliff, C., and Brickner, J.H. (2016). Transcription factors dynamically control the spatial organization of the yeast genome. Nucleus *7*, 369-374.

Randise-Hinchliff, C., Coukos, R., Sood, V., Sumner, M.C., Zdraljevic, S., Meldi Sholl, L., Garvey Brickner, D., Ahmed, S., Watchmaker, L., and Brickner, J.H. (2016). Strategies to regulate transcription factor-mediated gene positioning and interchromosomal clustering at the nuclear periphery. J Cell Biol *212*, 633-646.

Ranjitkar, P., Press, M.O., Yi, X., Baker, R., MacCoss, M.J., and Biggins, S. (2010). An E3 ubiquitin ligase prevents ectopic localization of the centromeric histone H3 variant via the centromere targeting domain. Mol Cell *40*, 455-464.

Raska, I., Shaw, P.J., and Cmarko, D. (2006). New insights into nucleolar architecture and activity. Int Rev Cytol *255*, 177-235.

Ravid, T., and Hochstrasser, M. (2008). Diversity of degradation signals in the ubiquitin-proteasome system. Nat Rev Mol Cell Biol *9*, 679-690.

Ray, J., Munn, P.R., Vihervaara, A., Lewis, J.J., Ozer, A., Danko, C.G., and Lis, J.T. (2019). Chromatin conformation remains stable upon extensive transcriptional changes driven by heat shock. Proc Natl Acad Sci U S A *116*, 19431-19439.

Regot, S., de Nadal, E., Rodriguez-Navarro, S., Gonzalez-Novo, A., Perez-Fernandez, J., Gadal, O., Seisenbacher, G., Ammerer, G., and Posas, F. (2013). The Hog1 stress-activated protein kinase targets nucleoporins to control mRNA export upon stress. J Biol Chem *288*, 17384-17398.

Reichelt, R., Holzenburg, A., Buhle, E.L., Jr., Jarnik, M., Engel, A., and Aebi, U. (1990). Correlation between structure and mass distribution of the nuclear pore complex and of distinct pore complex components. J Cell Biol *110*, 883-894.

Rekulapally, P., and Suresh, S.N. (2019). Nucleolus: A Protein Quality Control Compartment. Trends Biochem Sci *44*, 993-995.

Rexach, M., and Blobel, G. (1995). Protein import into nuclei: association and dissociation reactions involving transport substrate, transport factors, and nucleoporins. Cell *83*, 683-692.

Reyes-Turcu, F.E., and Grewal, S.I. (2012). Different means, same end-heterochromatin formation by RNAi and RNAi-independent RNA processing factors in fission yeast. Curr Opin Genet Dev *22*, 156-163.

Rhind, N., Chen, Z., Yassour, M., Thompson, D.A., Haas, B.J., Habib, N., Wapinski, I., Roy, S., Lin, M.F., Heiman, D.I*., et al.* (2011). Comparative functional genomics of the fission yeasts. Science *332*, 930-936.

Ribbeck, K., Lipowsky, G., Kent, H.M., Stewart, M., and Gorlich, D. (1998). NTF2 mediates nuclear import of Ran. EMBO J *17*, 6587-6598.

Ribeiro, M.J., Reinders, A., Boller, T., Wiemken, A., and De Virgilio, C. (1997). Trehalose synthesis is important for the acquisition of thermotolerance in Schizosaccharomyces pombe. Molecular microbiology *25*, 571-581.

Richter, K., Haslbeck, M., and Buchner, J. (2010). The heat shock response: life on the verge of death. Mol Cell *40*, 253-266.

Riezman, H. (2004). Why do cells require heat shock proteins to survive heat stress? Cell Cycle *3*, 61-63.

Rockel, T.D., Stuhlmann, D., and von Mikecz, A. (2005). Proteasomes degrade proteins in focal subdomains of the human cell nucleus. J Cell Sci *118*, 5231-5242.

Rodriguez, M.S., Gwizdek, C., Haguenauer-Tsapis, R., and Dargemont, C. (2003). The HECT ubiquitin ligase Rsp5p is required for proper nuclear export of mRNA in Saccharomyces cerevisiae. Traffic *4*, 566-575.

Rodriguez-Bravo, V., Maciejowski, J., Corona, J., Buch, H.K., Collin, P., Kanemaki, M.T., Shah, J.V., and Jallepalli, P.V. (2014). Nuclear pores protect genome integrity by assembling a premitotic and Mad1-dependent anaphase inhibitor. Cell *156*, 1017-1031.

Rodriguez-Navarro, S., Fischer, T., Luo, M.J., Antunez, O., Brettschneider, S., Lechner, J., Perez-Ortin, J.E., Reed, R., and Hurt, E. (2004). Sus1, a functional component of the SAGA histone acetylase complex and the nuclear pore-associated mRNA export machinery. Cell *116*, 75-86.

Rodriguez-Navarro, S., and Hurt, E. (2011). Linking gene regulation to mRNA production and export. Curr Opin Cell Biol *23*, 302-309.

Roguev, A., Wiren, M., Weissman, J.S., and Krogan, N.J. (2007). High-throughput genetic interaction mapping in the fission yeast Schizosaccharomyces pombe. Nat Methods *4*, 861-866.

Rohner, S., Kalck, V., Wang, X., Ikegami, K., Lieb, J.D., Gasser, S.M., and Meister, P. (2013). Promoter- and RNA polymerase II-dependent hsp-16 gene association with nuclear pores in Caenorhabditis elegans. J Cell Biol *200*, 589-604.

Rollenhagen, C., Hodge, C.A., and Cole, C.N. (2004). The nuclear pore complex and the DEAD box protein Rat8p/Dbp5p have nonessential features which appear to facilitate mRNA export following heat shock. Mol Cell Biol *24*, 4869-4879.

Rollenhagen, C., Hodge, C.A., and Cole, C.N. (2007). Following temperature stress, export of heat shock mRNA occurs efficiently in cells with mutations in genes normally important for mRNA export. Eukaryot Cell *6*, 505-513.

Rose, A., and Meier, I. (2004). Scaffolds, levers, rods and springs: diverse cellular functions of long coiled-coil proteins. Cell Mol Life Sci *61*, 1996-2009.

Rosenbaum, J.C., and Gardner, R.G. (2011). How a disordered ubiquitin ligase maintains order in nuclear protein homeostasis. Nucleus *2*, 264-270.

Rougemaille, M., Villa, T., Gudipati, R.K., and Libri, D. (2008). mRNA journey to the cytoplasm: attire required. Biology of the cell / under the auspices of the European Cell Biology Organization *100*, 327-342.

Rout, M.P., Aitchison, J.D., Suprapto, A., Hjertaas, K., Zhao, Y., and Chait, B.T. (2000). The yeast nuclear pore complex: composition, architecture, and transport mechanism. J Cell Biol *148*, 635-651.

Rout, M.P., and Wente, S.R. (1994). Pores for thought: nuclear pore complex proteins. Trends Cell Biol *4*, 357-365.

Rowley, A., Johnston, G.C., Butler, B., Werner-Washburne, M., and Singer, R.A. (1993). Heat shock-mediated cell cycle blockage and G1 cyclin expression in the yeast Saccharomyces cerevisiae. Mol Cell Biol *13*, 1034-1041.

Roy, B., and Sanyal, K. (2011). Diversity in requirement of genetic and epigenetic factors for centromere function in fungi. Eukaryot Cell *10*, 1384-1395.

Roy, B., Varshney, N., Yadav, V., and Sanyal, K. (2013). The process of kinetochore assembly in yeasts. FEMS Microbiol Lett *338*, 107-117.

Ruault, M., Dubarry, M., and Taddei, A. (2008). Re-positioning genes to the nuclear envelope in mammalian cells: impact on transcription. Trends Genet *24*, 574-581.

Ruiz-Roig, C., Vieitez, C., Posas, F., and de Nadal, E. (2010). The Rpd3L HDAC complex is essential for the heat stress response in yeast. Molecular microbiology *76*, 1049-1062.

Russell, J., and Zomerdijk, J.C. (2005). RNA-polymerase-I-directed rDNA transcription, life and works. Trends Biochem Sci *30*, 87-96.

Russell, S.J., Steger, K.A., and Johnston, S.A. (1999). Subcellular localization, stoichiometry, and protein levels of 26 S proteasome subunits in yeast. J Biol Chem *274*, 21943-21952.

Saavedra, C., Tung, K.S., Amberg, D.C., Hopper, A.K., and Cole, C.N. (1996). Regulation of mRNA export in response to stress in Saccharomyces cerevisiae. Genes Dev *10*, 1608-1620.

Saavedra, C.A., Hammell, C.M., Heath, C.V., and Cole, C.N. (1997). Yeast heat shock mRNAs are exported through a distinct pathway defined by Rip1p. Genes Dev *11*, 2845-2856.

Sadis, S., Hickey, E., and Weber, L.A. (1988). Effect of heat shock on RNA metabolism in HeLa cells. J Cell Physiol *135*, 377-386.

Saeki, Y., and Tanaka, K. (2012). Assembly and function of the proteasome. Methods in molecular biology *832*, 315-337.

Saguez, C., Olesen, J.R., and Jensen, T.H. (2005). Formation of export-competent mRNP: escaping nuclear destruction. Curr Opin Cell Biol *17*, 287-293.

Sahara, K., Kogleck, L., Yashiroda, H., and Murata, S. (2014). The mechanism for molecular assembly of the proteasome. Adv Biol Regul *54*, 51-58.

Sakurai, H., and Ota, A. (2011). Regulation of chaperone gene expression by heat shock transcription factor in Saccharomyces cerevisiae: importance in normal cell growth, stress resistance, and longevity. FEBS letters *585*, 2744-2748.

Sakurai, H., and Takemori, Y. (2007). Interaction between heat shock transcription factors (HSFs) and divergent binding sequences: binding specificities of yeast HSFs and human HSF1. J Biol Chem *282*, 13334-13341.

Salas-Pino, S., Gallardo, P., Barrales, R.R., Braun, S., and Daga, R.R. (2017). The fission yeast nucleoporin Alm1 is required for proteasomal degradation of kinetochore components. J Cell Biol *216*, 3591-3608.

Salat-Canela, C., Paulo, E., Sanchez-Mir, L., Carmona, M., Ayte, J., Oliva, B., and Hidalgo, E. (2017). Deciphering the role of the signal- and Sty1 kinase-dependent phosphorylation of the stress-responsive transcription factor Atf1 on gene activation. J Biol Chem *292*, 13635-13644.

Salomons, F.A., Acs, K., and Dantuma, N.P. (2010). Illuminating the ubiquitin/proteasome system. Exp Cell Res *316*, 1289-1295.

Sambrook, J.F., E. F. ; Maniatis, T. (1989). Molecular cloning: a laboratory manual. (Cold Spring Harbor, NY: Cold Spring Harbor Laboratory Press).

Sambrook, J.F.a.R., D.W. (2001). Molecular Cloning: A Laboratory Manual (Cold Spring Harbor Laboratory Press).

Samejima, I., and Yanagida, M. (1994). Identification of cut8+ and cek1+, a novel protein kinase gene, which complement a fission yeast mutation that blocks anaphase. Mol Cell Biol *14*, 6361-6371.

Sanchez, Y., and Lindquist, S.L. (1990). HSP104 required for induced thermotolerance. Science *248*, 1112-1115.

Sanchez-Mir, L., Salat-Canela, C., Paulo, E., Carmona, M., Ayte, J., Oliva, B., and Hidalgo, E. (2018). Phospho-mimicking Atf1 mutants bypass the transcription activating function of the MAP kinase Sty1 of fission yeast. Curr Genet *64*, 97-102.

Sanchez-Perez, I., Renwick, S.J., Crawley, K., Karig, I., Buck, V., Meadows, J.C., Franco-Sanchez, A., Fleig, U., Toda, T., and Millar, J.B. (2005). The DASH complex and Klp5/Klp6 kinesin coordinate bipolar chromosome attachment in fission yeast. EMBO J *24*, 2931-2943.

Santaguida, S., and Musacchio, A. (2009). The life and miracles of kinetochores. EMBO J *28*, 2511-2531.

Santhanam, A., Hartley, A., Duvel, K., Broach, J.R., and Garrett, S. (2004). PP2A phosphatase activity is required for stress and Tor kinase regulation of yeast stress response factor Msn2p. Eukaryot Cell *3*, 1261-1271.

Santos-Rosa, H., Moreno, H., Simos, G., Segref, A., Fahrenkrog, B., Pante, N., and Hurt, E. (1998). Nuclear mRNA export requires complex formation between Mex67p and Mtr2p at the nuclear pores. Mol Cell Biol *18*, 6826-6838.

Sarge, K.D., Murphy, S.P., and Morimoto, R.I. (1993). Activation of heat shock gene transcription by heat shock factor 1 involves oligomerization, acquisition of DNA-binding activity, and nuclear localization and can occur in the absence of stress. Mol Cell Biol *13*, 1392-1407.

Saroufim, M.A., Bensidoun, P., Raymond, P., Rahman, S., Krause, M.R., Oeffinger, M., and Zenklusen, D. (2015). The nuclear basket mediates perinuclear mRNA scanning in budding yeast. J Cell Biol *211*, 1131-1140.

Sato, M., Dhut, S., and Toda, T. (2005). New drug-resistant cassettes for gene disruption and epitope tagging in Schizosaccharomyces pombe. Yeast *22*, 583-591.

Sauer, R.T., and Baker, T.A. (2011). AAA+ proteases: ATP-fueled machines of protein destruction. Annu Rev Biochem *80*, 587-612.

Savulescu, A.F., Rotem, A., and Harel, A. (2011). Proteasomes crossing the nuclear border. Nucleus *2*, 258-263.

Scharf, A., Rockel, T.D., and von Mikecz, A. (2007). Localization of proteasomes and proteasomal proteolysis in the mammalian interphase cell nucleus by systematic application of immunocytochemistry. Histochemistry and cell biology *127*, 591-601.

Schauber, C., Chen, L., Tongaonkar, P., Vega, I., Lambertson, D., Potts, W., and Madura, K. (1998). Rad23 links DNA repair to the ubiquitin/proteasome pathway. Nature *391*, 715-718.

Scheer, U., and Hock, R. (1999). Structure and function of the nucleolus. Curr Opin Cell Biol *11*, 385-390.

Schenstrom, S.M., Rebula, C.A., Tatham, M.H., Hendus-Altenburger, R., Jourdain, I., Hay, R.T., Kragelund, B.B., and Hartmann-Petersen, R. (2018). Expanded Interactome of the Intrinsically Disordered Protein Dss1. Cell Rep *25*, 862-870.

Scherthan, H., Bahler, J., and Kohli, J. (1994). Dynamics of chromosome organization and pairing during meiotic prophase in fission yeast. J Cell Biol *127*, 273-285.

Schleiffer, A., Maier, M., Litos, G., Lampert, F., Hornung, P., Mechtler, K., and Westermann, S. (2012). CENP-T proteins are conserved centromere receptors of the Ndc80 complex. Nat Cell Biol *14*, 604-613.

Schmid, M., Arib, G., Laemmli, C., Nishikawa, J., Durussel, T., and Laemmli, U.K. (2006). Nup-PI: the nucleopore-promoter interaction of genes in yeast. Mol Cell *21*, 379-391.

Schmid, M., and Jensen, T.H. (2008). Quality control of mRNP in the nucleus. Chromosoma *117*, 419-429.

Schmid, M., Poulsen, M.B., Olszewski, P., Pelechano, V., Saguez, C., Gupta, I., Steinmetz, L.M., Moore, C., and Jensen, T.H. (2012). Rrp6p controls mRNA poly(A) tail length and its decoration with poly(A) binding proteins. Mol Cell *47*, 267-280.

Schmitt, A.P., and McEntee, K. (1996). Msn2p, a zinc finger DNA-binding protein, is the transcriptional activator of the multistress response in Saccharomyces cerevisiae. Proc Natl Acad Sci U S A *93*, 5777-5782.

Schmitt, C., von Kobbe, C., Bachi, A., Pante, N., Rodrigues, J.P., Boscheron, C., Rigaut, G., Wilm, M., Seraphin, B., Carmo-Fonseca, M*., et al.* (1999). Dbp5, a DEAD-box protein required for mRNA export, is recruited to the cytoplasmic fibrils of nuclear pore complex via a conserved interaction with CAN/Nup159p. EMBO J *18*, 4332-4347.

Schoenfelder, S., Clay, I., and Fraser, P. (2010). The transcriptional interactome: gene expression in 3D. Curr Opin Genet Dev *20*, 127-133.

Schubert, T., and Kohler, A. (2016). Mediator and TREX-2: Emerging links between transcription initiation and mRNA export. Nucleus *7*, 126-131.

Schwartz, T.U. (2016). The Structure Inventory of the Nuclear Pore Complex. J Mol Biol *428*, 1986-2000.

Schwarzacher, H.G., and Wachtler, F. (1993). The nucleolus. Anat Embryol (Berl) *188*, 515-536.

Schweizer, N., Ferras, C., Kern, D.M., Logarinho, E., Cheeseman, I.M., and Maiato, H. (2013). Spindle assembly checkpoint robustness requires Tpr-mediated regulation of Mad1/Mad2 proteostasis. J Cell Biol *203*, 883-893.

Scott, R.J., Lusk, C.P., Dilworth, D.J., Aitchison, J.D., and Wozniak, R.W. (2005). Interactions between Mad1p and the nuclear transport machinery in the yeast Saccharomyces cerevisiae. Mol Biol Cell *16*, 4362-4374.

Screpanti, E., De Antoni, A., Alushin, G.M., Petrovic, A., Melis, T., Nogales, E., and Musacchio, A. (2011). Direct binding of Cenp-C to the Mis12 complex joins the inner and outer kinetochore. Curr Biol *21*, 391-398.

Segref, A., Sharma, K., Doye, V., Hellwig, A., Huber, J., Luhrmann, R., and Hurt, E. (1997). Mex67p, a novel factor for nuclear mRNA export, binds to both poly(A)+ RNA and nuclear pores. EMBO J *16*, 3256-3271.

Selvanathan, S.P., Thakurta, A.G., Dhakshnamoorthy, J., Zhou, M., Veenstra, T.D., and Dhar, R. (2010). Schizosaccharomyces pombe Dss1p is a DNA damage checkpoint protein that recruits Rad24p, Cdc25p, and Rae1p to DNA double-strand breaks. J Biol Chem *285*, 14122-14133.

Senechal, P., Arseneault, G., Leroux, A., Lindquist, S., and Rokeach, L.A. (2009). The Schizosaccharomyces pombe Hsp104 disaggregase is unable to propagate the [PSI] prion. PLoS One *4*, e6939.

Shalgi, R., Hurt, J.A., Lindquist, S., and Burge, C.B. (2014). Widespread inhibition of posttranscriptional splicing shapes the cellular transcriptome following heat shock. Cell Rep *7*, 1362-1370.

Shaner, N.C., Campbell, R.E., Steinbach, P.A., Giepmans, B.N., Palmer, A.E., and Tsien, R.Y. (2004). Improved monomeric red, orange and yellow fluorescent proteins derived from Discosoma sp. red fluorescent protein. Nat Biotechnol *22*, 1567-1572.

Shankaranarayana, G.D., Motamedi, M.R., Moazed, D., and Grewal, S.I. (2003). Sir2 regulates histone H3 lysine 9 methylation and heterochromatin assembly in fission yeast. Curr Biol *13*, 1240-1246.

Shav-Tal, Y., Blechman, J., Darzacq, X., Montagna, C., Dye, B.T., Patton, J.G., Singer, R.H., and Zipori, D. (2005). Dynamic sorting of nuclear components into distinct nucleolar caps during transcriptional inhibition. Mol Biol Cell *16*, 2395-2413.

Shaw, P.J., and Jordan, E.G. (1995). The nucleolus. Annual review of cell and developmental biology *11*, 93-121.

Sheinberger, J., and Shav-Tal, Y. (2017). mRNPs meet stress granules. FEBS letters *591*, 2534-2542.

Shi, Y., Mosser, D.D., and Morimoto, R.I. (1998). Molecular chaperones as HSF1-specific transcriptional repressors. Genes Dev *12*, 654-666.

Shibata, S., Matsuoka, Y., and Yoneda, Y. (2002). Nucleocytoplasmic transport of proteins and poly(A)+ RNA in reconstituted Tpr-less nuclei in living mammalian cells. Genes to cells : devoted to molecular & cellular mechanisms *7*, 421-434.

Shichino, Y., Otsubo, Y., Yamamoto, M., and Yamashita, A. (2020). Meiotic gene silencing complex MTREC/NURS recruits the nuclear exosome to YTH-RNA-binding protein Mmi1. PLoS Genet *16*, e1008598.

Shin, C., Feng, Y., and Manley, J.L. (2004). Dephosphorylated SRp38 acts as a splicing repressor in response to heat shock. Nature *427*, 553-558.

Shiozaki, K., Shiozaki, M., and Russell, P. (1997). Mcs4 mitotic catastrophe suppressor regulates the fission yeast cell cycle through the Wik1-Wis1-Spc1 kinase cascade. Mol Biol Cell *8*, 409-419.

Shiozaki, K., Shiozaki, M., and Russell, P. (1998). Heat stress activates fission yeast Spc1/StyI MAPK by a MEKK-independent mechanism. Mol Biol Cell *9*, 1339-1349.

Shiroiwa, Y., Hayashi, T., Fujita, Y., Villar-Briones, A., Ikai, N., Takeda, K., Ebe, M., and Yanagida, M. (2011). Mis17 is a regulatory module of the Mis6-Mal2-Sim4 centromere complex that is required for the recruitment of CenH3/CENP-A in fission yeast. PLoS One *6*, e17761.

Shorbagi, S., and Brown, I.R. (2016). Dynamics of the association of heat shock protein HSPA6 (Hsp70B') and HSPA1A (Hsp70-1) with stress-sensitive cytoplasmic and nuclear structures in differentiated human neuronal cells. Cell stress & chaperones *21*, 993-1003.

Shou, W., Seol, J.H., Shevchenko, A., Baskerville, C., Moazed, D., Chen, Z.W., Jang, J., Shevchenko, A., Charbonneau, H., and Deshaies, R.J. (1999). Exit from mitosis is triggered by Tem1-dependent release of the protein phosphatase Cdc14 from nucleolar RENT complex. Cell *97*, 233-244.

Shulga, N., Mosammaparast, N., Wozniak, R., and Goldfarb, D.S. (2000). Yeast nucleoporins involved in passive nuclear envelope permeability. J Cell Biol *149*, 1027-1038.

Sicard, H., Faubladier, M., Noaillac-Depeyre, J., Leger-Silvestre, I., Gas, N., and Caizergues-Ferrer, M. (1998). The role of the Schizosaccharomyces pombe gar2 protein in nucleolar structure and function depends on the concerted action of its highly charged N terminus and its RNA-binding domains. Mol Biol Cell *9*, 2011-2023.

Siebrasse, J.P., Kaminski, T., and Kubitscheck, U. (2012). Nuclear export of single native mRNA molecules observed by light sheet fluorescence microscopy. Proc Natl Acad Sci U S A *109*, 9426-9431.

Silla, T., Karadoulama, E., Makosa, D., Lubas, M., and Jensen, T.H. (2018). The RNA Exosome Adaptor ZFC3H1 Functionally Competes with Nuclear Export Activity to Retain Target Transcripts. Cell Rep *23*, 2199-2210.

Silva, P., Barbosa, J., Nascimento, A.V., Faria, J., Reis, R., and Bousbaa, H. (2011). Monitoring the fidelity of mitotic chromosome segregation by the spindle assembly checkpoint. Cell Prolif *44*, 391-400.

Singh, G., Pratt, G., Yeo, G.W., and Moore, M.J. (2015). The Clothes Make the mRNA: Past and Present Trends in mRNP Fashion. Annu Rev Biochem *84*, 325-354.

Singh, N.S., Shao, N., McLean, J.R., Sevugan, M., Ren, L., Chew, T.G., Bimbo, A., Sharma, R., Tang, X., Gould, K.L.*, et al.* (2011). SIN-inhibitory phosphatase complex promotes Cdc11p dephosphorylation and propagates SIN asymmetry in fission yeast. Curr Biol *21*, 1968-1978.

Siniossoglou, S., Lutzmann, M., Santos-Rosa, H., Leonard, K., Mueller, S., Aebi, U., and Hurt, E. (2000). Structure and assembly of the Nup84p complex. J Cell Biol *149*, 41-54.

Siniossoglou, S., Wimmer, C., Rieger, M., Doye, V., Tekotte, H., Weise, C., Emig, S., Segref, A., and Hurt, E.C. (1996). A novel complex of nucleoporins, which includes Sec13p and a Sec13p homolog, is essential for normal nuclear pores. Cell *84*, 265-275.

Sirri, V., Urcuqui-Inchima, S., Roussel, P., and Hernandez-Verdun, D. (2008). Nucleolus: the fascinating nuclear body. Histochemistry and cell biology *129*, 13-31.

Skaggs, H.S., Xing, H., Wilkerson, D.C., Murphy, L.A., Hong, Y., Mayhew, C.N., and Sarge, K.D. (2007). HSF1-TPR interaction facilitates export of stress-induced HSP70 mRNA. J Biol Chem *282*, 33902-33907.

Skruzny, M., Schneider, C., Racz, A., Weng, J., Tollervey, D., and Hurt, E. (2009). An endoribonuclease functionally linked to perinuclear mRNP quality control associates with the nuclear pore complexes. PLoS Biol *7*, e8.

Sloan, K.E., Gleizes, P.E., and Bohnsack, M.T. (2016). Nucleocytoplasmic Transport of RNAs and RNA-Protein Complexes. J Mol Biol *428*, 2040-2059.

Smoyer, C.J., and Jaspersen, S.L. (2019). Patrolling the nucleus: inner nuclear membrane-associated degradation. Curr Genet *65*, 1099-1106.

Soheilypour, M., and Mofrad, M.R. (2016). Regulation of RNA-binding proteins affinity to export receptors enables the nuclear basket proteins to distinguish and retain aberrant mRNAs. Sci Rep *6*, 35380.

Soheilypour, M., and Mofrad, M.R.K. (2018). Quality control of mRNAs at the entry of the nuclear pore: Cooperation in a complex molecular system. Nucleus *9*, 202-211.

Solis, E.J., Pandey, J.P., Zheng, X., Jin, D.X., Gupta, P.B., Airoldi, E.M., Pincus, D., and Denic, V. (2016). Defining the Essential Function of Yeast Hsf1 Reveals a Compact Transcriptional Program for Maintaining Eukaryotic Proteostasis. Mol Cell *63*, 60-71.

Solmaz, S.R., Chauhan, R., Blobel, G., and Melcak, I. (2011). Molecular architecture of the transport channel of the nuclear pore complex. Cell *147*, 590-602.

Solomon, J.M., Rossi, J.M., Golic, K., McGarry, T., and Lindquist, S. (1991). Changes in hsp70 alter thermotolerance and heat-shock regulation in Drosophila. New Biol *3*, 1106-1120.

Sommer, P., and Nehrbass, U. (2005). Quality control of messenger ribonucleoprotein particles in the nucleus and at the pore. Curr Opin Cell Biol *17*, 294-301.

Sood, V., and Brickner, J.H. (2014). Nuclear pore interactions with the genome. Curr Opin Genet Dev *25*, 43-49.

Sorger, P.K. (1991). Heat shock factor and the heat shock response. Cell *65*, 363-366.

Sorger, P.K., Lewis, M.J., and Pelham, H.R. (1987). Heat shock factor is regulated differently in yeast and HeLa cells. Nature *329*, 81-84.

Sorger, P.K., and Pelham, H.R. (1988). Yeast heat shock factor is an essential DNA-binding protein that exhibits temperature-dependent phosphorylation. Cell *54*, 855-864.

Sorokin, A.V., Kim, E.R., and Ovchinnikov, L.P. (2007). Nucleocytoplasmic transport of proteins. Biochemistry (Mosc) *72*, 1439-1457.

Soucek, S., Corbett, A.H., and Fasken, M.B. (2012). The long and the short of it: the role of the zinc finger polyadenosine RNA binding protein, Nab2, in control of poly(A) tail length. Biochim Biophys Acta *1819*, 546-554.

Soucek, S., Zeng, Y., Bellur, D.L., Bergkessel, M., Morris, K.J., Deng, Q., Duong, D., Seyfried, N.T., Guthrie, C., Staley, J.P.*, et al.* (2016). The Evolutionarily-conserved Polyadenosine RNA Binding Protein, Nab2, Cooperates with Splicing Machinery to Regulate the Fate of pre-mRNA. Mol Cell Biol *36*, 2697-2714.

Souquet, B., Freed, E., Berto, A., Andric, V., Auduge, N., Reina-San-Martin, B., Lacy, E., and Doye, V. (2018). Nup133 Is Required for Proper Nuclear Pore Basket Assembly and Dynamics in Embryonic Stem Cells. Cell Rep *25*, 1994.

St-Andre, O., Lemieux, C., Perreault, A., Lackner, D.H., Bahler, J., and Bachand, F. (2010). Negative regulation of meiotic gene expression by the nuclear poly(a)-binding protein in fission yeast. J Biol Chem *285*, 27859-27868.

Stefanovsky, V.Y., Pelletier, G., Hannan, R., Gagnon-Kugler, T., Rothblum, L.I., and Moss, T. (2001). An immediate response of ribosomal transcription to growth factor stimulation in mammals is mediated by ERK phosphorylation of UBF. Mol Cell *8*, 1063-1073.

Steglich, B., Stralfors, A., Khorosjutina, O., Persson, J., Smialowska, A., Javerzat, J.P., and Ekwall, K. (2015). The Fun30 chromatin remodeler Fft3 controls nuclear organization and chromatin structure of insulators and subtelomeres in fission yeast. PLoS Genet *11*, e1005101.

Stegmeier, F., and Amon, A. (2004). Closing mitosis: the functions of the Cdc14 phosphatase and its regulation. Annu Rev Genet *38*, 203-232.

Stewart, M. (2010). Nuclear export of mRNA. Trends Biochem Sci *35*, 609-617.

Stewart, M. (2019). Polyadenylation and nuclear export of mRNAs. J Biol Chem *294*, 2977-2987.

Stoler, S., Keith, K.C., Curnick, K.E., and Fitzgerald-Hayes, M. (1995). A mutation in CSE4, an essential gene encoding a novel chromatin-associated protein in yeast, causes chromosome nondisjunction and cell cycle arrest at mitosis. Genes Dev *9*, 573-586.

Strahm, Y., Fahrenkrog, B., Zenklusen, D., Rychner, E., Kantor, J., Rosbach, M., and Stutz, F. (1999). The RNA export factor Gle1p is located on the cytoplasmic fibrils of the NPC and physically interacts with the FG-nucleoporin Rip1p, the DEAD-box protein Rat8p/Dbp5p and a new protein Ymr 255p. EMBO J *18*, 5761-5777.

Stralfors, A., Walfridsson, J., Bhuiyan, H., and Ekwall, K. (2011). The FUN30 chromatin remodeler, Fft3, protects centromeric and subtelomeric domains from euchromatin formation. PLoS Genet *7*, e1001334.

Strambio-de-Castillia, C., Blobel, G., and Rout, M.P. (1999). Proteins connecting the nuclear pore complex with the nuclear interior. J Cell Biol *144*, 839-855.

Strambio-De-Castillia, C., Niepel, M., and Rout, M.P. (2010). The nuclear pore complex: bridging nuclear transport and gene regulation. Nat Rev Mol Cell Biol *11*, 490-501.

Strassburg, K., Walther, D., Takahashi, H., Kanaya, S., and Kopka, J. (2010). Dynamic transcriptional and metabolic responses in yeast adapting to temperature stress. OMICS *14*, 249-259.

Strasser, K., Bassler, J., and Hurt, E. (2000). Binding of the Mex67p/Mtr2p heterodimer to FXFG, GLFG, and FG repeat nucleoporins is essential for nuclear mRNA export. J Cell Biol *150*, 695-706.

Strasser, K., and Hurt, E. (2000). Yra1p, a conserved nuclear RNA-binding protein, interacts directly with Mex67p and is required for mRNA export. EMBO J *19*, 410-420.

Strasser, K., and Hurt, E. (2001). Splicing factor Sub2p is required for nuclear mRNA export through its interaction with Yra1p. Nature *413*, 648-652.

Strasser, K., Masuda, S., Mason, P., Pfannstiel, J., Oppizzi, M., Rodriguez-Navarro, S., Rondon, A.G., Aguilera, A., Struhl, K., Reed, R.*, et al.* (2002). TREX is a conserved complex coupling transcription with messenger RNA export. Nature *417*, 304-308.

Strawn, L.A., Shen, T., Shulga, N., Goldfarb, D.S., and Wente, S.R. (2004). Minimal nuclear pore complexes define FG repeat domains essential for transport. Nat Cell Biol *6*, 197-206.

Strawn, L.A., Shen, T., and Wente, S.R. (2001). The GLFG regions of Nup116p and Nup100p serve as binding sites for both Kap95p and Mex67p at the nuclear pore complex. J Biol Chem *276*, 6445-6452.

Stutz, F., and Izaurralde, E. (2003). The interplay of nuclear mRNP assembly, mRNA surveillance and export. Trends Cell Biol *13*, 319-327.

Stutz, F., Kantor, J., Zhang, D., McCarthy, T., Neville, M., and Rosbash, M. (1997). The yeast nucleoporin rip1p contributes to multiple export pathways with no essential role for its FG-repeat region. Genes Dev *11*, 2857-2868.

Stuwe, T., Bley, C.J., Thierbach, K., Petrovic, S., Schilbach, S., Mayo, D.J., Perriches, T., Rundlet, E.J., Jeon, Y.E., Collins, L.N.*, et al.* (2015a). Architecture of the fungal nuclear pore inner ring complex. Science *350*, 56-64.

Stuwe, T., Correia, A.R., Lin, D.H., Paduch, M., Lu, V.T., Kossiakoff, A.A., and Hoelz, A. (2015b). Nuclear pores. Architecture of the nuclear pore complex coat. Science *347*, 1148-1152.

Su, Y., Pelz, C., Huang, T., Torkenczy, K., Wang, X., Cherry, A., Daniel, C.J., Liang, J., Nan, X., Dai, M.S.*, et al.* (2018). Post-translational modification localizes MYC to the nuclear pore basket to regulate a subset of target genes involved in cellular responses to environmental signals. Genes Dev *32*, 1398-1419.

Subramanian, L., Toda, N.R., Rappsilber, J., and Allshire, R.C. (2014). Eic1 links Mis18 with the CCAN/Mis6/Ctf19 complex to promote CENP-A assembly. Open Biol *4*, 140043.

Sugimoto, K., Kuriyama, K., Shibata, A., and Himeno, M. (1997). Characterization of internal DNA-binding and C-terminal dimerization domains of human centromere/kinetochore autoantigen CENP-C in vitro: role of DNA-binding and self-associating activities in kinetochore organization. Chromosome research : an international journal on the molecular, supramolecular and evolutionary aspects of chromosome biology *5*, 132-141.

Sugiyama, T., Cam, H., Verdel, A., Moazed, D., and Grewal, S.I. (2005). RNA-dependent RNA polymerase is an essential component of a self-enforcing loop coupling heterochromatin assembly to siRNA production. Proc Natl Acad Sci U S A *102*, 152-157.

Sugiyama, T., Cam, H.P., Sugiyama, R., Noma, K., Zofall, M., Kobayashi, R., and Grewal, S.I. (2007). SHREC, an effector complex for heterochromatic transcriptional silencing. Cell *128*, 491-504.

Sugiyama, T., and Sugioka-Sugiyama, R. (2011). Red1 promotes the elimination of meiosis-specific mRNAs in vegetatively growing fission yeast. EMBO J *30*, 1027-1039.

Sugiyama, T., Wanatabe, N., Kitahata, E., Tani, T., and Sugioka-Sugiyama, R. (2013). Red5 and three nuclear pore components are essential for efficient suppression of specific mRNAs during vegetative growth of fission yeast. Nucleic Acids Res *41*, 6674-6686.

Sullivan, K.F., Hechenberger, M., and Masri, K. (1994). Human CENP-A contains a histone H3 related histone fold domain that is required for targeting to the centromere. J Cell Biol *127*, 581-592.

Suma, M., Kitagawa, T., Nakase, Y., Nakazawa, N., Yanagida, M., and Matsumoto, T. (2018). Fission Yeast CENP-C (Cnp3) Plays a Role in Restricting the Site of CENP-A Accumulation. G3 (Bethesda) *8*, 2723-2733.

Sun, J., Shi, Y., and Yildirim, E. (2019). The Nuclear Pore Complex in Cell Type-Specific Chromatin Structure and Gene Regulation. Trends Genet *35*, 579-588.

Sun, L.L., Li, M., Suo, F., Liu, X.M., Shen, E.Z., Yang, B., Dong, M.Q., He, W.Z., and Du, L.L. (2013). Global analysis of fission yeast mating genes reveals new autophagy factors. PLoS Genet *9*, e1003715.

Suntharalingam, M., and Wente, S.R. (2003). Peering through the pore: nuclear pore complex structure, assembly, and function. Dev Cell *4*, 775-789.

Swaffer, M.P., Jones, A.W., Flynn, H.R., Snijders, A.P., and Nurse, P. (2018). Quantitative Phosphoproteomics Reveals the Signaling Dynamics of Cell-Cycle Kinases in the Fission Yeast Schizosaccharomyces pombe. Cell Rep *24*, 503-514.

Szymborska, A., de Marco, A., Daigle, N., Cordes, V.C., Briggs, J.A., and Ellenberg, J. (2013). Nuclear pore scaffold structure analyzed by super-resolution microscopy and particle averaging. Science *341*, 655-658.

Taddei, A., Van Houwe, G., Hediger, F., Kalck, V., Cubizolles, F., Schober, H., and Gasser, S.M. (2006). Nuclear pore association confers optimal expression levels for an inducible yeast gene. Nature *441*, 774-778.

Takahashi, K., Chen, E.S., and Yanagida, M. (2000). Requirement of Mis6 centromere connector for localizing a CENP-A-like protein in fission yeast. Science *288*, 2215-2219.

Takahashi, K., Takayama, Y., Masuda, F., Kobayashi, Y., and Saitoh, S. (2005). Two distinct pathways responsible for the loading of CENP-A to centromeres in the fission yeast cell cycle. Philosophical transactions of the Royal Society of London Series B, Biological sciences *360*, 595-606; discussion 606-597.

Takahashi, K., Yamada, H., and Yanagida, M. (1994). Fission yeast minichromosome loss mutants mis cause lethal aneuploidy and replication abnormality. Mol Biol Cell *5*, 1145-1158.

Takayama, Y., Sato, H., Saitoh, S., Ogiyama, Y., Masuda, F., and Takahashi, K. (2008). Biphasic incorporation of centromeric histone CENP-A in fission yeast. Mol Biol Cell *19*, 682-690.

Takeda, K., Tonthat, N.K., Glover, T., Xu, W., Koonin, E.V., Yanagida, M., and Schumacher, M.A. (2011). Implications for proteasome nuclear localization revealed by the structure of the nuclear proteasome tether protein Cut8. Proc Natl Acad Sci U S A *108*, 16950-16955.

Takeda, K., and Yanagida, M. (2005). Regulation of nuclear proteasome by Rhp6/Ubc2 through ubiquitination and destruction of the sensor and anchor Cut8. Cell *122*, 393-405.

Takeuchi, K., and Fukagawa, T. (2012). Molecular architecture of vertebrate kinetochores. Exp Cell Res *318*, 1367-1374.

Takeuchi, K., Nishino, T., Mayanagi, K., Horikoshi, N., Osakabe, A., Tachiwana, H., Hori, T., Kurumizaka, H., and Fukagawa, T. (2014). The centromeric nucleosome-like CENP-T-W-S-X complex induces positive supercoils into DNA. Nucleic Acids Res *42*, 1644-1655.

Tan, W., Zolotukhin, A.S., Bear, J., Patenaude, D.J., and Felber, B.K. (2000). The mRNA export in Caenorhabditis elegans is mediated by Ce-NXF-1, an ortholog of human TAP/NXF and Saccharomyces cerevisiae Mex67p. RNA *6*, 1762-1772.

Tan-Wong, S.M., Wijayatilake, H.D., and Proudfoot, N.J. (2009). Gene loops function to maintain transcriptional memory through interaction with the nuclear pore complex. Genes Dev *23*, 2610-2624.

Tanaka, K., Chang, H.L., Kagami, A., and Watanabe, Y. (2009). CENP-C functions as a scaffold for effectors with essential kinetochore functions in mitosis and meiosis. Dev Cell *17*, 334-343.

Tani, T., Derby, R.J., Hiraoka, Y., and Spector, D.L. (1995). Nucleolar accumulation of poly (A)+ RNA in heat-shocked yeast cells: implication of nucleolar involvement in mRNA transport. Mol Biol Cell *6*, 1515-1534.

Tani, T., Derby, R.J., Hiraoka, Y., and Spector, D.L. (1996). Nucleolar accumulation of poly (A)+ RNA in heat-shocked yeast cells: implication of nucleolar involvement in mRNA transport. Mol Biol Cell *7*, 173-192.

Tanizawa, H., Iwasaki, O., Tanaka, A., Capizzi, J.R., Wickramasinghe, P., Lee, M., Fu, Z., and Noma, K. (2010). Mapping of long-range associations throughout the fission yeast genome reveals global genome organization linked to transcriptional regulation. Nucleic Acids Res *38*, 8164-8177.

Tapia-Alveal, C., Outwin, E.A., Trempolec, N., Dziadkowiec, D., Murray, J.M., and O'Connell, M.J. (2010). SMC complexes and topoisomerase II work together so that sister chromatids can work apart. Cell Cycle *9*, 2065-2070.

Tapley, E.C., and Starr, D.A. (2013). Connecting the nucleus to the cytoskeleton by SUN-KASH bridges across the nuclear envelope. Curr Opin Cell Biol *25*, 57-62.

Taricani, L., Tejada, M.L., and Young, P.G. (2002). The fission yeast ES2 homologue, Bis1, interacts with the Ish1 stress-responsive nuclear envelope protein. J Biol Chem *277*, 10562-10572.

Tasto, J.J., Carnahan, R.H., McDonald, W.H., and Gould, K.L. (2001). Vectors and gene targeting modules for tandem affinity purification in Schizosaccharomyces pombe. Yeast *18*, 657-662.

Tatebe, H., and Yanagida, M. (2000). Cut8, essential for anaphase, controls localization of 26S proteasome, facilitating destruction of cyclin and Cut2. Curr Biol *10*, 1329-1338.

Tchelidze, P., Benassarou, A., Kaplan, H., O'Donohue, M.F., Lucas, L., Terryn, C., Rusishvili, L., Mosidze, G., Lalun, N., and Ploton, D. (2017). Nucleolar sub-compartments in motion during rRNA synthesis inhibition: Contraction of nucleolar condensed chromatin and gathering of fibrillar centers are concomitant. PLoS One *12*, e0187977.

Terry, L.J., and Wente, S.R. (2007). Nuclear mRNA export requires specific FG nucleoporins for translocation through the nuclear pore complex. J Cell Biol *178*, 1121-1132.

Terry, L.J., and Wente, S.R. (2009). Flexible gates: dynamic topologies and functions for FG nucleoporins in nucleocytoplasmic transport. Eukaryot Cell *8*, 1814-1827.

Tetenbaum-Novatt, J., and Rout, M.P. (2010). The mechanism of nucleocytoplasmic transport through the nuclear pore complex. Cold Spring Harb Symp Quant Biol *75*, 567-584.

Texari, L., and Stutz, F. (2015). Sumoylation and transcription regulation at nuclear pores. Chromosoma *124*, 45-56.

Thadani, R., Uhlmann, F., and Heeger, S. (2012). Condensin, chromatin crossbarring and chromosome condensation. Curr Biol *22*, R1012-1021.

Thakurta, A.G., Gopal, G., Yoon, J.H., Kozak, L., and Dhar, R. (2005). Homolog of BRCA2-interacting Dss1p and Uap56p link Mlo3p and Rae1p for mRNA export in fission yeast. EMBO J *24*, 2512-2523.

Thakurta, A.G., Gopal, G., Yoon, J.H., Saha, T., and Dhar, R. (2004). Conserved nuclear export sequences in Schizosaccharomyces pombe Mex67 and human TAP function in mRNA export by direct nuclear pore interactions. J Biol Chem *279*, 17434-17442.

Thakurta, A.G., Selvanathan, S.P., Patterson, A.D., Gopal, G., and Dhar, R. (2007). The nuclear export signal of splicing factor Uap56p interacts with nuclear pore-associated protein Rae1p for mRNA export in Schizosaccharomyces pombe. J Biol Chem *282*, 17507-17516.

Thielmann, H.W., and Popanda, O. (1998). Irradiation with ultraviolet light and gamma-rays increases the level of DNA topoisomerase II in nuclei of normal and xeroderma pigmentosum fibroblasts. Int J Oncol *12*, 265-271.

Thomsen, R., Libri, D., Boulay, J., Rosbash, M., and Jensen, T.H. (2003). Localization of nuclear retained mRNAs in Saccharomyces cerevisiae. RNA *9*, 1049-1057.

Thon, G., and Verhein-Hansen, J. (2000). Four chromo-domain proteins of Schizosaccharomyces pombe differentially repress transcription at various chromosomal locations. Genetics *155*, 551-568.

Tibbles, L.A., and Woodgett, J.R. (1999). The stress-activated protein kinase pathways. Cell Mol Life Sci *55*, 1230-1254.

Tieg, B., and Krebber, H. (2013). Dbp5 - from nuclear export to translation. Biochim Biophys Acta *1829*, 791-798.

Tirosh, I., Wong, K.H., Barkai, N., and Struhl, K. (2011). Extensive divergence of yeast stress responses through transitions between induced and constitutive activation. Proc Natl Acad Sci U S A *108*, 16693-16698.

Toda, T., Hsu, J.Y., Linker, S.B., Hu, L., Schafer, S.T., Mertens, J., Jacinto, F.V., Hetzer, M.W., and Gage, F.H. (2017). Nup153 Interacts with Sox2 to Enable Bimodal Gene Regulation and Maintenance of Neural Progenitor Cells. Cell Stem Cell *21*, 618-634 e617.

Tomko, R.J., Jr., Funakoshi, M., Schneider, K., Wang, J., and Hochstrasser, M. (2010). Heterohexameric ring arrangement of the eukaryotic proteasomal ATPases: implications for proteasome structure and assembly. Mol Cell *38*, 393-403.

Tong, A.H., Evangelista, M., Parsons, A.B., Xu, H., Bader, G.D., Page, N., Robinson, M., Raghibizadeh, S., Hogue, C.W., Bussey, H.*, et al.* (2001). Systematic genetic analysis with ordered arrays of yeast deletion mutants. Science *294*, 2364-2368.

Tran, E.J., and Wente, S.R. (2006). Dynamic nuclear pore complexes: life on the edge. Cell *125*, 1041-1053.

Tran, E.J., Zhou, Y., Corbett, A.H., and Wente, S.R. (2007). The DEAD-box protein Dbp5 controls mRNA export by triggering specific RNA:protein remodeling events. Mol Cell *28*, 850-859.

Trautmann, S., Wolfe, B.A., Jorgensen, P., Tyers, M., Gould, K.L., and McCollum, D. (2001). Fission yeast Clp1p phosphatase regulates G2/M transition and coordination of cytokinesis with cell cycle progression. Curr Biol *11*, 931-940.

Trazzi, S., Bernardoni, R., Diolaiti, D., Politi, V., Earnshaw, W.C., Perini, G., and Della Valle, G. (2002). In vivo functional dissection of human inner kinetochore protein CENP-C. J Struct Biol *140*, 39-48.

Trazzi, S., Perini, G., Bernardoni, R., Zoli, M., Reese, J.C., Musacchio, A., and Della Valle, G. (2009). The C-terminal domain of CENP-C displays multiple and critical functions for mammalian centromere formation. PLoS One *4*, e5832.

Trcek, T., Chao, J.A., Larson, D.R., Park, H.Y., Zenklusen, D., Shenoy, S.M., and Singer, R.H. (2012). Single-mRNA counting using fluorescent in situ hybridization in budding yeast. Nature protocols *7*, 408-419.

Treger, J.M., Schmitt, A.P., Simon, J.R., and McEntee, K. (1998). Transcriptional factor mutations reveal regulatory complexities of heat shock and newly identified stress genes in Saccharomyces cerevisiae. J Biol Chem *273*, 26875-26879.

Trinklein, N.D., Murray, J.I., Hartman, S.J., Botstein, D., and Myers, R.M. (2004). The role of heat shock transcription factor 1 in the genome-wide regulation of the mammalian heat shock response. Mol Biol Cell *15*, 1254-1261.

Trott A., M.K.A. (2003). The yeast response to heat shock, Vol Topics in Current Genetics (Berlin, Heidelberg: Springer).

Truman, A.W., Millson, S.H., Nuttall, J.M., Mollapour, M., Prodromou, C., and Piper, P.W. (2007). In the yeast heat shock response, Hsf1-directed induction of Hsp90 facilitates the activation of the Slt2 (Mpk1) mitogen-activated protein kinase required for cell integrity. Eukaryot Cell *6*, 744-752.

Tudek, A., Lloret-Llinares, M., and Jensen, T.H. (2018a). The multitasking polyA tail: nuclear RNA maturation, degradation and export. Philosophical transactions of the Royal Society of London Series B, Biological sciences *373*.

Tudek, A., Schmid, M., Makaras, M., Barrass, J.D., Beggs, J.D., and Jensen, T.H. (2018b). A Nuclear Export Block Triggers the Decay of Newly Synthesized Polyadenylated RNA. Cell Rep *24*, 2457-2467 e2457.

Tutucci, E., and Stutz, F. (2011). Keeping mRNPs in check during assembly and nuclear export. Nat Rev Mol Cell Biol *12*, 377-384.

Umlauf, D., Bonnet, J., Waharte, F., Fournier, M., Stierle, M., Fischer, B., Brino, L., Devys, D., and Tora, L. (2013). The human TREX-2 complex is stably associated with the nuclear pore basket. J Cell Sci *126*, 2656-2667.

Unno, M., Mizushima, T., Morimoto, Y., Tomisugi, Y., Tanaka, K., Yasuoka, N., and Tsukihara, T. (2002). The structure of the mammalian 20S proteasome at 2.75 A resolution. Structure *10*, 609-618.

Upla, P., Kim, S.J., Sampathkumar, P., Dutta, K., Cahill, S.M., Chemmama, I.E., Williams, R., Bonanno, J.B., Rice, W.J., Stokes, D.L.*, et al.* (2017). Molecular Architecture of the Major Membrane Ring Component of the Nuclear Pore Complex. Structure *25*, 434-445.

Vabulas, R.M., Raychaudhuri, S., Hayer-Hartl, M., and Hartl, F.U. (2010). Protein folding in the cytoplasm and the heat shock response. Cold Spring Harb Perspect Biol *2*, a004390.

Vainberg, I.E., Dower, K., and Rosbash, M. (2000). Nuclear export of heat shock and non-heat-shock mRNA occurs via similar pathways. Mol Cell Biol *20*, 3996-4005.

Van de Vosse, D.W., Wan, Y., Lapetina, D.L., Chen, W.M., Chiang, J.H., Aitchison, J.D., and Wozniak, R.W. (2013). A role for the nucleoporin Nup170p in chromatin structure and gene silencing. Cell *152*, 969-983.

Van de Vosse, D.W., Wan, Y., Wozniak, R.W., and Aitchison, J.D. (2011). Role of the nuclear envelope in genome organization and gene expression. Wiley Interdiscip Rev Syst Biol Med *3*, 147-166.

van Emden, T.S., Forn, M., Forne, I., Sarkadi, Z., Capella, M., Martin Caballero, L., Fischer-Burkart, S., Bronner, C., Simonetta, M., Toczyski, D.*, et al.* (2019). Shelterin and subtelomeric DNA sequences control nucleosome maintenance and genome stability. EMBO reports *20*.

Vaquerizas, J.M., Suyama, R., Kind, J., Miura, K., Luscombe, N.M., and Akhtar, A. (2010). Nuclear pore proteins nup153 and megator define transcriptionally active regions in the Drosophila genome. PLoS Genet *6*, e1000846.

Varetti, G., Guida, C., Santaguida, S., Chiroli, E., and Musacchio, A. (2011). Homeostatic control of mitotic arrest. Mol Cell *44*, 710-720.

Varma, D., and Salmon, E.D. (2012). The KMN protein network--chief conductors of the kinetochore orchestra. J Cell Sci *125*, 5927-5936.

Velazquez, J.M., and Lindquist, S. (1984). hsp70: nuclear concentration during environmental stress and cytoplasmic storage during recovery. Cell *36*, 655-662.

Verdel, A., Jia, S., Gerber, S., Sugiyama, T., Gygi, S., Grewal, S.I., and Moazed, D. (2004). RNAi-mediated targeting of heterochromatin by the RITS complex. Science *303*, 672-676.

Verdel, A., and Moazed, D. (2005). RNAi-directed assembly of heterochromatin in fission yeast. FEBS letters *579*, 5872-5878.

Verghese, J., Abrams, J., Wang, Y., and Morano, K.A. (2012). Biology of the heat shock response and protein chaperones: budding yeast (Saccharomyces cerevisiae) as a model system. Microbiol Mol Biol Rev *76*, 115-158.

Veri, A.O., Robbins, N., and Cowen, L.E. (2018). Regulation of the heat shock transcription factor Hsf1 in fungi: implications for temperature-dependent virulence traits. FEMS yeast research *18*.

Verrier, L., Taglini, F., Barrales, R.R., Webb, S., Urano, T., Braun, S., and Bayne, E.H. (2015). Global regulation of heterochromatin spreading by Leo1. Open Biol *5*.

Vigh, L., Nakamoto, H., Landry, J., Gomez-Munoz, A., Harwood, J.L., and Horvath, I. (2007). Membrane regulation of the stress response from prokaryotic models to mammalian cells. Ann N Y Acad Sci *1113*, 40-51.

Vinciguerra, P., Iglesias, N., Camblong, J., Zenklusen, D., and Stutz, F. (2005). Perinuclear Mlp proteins downregulate gene expression in response to a defect in mRNA export. EMBO J *24*, 813-823.

Vinciguerra, P., and Stutz, F. (2004). mRNA export: an assembly line from genes to nuclear pores. Curr Opin Cell Biol *16*, 285-292.

Viphakone, N., Hautbergue, G.M., Walsh, M., Chang, C.T., Holland, A., Folco, E.G., Reed, R., and Wilson, S.A. (2012). TREX exposes the RNA-binding domain of Nxf1 to enable mRNA export. Nat Commun *3*, 1006.

Viphakone, N., Sudbery, I., Griffith, L., Heath, C.G., Sims, D., and Wilson, S.A. (2019). Co-transcriptional Loading of RNA Export Factors Shapes the Human Transcriptome. Mol Cell *75*, 310-323 e318.

Viphakone, N., Voisinet-Hakil, F., and Minvielle-Sebastia, L. (2008). Molecular dissection of mRNA poly(A) tail length control in yeast. Nucleic Acids Res *36*, 2418-2433.

Visintin, R., Hwang, E.S., and Amon, A. (1999). Cfi1 prevents premature exit from mitosis by anchoring Cdc14 phosphatase in the nucleolus. Nature *398*, 818-823.

Vjestica, A., Zhang, D., Liu, J., and Oliferenko, S. (2013). Hsp70-Hsp40 chaperone complex functions in controlling polarized growth by repressing Hsf1-driven heat stress-associated transcription. PLoS Genet *9*, e1003886.

Voellmy, R. (2004). Transcriptional regulation of the metazoan stress protein response. Prog Nucleic Acid Res Mol Biol *78*, 143-185.

Voellmy, R., and Boellmann, F. (2007). Chaperone regulation of the heat shock protein response. Advances in experimental medicine and biology *594*, 89-99.

Vogel, J.L., Parsell, D.A., and Lindquist, S. (1995). Heat-shock proteins Hsp104 and Hsp70 reactivate mRNA splicing after heat inactivation. Curr Biol *5*, 306-317.

Voges, D., Zwickl, P., and Baumeister, W. (1999). The 26S proteasome: a molecular machine designed for controlled proteolysis. Annu Rev Biochem *68*, 1015-1068.

Vollmer, B., and Antonin, W. (2014). The diverse roles of the Nup93/Nic96 complex proteins - structural scaffolds of the nuclear pore complex with additional cellular functions. Biol Chem *395*, 515-528.

Vollmer, B., Schooley, A., Sachdev, R., Eisenhardt, N., Schneider, A.M., Sieverding, C., Madlung, J., Gerken, U., Macek, B., and Antonin, W. (2012). Dimerization and direct membrane interaction of Nup53 contribute to nuclear pore complex assembly. EMBO J *31*, 4072-4084.

Volpe, T., and Martienssen, R.A. (2011). RNA interference and heterochromatin assembly. Cold Spring Harb Perspect Biol *3*, a003731.

Volpe, T.A., Kidner, C., Hall, I.M., Teng, G., Grewal, S.I., and Martienssen, R.A. (2002). Regulation of heterochromatic silencing and histone H3 lysine-9 methylation by RNAi. Science *297*, 1833-1837.

Vomastek, T., Iwanicki, M.P., Burack, W.R., Tiwari, D., Kumar, D., Parsons, J.T., Weber, M.J., and Nandicoori, V.K. (2008). Extracellular signal-regulated kinase 2 (ERK2) phosphorylation sites and docking domain on the nuclear pore complex protein Tpr cooperatively regulate ERK2-Tpr interaction. Mol Cell Biol *28*, 6954-6966.

von Appen, A., Kosinski, J., Sparks, L., Ori, A., DiGuilio, A.L., Vollmer, B., Mackmull, M.T., Banterle, N., Parca, L., Kastritis, P.*, et al.* (2015). In situ structural analysis of the human nuclear pore complex. Nature *526*, 140-143.

Vujanac, M., Fenaroli, A., and Zimarino, V. (2005). Constitutive nuclear import and stress-regulated nucleocytoplasmic shuttling of mammalian heat-shock factor 1. Traffic *6*, 214-229.

Wahle, E. (1995). Poly(A) tail length control is caused by termination of processive synthesis. J Biol Chem *270*, 2800-2808.

Walde, S., and Kehlenbach, R.H. (2010). The Part and the Whole: functions of nucleoporins in nucleocytoplasmic transport. Trends Cell Biol *20*, 461-469.

Wallace, E.W., Kear-Scott, J.L., Pilipenko, E.V., Schwartz, M.H., Laskowski, P.R., Rojek, A.E., Katanski, C.D., Riback, J.A., Dion, M.F., Franks, A.M.*, et al.* (2015). Reversible, Specific, Active Aggregates of Endogenous Proteins Assemble upon Heat Stress. Cell *162*, 1286-1298.

Walther, D., Strassburg, K., Durek, P., and Kopka, J. (2010). Metabolic pathway relationships revealed by an integrative analysis of the transcriptional and metabolic temperature stress-response dynamics in yeast. OMICS *14*, 261-274.

Walther, T.C., Alves, A., Pickersgill, H., Loiodice, I., Hetzer, M., Galy, V., Hulsmann, B.B., Kocher, T., Wilm, M., Allen, T.*, et al.* (2003). The conserved Nup107-160 complex is critical for nuclear pore complex assembly. Cell *113*, 195-206.

Wang, M., Tao, X., Jacob, M.D., Bennett, C.A., Ho, J.J.D., Gonzalgo, M.L., Audas, T.E., and Lee, S. (2018). Stress-Induced Low Complexity RNA Activates Physiological Amyloidogenesis. Cell Rep *24*, 1713-1721 e1714.

Warner, J.R. (1999). The economics of ribosome biosynthesis in yeast. Trends Biochem Sci *24*, 437-440.

Watanabe, N., Ikeda, T., Mizuki, F., and Tani, T. (2012). Characterization of the ptr5+ gene involved in nuclear mRNA export in fission yeast. Biochemical and biophysical research communications *418*, 62-66.

Watt, S., Mata, J., Lopez-Maury, L., Marguerat, S., Burns, G., and Bahler, J. (2008). urg1: a uracil-regulatable promoter system for fission yeast with short induction and repression times. PLoS One *3*, e1428.

Wehmer, M., and Sakata, E. (2016). Recent advances in the structural biology of the 26S proteasome. Int J Biochem Cell Biol *79*, 437-442.

Wei, N., and Deng, X.W. (2003). The COP9 signalosome. Annual review of cell and developmental biology *19*, 261-286.

Weighardt, F., Cobianchi, F., Cartegni, L., Chiodi, I., Villa, A., Riva, S., and Biamonti, G. (1999). A novel hnRNP protein (HAP/SAF-B) enters a subset of hnRNP complexes and relocates in nuclear granules in response to heat shock. J Cell Sci *112 (Pt 10)*, 1465-1476.

Weirich, C.S., Erzberger, J.P., Berger, J.M., and Weis, K. (2004). The N-terminal domain of Nup159 forms a beta-propeller that functions in mRNA export by tethering the helicase Dbp5 to the nuclear pore. Mol Cell *16*, 749-760.

Welch, W.J., and Feramisco, J.R. (1984). Nuclear and nucleolar localization of the 72,000-dalton heat shock protein in heat-shocked mammalian cells. J Biol Chem *259*, 4501-4513.

Welch, W.J., and Suhan, J.P. (1985). Morphological study of the mammalian stress response: characterization of changes in cytoplasmic organelles, cytoskeleton, and nucleoli, and appearance of intranuclear actin filaments in rat fibroblasts after heat-shock treatment. J Cell Biol *101*, 1198-1211.

Wente, S.R., and Rout, M.P. (2010). The nuclear pore complex and nuclear transport. Cold Spring Harb Perspect Biol *2*, a000562.

Werner-Washburne, M., Stone, D.E., and Craig, E.A. (1987). Complex interactions among members of an essential subfamily of hsp70 genes in Saccharomyces cerevisiae. Mol Cell Biol *7*, 2568-2577.

West, R.R., Vaisberg, E.V., Ding, R., Nurse, P., and McIntosh, J.R. (1998). cut11(+): A gene required for cell cycle-dependent spindle pole body anchoring in the nuclear envelope and bipolar spindle formation in Schizosaccharomyces pombe. Mol Biol Cell *9*, 2839-2855.

Westerheide, S.D., Anckar, J., Stevens, S.M., Jr., Sistonen, L., and Morimoto, R.I. (2009). Stress-inducible regulation of heat shock factor 1 by the deacetylase SIRT1. Science *323*, 1063-1066.

Westermann, S., and Schleiffer, A. (2013). Family matters: structural and functional conservation of centromere-associated proteins from yeast to humans. Trends Cell Biol *23*, 260-269.

Wilhelm, B.T., Marguerat, S., Watt, S., Schubert, F., Wood, V., Goodhead, I., Penkett, C.J., Rogers, J., and Bahler, J. (2008). Dynamic repertoire of a eukaryotic transcriptome surveyed at single-nucleotide resolution. Nature *453*, 1239-1243.

Wilkinson, C.R., Wallace, M., Morphew, M., Perry, P., Allshire, R., Javerzat, J.P., McIntosh, J.R., and Gordon, C. (1998). Localization of the 26S proteasome during mitosis and meiosis in fission yeast. EMBO J *17*, 6465-6476.

Wilkinson, C.R., Wallace, M., Seeger, M., Dubiel, W., and Gordon, C. (1997). Mts4, a non-ATPase subunit of the 26 S protease in fission yeast is essential for mitosis and interacts directly with the ATPase subunit Mts2. J Biol Chem *272*, 25768-25777.

Wilkinson, M.G., Samuels, M., Takeda, T., Toone, W.M., Shieh, J.C., Toda, T., Millar, J.B., and Jones, N. (1996). The Atf1 transcription factor is a target for the Sty1 stress-activated MAP kinase pathway in fission yeast. Genes Dev *10*, 2289-2301.

Williams, J.S., Hayashi, T., Yanagida, M., and Russell, P. (2009). Fission yeast Scm3 mediates stable assembly of Cnp1/CENP-A into centromeric chromatin. Mol Cell *33*, 287-298.

Winey, M., Yarar, D., Giddings, T.H., Jr., and Mastronarde, D.N. (1997). Nuclear pore complex number and distribution throughout the Saccharomyces cerevisiae cell cycle by three-dimensional reconstruction from electron micrographs of nuclear envelopes. Mol Biol Cell *8*, 2119-2132.

Wojcik, C., Benchaib, M., Lornage, J., Czyba, J.C., and Guerin, J.F. (2000). Localization of proteasomes in human oocytes and preimplantation embryos. Mol Hum Reprod *6*, 331-336.

Wood, V., Gwilliam, R., Rajandream, M.A., Lyne, M., Lyne, R., Stewart, A., Sgouros, J., Peat, N., Hayles, J., Baker, S.*, et al.* (2002). The genome sequence of Schizosaccharomyces pombe. Nature *415*, 871-880.

Wood, V., Harris, M.A., McDowall, M.D., Rutherford, K., Vaughan, B.W., Staines, D.M., Aslett, M., Lock, A., Bahler, J., Kersey, P.J.*, et al.* (2012). PomBase: a comprehensive online resource for fission yeast. Nucleic Acids Res *40*, D695-699.

Woodward, L.A., Mabin, J.W., Gangras, P., and Singh, G. (2017). The exon junction complex: a lifelong guardian of mRNA fate. Wiley interdisciplinary reviews RNA *8*.

Woolcock, K.J., and Buhler, M. (2013). Nuclear organisation and RNAi in fission yeast. Curr Opin Cell Biol *25*, 372-377.

Woolcock, K.J., Stunnenberg, R., Gaidatzis, D., Hotz, H.R., Emmerth, S., Barraud, P., and Buhler, M. (2012). RNAi keeps Atf1-bound stress response genes in check at nuclear pores. Genes Dev *26*, 683-692.

Xu, J., Yanagisawa, Y., Tsankov, A.M., Hart, C., Aoki, K., Kommajosyula, N., Steinmann, K.E., Bochicchio, J., Russ, C., Regev, A.*, et al.* (2012). Genome-wide identification and characterization of replication origins by deep sequencing. Genome Biol *13*, R27.

Xu, M., and Cook, P.R. (2008). The role of specialized transcription factories in chromosome pairing. Biochim Biophys Acta *1783*, 2155-2160.

Yamada, J., Phillips, J.L., Patel, S., Goldfien, G., Calestagne-Morelli, A., Huang, H., Reza, R., Acheson, J., Krishnan, V.V., Newsam, S.*, et al.* (2010). A bimodal distribution of two distinct categories of intrinsically disordered structures with separate functions in FG nucleoporins. Mol Cell Proteomics *9*, 2205-2224.

Yamada, T., Fischle, W., Sugiyama, T., Allis, C.D., and Grewal, S.I. (2005). The nucleation and maintenance of heterochromatin by a histone deacetylase in fission yeast. Mol Cell *20*, 173-185.

Yamagishi, M., and Nomura, M. (1988). Deficiency in both type I and type II DNA topoisomerase activities differentially affect rRNA and ribosomal protein synthesis in Schizosaccharomyces pombe. Curr Genet *13*, 305-314.

Yamagishi, Y., Sakuno, T., Goto, Y., and Watanabe, Y. (2014). Kinetochore composition and its function: lessons from yeasts. FEMS Microbiol Rev *38*, 185-200.

Yamamoto, A., Mizukami, Y., and Sakurai, H. (2005). Identification of a novel class of target genes and a novel type of binding sequence of heat shock transcription factor in Saccharomyces cerevisiae. J Biol Chem *280*, 11911-11919.

Yamamoto, N., Maeda, Y., Ikeda, A., and Sakurai, H. (2008). Regulation of thermotolerance by stress-induced transcription factors in Saccharomyces cerevisiae. Eukaryot Cell *7*, 783-790.

Yamanaka, S., Yamashita, A., Harigaya, Y., Iwata, R., and Yamamoto, M. (2010). Importance of polyadenylation in the selective elimination of meiotic mRNAs in growing S. pombe cells. EMBO J *29*, 2173-2181.

Yang, H.J., Asakawa, H., Haraguchi, T., and Hiraoka, Y. (2015). Nup132 modulates meiotic spindle attachment in fission yeast by regulating kinetochore assembly. J Cell Biol *211*, 295-308.

Yang, K., Yang, J., and Yi, J. (2018). Nucleolar Stress: hallmarks, sensing mechanism and diseases. Cell Stress *2*, 125-140.

Yang, Q., Rout, M.P., and Akey, C.W. (1998). Three-dimensional architecture of the isolated yeast nuclear pore complex: functional and evolutionary implications. Mol Cell *1*, 223-234.

Yoon, J.H. (2004). Schizosaccharomyces pombe rsm1 genetically interacts with spmex67, which is involved in mRNA export. Journal of microbiology *42*, 32-36.

Yoon, J.H., Love, D.C., Guhathakurta, A., Hanover, J.A., and Dhar, R. (2000). Mex67p of Schizosaccharomyces pombe interacts with Rae1p in mediating mRNA export. Mol Cell Biol *20*, 8767-8782.

Yoon, J.H., Whalen, W.A., Bharathi, A., Shen, R., and Dhar, R. (1997). Npp106p, a Schizosaccharomyces pombe nucleoporin similar to Saccharomyces cerevisiae Nic96p, functionally interacts with Rae1p in mRNA export. Mol Cell Biol *17*, 7047-7060.

Yoshida, J., and Tani, T. (2005). Hsp16p is required for thermotolerance in nuclear mRNA export in fission yeast Schizosaccharomyces pombe. Cell structure and function *29*, 125-138.

Yoshida, M., and Sazer, S. (2004). Nucleocytoplasmic transport and nuclear envelope integrity in the fission yeast Schizosaccharomyces pombe. Methods *33*, 226-238.

Yoshida, T., Shimada, K., Oma, Y., Kalck, V., Akimura, K., Taddei, A., Iwahashi, H., Kugou, K., Ohta, K., Gasser, S.M.*, et al.* (2010). Actin-related protein Arp6 influences H2A.Z-dependent and -independent gene expression and links ribosomal protein genes to nuclear pores. PLoS Genet *6*, e1000910.

Yost, H.J., and Lindquist, S. (1986). RNA splicing is interrupted by heat shock and is rescued by heat shock protein synthesis. Cell *45*, 185-193.

Yost, H.J., and Lindquist, S. (1991). Heat shock proteins affect RNA processing during the heat shock response of Saccharomyces cerevisiae. Mol Cell Biol *11*, 1062-1068.

Youn, J.Y., Dunham, W.H., Hong, S.J., Knight, J.D.R., Bashkurov, M., Chen, G.I., Bagci, H., Rathod, B., MacLeod, G., Eng, S.W.M.*, et al.* (2018). High-Density Proximity Mapping Reveals the Subcellular Organization of mRNA-Associated Granules and Bodies. Mol Cell *69*, 517-532 e511.

Yung, B.Y., Busch, R.K., Busch, H., Mauger, A.B., and Chan, P.K. (1985). Effects of actinomycin D analogs on nucleolar phosphoprotein B23 (37,000 daltons/pI 5.1). Biochem Pharmacol *34*, 4059-4063.

Zander, G., Hackmann, A., Bender, L., Becker, D., Lingner, T., Salinas, G., and Krebber, H. (2016). mRNA quality control is bypassed for immediate export of stress-responsive transcripts. Nature *540*, 593-596.

Zander, G., and Krebber, H. (2017). Quick or quality? How mRNA escapes nuclear quality control during stress. RNA Biol *14*, 1642-1648.

Zenklusen, D., Vinciguerra, P., Strahm, Y., and Stutz, F. (2001). The yeast hnRNP-Like proteins Yra1p and Yra2p participate in mRNA export through interaction with Mex67p. Mol Cell Biol *21*, 4219-4232.

Zenklusen, D., Vinciguerra, P., Wyss, J.C., and Stutz, F. (2002). Stable mRNP formation and export require cotranscriptional recruitment of the mRNA export factors Yra1p and Sub2p by Hpr1p. Mol Cell Biol *22*, 8241-8253.

Zhang, D., and Oliferenko, S. (2014). Tts1, the fission yeast homologue of the TMEM33 family, functions in NE remodeling during mitosis. Mol Biol Cell *25*, 2970-2983.

Zhang, K., Daigle, J.G., Cunningham, K.M., Coyne, A.N., Ruan, K., Grima, J.C., Bowen, K.E., Wadhwa, H., Yang, P., Rigo, F.*, et al.* (2018). Stress Granule Assembly Disrupts Nucleocytoplasmic Transport. Cell *173*, 958-971 e917.

Zhang, K., Mosch, K., Fischle, W., and Grewal, S.I. (2008). Roles of the Clr4 methyltransferase complex in nucleation, spreading and maintenance of heterochromatin. Nat Struct Mol Biol *15*, 381-388.

Zhao, A., Guo, A., Liu, Z., and Pape, L. (1997). Molecular cloning and analysis of Schizosaccharomyces pombe Reb1p: sequence-specific recognition of two sites in the far upstream rDNA intergenic spacer. Nucleic Acids Res *25*, 904-910.

Zhao, R., and Houry, W.A. (2005). Hsp90: a chaperone for protein folding and gene regulation. Biochem Cell Biol *83*, 703-710.

Zhao, X., Wu, C.Y., and Blobel, G. (2004). Mlp-dependent anchorage and stabilization of a desumoylating enzyme is required to prevent clonal lethality. J Cell Biol *167*, 605-611.

Zheng, X., Krakowiak, J., Patel, N., Beyzavi, A., Ezike, J., Khalil, A.S., and Pincus, D. (2016). Dynamic control of Hsf1 during heat shock by a chaperone switch and phosphorylation. eLife *5*.

Zhou, Y., Zhu, J., Schermann, G., Ohle, C., Bendrin, K., Sugioka-Sugiyama, R., Sugiyama, T., and Fischer, T. (2015). The fission yeast MTREC complex targets CUTs and unspliced pre-mRNAs to the nuclear exosome. Nat Commun *6*, 7050.

Zimmer, C., and Fabre, E. (2011). Principles of chromosomal organization: lessons from yeast. J Cell Biol *192*, 723-733.

Zimowska, G., Aris, J.P., and Paddy, M.R. (1997). A Drosophila Tpr protein homolog is localized both in the extrachromosomal channel network and to nuclear pore complexes. J Cell Sci *110 (Pt 8)*, 927-944.

Zofall, M., and Grewal, S.I. (2006). RNAi-mediated heterochromatin assembly in fission yeast. Cold Spring Harb Symp Quant Biol *71*, 487-496.

Zou, J., Guo, Y., Guettouche, T., Smith, D.F., and Voellmy, R. (1998). Repression of heat shock transcription factor HSF1 activation by HSP90 (HSP90 complex) that forms a stress-sensitive complex with HSF1. Cell *94*, 471-480.

Zuccolo, M., Alves, A., Galy, V., Bolhy, S., Formstecher, E., Racine, V., Sibarita, J.B., Fukagawa, T., Shiekhattar, R., Yen, T., *et al.* (2007). The human Nup107-160 nuclear pore subcomplex contributes to proper kinetochore functions. EMBO J *26*, 1853-1864.

Zuleger, N., Robson, M.I., and Schirmer, E.C. (2011). The nuclear envelope as a chromatin organizer. Nucleus *2*, 339-349.

Research performed over the last years has changed the view of NPCs as simple nucleo-cytoplasmic trafficking channels into a more comprehensive understanding of the multiples roles of the NPCs, which range from chromatin regulation to the maintenance of genome integrity. The most nucleoplasm-facing structure of the NPC is the nuclear basket. While in higher eukaryotes the main structural component of the nuclear basket is the translocated promoter region (TPR) nucleoporin, most yeasts possess two orthologs: Mlp1/Mlp2 in *Saccharomyces cerevisiae* and Nup211/Alm1 in *Schizosaccharomyces pombe*. Although it is known that most nuclear basket functions have been conserved along evolution, it remains unclear how TPR nucleoporins are assembled into the NPCs and the roles that they perform in the fission yeast.

Previous data from our laboratory described that the absence of Alm1 leads to chromosome missegregation and altered kinetochore behaviour. In order to avoid erroneous microtubule-kinetochore attachments and chromosome segregation defects, it is required a proper centromere and kinetochore structural organization, which is regulated by proteasomal degradation. Proteasome is enriched in the nucleus, specially at the nuclear periphery, although how this localization is regulated and its biological implications are unclear. In the first part of this thesis, we have characterized the role of the nuclear basket component Alm1 in the spatial regulation of the proteasome, which is key for chromosome segregation through the regulation of the kinetochore homeostasis.

The different steps of mRNA biogenesis, including transcription, processing, quality control and export are closely coordinated, and the nuclear basket has been proposed to act as a physical platform that couples such processes. *nup211*$^{+}$ was previously described as required for mRNA export. However, it remains unknown its specific role in mRNA docking and export. In the second part of this thesis, we have characterized how the two TPR nucleoporins in the fission yeast, Nup211 and Alm1, are assembled into the nuclear basket and how they anchor to the NPC. Additionally, we have performed a genetic and functional analysis to dissect the functions of Nup211 and Alm1 in mRNA docking, quality control and export.

Heat shock deeply compromise cell viability due to protein denaturation and aggregation. In order to ensure survival cells activate the evolutionary conserved *heat shock response* (HSR), which results in profound changes in mRNA metabolism and nuclear organization. How this switch is achieved is not fully understood. In the third part of this study, we have characterized how heat stress leads to the inhibition of bulk mRNA export and the arrest of cell growth, concomitant with the aggregation of NPC components, the mRNA processing and export machinery, cell cycle regulators, and protective chaperones and disaggregases into ring-like structures proximal to the nucleolus. We propose that these structures, named "nucleolar rings" (NuRs), are formed by the reversible aggregation of nuclear components, and constitute storage sites for those activities that are inhibited during HS and have to be protected in order to re-start cellular metabolism when normal conditions are restored.